Filling the gap in environmental analysis: enrichment of ionizable micropollutants by electromembrane extraction or field-step electrophoresis and their analysis by capillary electrophoresis and liquid chromatography mass spectrometry for (non-)target screening

Dissertation

der Mathematisch-Naturwissenschaftlichen Fakultät

der Eberhard Karls Universität Tübingen

zur Erlangung des Grades eines

Doktors der Naturwissenschaften

(Dr. rer. nat.)

vorgelegt von

Tobias Rösch

aus Göppingen

Tübingen

2021

Gedruckt mit Genehmigung der Mathematisch-Naturwissenschaftlichen Fakultät der Eberhard Karls Universität Tübingen.

Für meine Eltern – Danke für alles.

Danksagung

Die vorliegende Arbeit baut auf der teils unermüdlichen Unterstützung vieler Personen auf, ohne die vieles in dieser Form nicht möglich gewesen wäre. An dieser Stelle möchte ich einigen davon danken.

Prof. Dr. Carolin Huhn möchte ich für die Möglichkeit danken, die Arbeit in ihrem Arbeitskreis abzuschließen. Vielen Dank für deine engagierte Betreuung und Aufmerksamkeit, für die vielen Gelegenheiten, sich auch auf Konferenzen fachlich auszutauschen, und vor allem auch danke für deine stetige Bereitschaft zu intensiven und kritischen Diskussionen bis hin zum letzten Tag. Ich danke dir für den großen wissenschaftlichen Freiraum, den du mir gegeben hast und der auch wesentlich zum Gelingen dieser Arbeit beigetragen hat.

Bei Prof. Dr. Günter Gauglitz bedanke ich mich herzlich für die Übernahme des Zweitgutachtens. Prof. Dr. Michael Lämmerhofer und Prof. Dr. Udo Weimar möchte ich für Ihre Bereitschaft, sich im Rahmen der mündlichen Promotionsprüfung mit dieser Arbeit auseinanderzusetzen, herzlich danken.

Was wäre ein Doktorand ohne seine Mitstreiterinnen und Mitstreiter: Benjamin Rudisch und Sarah Knoll. An dieser Stelle ein herzliches Dankeschön für eure moralische und fachliche Unterstützung sowie die unermüdliche Bereitschaft, euer Wissen mit mir zu teilen und zum Gelingen dieser Arbeit beizutragen. Aber auch Michel Banet, Hannes Graf, Dr. Martin Meixner, Dr. Tanja Melzer, Dr. Sonja Metternich, Dr. Anna-Jorina Wicht, Benedikt Wimmer und Viola Wurster möchte ich hier erwähnen. Vielen Dank für die schönen gemeinsamen Konferenzen, den fachlichen Austausch und das Feedback bei Problemstellungen und Ideen, die Übernahme von Korrekturen usw.

Manche dieser Ergebnisse wären ohne die engagierte und fleißige Arbeit meiner Praktikantinnen und Praktikanten in diesem Zeitrahmen nicht möglich gewesen. Stephanie Bock, Christina Breitenstein, Birgit Dittrich, Eric Juriatti und Nadja Kalinke: Danke für das Probenvorbereiten, danke für das Membranenherstellen und vor allem danke für das wiederholte Auf- und Abbauen der Anreicherungszelle.

Bedanken möchte ich mich weiterhin bei der gesamten 6. Ebene, also allen Mitarbeitern rund um die Arbeitskreise von Prof. Dr. Reinhold Fink, Prof. Dr. Günter Gauglitz und Prof. Dr. Stefan Schwarzer. Ich danke allen herzlich, sei es für die Zurverfügungstellung von Chemikalien und Geräten als auch für den fachlichen und persönlichen Austausch im Kaffeeraum oder beim gemeinsamen Mittagessen.

Einige Teile dieser Arbeit basieren auf der erfolgreichen Zusammenarbeit mit Kooperationspartnern. An dieser Stelle möchte ich mich explizit bei Herrn Dr. Gerhard Weber und seinen Mitarbeitern (FFE Service) für die angenehme Zusammenarbeit bei der Planung und Umsetzung der gemeinsam ausgearbeiteten Ideen sowie der freundlichen Betreuung vor Ort bedanken. Des Weiteren bedanke ich mich herzlich bei den beteiligten Mitarbeitern der Landeswasserversorgung Langenau, vor allem bei Dr. Tobias Bader. Vielen Dank für die schnellen Rückmeldungen und hilfreichen Diskussionen.

Erklärung nach § 6 Abs. 2 der PromO der Mathematisch-Naturwissenschaftlichen Fakultät

Chapter 2: Literature research and writing was done by me (Sections *Dispersive liquid-liquid microextraction*, *Electric field-driven sample preparation*, *Ion chromatography* and *Electromigrative separation techniques*) and Sarah Knoll (Sections *Solid-phase extraction*, *QuEChERS extraction*, *Hydrophilic interaction liquid chromatography*, *Supercritical fluid chromatography* and *Mixed-mode liquid chromatography*). The other Sections were elaborated together equally. Statistical evaluation and creation of Figures 2-1 and 2-2 were done by me. Carolin Huhn aided with valuable input and the correction of the manuscript. This introductory chapter was published as a review article in Analytical & Bioanalytical Chemistry, September 2020, Volume 412, Issue 24, pp. 6149-6165 [1].

Chapter 3: The study design and discussion of results was jointly done by Carolin Huhn and me. The method development and optimization of the CE-MS system applicable for environmental samples were done by me. Alexandra Haake assisted with the investigation of the effects on organic solvents during her Bachelor thesis. The optimization of the SPE protocol was conducted by me with input from Sarah Knoll. QuEChERS extraction and biota sample preparation were accomplished by Birgit Dittrich under my supervision. Writing of the manuscript was done by me, Carolin Huhn corrected the manuscript.

Chapter 4: I developed the HILIC method with input from Sarah Knoll with regard to suitable eluent compositions. I conducted all experimental work for this chapter, as well as data evaluation and visualization, literature research and writing. Carolin Huhn corrected the manuscript.

Chapter 5: The instrumental setup was designed in collaboration with Benjamin Rudisch and the workshop (Alexander Schnapper and Christof Binder) to guarantee feasibility of my ideas for a suitable instrumental setup. The optimization of the membrane composition and the flow-through cell were partly conducted by student coworkers Stephanie Bock, Christina Breitenstein, Eric Juriatti and Nadja Kalinke under my supervision. The 3D-printed sample channel was generously provided by Yannick Lubick. Nadja Kalinke additionally executed the EME experiments of the Box-Behnken- Design. Data evaluation and visualization, as well as literature research and writingwere completely done by me. Results were discussed with Carolin Huhn throughout the work. Carolin Huhn corrected the manuscript.

Chapter 6: The idea to use FFE for the enrichment in FSE experiments was based on previous work already described by Jorina Wicht in her PhD Thesis (2019 Tübingen [2]). Sample collection, analysis of the fractions and data analysis was done by me. Optimization of FSE separation and fractionation experiments were conducted by Gerhard Weber and his employees of FFE Service. Discussions between Carolin Huhn,

Gerhard Weber and me led to an optimization of the FSE system in a second set of experiments. All study parameters excluding the FSE parameters were designed by me. Non-target screenings were conducted by Tobias Bader from the Landeswasserversorgung Langenau. Summary of data and overall data compilation as well as writing of the manuscript was done by me. All partners aided in corrections with joint discussions.

Table of contents

Table of contents

Abbreviations

ASD	average symmetry deviation
AT	analysis time
BBD	Box-Behnken-Design
BGE	background electrolyte
BPE	base peak electropherogram
CE	capillary electrophoresis
CN	charge number
CSV	calculated symmetry value
CTA	cellulose triacetate
DAD	diode array detector
DCM	dichloromethane
DEHPA	di-(2-ethylhexyl) phosphoric acid
d-SPE	dispersive solid-phase extraction
EC	evaporative concentration
EF	enrichment factor
EIC	extracted ion chromatogram
EIE	extracted ion electropherogram
EME	electromembrane extraction
EOF	electroosmotic flow
ESI	electrospray ionization
FA	formic acid
FFE	free flow electrophoresis
FPNE	2-fluorophenyl 2-nitrophenyl ether
FSE	field-step electrophoresis
HAc	acetic acid
HILIC	hydrophilic interaction liquid chromatography
HPLC	high-performance liquid chromatography
IC	ion chromatography
ICP	inductively coupled plasma
ISTD	isotope-labeled standard
ITP	isotachophoresis
LC	liquid chromatography
LOD	limit of detection
ME	matrix effect
MeCN	acetonitrile
MeOH	methanol
MEPS	microextraction by packed sorbent

MMLC	mixed-mode liquid chromatography
MS	mass spectrometry
MS/MS	tandem mass spectrometry
MT	migration time
MW	migration window
NACE	non-aqueous capillary electrophoresis
NPOE	2-nitrophenyl octyl ether
PA	peak area
PEEK	polyether ether ketone
PH	peak height
pI	isoelectric point
PIM	polymer inclusion membrane
QuEChERS	Quick, Easy, Cheap, Efficient, Rugged, Safe
RPLC	reversed-phase liquid chromatography
RSD	relative standard deviation
RT	retention time
S/N	signal to noise
SFC	supercritical fluid chromatography
SLM	supported liquid membrane
SP	separation power
SPE	solid-phase extraction
SPME	solid-phase microextraction
TCR	total chromatographic resolution
TEA	triethylamin
TEHP	tris (2-ethylhexyl) phosphate
TIC	total ion chromatogram
tITP	transient isotachophoresis
VEF	volume enrichment factor
vPICs	very polar and ionic compounds
WWTP	wastewater treatment plant
ZIC	zwitterionic

Abstract

In environmental analysis, the so called "analytical gap" (Reemtsma, Environ Sci Technol 2016, 50, 19, 10308-10315) demands for new strategies for monitoring polar micropollutants and their transformation products, especially ionic and ionizable compounds in environmental samples. Various approaches with hydrophilic interaction liquid chromatography coupled to mass spectrometry (HILIC-MS) as well as with ion chromatography-MS have been published in the last few years, but still some limitations and challenges remained.

With its high separation efficiency and good matrix tolerance, capillary electrophoresis-mass spectrometry is well suited for the analysis of ionic and ionizable compounds. In this work, it was possible to establish a non-aqueous capillary electrophoresis (NACE)-MS method applicable for the analysis of micropollutants (cationic, anionic and non-charged analytes) in environmental waters and biota samples. The method showed good precision with average relative standard deviations (RSD) for migration time of 1.4% and peak area of 5.3%. Detection limits (on average) of 4.2 µg/l were reached in aqueous samples and biota extracts. A comparison concerning detection limits, matrix effects and selectivity with two chromatographic separation methods developed (reversed phase liquid chromatography-MS (RPLC-MS) and HILIC-MS) demonstrated the high potential of the NACE-MS method, though sensitivity was insufficient. For preconcentration, classical solid-phase extraction (SPE)/NACE-MS was applied to quantify the artificial sweetener acesulfame and the pharmaceutical hydrochlorothiazide, but further enrichment of micropollutants was necessary. The development of new methods to preconcentrate analytes with high coverage was the focus of this work's second part. Instrumental strategies were developed to enrich ionic and ionizable substances in environmental samples with the aid of electric fields to establish a sample preparation step which did not discriminate substance classes, e.g. according to charge number or polarity. All methods were shown to be applicable for suspect and non-target screening. Based on previous results in the literature, a dual electromembrane extraction (EME) flow-through cell was developed and optimized. It proved compatible with chromatographic and electrophoretic separation techniques and was applied to river water. The EME/NACE-MS setup was suitable to enrich both cationic and anionic analytes possessing a wide range of physicochemical characteristics with average enrichment factors of 40 (cations) and 20 (anions). The high coverage that was reached even for highly polar analytes like metformin and sulfamic acid when using optimized polymer inclusion membranes demonstrated the potential of EME for non-target screening as well. Matrix effects were investigated for river water samples.

A new sample preparation method for environmental sciences based on free flow electrophoresis (FFE) was implemented. The sample was introduced continuously into a low-conductivity buffer zone. Acidic analytes present in the sample were stacked at the boundary to a high-conductivity zone upon application of an electric field perpendicular to the sample flow. This step mode FFE, called field-step electrophoresis (FSE), proved suitable for the focusing of acidic analytes with pK_a values of up to 10, demonstrating a broad range. In most cases, model analytes spiked into FSE samples could be recovered

in only one, but never more than two fractions. Neutral matrix compounds and cations present in environmental water as well as highly mobile inorganic anions passing the stacking boundary were removed successfully. FSE media were chosen to be volatile. Thus, solvent exchange and analyte enrichment via preconcentration were possible. The protocol was compatible with downstream analysis by RPLC-, HILIC- and CE-MS. The highly reproducible FSE/RPLC-MS procedure (RSD of peak areas 3-6%) was successfully used for non-target screening in a river water samples as a proof of concept demonstrating its high potential for environmental sciences. Both EME and FSE were found to be independent of analyte polarity and can thus be used complementarily to the sample preparation techniques already established in environmental analysis, e.g. SPE. Concluding, two new sample preparation methods compatible with chromatographic- and electromigrative-based separation techniques were developed. For analysis, a dual HILIC method and a new NACE-MS method were introduced and validated for their application in environmental sciences, all explicitly devoted to the analysis of polar and ionic micropollutants. Throughout the work, the analysis of environmental samples provedthe applicability of the methods.

.

Zusammenfassung

In der Umweltanalytik erfordert die „analytische Lücke" (Reemtsma, Environ Sci Technol 2016, 50, 19, 10308-10315) neue Strategien zur Überwachung polarer Mikroschadstoffe und ihrer Umwandlungsprodukte, insbesondere ionischer und ionisierbarer Verbindungen in Umweltproben. In den letzten Jahren wurden verschiedene analytische Lösungsansätze mit hydrophiler Interaktionsflüssigkeitschromatographie gekoppelt mit Massenspektrometrie (HILIC-MS) sowie mit Ionenchromatographie-MS veröffentlicht, jedoch blieben einige Einschränkungen und Herausforderungen bestehen.

Die Kapillarelektrophorese-Massenspektrometrie ist mit ihrer hohen Trennleistung und guten Matrixtoleranz für die Analyse ionischer Verbindungen geeignet. In dieser Arbeit konnte eine nicht-wässrige Kapillarelektrophorese (NACE)-MS-Methode etabliert werden, die für die Analyse von Mikroschadstoffen (kationische, anionische und nicht geladene Analyten) in Umweltgewässern und Biota-Proben anwendbar ist. Die Methode zeigte eine hohe Präzision mit relativen Standardabweichungen (RSD) von im Durchschnitt 1,4 % für Migrationszeiten und 5,3 % für die Peakflächen. In wässrigen Proben und Biota-Extrakten wurden durchschnittliche Nachweisgrenzen von 4,2 µg/l erreicht. Ein Vergleich von zwei neu entwickelten chromatographischen Trennmethoden (Umkehrphasenchromatographie-MS (RPLC-MS) und HILIC-MS) bezüglich Nachweisgrenzen, Matrixeffekten und Selektivität zeigte das hohe Potenzial der NACE-MS-Methode für ein Non-Target Screening ionisierbarer Substanzen. Allerdings war die Sensitivität nicht ausreichend. Zur Anreicherung wurde die klassische Festphasenextraktion (SPE) verwendet, was die Quantifizierung des künstlichen Süßstoffes Acesulfam und des häufig verschriebenen Arzneimittels Hydrochlorothiazid ermöglichte. Eine weitere Anreicherung von Mikroschadstoffen war allerdings notwendig, da die Empfindlichkeit noch nicht für alle Modellanalyten gleichermaßen ausreichend war. Die Entwicklung neuer Methoden zur Anreicherung von Analyten stand im Fokus des zweiten Teils dieser Arbeit. Dabei wurde vor allem darauf geachtet, dass ein breiter Analytbereich abgedeckt werden konnte. Es wurden instrumentelle Strategien und Methoden entwickelt, um ionische und ionisierbare Substanzen in Umweltproben mithilfe elektrischer Felder anzureichern, um eine Probenvorbereitung mit einer sehr hohen Analytabdeckung bezüglich der Polarität der ionisierbaren Analyten zu erhalten. Alle Methoden erwiesen sich als anwendbar für das Suspect- oder Non-Target Screening.

Basierend auf früheren Ergebnissen in der Forschungsliteratur wurde eine Durchflusszelle für die duale Elektromembran-Extraktion (EME) entwickelt und optimiert. Die Anreicherungsmethode erwies sich als kompatibel mit chromatographischen und elektrophoretischen Trenntechniken und wurde auf Flusswasser angewandt. Der EME/NACE-MS-Aufbau war dazu geeignet, sowohl kationische als auch anionische Analyten, die ein breites Spektrum physikalisch- chemischer Eigenschaften abdeckten, mit durchschnittlichen Anreicherungsfaktoren von 40 (Kationen) und 20 (Anionen) anzureichern. Die erfolgreiche Anwendung auf hochpolare Analyten wie Metformin und Sulfaminsäure, die bei der Verwendung optimierter Polymer-Inclusion-Membranen gezeigt wurde, demonstrierte das Potenzial

von EME auch für Non-Target Screenings. Intensiv wurden Matrixeffekte bei Flusswasserproben untersucht.

Eine neue Probenvorbereitungsmethode für die Umweltwissenschaften basierend auf der Free Flow Electrophoresis (FFE) wurde implementiert. Die Probe wurde kontinuierlich in eine Pufferzone mit niedriger Leitfähigkeit eingeführt. In der Probe vorhandene säurebildende Analyten wurden an der Grenze zu einer Zone hoher Leitfähigkeit nach Anlegen eines elektrischen Felds senkrecht zum Probenfluss gestackt. Dieser auch als Field-Step Electrophoresis (FSE) bezeichnete FFE-Modus erwies sich als geeignet für die Fokussierung eines breiten Spektrums saurer Analyten mit pK_S-Werten bis zu 10. In den meisten Fällen konnten in FSE-Proben gespikte Modellanalyten in nur einer, aber nie in mehr als in zwei Fraktionen wiedergefunden werden. Neutrale Matrixkomponenten und Kationen, die in Umweltwasser vorhanden sind, sowie hochmobile anorganische Anionen, die die Grenzfläche der Aufkonzentrierung passieren können, wurden erfolgreich entfernt. FSE-Medien wurden so gewählt, dass sie flüchtig sind, sodass ein Lösungsmittelaustausch und eine Anreicherung durch Evaporation und Aufnahme in geringerem Volumen möglich waren. Die FSE-Probenvorbereitung war kompatibel mit nachgeschalteten Analysen durch RPLC-, HILIC- und CE-MS. Das FSE/RPLC-MS-Verfahren erwies sich als hoch reproduzierbar (RSD der Peakflächen 3-6%) und wurde erfolgreich für das Non-Target-Screening in Flusswasserproben in einer Machbarkeitsstudie eingesetzt, die sein hohes Potenzial für die Umweltwissenschaften demonstriert. Sowohl EME als auch FSE erwiesen sich als unabhängig von der Analytpolarität und können somit komplementär zu den bereits in der Umweltanalytik etablierten Probenvorbereitungstechniken eingesetzt werden, z.B. zu SPE.

Zusammenfassend wurden zwei neue Probenvorbereitungsmethoden entwickelt, die mit chromatographischen und elektromigrativen Trenntechniken kompatibel sind. Zwei separate HILIC-Methoden sowie eine neue NACE-MS-Methode für die Analyse von anionischen und kationischen Analyten konnten erfolgreich eingeführt werden. Ihre Anwendungen in den Umweltwissenschaften wurden explizit für die Analyse von polaren und ionischen Mikroverunreinigungen in Umweltproben getestet und beurteilt und so ihre Eignung für die Umweltanalytik nachgewiesen.

1. Motivation

Since Reemtsma et al. [3] coined the term "analytical gap" in environmental analysis in 2016, the scope in environmental sciences has broadened towards finding solutions for the analysis of persistent and mobile organic compounds in environmental waters as well as biota and soil samples. These analytes are usually highly polar and can pass more easily through established clean-up processes in wastewater treatment plants. Many transformation products belong to this class of analytes. As their fate and behavior in the environment is often unknown, new monitoring campaigns are necessary. In order to achieve this, not only targeted methods, but also suspect and non-target screenings are required [4].

Whereas reversed-phase liquid chromatography mass spectrometry (RPLC-MS) is already well established for the (non-target) analysis of non-polar compounds, there is no comprehensive method yet for the analysis of these polar and ionic compounds. New advancements in chromatographic-based separation methods like supercritical fluid chromatography or mixed-mode liquid chromatography show great potential, but so far, only hydrophilic interaction liquid chromatography coupled to MS (HILIC-MS) has been accepted to some extent [5]. Even for HILIC, no stationary phase generally applicable for comprehensive monitoring has evolved due to the strong selectivity differences among both stationary and mobile phases with their great variety of possible interactions for retention [5]. This results in a large number of stationary phases and various methods, which complicates the establishment of non-target libraries for identification. Additionally, especially in water analysis, the necessity of a high percentage of organic solvent, mostly acetonitrile, in the injection solution for HILIC separation, reduces the sensitivity for aqueous samples at least by a factor of 5 if no solvent exchange is implemented during the sample preparation method.

It has been shown that the majority of polar compounds is ionizable in the pH range between 4 and 10 [5], which offers the possibility to use separation techniques dedicated to the analysis of ionic compounds such as capillary electrophoresis (CE) or ion chromatography. Whereas for the latter, applications have only recently beenestablished using sensitive mass spectrometric detection [6], CE-MS is already widely accepted for non-targeted analysis in metabolomics [7, 8].

This thesis addresses the gap in the analysis of polar ionizable compounds in environmental sciences by establishing new methods for their analysis. First, the development of a new CE-MS method applicable to environmental samples is envisaged covering both anions and cations. Besides its general performance with regard to advantages and limitations, the compatibility with common sample preparation techniques (solid-phase extraction (SPE), evaporative concentration (EC)) and its application to environmental samples, namely surface water and biota, are investigated. Additionally, two separate chromatographic separation methods for polar anionic and cationic compounds using HILIC-MS are developed and validated, and their selectivity is compared with an established RPLC-MS method.

As concentrations are too low for direct injection in CE-MS, sample preparation steps are necessary. So far, most sample preparation techniques have addressed specific analytes or substance classes. Currently, most promising strategies are based on variations of SPE, namely mixed-bed SPE [9] and EC [10]. Both have been shown to cover a broad range of polar ionizable compounds including gap compounds [11]. To date, only a few mixed-bed SPE stationary phases are commercially available, and EC often suffers from considerable signal suppression [10]. They have hardly been investigated with respect to their ability to non-selectively preconcentrate specifically ionizable analytes. In this thesis, the coverage of different sample preparation techniques is thoroughly examined with a suitable set of model analytes.

The focus of this thesis lies on sample preparation techniques dedicated to ionizable compounds using electric fields for preconcentration. Electromembrane extraction (EME) was introduced in 2006 by Pedersen-Bjergaard and Rasmussen [12] and applications have increased drastically since then. The usually aqueous sample and acceptor solutions are separated by a membrane, mostly with tailored selectivity for selected analytes of interest [13]. The application of an electric field across the two compartments results in the transfer of analytes through the membrane into the acceptor solution of lower volume to reach an enrichment of the analytes. In this work, a new setup for dual EME of positively and negatively charged analytes is developed and validated. It was investigated whether EME can be used for screening approaches covering a broad polarity range as compared to the state of the art of selective preconcentration, which focuses mostly on either cations or anions, e.g. from biological samples.

In CE, on-line preconcentration techniques such as large volume sample stacking [14] or transient isotachophoresis [15] are common, though only a few μl can be injected. Therefore, the low detection limits to quantify micropollutants in environmental samples are still challenging. Free flow electrophoresis (FFE) offers the possibility to continuously inject sample, so that large injection volumes can be realized and fractions can be sampled from the separation [16]. Using a specific mode of FFE, namely field-step electrophoresis (FSE) [17], all (negatively) charged analytes present in the sample can be focused between two conductivity zones in only a few fractions. This procedure was originally established in protein fractionation, and this thesis attempts to adapt it for the application in environmental analysis and thus for small molecules. Preconcentration of analytes is intended using volatile FSE media to enable solvent exchange, which is also advantageous to the compatibility with downstream analysis.

Throughout this work, compatibility between sample preparation/enrichment methods and downstream analysis is investigated to define the most promising combinations, also taking into account enrichment efficiencies and matrix effects. Using large sets of model analytes, the coverage of all methods as well as any bias with regard to polarity and charge is thoroughly examined. Finally, all methods are used to quantify micropollutants in river or biota samples to demonstrate their applicability in environmental sciences.

2. Introduction: Trends in sample preparation and separation methods for the analysis of very polar and ionic compounds in environmental water and biota samples

This introductory chapter was published as a review article in in Analytical & Bioanalytical Chemistry, September 2020, Volume 412, Issue 24, pp. 6149-6165 [1].

2.1 Abstract

Recent years showed a boost in knowledge about the presence and fate of micropollutants in the environment. Instrumental and methodological developments mainly in liquid chromatography coupled to mass spectrometry hold a large share in this success story. These techniques soon complemented gas chromatography and enabled the analysis of more polar compounds including pesticides but also household chemicals, food additives and pharmaceuticals often present as traces in surface waters. In parallel sample preparation techniques evolved to extract and enrich these compounds from biota and water samples.

This review article looks at very polar and ionic compounds using the criterion log P $\leq$ 1. Considering about 240 compounds, we show that (simulated) log D values are often even lower than the corresponding log P values due to ionization of the compounds at our reference pH of 7.4. High polarity and charge are still challenging characteristics in the analysis of micropollutants and these compounds are hardly covered in current monitoring strategies of water samples. The situation is even more challenging in biota analysis given the large number of matrix constituents with similar properties. Currently, a large number of sample preparation and separation approaches are developed to meet the challenges of the analysis of very polar and ionic compounds. In addition to reviewing them, we show the reader some trends: for sample preparation, preconcentration and purification efforts by SPE will continue, possibly using upcoming mixed-mode stationary phases and mixed beds in order to increase comprehensiveness in monitoring applications. For biota analysis, miniaturization and parallelization are aspects of future research. For ionic or ionizable compounds, we see electromembrane extraction as a method of choice with a high potential to increase throughput by automation. For separation, predominantly coupled to mass spectrometry, hydrophilic interaction liquid chromatography applications will increase as the polarity range ideally complements reversed-phase liquid chromatography and instrumentation and expertise are available in most laboratories. Two-dimensional applications have not yet reached maturity in liquid phase separations to be applied in higher throughput. Possibly, the development and commercial availability of mixed-mode stationary phases make 2D applications obsolete in semi-targeted applications. An interesting alternative will enter routine analysis soon: supercritical fluid chromatography demonstrated an impressive analyte coverage but also the possibility to tailor selectivity for targeted approaches. For ionic and ionizable micropollutants, ion chromatography and capillary electrophoresis are amenable but may be used only for specialized applications such as the analysis of halogenated acids when

aspects like desalting and preconcentration are solved and the key advantages are fully elaborated by further research.

2.2 Introduction

Already in 1985 Richardson and Bowron [18] discussed the fate of pharmaceuticals in the (aquatic) environment. Over the last 35 years, the interest in their fate steadily increased as can be seen by a statistic for the keywords environmental and pharmaceutical (see Figure 2-1A). Recent years showed improvements throughout the whole analytical process. However, due to the different physicochemical properties of pharmaceuticals caused by a variety of functional groups, it is obvious that there is no analytical method for the successful simultaneous analysis of all contaminants in a sample. Whereas for the analysis of non-polar to medium polar compounds (log P > 1) successful and reliable analysis methods already exist, there is a lack of methods for the analysis of very polar and ionic compounds (vPICs). Reemtsma et al. [19] even pointed out that -at present- an analytical gap exists for these substances. Despite great effort in past years in environmental analysis, visible from the rising number of publications identified with the keywords environmental, pharmaceutical and ionic (see Figure 2-1A), still little is known about the occurrence, fate and potential ecological effects of vPICs and their mostly even more polar metabolites in the (aquatic) environment. Since these compounds are highly polar, often mobile and possibly also persistent, they have the potential to spread through the water cycle and even reach drinking water. For ionic compounds, the charge influences sorption and uptake, which is not well understood. With increasing awareness of their possible ecotoxicological relevance, for example effects on aquatic organisms and health threats, the demand of general public for tightened regulation is rising. This requires further research to increase knowledge and understanding of occurrence and effects. Consequently, sensitive and precise methods for the analysis of these mostly small organic compounds are needed.

We compiled data from recent articles dealing with the analysis of vPICs (log P ≤ 1) in the environment. Figure 2-1B classifies 237 different vPICs that were analyzed in 63 published cited here with regard to their application. Clearly, vPICs are present in all fields of applications. It is important to mention, that this group also contains other micropollutants than pharmaceuticals and their metabolites (which themselves are mostly more polar, e.g. abacavir and its metabolite abacavir carboxylate with log $D_{pH\ 7.4}$ values of 0.4 and -2.7, respectively (see also Table S2-1)). In fact, only less than about 40% of the compounds analyzed here are pharmaceuticals. Other substance classes like food supplements (for example (artificial) sweetener) or industrial compounds in general are quite common representatives for vPICs. In order to get a feeling for the polarity of the substances, Figure 2-2 shows the distribution of their log P values. Having in mind that at pH 7.4 over 70% of these compounds have charge numbers equal to or higher than 0.5, it is crucial to consider their corresponding log D values at pH 7.4 which are summarized in Figure 2-2 (details are presented in Table S2-1 in Section 2.8).
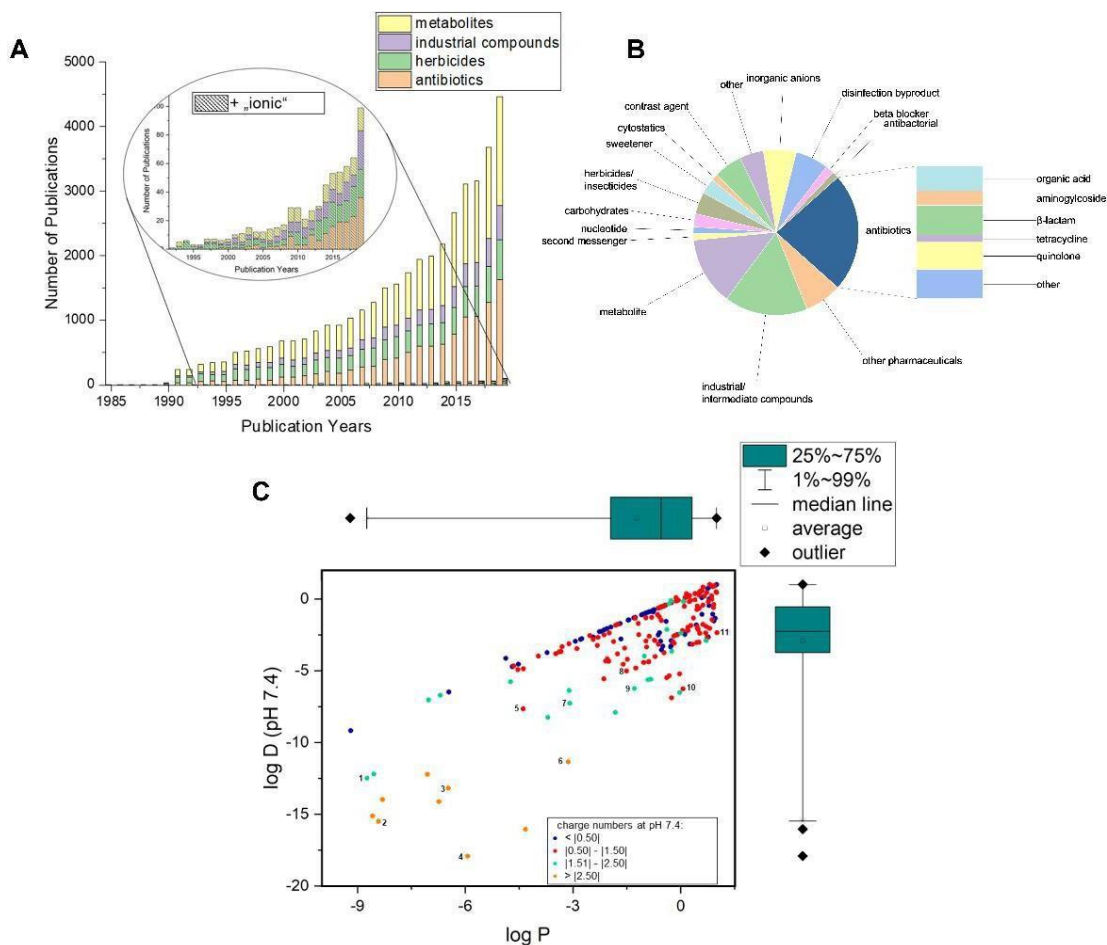
Figure 2-1 A: Non-exhaustive trend of numbers of published articles over the last 35 years listed in „Web of Science" using the keywords environmental + most common substance classes (metabolites, industrial compounds, herbicides or antibiotics, see also B) and additionally to it "ionic" in a second search (see enlarged section); B: classification of the 237 very polar and ionic compounds (vPICs, log P ≤ 1) analyzed in 63 cited articles. Details of the compounds can be found in Table S2-1 in Section 2.8. Only substance classes with ≥ 3 members are included; C: scatterplot with marginal boxplot of log P and the corresponding log $D_{pH\,7.4}$ values of the compounds. log P and log D data were extracted from Chemicalize provided by ChemAxon (10/05/2020). Colors code for different charge numbers (given as absolute number (modulus)). Selected analytes with large differences between log P and log D (see also Table S2-1) are: 1) Gd-BT-DO3A, 2) neomycin, 3) tobramycin, 4) Gd-DTPA, 5) cephalosporin C, 6) gentamicin, 7) glyphosate, 8) cephalozin, 9) 3-methylphosphinic acid, 10) itaconate and 11) 3,4-dihydroxyphenylacetic acid.

A Welch's t-test showed a statistically significant difference between the log P values and their corresponding log $D_{pH\,7.4}$ values. Details on the correlation of log P and log $D_{pH\,7.4}$ are also presented in Figure 2-1C. As expected, the average polarity of these compounds increases (log D decreases) which will result in different behavior in the environment. Several compounds such as gadolinium-based contrast agents or aminoglycoside antibiotics have large differences between log P and log $D_{pH\,7.4}$, see Figure 2-1C. Mass spectrometry (MS) is the detection method of choice to reach the required detection limits, as it provides identification strength and an additional separation dimension when coupled to the various separation techniques [5]. Current screening and environmental monitoring strategies for micropollutants often rely on solid-phase extraction (SPE) for sample preparation and liquid chromatography (LC), mostly C18 reversed-phase (RP)

stationary phases, for separation. Both SPE and reversed-phase liquid chromatography (RPLC) have limitations for vPICs. This is due to insufficient retention, leading to poor extraction efficiencies and poor separation of early eluting peaks in RPLC.
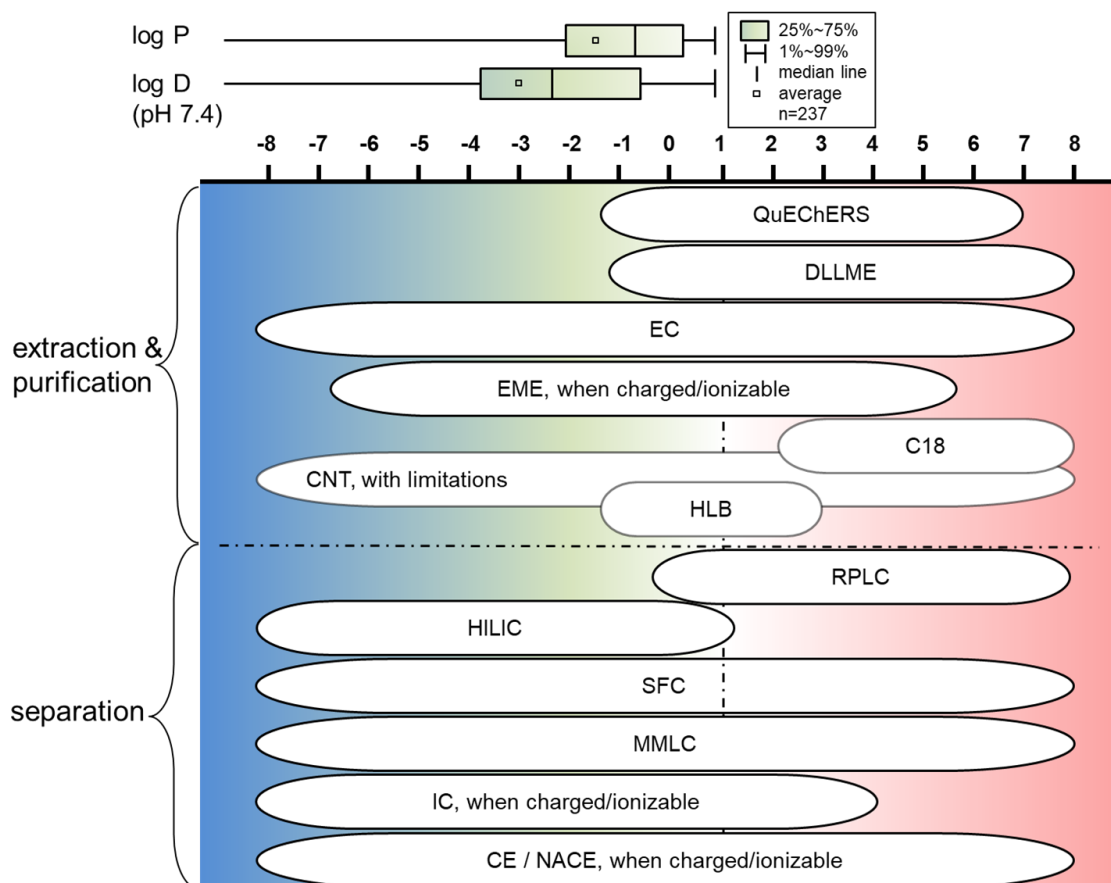
Figure 2-2: Distribution of log P and log $D_{pH\ 7.4}$ values of the compounds listed in Table S2-1 (classification according to application as in Figure 2-1B). Details of the correlation between log P and log $D_{pH\ 7.4}$ is shown in Figure 2-1C). Contours shows estimated log P scopes of the sample preparation and separation techniques as discussed in this article. Abbreviations: DLLME-dispersive liquid-liquid microextraction, EC-evaporative concentration, EME-electromembrane concentration, CNT-carbon nanotubes, HLB-hydrophilic-lipophilic balance, RPLC-reversed-phase liquid chromatography, HILIC-hydrophilic interaction liquid chromatography, SFC-supercritical fluid chromatography, MMLC-mixed-mode liquid chromatography, IC-ion chromatography, (NA)CE-(non-aqueous) capillary electrophoresis.

Figure 2-2 provides an overview on current analytical methods (sample preparation and separation) applicable for vPIC analysis and the range of log P/log D values, which can be covered (in part, however, of course not the whole range with a single analysis). Limitations regarding the polarity range covered are evident in many up-to-date reviews [20-23]. Various analytical approaches were tested to address polar micropollutants with hydrophilic interaction liquid chromatography (HILIC) being the most prominent method, followed by supercritical fluid chromatography (SFC), mixed-mode liquid chromatography (MMLC) and combinations thereof. We will discuss the applicability of ion chromatography (IC) and capillary electrophoresis (CE) suited for ionic and ionizable compounds (as the majority of polar compounds is ionizable). New instrumental developments e.g. for IC-MS will be discussed but also innovations, for example

improved stationary phases with a column material particle size less than 2 µm for ultrahigh-performance SFC (UHPSFC).

Environmental samples, especially biota samples, have complex matrices. Matrix effects seem to be relevant especially for very polar analytes [24]. They have to be addressed enhancing selectivity (both for separation and detection) and using sample preparation strategies. While common sample preparation techniques like SPE are still advancing quickly, multiresidue methods such as QuEChERS (quick, easy, cheap, effective, rugged and safe) found their way from food to environmental soil and biota analysis. We here want to discuss some alternatives, too, such as electromembrane extraction (EME), some of them only applicable for ionic and ionizable analytes.

In the past, there have been some reviews or trend articles already addressing the analysis of polar compounds [5, 20-22, 25]. In this review article we will focus on liquid phase separations coupled to MS and sample preparation strategies for the analysis of vPICs (log P ≤ 1) in environmental samples including water and biota. We critically discuss new developments in the field differentiating between targeted and non-targeted methods. We here want to discuss sample preparation in combination with different separation methods e.g. IC, CE and SFC and to elaborate recent trends and emphasize their potential for the analysis of vPICs in environmental samples in the future.

2.3 Trends in sample preparation

2.3.1 Sample preparation for environmental matrices

Beside robustness and reproducibility, the main objectives of sample preparation are the removal of matrix compounds, analyte recovery and especially analyte preconcentration whereas the latter two are also often combined in the term enrichment factor. Since most micropollutants in environmental samples are present at trace levels (ng/l to µg/l range) separation techniques alone are not able to reach these concentration levels, and they can be utilized only if sample enrichment is applied [26-29]. Moreover, smaller initial sample sizes (especially important in biota analysis of invertebrates), improvement in extraction selectivity for targeted analysis, but also coverage in non-target analysis are essential [5]. Coupling to analytical separation methods plays an important role [30]. Another aspect is green analytical chemistry, which has emerged in the 1990s, due to many analytical methods themselves generating a significant amount of chemical waste, resulting in a great environmental impact. It is required to reduce the amount and toxicity of applied solvents and reagents, especially by automation and miniaturization [31]. In this section, we focus on modern approaches for the sample preparation of polar and ionic analytes in water and biota samples.

2.3.2 Solid-phase extraction

Conventional off-line SPE is the method of choice for isolating and enriching organic micropollutants from environmental samples with a wide range of sorbents available [32]. Based on the nature of the analytes, a careful choice of the sorbent material allows obtaining high recoveries and enrichment factors, typically in the range of 2-1000. Ofall

sorbents available for SPE, Oasis HLB is the most common sorbent used for environmental samples. It is a copolymeric sorbent with hydrophilic and lipophilic properties and can be used for a wide range of target compounds. It is water-wettable and stable over the whole pH range. In environmental analysis it was used for the extraction of pharmaceuticals of various therapeutic classes from different matrices including wastewater [28, 33], sludge [34] and fish tissue [35]. However, the study of Boulard et al. [36] showed limitations of this material for polar pharmaceuticals and their transformation products with a log $D_{pH\,7}$ close to or below 0. Alternatives to Oasis HLB are carbonaceous SPE sorbents, as they combine polar and nonpolar interactions, making them suitable for a large polarity range (see Zahn et al. [5] for further discussion). In environmental analysis, they were applied for the analysis of polar pesticides [37] and herbicides [38].

Mixed-mode SPE sorbents became commercially available, which are able to retain compounds through both hydrophobic interactions and ionic interactions so that ionic or ionizable compounds can also be extracted [22]. For example, Scheurer et al. [39] used Strata X-CW columns to extract the ionic antidiabetic metformin from sewage and surface water with a relative recovery $\geq$ 90%. However, even SPE materials intended for polar compounds are often unable to retain the most polar compounds and ion exchange materials are limited to charged compounds [5]. Accordingly, either combinations of different SPE sorbents or alternative methods such as evaporative concentration (EC) are needed to enrich these compounds from matrices: Köke et al. [40] used mixed-bed SPE originally developed by Kern et al. [9] combining three SPE materials to enrich polar compounds from various environmental waters. The results were compared to a sample preparation method based on EC. The study showed that both approaches provided a higher coverage of analytes compared to Oasis HLB. Mean recoveries for the enriched analytes were similar, however, lower matrix effects were observed for the HLB method in HILIC-MS/MS. Mechelke et al. [10] compared EC to mixed-bed multilayer SPE for the enrichment of 590 organic substances from river water and wastewater. The results showed, that overall, EC was better suited for the enrichment of polar analytes (see also [5]), albeit considerable signal suppression was observed for the EC-enriched samples. However, there is still no method that covers the complete range of vPICs, therefore further research is necessary to increase the analyte coverage and to further reduce matrix effects especially for polar analytes in biota samples, which may have more naturally occurring interferents.

SPE can be applied on-line and off-line, with specific benefits and drawbacks of these two approaches. A major advantage of on-line SPE is that it analyzes the entire eluate from the SPE extract, hence providing better preconcentration factors, sensitivity and recovery than most off-line SPE approaches. In addition, on-line SPE has low solvent consumption requirements thereby decreasing the costs for organic solvents waste disposal [41]. Problems may arise from the compatibility with subsequent RPLC due to an insufficient elution strength [32]. However, Huntscha et al. [42] demonstrated that this problem can be avoided by adding water after the enrichment step to improve compatibility with the separation of polar compounds. In their study, a multiresidue method for the analysis of 88 polar organic micropollutants (with a broad range of physicochemical properties: log $D_{pH\,7.4}$ ranging from -4.2 to 4.2) in ground, surface and

wastewater using on-line mixed-bed multilayer SPE coupled to HPLC-MS was used. The majority of the compounds (~ 80%) were quantified below 10 ng/l in groundwater and surface water and below 100 ng/l in wastewater using a sample volume of 20 ml. The method showed good relative recoveries.

Major drawbacks of SPE are for example limited sorption capacity and clogging of sorbent pores by suspended particles/matrix compounds. An alternative extraction mode that prevents these problems is dispersive SPE (d-SPE). It provides a large active surface for sorption. Recently, many novel materials were developed. Cai et al. [43] showed a successful application of vortex-assisted dispersive micro-SPE based on a novel porous metal organic framework for the determination of amphenicols and the metabolite in aquaculture water. Under optimal conditions, the relative recoveries were > 70%. Since d-SPE requires two centrifugation steps, automation of the technique is difficult, thus may not be suitable for higher throughput. A further development of d-SPE is magnetic SPE (m-SPE) using sorbents with superparamagnetic properties and high adsorption capacity, so that filtration or centrifugation steps can be avoided. Among the most recent functionalized magnetic materials are magnetite (Fe_3O_4) nanoparticles coated with silica, different polymers, nanomaterials and ionic liquids [44]. In a study of Luo et al. [45], a magnetic composite made of graphene and Fe_3O_4 @ SiO_2 was prepared by simple adsorption. It was used as an extraction medium for the effective and efficient enrichment of six sulfonamide antibiotics in environmental water samples. However, SPE cannot be regarded a green method given its relatively high solvent consumption.

Another mode of SPE is solid-phase microextraction (SPME). It is fast, versatile, sensitive and solvent-free. The isolation and preconcentration of the analytes occur in a single step, providing a simple sample preparation. In its most popular configuration, the SPME device consists of a fused-silica rod coated with a thin layer of a suitable polymeric coating (e.g. polydimethylsiloxane, polyacrylate and carbowax). Since its introduction in 1990 by Pawliszyn [46], SPME applications significantly broadened also for the analysis of environmental samples [47-49]. Aresta et al. [50], for example, developed an SPME-LC-UV method for the determination of the polar antibiotic chloramphenicol in urine and environmental water samples. For SPME, polar carbowax fibers were used and provided sufficient extraction recoveries. However, SPME was shown to be less sensitive compared to SPE [51, 52]. Carbon nanotubes (CNTs) gained great interest [48], especially multi-walled CNTs with multiple layers of graphene [53] with their large surface-to-volume ratio and increased loadability. The extraction of non-polar, polar and even ionic species is possible via both hydrophobic and ionic interactions [48], e.g. for the analysis of polar sulfonylurea herbicides in environmental water samples [54]. Recent SPME approaches also focused on a lower ecological impact [55, 56].

As well as SPME, microextraction by packed sorbent (MEPS) is an equivalent to SPE and can be expected to become a very promising sample preparation technique in the future for several reasons: it is fast and simple to use, it can be fully automated, it can cope with much smaller sample volumes than full-scale SPE (as small as 10 µl), which is of interest especially for the analysis of e.g. plasma, urine or biota samples like insects. MEPS sorbents can be used more than 100 times (even for complex samples). MEPS uses the same sorbents as conventional SPE in cartridges. Thus, downscaling of most existing

SPE methods is possible. In MEPS, 1-4 mg sorbent are either inserted into the syringe (100-250 µl) as a plug or between the needle and the barrel in a cartridge. Sample extraction, enrichment and clean-up are accomplished directly on the packed sorbent [57]. The number of extraction cycles can be increased by drawing and ejecting the sample through the needle into the syringe several times (draw-eject), leading to a higher recovery [58]. Another key aspect of MEPS is the small solvent volume used for the elution of the analytes, which makes it good choice for on-line coupling with LC [59] and CE [60] separations. Mostly, pharmaceuticals in wastewater were analyzed in environmental applications [61]. Morales-Cid et al. [60] demonstrated a new and innovative way to integrate MEPS into commercial CE equipment. This method provided automated sample clean-up and preconcentration from only a few microliters of sample, which is interesting in biota analysis. The robustness of the proposed technical implementation was demonstrated by the use of a (MEPS)-non-aqueous capillary electrophoresis (NACE)-MS method used to determine the very polar fluoroquinolones in urine. The detection limits (LODs) were in the range of 6.3 – 10.6 µg/l and absolute recoveries were in the range of 71-109%.

2.3.3 Dispersive liquid-liquid microextraction

As a mode of liquid-liquid extraction, dispersive liquid-liquid microextraction was introduced by Rezaee et al. [62] for the extraction and preconcentration of organic analytes from water samples. A dispersed liquid phase is used to facilitate extraction from mostly small volumes (tens of µl range) of extraction solvent by fast equilibration due to the increased interfacial surface area between sample and extraction solvent. Many combinations with other sample preparation methods like SPE, single-drop microextraction or dispersive liquid-liquid microextraction itself allowed the purification and enrichment of a broad range of analytes (pharmaceuticals, pesticides, personal care products) in different samples (environmental samples, food, biological fluids) [63]. For hydrophilic compounds, recoveries have to be further improved. So far, the main strategy for the extraction of vPICs is compensating poor recoveries by high enrichment factors [64]. However, optimizations strategies such as using ionic liquids as extraction solvents and ultrasound assistance in the extraction process led to the successful extraction of the polar fluoroquinolones (7 out of 8 with log P < 1) in groundwater samples [65]. In order to enable automated methods, there are new approaches to omit the dispenser solvent which could eliminate the centrifugation step and enable higher throughput [66].

2.3.4 QuEChERS extraction

According to the current trend in analytical chemistry to develop environmentally friendly methods, QuEChERS extraction has become increasingly popular in many fields [67]. The extraction method was originally developed by Anastassiades in 2003 [68] to determine pesticides in fruits and vegetables. Since then, the method has been optimized and adjusted for different analytes and environmental matrices. E.g. QuEChERS was used to extract pharmaceuticals from sewage and surface water [69], drinking water, treatment plant sludge [70], soil [71], invertebrates [2] and fish tissue [72, 73]. The method is based on liquid-liquid extraction with mainly acetonitrile (partly also acetone or ethyl acetate) and

water, often followed by a d-SPE for cleanup. Due to the miscibility of acetonitrile and water, a mixture of salts (NaCl and MgSO$_4$) must be added to induce phase separation [68]. The ratio/volume of solvents and salts is used to optimize phase polarities and thus extraction efficiencies. For highly polar compounds, methanol can be added to enhance the recovery: for the quantification of quinolones and tetracyclines from fish tissue an extraction solution based on a mixture of acetonitrile and methanol (75:25, v/v) resulted in relative recoveries ranging from 69% to 125% [74]. In contrast to food samples, the size and quantity of environmental biota samples is often limited. Therefore, the sample extraction techniques originally developed for food analysis, have to be adapted. Often, miniaturization is necessary for invertebrate samples [2], for example, carbamazepine and fluoxetine were quantified in single individuals of benthic invertebrates with relative recoveries > 85% [72]. Many non-polar and fatty compounds present in the mollusk matrix were removed using hexane as a third liquid phase during extraction. Overall, with its simplicity, environmental sustainability and its compatibility with all relevant separation techniques, we suppose QuEChERS extraction to be increasingly applied in the future. However, we expect that not all vPICs can be extracted with acceptable efficiency.

2.3.5 Electric field-driven sample preparation

There are new approaches using electric fields as auxiliary force to accelerate mass transfer of ionic analytes during extraction. Among them, electromembrane extraction (EME) has probably gained highest attention so far due to its simple setup. Introduced in 2006 by Pedersen-Bjergaard et al. [12], the usually aqueous sample and acceptor solutions are separated by a membrane, which can either be a supported liquid membrane (SLM) or a polymer-imprinted membrane. Application of an electric field across the two compartments results in migration of analytes according to their charge and electrophoretic mobility (both in the donor and acceptor solution but also in the membrane). This strategy has three benefits: (1) by using a smaller acceptor solution volume, enrichment of the analytes occurs together with (2) a clean-up from non-charged and oppositely charged matrix compounds, and (3) selectivity tuning by the membrane composition is possible (see below). This approach is only applicable for the extraction of ionizable and ionic compounds from various liquid samples or extracts. High matrix tolerance and compatibility with common analytical techniques like LC, GC and CE have already been demonstrated [75]. Selectivity regarding the polarity of compounds can be tuned with different membrane compositions. In 2014, for example, Koruni et al. [76] presented the simultaneous extraction of both acidic and basic drugs over a broad range of polarities using two SLMs of different composition. However, further improvements to also target highly polar charged compounds are necessary and are addressed in current research [77]. In principle, EME is very environmentally friendly and potentially automatable, so we expect increased attention in the future, especially for water analysis. For extracts of biota or soil samples, this method is not (yet) established as mostly organic solvents are used for extraction. One possibility may be to evaporate the organic solvent and reconstituting the residue in water. Further research needs to address shortcomings such as low speed, low degree of automation, sensitivity and recovery. Most studies so

far used optimized methods for selected analytes, they have not yet been implemented for screening purposes.

2.4 Chromatographic techniques

In this chapter we focus on trends in chromatographic techniques especially useful for the analysis of vPICs or for a broad analyte coverage in environmental samples, such as HILIC, SFC and MMLC. Their advantages, disadvantages and application to environmental samples are elaborated.

2.4.1 Hydrophilic interaction liquid chromatography

In the last decade, HILIC-MS established itself as a valuable complementary approach to RPLC for the determination of highly hydrophilic, polar and ionic compounds. This is also confirmed by the increase of HILIC applications [20] in various fields such as biology [78], food [79] and environmental science [39, 80]. Based on a combination of a polar stationary phase with a low aqueous and high organic content in the mobile phase, HILIC is able to improve chromatographic retention, resolution and thus sensitivity for polar compounds [21], which may otherwise elute in or close to the void volume in RPLC. Further advantages over RPLC are higher applicable flow rates due the high organic content of the mobile phase and hence its lower viscosity. It is well suited for large volume injections of extracts with high organic content, often of interest in biota analysis. For the same reason, HILIC is also well compatible with on-line SPE as demonstrated by Fontanals et al. [32] with their first fully automated method based on on-line SPE coupled to HILIC-MS to determine a group of polar drugs and pharmaceuticals (log $D_{pH\ 7}$ ranging from -1.8 to 1.4) in environmental water samples. The method had analyte recoveries near 100% and LODs $\leq$ 2 ng/l for most of the compounds. However, the high organic content of the mobile phase is a disadvantage when water samples are analyzed: the direct injection of large volumes of water as routinely done in RPLC (up to 100 µl) is not possible because of the high elution strength of water in HILIC [81]. Instead, dilution to ca. 80% acetonitrile is often required, significantly increasing LODs. In environmental analysis, HILIC was applied for the targeted analysis of polar herbicides [82], pesticides [83] and pharmaceuticals, such as antibiotics [28], drugs of abuse [32], cytostatics [84], antidiabetics [39, 85] and contrast agents [86, 87]. HILIC was successfully used as a complementary method to RPLC for the non-target screening of emerging polar organic compounds in wastewater [88]. To further extend the applicability of HILIC to a wider range of pharmaceutical compounds, various new HILIC stationary phases may be applied. Silica-based materials, in particular bare and amide-bonded silica, zwitterionic and diol stationary phases, remain by far the most widely used stationary phases for HILIC in environmental applications with MS-compatible mobile phases [21]. In terms of green chemistry, HILIC is surely not advantageous due to the large amount of acetonitrile needed, necessitating a search for eco-friendlier alternatives. An example was given by dos Santos Pereira et al. [89], who demonstrated that biodegradable ethanol successfully replaced acetonitrile in the separation of vPICs. Another possibility to reduce the amount of organic solvents could be miniaturization of the analytical column, which is already a trend in bioanalysis [90].

However, this may be at the cost of a lowered sample loadability and is thus an option for biota but not for water analysis. Overall, we expect HILIC applications to increase as its polarity range almost ideally complements RPLC analysis (see Figure 2-2), while the same equipment can be used. Multidimensional applications combining RPLC and HILIC are discussed in Section 2.6.

2.4.2 Supercritical fluid chromatography

In recent years SFC experienced a significant revival due to improvements in instrumentation, resulting in higher reliability and robustness [91]. Moreover, the advent of sub-2-µm particles and superficially porous particles in the stationary phases encouraged the use of UHPSFC [5]. This gave rise to a further improvement of resolution and faster analyses, however, without the need for high pump pressure as encountered in ultra-high-performance LC. Hyphenation to MS is increasingly used, which opened the way to new application fields such as bioanalysis, omics sciences, plant, food, and environmental analyses [91]. The mobile phase of modern SFC usually consists of compressed carbon dioxide, making it a "green method" [92]. Small volumes of modifiers such as methanol are added to tailor selectivity addressing different polarity ranges and optimize resolution. Regarding stationary phase chemistries, a large variety of stationary phases, from the most polar silica to the least polar well-endcapped or densely bonded alkyl-bonded silica, is now available, which enables to tailor selectivity [5, 93].
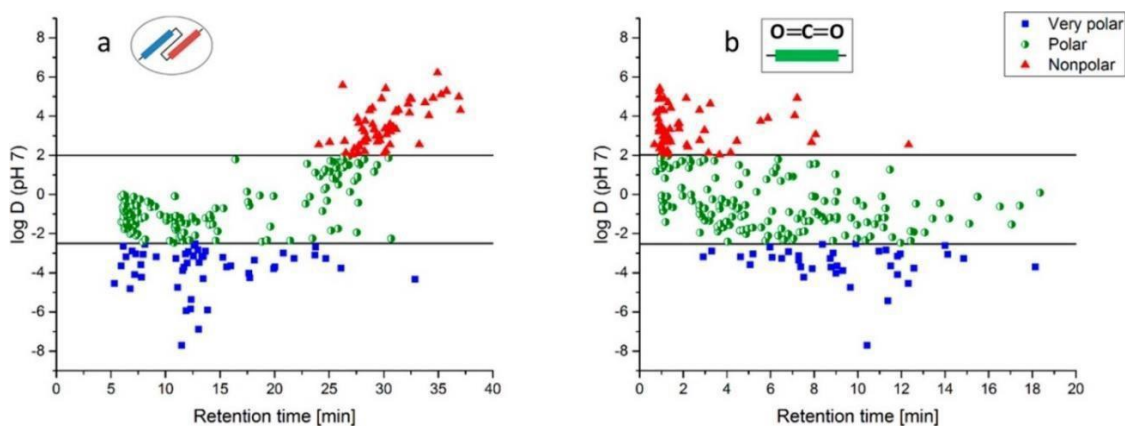
Figure 2-3: Plots of log $D_{pH\ 7}$ vs. Retention time of standard compounds analyzed by RPLC-HILIC-TOF-MS (a) and SFC-TOF-MS (b). Very polar compounds (log D < -2.5, blue rectangles) are mainly retained by HILIC in the RPLC-HILIC coupling, while nonpolar compounds (log D > 2.0, red triangles) are exclusively retained by RPLC. Polar compounds are retained in both, HILIC and RPLC, but retention in HILIC seems to be more likely with increased polarity. In SFC (b), nonpolar compounds are retained less than very polar compounds. The retention patterns in the RPLC-HILIC coupling (a) show two groups that represent HILIC- (RT < 16 min) and RPLC- retained compounds (RT > 16 min). Compound log D increases with RT in RPLC, while the opposite occurs in HILIC. This retention behavior known from normal phase LC can partly be observed in SFC separations, too. (b). Reprinted with permission from [92]. © 2020 American Chemical Society

In a seminal paper, two chromatographic separation strategies were compared, a serial RPLC-HILIC coupling vs. SFC [92]. For SFC, a zwitterionic HILIC column and a binary gradient of CO_2 and 20 mM ammonium acetate in methanol (modifier) was used. Both systems were able to retain nearly all the 274 environmentally relevant compounds with very different polarities (log $D_{pH\ 7}$ ranging from -7.7 to 7.7) providing a more comprehensive analysis than common RPLC-MS (see also Figure 2-3). Such at least partially orthogonal methods can be used for cross-validation.

2.4.3 Mixed-mode liquid chromatography

Mixed-mode stationary phases are gaining attention as more and more applications are published and new commercial columns appear on the market [94]. The main advantage of MMLC is that it provides more than one type of interaction between the stationary phase and the analytes, allowing the simultaneous determination of compounds with a wide range of physicochemical properties (e.g. ionic, basic, acidic and neutral chemicals, or hydrophilic and hydrophobic) in one run [95, 96]. The three most common types of MMLC are RP-ion exchange, HILIC-ion exchange, and RP-HILIC [97], which extends the application range of these methods but partially also combines their weaknesses and drawbacks [5]. Stationary phases are silica- or polymer-based, different hybrid and monolithic mixed-mode stationary phases are available [98]. The particle size of the current commercial sorbents is usually in the range of 3-7 µm and the stationary phases are synthesized on fully porous particles. In the near future, it can be expected that commercial sub-2-µm particles and superficially porous materials will be developed. This will lead to better separation efficiency and analysis time. Initially, mixed-mode columns were applied in bioanalysis, but their application was expanded to a variety of fields, including pharmaceutical analysis [99], metabolism studies [100, 101] and recently also to environmental analysis [102-107]. González-Mariño et al. [107] described the first application of RP-ion exchange mixed-mode LC for the determination of drugs of abuse in wastewater. MMLC was shown to be a good alternative to traditional RPLC and HILIC for the separation of vPICs. Montes et al. [106] used a targeted MMLC-MS for the quantitative determination of 23 persistent and mobile organic contaminants (log $D_{pH\,7}$ ranging from -3.7 to 3.4) in surface and drinking water samples. In comparison to RPLC, MMLC proved superior in both retention and peak shape for ionic compounds, while also performing well for neutrals. In contrast to HILIC, the mobile phase of MMLC has a high aqueous content (as in RPLC), therefore it is well suited for the direct injection of water samples. Further advantages of MMLC include the higher flexibility in adjusting separation selectivity and the possibility to use the mixed-mode sorbent in different elution modes [98]. MMLC can thus be an alternative to 2D applications. Beside many benefits, there are also some drawbacks related with these stationary phases. For example, when more than one type of interaction is active, asymmetric signals may evolve and thus reduced separation efficiency. Furthermore, method development has to consider the different separation modes and counteracting effects of optimization parameters may complicate this process. This necessitates compromises in separation performance, when analytes with a broad range of physicochemical characteristics are included. Additionally, Zahn et al. [5] indicated some limitations for RP-ion exchange columns, which are similar to the two retention mechanisms: poor retention of polar but neutral compounds and additionally the reliance on high electrolyte concentrations in the eluent to elute strongly retained ionic compounds which may cause detrimental effects in ESI [105]. However, with new mixed-mode stationary phases appearing on the market, MMLC-MS can be tailored to the polarity range of interest for specific questions and may be ideal for targeted or semi-non-target screening of classes of compounds.

2.4.4 Ion chromatography

IC as a special mode of LC has already proven to be a powerful tool for the analysis of ionic compounds, mostly inorganic anions and cations in water samples and biological fluids [108] as well as small organic compounds in a broad range of sample types such as milk [109] or biological fluids [110], but also environmental samples [111]. For reliable IC analysis, for example of wastewater treatment effluents, sample preparation is often mandatory given the high matrix (salt) load of many environmental samples (see Section 2.3.1). Zakaria et al. [112] listed three major strategies for sample pretreatment:

1) samples may be purified by suitable ion exchange resins, for example silver cartridges for the removal of chloride [113], 2) use of sensitive methods like inductively coupled plasma (ICP)-MS after strongly diluting the samples [114] or 3) use of high capacity columns to increase loadability [115]. We see an additional possibility in the use of electric fields (see Section 2.3.5) as both, sample preparation and separation method require charged analytes. An EME-IC system for the analysis of inorganic anions was presented [116]. Another option is the use of 2D-IC techniques [117] (see also Section 2.6), as applied e.g. for the analysis of bromate, chlorate and five haloacetic acids in water [118]. Similar trends as in LC towards higher pressure and smaller particle sizes (see above) can be expected for IC to reach higher separation efficiencies and lower detection limits.

The successful analysis of acidic pharmaceuticals in biological fluids using IC with sensitive fluorescence detection after labeling was reported by Muhammad et al. [110]. A further increase in sensitivity is obtained when coupling IC with MS [119] upon further improvements of the interfaces. Recently, Stoll [6] summarized the state of the art of IC-MS. Limitations of current IC(-MS) instrumentation especially for (semi-)screening methods include the rather long column equilibration times and possible signal quenching by interactions of analytes with suppressors [120]. Publications in the field show a limited choice of suitable eluents as they must have a suitably high elution strength while being MS-compatible. Limitations for both ICP-MS and electrospray ionization (ESI)-MS were reported, describing decreased sensitivity in ICP-MS by using carbonate/bicarbonate eluents without a suppressor as a result of contamination of skimmer cones [121] and a general signal suppression in ESI due to high concentrations of eluents [122]. Overall, improvements with optimized elution buffers [122] as well as instrumentation and system design [123] are still subject to current research. Another approach is the reduction of the column inner diameters to 0.4 mm [124] or to use an organic make-up solvent such as acetonitrile or isopropanol [125] to increase MS sensitivity.

The two major MS interfaces used for IC are ICP and ESI. Whereas IC-ICP-MS is suitable for elemental analysis in a broad range of different samples including for example organic compounds with halogen substituents, IC-ESI-MS enables to analyze low molecular mass organic compounds. The general advantages of ICP-MS for different environmentally relevant pollutant species (e.g. pharmaceuticals, flame retardants, pesticides, …) were worked out nicely by Pfröfrock and Prange [126]. With ICP-MS, the detection and selective screening of different molecules containing covalently bound (hetero-)elements such as phosphorus, arsenic or halogens is possible. Sacher et al. [127], for example, developed an IC-ICP-MS method for iodinated X-ray contrast agents in

surface water. Whereas a full non-target screening cannot be reached with IC-ICP-MS, it may be possible to target sulfur species in a screening approach, interesting to study the transformation of pharmaceuticals and pesticides to sulfur- or phosphor-containing species, for example, metolachlor with charged transformation products [128]. In addition, quantification is possible without internal standards, if the stoichiometry is known [129, 130]. Especially the complementary combination of ICP-MS for screening and ESI-MS for identification is an interesting approach [131, 132], which will likely be applied more often in the future.

Speciation analysis by IC-ICP-MS for environmental analysis was summarized in a book edited by Michalski [133]. For biota, the potential of IC-ICP-MS has already been exploited for the detection of arsenic and selenium species in fish tissue by Reyes et al. [134] but to our knowledge not yet for pharmaceuticals. IC-ICP-MS with its high selectivity will be of future interest especially for targeted or selective screening approaches in samples of high matrix load such as biota samples. Generally, this can enable a broader screening of vPICs and their transformation products in biota, especially for compounds with iodine or bromine, which are rare in biological samples.

Successful applications of IC-ESI-MS for the analysis of environmental samples show the increasing interest for the analysis of pesticides in food samples. Polar pesticides being charged over a broad pH range like glyphosate, ethephon [122] or paraquat [135] were successfully analyzed in food samples by IC-ESI-MS/MS. In environmental samples, this technique is mostly applied for the analysis of inorganic anions and cations as well as small organic acids [136]. However, in recent years, there has been progress in the analysis of polar pesticides in environmental waters by IC-MS. Glyphosate and two of its metabolites (all log P < -2) were successfully analyzed in surface and drinking waters reaching LODs in the low ng/l range [137]. The analysis of haloacetic acids in drinking water was also successful [138], which is very fortunate given the new regulations in the European Union (Water Framework Directive, WFD, 2000/60/EC) requiring the sensitive analysis of these compounds. We expect further applications for the analysis of wastewater micropollutants and semi-targeted screenings, as they already proved valuable in forensic analysis of gunshot residues [139].

2.5 Electromigrative separation techniques

Electromigrative separation techniques like CE are an alternative to IC for the analysis of ionic or ionizable micropollutants. The general applicability and potential of CE in environmental analysis was shown in numerous applications of pesticide analysis summarized in recent reviews [140, 141]. The use and state of the art of CE analysis of various pharmaceuticals in environmental samples was described by Hamdan in 2017 [142]. Electromigrative separation techniques like CE are an alternative to IC for the analysis of ionic or ionizable micropollutants. The general applicability and potential of CE in environmental analysis was shown in numerous applications of pesticide analysis summarized in recent reviews [140, 141]. The use and state of the art of CE analysis of various pharmaceuticals in environmental samples was described by Hamdan in 2017 [142].

Whereas CE is already well established for the analysis of small molecules in human body fluids [143], the use of electromigration separation techniques for the analysis of vPICs in environmental samples is still challenging. The loadability for the commonly used capillaries of only 50 µm inner diameter is limited and often gives rise to relatively high detection limits. This can be overcome improving sample preparation and enrichment methods dedicated to CE, e.g. sample preparation using on- or off-line SP(M)E, see Hamdan [142]. On-line enrichment is possible via large volume sample stacking [14], field-amplified sample injection [144] and (transient) isotachophoresis [15, 145]. Off-line electro-driven enrichment techniques like EME are gaining more and more popularity [146] and their hyphenation with CE for the analysis of environmental samples was reported [147], see also Section 2.3.5. There are optimized CE-diode array detection (DAD) methods which reach detection limits in the medium ng/l range [148], however, these are rather exceptional. More often, MS [149] and sometimes fluorescence detection [150], mostly after derivatization [151], are used.

As for LC, MS is the detection method of choice for non-target screenings, but today, most CE-MS methods are still established in research laboratories only, although 1) there are less restrictions compared to IC-MS hyphenation (for example eluent composition) and 2) ESI-MS-interfaces compatible with both LC and CE separation systems are available. In addition, solvent consumption is low compared to chromatographic techniques, which makes CE and CE-MS interesting as "green" alternatives. Although many CE(-MS) methods barely reach detection limits below 1 µg/l [142], there are already promising approaches combining CE-MS with different sample preparation methods [152, 153]. Additionally, an enrichment free approach was recently published by Höcker et al. [154] enabling the analysis of anionic micropollutants like haloacetic acids and halomethane sulfonic acids in drinking water, reaching LOQs between 30 and 500 ng/l.

CE was shown to be well suited for the analysis of biological fluids, but there are only few examples for its use in biota analysis: Deng et al. [155] analyzed the polar antibiotic tetracycline in crucian carp muscle using electrochemiluminescence detection. Sun et al. [156] analyzed sulfonamides in shrimp, sardine and anchovy with DAD. Both methods reached detection limits in the µg/l range. Coupling CE to sensitive MS detection even led to detection limits in the upper ng/l (low ng/g) range for the analysis of the anti-diabetic drug metformin in fish without sample preconcentration [157], requiring only small sample volumes, which enabled analyzing individual fish organs.

2.6   2D applications

The aim of 2D approaches are: 1) maximum sample information, the comprehensive analysis of micropollutants over a broad range of physicochemical characteristics (today mostly polarity) for non-target analysis. For this, RPLC-HILIC has already been established by Bieber et al. [92]. Similar approaches are well known in peptide analysis [158]. 2) With 2D techniques peak capacity can be increased using ideally orthogonal separation selectivity in the second dimension. The two separation dimensions can either be coupled consecutively or by heart-cutting selected zones to enhance resolution and minimize matrix effects, e.g. comprehensive couplings of ICxRPLC [159] or ICxCE [160].

Chromatographic and electromigration separations were successfully combined in bioanalysis [161]. 3) The first dimension may also be used as a clean-up step as shown for IC-IC by Zakaria et al. [112] using the first dimension to eliminate inorganic salt components prior to the quantification of bromate in sea water samples. Although LODs of only 60 µg/l of bromate were obtained, this approach might also be interesting for the analysis of pharmaceuticals in environmental samples containing high concentrations of salt using IC with sensitive MS detection. Possibly, additional preconcentration and desalting steps, e.g. using SPE are necessary to meet the required detection limits.

It has to be noted, that comprehensive applications are generally limited by the first dimension with regard to polarity or charge. Improved instrumental setups for hyphenation and testing some of the new materials available today (for example MMLC stationary phases, see Section 2.4.3) can result in increased matrix tolerance and higher sensitivity for complex samples. Stevenson et al. [162] developed an off-line 2D-LC separation of a β-lactoglobulin tryptic digest with the same mixed-mode stationary phase in both dimensions. In the first dimension, the mobile phase pH was 7, while it was adjusted to pH 2 in the second dimension evoking different separation mechanisms. Greater separation efficiency was observed for the mixed-mode column in comparison to classical C18, thereby providing larger peak capacity than the C18 column. Similar applications will be of interest in environmental analysis. With the advent of commercial equipment for 2D applications, its application in environmental analysis will surely rise, though merely for research than for routine analysis. A major limitation is the data evaluation, where further software developments are required.

2.7   Summary on future perspectives

The impressive development of new analytical methods enabled the analysis of many vPICs in environmental samples. These developments comprise new materials, instrumentation, miniaturization and automation both for sample preparation and separation. In this article, we showed that some current trends are partly due to a revival of methods such as SFC, partly due to the use of developments from other fields such as QuEChERS extraction from food science, and MMLC from pharmaceutical analysis or some 2D applications from bioanalysis. In the following, we want to summarize future perspectives.

Due to the high demand for improved limits of detection and selectivity, many new SPE materials for vPICs were commercialized but none of the sorbents available can cover the whole range of compounds. Especially, the retention of very polar analytes is still an issue. Both mixed-bed SPE and EC were shown to also cover very polar compounds. However, only a few mixed-bed cartridges are commercially available and EC does not include a sample clean-up. New materials like carbon-based nanomaterials can be used to improve the extraction efficiency but they are mostly suitable only for target analysis or specialized applications.

For ionic and ionizable compounds, we expect electro-based enrichment techniques to find applications beyond inorganic ions [116], especially for the analysis of ionic or ionizable pharmaceuticals in environmental samples. For electro-based enrichment

techniques, further effort is required to achieve an acceptable degree of sample throughput by automation and miniaturization for both monitoring strategies and (eco)toxicological research. For matrix removal, these developments are believed to be prioritized compared to on-line sample pretreatment and 2D approaches.

We are convinced that HILIC will complement RPLC routine analysis as the expertise for liquid chromatography is high and implementation is straightforward. Future research will show which stationary phases will become the gold standard in the future. SFC research is very active and due to the development of modern instrumentation, reproducible results are obtained today. In the pharmaceutical industry, SFC can already replace RPLC as a routine technique for the separation of chiral substances on a preparative scale [163]. In environmental analysis, the actual potential of SFC can only be estimated, since applications are still rare. However, it is anticipated that SFC may partly replace RPLC, as a wider polarity range is covered, even when compared to 2D techniques such as RPLC-HILIC. SFC may then become a suitable tool also for monitoring campaigns. Thus, it will be interesting to see if 2D techniques will find more application in environmental analysis as currently seen in bioanalysis, especially peptide analysis. While instrumental developments led to the commercial availability of dedicated instrumentation for comprehensive 2D-LC, software tools still show limitations. Possibly, MMLC will open up new possibilities in 2D separation methods, when used as a first dimension with a broad analyte coverage. We see a great potential in MMLC since it improves the separation of vPICs (both basic and acidic) while also retaining neutral chemicals. MMLC thus combines the benefits of different chromatographic modes. Manufacturers of stationary phases also reacted with increased production of MMLC stationary phases.

Finally, attractive alternatives for ionizable compounds, also with regard to "green chemistry" are IC-MS and CE-MS. However, environmental CE-MS applications afford more research for analyte enrichment and IC-MS applications for improved stationary phases for a greater choice of MS-compatible eluents. It is difficult to judge if CE-MS with a lower instrumental requirement than IC-MS will be implemented in laboratories dominated by chromatographic expertise.

In our opinion, the gap described in 2016 by Reemtsma et al. [19] for the analysis of persistent and mobile organic compounds still exists. With the latest developments in analytical chemistry, filling this gap seems feasible. However, most methods which are well suited have not yet left laboratory scale applications so that their applicability in monitoring campaigns remains to be shown. Establishing new analytical processes in general is a time-consuming process for laboratories. Acceptance by the community and regulatory bodies is another hindrance. Often, modified or optimized established methods are accepted more quickly and are easier to implement with regard to existing instrumentation and expertise. However, with the slow implementation of new methodology, chances are missed to increase efficiency, scope, matrix tolerance, environmental friendliness, etc.

All in all, however, we have to keep in mind, that no method is capable to fulfill all requirements from environmental science and (eco)toxicology given the wealth of

compounds with their broad range of physicochemical characteristics. New strategies have to find compromises between different needs, e.g. analyte coverage, matrix compatibility or analysis time and costs. Additionally, other drivers like automation, miniaturization in biota analysis and organic solvent consumption have to be considered for current and future developments for the analysis of vPICs.

2.8 Supporting information

The here presented Supporting Information contains a table presenting a non-comprehensive, alphabetically ordered list of 237 compounds with log P values ≤ 1 analyzed in 63 cited articles. Research and review articles with more than 40 analyzed/listed compounds were excluded. All properties (pK$_a$ values, log P and log D values and charge state) were calculated with Chemicalize provided by ChemAxon. The column "function" contains one of the main uses from which the pie chart in Figure 2-1B was generated.

Table S2-1: Non-comprehensive, alphabetically ordered list of 237 compounds with log P values ≤ 1 analyzed in 63 here cited articles. Research and review articles with more than 40 analyzed/listed compounds were excluded. All properties (pK$_a$ values, log P and log D values and charge state) were calculated with Chemicalize provided by ChemAxon (10/05/2020).

analyte	strongest		log P	log D$_{pH}$			charge number at pH 7.4	function
	acidic pKa	basic pK$_a$		1.7	7.4	8.0		
2′,2′-difluoro-deoxyuridine	9.9		-1.1	-1.1	-1.1	-1.1	0.0	human metabolites
2-phenyl-5-benzimidazole-sulfonic acid	-2.2	4.9	-0.1	-0.1	0.1	0.1	-1.0	UV filter
2-phenylbenz-imidazole-5-sulphonic acid	-2.2	4.9	-0.1	-0.1	0.1	0.1	-1.0	UV filter
3,4-dihydroxy-phenylacetic acid	3.6		1.0	1.0	-2.3	-2.5	-1.0	human metabolites
3-methylphosphinico-propionic acid	2.0		-1.3	-1.5	-6.2	-6.7	-2.0	pesticide metabolite
4-acetamido-antipyrine	12.5	-0.8	0.2	0.2	0.2	0.2	0.0	drug metabolites
4-formylamino-antipyrine	12.7	-0.8	0.1	0.1	0.1	0.1	0.0	drug metabolites
4-methylamino-antipyrine		1.2	0.8	0.6	0.8	0.8	0.0	drug metabolites
4-methylthiosemi-carbazide	14.1	3.9	-0.6	-2.7	-0.6	-0.6	0.0	intermediate compound
5-fluorouracil	7.2		-0.7	-0.7	-1.1	-1.5	-0.6	cytostatics
6-acetylmorphine	10.2	9.0	0.9	-2.3	-0.4	0.2	1.0	drug metabolite
abacavir	15.4	5.8	0.4	-1.6	0.4	0.4	0.2	nucleoside reverse transcriptase inhibitors
abacavir carboxylate	3.8	5.8	-1.2	-1.3	-2.5	-2.7	-0.8	drug metabolite
acephate	10.5		-0.3	-0.3	-0.3	-0.3	0.0	insecticide
acesulfame	3.0		-0.6	-0.6	-1.5	-1.5	-1.0	artificial sweetener
acetaminophen	9.5		0.9	0.9	0.9	0.9	0.0	analgesics and antipyretics

Introduction: Trends in sample preparation and separation methods for the analysis of very polar and ionic compounds in environmental water and biota samples

analyte	strongest acidic pKa	basic pKₐ	log P	log D$_{pH}$ 1.7	7.4	8.0	charge number at pH 7.4	function
acetic acid	4.5		-0.2	-0.2	-3.0	-3.4	-1.0	intermediate compound
acrylamide	0.0		-0.3	-0.3	-0.3	-0.3	0.0	intermediate compound
acyclovir	12.0	3.0	-1.0	-2.1	-1.0	-1.0	0.0	antiviral
amidosulfuron	3.2	2.5	-1.2	-1.8	-1.7	-1.7	-1.0	herbicide
amikacin	12.2	9.6	-8.6	-20.7	-15.1	-12.9	3.8	aminoglycoside antibiotics
aminopyralid	1.1	5.0	0.3	0.2	-1.8	-2.0	-1.0	herbicide
amoxicillin	3.2	7.2	-2.3	-3.0	-2.7	-3.0	-0.6	β-lactam antibiotic
AMP[1]	1.2	3.9	-4.8	-4.5	-5.8	-6.3	-2.0	nucleotide
AMPA[2]	1.9	9.4	-2.3	-2.5	-3.2	-4.3	-1.0	pesticide metabolite
ampicillin	3.2	7.2	-2.0	-2.7	-2.4	-2.7	-0.6	penicillin
ascorbate	4.2		-1.3	-2.1	-4.8	-4.9	-1.1	vitamin
aspartame	3.5	8.5	-2.2	-3.0	-2.3	-2.3	-0.1	artificial sweetener
atenolol	14.1	9.7	0.4	-2.8	-1.8	-1.2	1.0	beta blocker
atrazine-hydroxydesethyl	12.6	5.6	1.0	-0.8	1.0	1.0	0.0	pesticide metabolite
azide	5.1		0.1	0.0	-0.2	-0.2	-1.0	intermediate compound
barbitone	7.5		0.7	0.7	0.5	0.1	-0.5	hypnotic
bentazon	2.0		0.8	0.6	-0.2	-0.2	-1.0	herbicide
benzene-sulfonamide	10.2		0.6	0.6	0.6	0.6	0.0	intermediate compound
benzoylecgonine	3.2	9.5	-0.6	-1.3	-0.6	-0.6	0.0	drug metabolites
bromate	1.3		0.2	-0.4	-2.2	-2.2	-1.0	inorganic anion
bromide	-8.0		0.8	1.0	1.0	1.0	-1.0	inorganic anion
bromochloro acetic acid	2.0		0.8	0.6	-2.8	-2.8	-1.0	disinfection byproduct
bromomethane sulfonic acid	-2.1		0.0	-2.4	-2.4	-2.4	-1.0	disinfection byproduct
butyric acid	4.9		0.9	0.9	-1.5	-2.0	-1.0	industrial chemical
caffeine		-1.2	-0.6	-0.6	-0.6	-0.6	0.0	psychoactive drug
cAMP[3]	1.8	3.9	-3.4	-3.3	-3.7	-3.7	-1.0	second messenger
carbonate	3.5		0.3	0.2	-3.1	-3.2	-1.0	other
cCMP[4]	1.8	4.2	-2.0	-2.3	-4.3	-4.4	-1.0	second messenger
cefadroxil	3.3	7.2	-2.5	-3.2	-2.8	-3.2	-0.6	β-lactam antibiotic
cefoperazone	3.2	-2.0	-0.9	-0.9	-4.4	-4.4	-1.0	β-lactam antibiotic
cefotaxime	2.7	3.6	-1.5	-2.0	-4.2	-4.2	-1.0	β-lactam antibiotic
cefradin	3.3	7.6	-2.5	-3.2	-2.6	-2.9	-0.4	β-lactam antibiotic
ceftiofur	2.5	3.5	0.1	-0.3	-2.5	-2.5	-1.0	β-lactam antibiotic
cefuroxime	3.0	-1.2	-0.9	-0.9	-4.4	-4.4	-1.0	β-lactam antibiotic
cephalexin	3.3	7.2	-2.1	-2.9	-2.5	-2.9	-0.6	β-lactam antibiotic
cephalosporin C	1.8	9.2	-4.4	-4.5	-7.6	-7.8	-1.0	β-lactam antibiotic
cephapirin	3.4	5.0	-2.1	-1.9	-4.2	-4.4	-1.0	β-lactam antibiotic
cephazolin	2.8	0.3	-1.5	-1.6	-5.0	-5.0	-1.0	β-lactam antibiotic
cGMP[5]	1.8	2.9	-2.1	-2.2	-4.3	-4.3	-1.0	second messenger
chloramphenicol	8.7		0.9	0.9	0.9	0.8	-0.1	broadband antibiotic
chlorate	4.6		0.0	0.0	-2.2	-2.3	-1.0	inorganic anion
chloride	-7.0		0.6	0.8	0.8	0.8	-1.0	inorganic anion
chlorite	-4.6		0.2	-2.2	-2.2	-2.2	-1.0	inorganic anion
chlormequat			-3.3	-3.3	-3.3	-3.3	1.0	pesticide
chloromethane-sulfonic acid	-2.3		-0.2	-2.6	-2.6	-2.6	-1.0	disinfection byproduct

analyte	strongest		log P	log D$_{pH}$			charge number at pH 7.4	function
	acidic pKa	basic pK$_a$		1.7	7.4	8.0		
chlortetracycline	7.0	6.2	-2.9	-3.6	-3.5	-4.0	-0.8	tetracycline antibiotic
choline	14.0		-4.7	-4.7	-4.7	-4.7	1.0	essential nutrient
chromate	-2.3		-3.7	-9.2	-8.2	-8.2	-2.0	inorganic anion
ciprofloxacin	5.6	8.8	-0.9	-1.7	-0.9	-0.9	0.0	fluoroquinolone
citrate	3.1		-1.3	-1.3	-9.5	-10.5	-3.0	organic acid
clindamycin-sulfoxide	12.3	7.5	-1.0	-4.5	-1.3	-1.1	0.5	drug metabolites
CMP[6]	1.8	2.9	-2.1	-2.2	-4.3	-4.3	-1.0	nucleotide
cyanate	-1.3		-0.5	-3.2	-3.5	-3.5	-1.0	other
cyanuric acid	5.6		1.0	1.0	1.0	1.0	0.0	intermediate compound
cyclamate	-0.8		0.6	-1.5	-1.8	-1.8	-1.0	artificial sweetener
cytarabine	12.6	4.2	-2.8	-4.7	-2.8	-2.8	0.0	cytostatics
danofloxacin	5.5	7.3	0.1	-1.6	-0.2	-0.6	-0.5	fluoroquinolone
desmethyl rantinidine		8.4	0.6	-2.7	-0.4	0.1	0.9	drug metabolite
dibromo acetic acid	1.6		0.7	0.4	-2.9	-2.9	-1.0	disinfection byproduct
dibromo butyric acid	2.8		0.9	0.8	-2.7	-2.7	-1.0	disinfection byproduct
dibromo methane sulfonic acid	-2.4		1.0	-1.3	-1.3	-1.3	-1.0	disinfection byproduct
dibromo propionic acid	2.5		0.8	0.7	-2.8	-2.8	-1.0	disinfection byproduct
diethanol amine	15.3	9.3	-1.6	-4.8	-3.4	-2.9	1.0	intermediate compound
diethyl amine		10.6	0.5	-2.7	-2.4	-2.0	1.0	intermediate compound
diethyl phosphate	2.0		0.5	0.3	-1.9	-1.9	-1.0	other
difluoro acetic acid	2.0		0.2	0.0	-3.3	-3.3	-1.0	disinfection byproduct
diisopropanol amine	15.0	9.6	-0.7	-4.0	-2.9	-2.3	1.0	intermediate compound
dimethyl amine		10.5	-0.2	-3.4	-3.1	-2.6	1.0	intermediate compound
diquat			-7.0	-7.0	-7.0	-7.0	2.0	herbicide
doxycycline	7.3	5.8	-3.3	-4.1	-3.7	-4.1	-0.6	antibiotic
DTPA-BMA-Gd	1.0	8.3	-8.7	-8.9	-12.5	-13.1	-1.9	contrast agent
emitricitabine S-oxide	14.0	1.4	-2.3	-2.5	-2.3	-2.3	0.0	pesticide metabolite
emtricitabine	14.3	1.7	-0.9	-1.2	-0.9	-0.9	0.0	nucleoside reverse-transcriptase inhibitor
emtricitabine carboxylate	3.3	1.5	-0.7	-0.8	-4.0	-4.1	-1.0	drug metabolite
enalapril	3.7	5.2	0.6	-0.8	-1.1	-1.2	-1.0	ACE inhibitor
enrofloxacin	5.6	7.2	0.5	-1.2	0.3	-0.1	-0.6	fluoroquinolone
ethephon	1.8		-0.6	-0.8	-2.9	-3.1	-1.2	plant growth regulator
ethyl glucuronide	3.5		-1.6	-1.6	-4.5	-5.0	-1.0	human metabolites
ethyl sulfate	-2.1		-0.1	-2.5	-2.5	-2.5	-1.0	intermediate compound
ethylenthiourea	13.9	6.4	-0.3	-3.2	-0.1	-0.1	0.2	intermediate compound
flonicamid	12.6	3.4	0.2	-0.7	0.2	0.2	0.0	insecticide

analyte	strongest acidic pKa	basic pK$_a$	log P	log D$_{pH}$ 1.7	log D$_{pH}$ 7.4	log D$_{pH}$ 8.0	charge number at pH 7.4	function
florfenicol	8.5		0.7	0.7	0.6	0.6	-0.1	broadband antibiotic
florfenicol-amine	13.6	8.1	-0.4	-3.5	-1.2	-0.8	0.8	broadband antibiotic
fluconazole	12.7	2.3	0.6	0.6	0.6	0.6	0.0	antifungal medication
fluoride	3.2		0.2	0.2	0.4	0.4	-1.0	inorganic anion
formate	4.3		-0.3	-0.3	-3.3	-3.6	-1.0	organic acid
fosetyl-Al		-1.9	0.2	0.2	0.2	0.2	0.0	fungicide
fructose	10.3		-2.8	-2.8	-2.8	-2.8	0.0	carbohydrates
fumarate	3.4		0.0	-0.1	-6.5	-6.9	-2.0	food additive
gabapentin	4.6	9.9	-1.3	-2.0	-1.3	-1.3	0.0	anticonvulsant, antiepileptic
gadodiamide	-6.6	-0.3	-16.2	-15.4	-14.6	-14.8	1.3	contrast agent
Gd-BOPTA	1.7	8.9	-4.3	-5.1	-16.0	-16.9	-3.7	contrast agent
Gd-BT-DO3A/Gadovist	1.2	7.8	-8.6	-9.3	-12.2	-13.0	-2.2	contrast agent
Gd-DOTA	1.2	7.5	-6.7	-7.0	-14.1	-15.2	-3.4	contrast agent
Gd-DTPA	-1.0	8.8	-5.9	-6.5	-17.9	-18.8	-3.9	contrast agent
gemcitabine	11.5	3.7	-1.5	-3.1	-1.5	-1.5	0.0	cytostatics
gentamicin	12.6	10.1	-3.1	-18.7	-11.3	-8.8	4.5	aminoglycoside antibiotic
glufosinate	1.9	9.5	-3.5	-3.6	-6.7	-6.7	-1.0	herbicide
glycolic acid	3.5		-1.0	-1.1	-4.4	-4.5	-1.0	other
glyphosate	-0.6	9.6	-3.1	-3.1	-7.3	-7.8	-1.9	herbicide
GMP[7]	1.2	2.8	-3.1	-3.4	-6.4	-6.9	-2.0	nucleotide
guanylurea	13.6	9.8	-1.8	-4.1	-3.8	-3.5	1.0	drug metabolite
hydrochlorothiazide	9.1		-0.6	-0.6	-0.6	-0.6	0.0	diuretics
iodate	0.9		0.2	-0.7	-2.2	-2.2	-1.0	inorganic anion
iodixanol	11.4	-1.1	-2.1	-2.1	-2.1	-2.1	0.0	contrast agent
iohexol	11.7	-1.4	-2.0	-2.0	-2.0	-2.0	0.0	contrast agent
iomeprol	11.7	-1.4	-1.5	-1.5	-1.5	-1.5	0.0	contrast agent
iopamidol	11.0	-1.6	-0.7	-0.7	-0.7	-0.7	0.0	contrast agent
iopentol	11.7	-1.4	-1.3	-1.3	-1.3	-1.3	0.0	contrast agent
iopromide	11.1	-1.4	-0.4	-0.5	-0.4	-0.5	0.0	contrast agent
ioversol	11.7	-1.4	-2.1	-2.1	-2.1	-2.1	0.0	contrast agent
ipratropium	15.2		-1.8	-1.8	-1.8	-1.8	1.0	bronchodilators
itaconate	3.6		0.1	0.1	-6.3	-6.7	-2.0	intermediate compound
kanamycin	12.1	9.3	-7.1	-19.2	-12.2	-10.3	3.5	aminoglycoside antibiotic
lactate	3.8		-0.5	-0.5	-3.7	-3.9	-1.0	human metabolites
lamivudine	14.3	4.3	-1.1	-3.0	-1.1	-1.1	0.0	nucleoside reverse transcriptase inhibitors
l-carnitine	4.2		-4.9	-4.9	-4.1	-4.1	0.0	human metabolites
levofloxacin-ofloxacin	5.4	6.7	0.1	-1.9	-0.5	-1.0	-0.8	fluoroquinolone
lomefloxacin	5.5	8.8	-0.4	-1.2	-0.4	-0.5	0.0	fluoroquinolone
maleate	2.9		0.0	-0.1	-5.2	-5.8	-2.0	organic acid
malonate	2.4		-0.3	-0.4	-5.3	-5.9	-2.0	organic acid
maltose	11.3		-4.7	-4.7	-4.7	-4.7	0.0	carbohydrate
maltotriose	11.2		-6.5	-6.5	-6.5	-6.5	0.0	carbohydrates
marbofloxacin	5.3	6.7	-0.6	-2.6	-1.2	-1.7	-0.8	fluoroquinolone
melamine		9.6	-0.6	-3.6	-2.3	-2.0	1.0	intermediate compound
mepiquat			-3.1	-3.1	-3.1	-3.1	1.0	plant growth regulator
metformin		12.3	-0.9	-5.8	-5.6	-5.4	2.0	antidiabetic

analyte	strongest		log P	log D$_{pH}$			charge number at pH 7.4	function
	acidic pKa	basic pK$_a$		1.7	7.4	8.0		
methane-sulfonic acid	-1.6		-1.0	-3.3	-3.3	-3.3	-1.0	intermediate compound
methylisothiazoline	4.5		0.9	-1.8	0.9	0.9	0.0	intermediate compound
metronidazole	15.4	3.0	-0.5	-1.4	-0.5	-0.5	0.0	nitroimidazole antibiotics
monobromo acetic acid	2.6		0.5	0.5	-3.0	-3.0	-1.0	disinfection byproduct
monobromo-propionic acid	3.2		0.7	0.7	-2.7	-2.8	-1.0	disinfection byproduct
monochloro acetic acid	3.1		0.3	0.3	-3.2	-3.2	-1.0	disinfection byproduct
monochloro butyric acid	4.0		0.8	0.8	-2.3	-2.6	-1.0	disinfection byproduct
monochloro propionic acid	3.7		0.6	0.6	-2.7	-2.9	-1.0	disinfection byproduct
monoethanol amine	14.8	9.4	-1.0	-4.0	-2.9	-2.4	1.0	intermediate compound
monoethyl amine		10.2	-0.3	-3.3	-2.9	-2.4	1.0	intermediate compound
monoethyl phosphate	1.8		-0.3	-0.5	-3.3	-3.8	-1.9	intermediate compound
monofluoro acetic acid	3.1		-0.2	-0.2	-3.6	-3.7	-1.0	disinfection byproduct
monoisopropanol amine	14.5	9.6	-0.7	-3.8	-2.9	-2.3	1.0	intermediate compound
monomethyl amine		10.1	-0.6	-3.7	-3.2	-2.7	1.0	intermediate compound
mono-n-butyl phosphoric acid	1.8		0.7	0.4	-2.4	-2.9	-1.9	intermediate compound
morphine	10.3	9.1	0.9	-2.3	-0.6	0.0	1.0	opioid
morpholine		8.5	-0.4	-3.7	-1.6	-1.0	0.9	intermediate compound
moxifloxacin	5.5	9.5	-0.5	-1.3	-0.5	-0.5	0.0	fluoroquinolone
N,N-dimethylsulfamide			-0.6	-0.6	-0.6	-0.6		herbicide metabolite
N^4-acetylsulfa-merazine	6.9	-1.8	0.6	0.6	0.1	-0.2	-0.8	drug metabolite
N^4-acetylsulfa-methoxazole	5.9	0.4	0.9	0.8	0.0	-0.1	-1.0	drug metabolite
nadolol	13.6	9.8	0.9	-2.4	-1.4	-0.9	1.0	beta blocker
nalidixic acid	5.8	4.7	0.8	-0.7	-0.5	-1.0	-0.9	fluoroquinolones
n-butyl amine		10.2	0.7	-2.3	-1.9	-1.5	1.0	intermediate compound
neohesperidin dihydrochalcone	8.8		0.8	0.8	0.7	0.7	-0.1	artificial sweetener
neomycin	12.2	9.7	-8.4	-26.6	-15.5	-12.7	5.1	aminoglycoside antibiotic
nitrate	-1.4		-0.2	-2.6	-2.6	-2.6	-1.0	inorganic anion
nitrite	3.4		0.2	0.2	0.2	0.2	-1.0	inorganic anion
norephedrine	13.9	9.4	0.9	-2.2	-1.1	-0.5	1.0	sympathomimetic
norfloxacin	5.6	8.8	-1.0	-1.8	-1.0	-1.0	0.0	fluoroquinolone
O,O-diethyl phosphate	2.0		0.5	0.3	-1.9	-1.9	-1.0	pesticide metabolite
oxalate	1.4		-0.3	-0.8	-6.9	-7.2	-2.0	organic acid
oxipurinol	6.3	2.1	-1.7	-2.2	-2.8	-3.2	0.1	drug metabolite

| analyte | strongest | | log P | log D_{pH} | | | charge number at pH 7.4 | function |
	acidic pKa	basic pK$_a$		1.7	7.4	8.0		
oxytetracycline	7.3	5.8	-4.5	-5.3	-4.9	-5.5	-0.7	tetracycline antibiotic
paracetamol	9.5		0.9	0.9	0.9	0.9	0.0	aniline analgesics
paraquat			-6.7	-6.7	-6.7	-6.7	2.0	herbicide
paromomycin	12.2	9.6	-8.3	-23.5	-14.0	-11.7	4.4	aminoglycoside antibiotic
pefloxacin	5.6	7.0	0.3	-1.7	-0.1	-0.6	-0.7	quinolone
penicillin V	3.4		0.8	0.8	-2.6	-2.7	-1.0	penicillin
perchlorate	-7.1		-0.1	-2.5	-2.5	-2.5	-1.0	inorganic anion
phosphate	1.8		-1.0	-1.3	-4.0	-4.5	-1.9	inorganic anion
pimaricin	3.6	9.1	-1.7	-2.4	-1.7	-1.7	0.0	antifungal medication
piperacillin	3.5		-0.3	-0.3	-3.6	-3.8	-1.0	β-lactam antibiotic
propionic acid	4.8		0.5	0.5	-2.1	-2.6	-1.0	organic acid
quadrol	14.7	9.1	-0.9	-7.4	-2.6	-2.0	1.0	intermediate compound
ranitidine		7.8	1.0	-2.5	0.5	0.8	0.7	H$_2$ receptor antagonist
rantinidine N-oxide	15.0	3.8	-0.1	-0.2	-0.1	-0.1	0.0	drug metabolite
rantinidine S-oxide		7.7	-0.8	-4.3	-1.3	-1.0	0.7	drug metabolite
ribose	12.3		-2.9	-2.9	-2.9	-2.9	0.0	carbohydrates
ristocetin A	3.2	9.7	-9.2	-12.6	-9.2	-9.2	0.2	glycopeptide antibiotic
saccharine	1.9		0.5	0.3	-0.5	-0.5	-1.0	artificial sweetener
salbutamol	10.1	9.4	0.3	-2.4	-1.3	-0.8	1.0	antiasthmatic agent
sarafloxacin	5.6	8.8	0.5	-0.3	0.5	0.5	0.0	quinolone
sorbitol	12.6		-3.7	-3.7	-3.7	-3.7	0.0	nutritive sweetener
sotalol	10.1	9.4	-0.4	-3.2	-2.1	-1.6	1.0	beta blocker
succinate	3.6		-0.4	-0.4	-5.5	-6.2	-2.0	organic acid
sucralose	11.9		-0.5	-0.5	-0.5	-0.5	0.0	artificial sweetener
sucrose	11.8		-4.5	-4.5	-4.5	-4.5	0.0	carbohydrates
sulfachlor-pyridazine	6.6	2.0	0.9	0.4	0.2	0.2	-0.9	sulfonamide antibiotic
sulfadiazine	7.0	2.0	0.4	-0.1	-0.1	-0.3	-0.7	sulfonamide antibiotic
sulfadimidine	7.0	2.0	0.7	0.2	0.2	-0.1	-0.7	sulfonamide antibacterial
sulfameter	7.1	2.0	0.2	-0.2	-0.2	-0.5	-0.7	sulfonamide antibacterial
sulfamethazine	7.0	2.0	0.7	0.2	0.2	-0.1	-0.7	sulfonamide antibacterial
sulfamethoxazole	6.2	2.0	0.8	0.3	0.0	-0.1	-1.0	sulfonamide antibiotic
sulfate	-3.0		-0.8	-3.4	-5.6	-5.6	-2.0	inorganic anion
sulfathiazole	6.9	2.0	1.0	0.5	0.5	0.2	-0.8	sulfonamide antibiotic
tartrate	2.7		-1.8	-1.9	-7.9	-8.4	-2.0	organic acid
terbutaline	8.9	9.8	0.4	-1.9	-0.7	-0.2	1.0	beta adrenergic receptor agonists
tetracycline	7.2	6.2	-3.5	-4.2	-3.8	-4.3	-0.6	tetracycline antibiotic
tetraethyl-ammonium			-2.5	-2.5	-2.5	-2.5	1.0	other
tetramethyl-ammonium			-4.0	-4.0	-4.0	-4.0	1.0	other

analyte	strongest		log P	log D$_{pH}$			charge number at pH 7.4	function
	acidic pKa	basic pK$_a$		1.7	7.4	8.0		
tetrapropyl-ammonium			-0.5	-0.5	-0.5	-0.5	1.0	other
TFNA[8] (flonicamid metabolite)	2.6	4.0	0.8	0.4	-2.0	-2.2	-1.0	pesticide metabolite
TFNG[9] (flonicamid metabolite)	2.8	3.5	-0.5	-0.7	-3.3	-3.3	-1.0	pesticide metabolite
theophylline	7.8	-0.8	-0.8	-0.8	-0.9	-1.1	-0.3	methylxanthine
thiamphenicol	8.8		-0.2	-0.2	-0.2	-0.3	0.0	broadband antibiotic
thifensulfuron-methyl	5.2	1.3	0.5	0.0	-2.0	-2.6	-1.0	herbicide
thiocyanate	0.5		0.5	-0.4	-0.6	-0.6	-1.0	other
thiosemicarbazide	14.5	3.9	-0.8	-2.9	-0.8	-0.8	0.0	intermediate compound
thiosulfate	-2.3		-0.1	-2.5	-2.5	-2.5	-1.0	intermediate compound
thiourea	15.2		-0.5	-0.5	-0.5	-0.5	0.0	intermediate compound
threonate	3.4		-2.2	-2.2	-5.6	-5.6	-1.0	sugar
tiotropium	10.4		-1.8	-1.8	-1.8	-1.7	1.0	anticholinergics
tobramycin	12.5	9.5	-6.5	-21.6	-13.2	-10.7	4.4	aminoglycoside antibiotic
toyocamycin	12.5	6.5	-1.3	-3.3	-1.3	-1.3	0.6	drug metabolite
triethanol amine	15.1	8.4	-1.9	-5.4	-3.0	-2.5	0.9	intermediate compound
trifluoroacetic acid	1.0		0.9	0.1	-2.6	-2.6	-1.0	disinfection byproduct
triisopropanol amine	14.8	9.3	-0.6	-4.1	-2.5	-1.9	1.0	intermediate compound
trimethyl amine		9.6	0.2	-3.3	-2.0	-1.4	1.0	intermediate compound
trimethyl sulfonium			-0.1	-0.1	-0.1	-0.1	1.0	ionic liquid
uracil 1-β-d-arabinofuranoside	9.1		-2.8	-2.8	-2.8	-2.8	0.0	human metabolites
vancomycin	3.4	9.9	-4.4	-7.4	-4.9	-4.4	0.9	glycopeptide antibiotic
vanillactic acid	3.4		0.7	0.7	-2.7	-2.8	-1.0	drug metabolite
vanilmandelic acid	3.1		0.4	0.4	-3.0	-3.1	-1.0	drug metabolite

[1] AMP – adenosine monophosphate; [2] AMPA – α-amino-3-hydroxy-5-methyl-4-isoxazolepropionic acid; [3] cAMP – cyclic adenosine monophosphate; [4] cCMP – cyclic cytidine monophosphate; [5] cGMP – cyclic guanosine monophosphate; [6] CMP – cytidine monophosphate; [7] GMP – guanosine monophosphate; [8] TFNA – 4-trifluoromethyl nicotinic acid; [9] TFNG – N-(4-trifluoromethylnicotinoyl)glycine)

3. Screening of ionizable micropollutants in environmental waters and biota by non-aqueous capillary electrophoresis mass spectrometry

3.1 Abstract

The growing requirements for the reliable analysis of polar compounds in environmental samples with sufficient sensitivity necessitates further advancements in analytical methods. Especially highly polar and ionic compounds are hardly covered in current monitoring strategies of aqueous and biota samples. Various sample preparation techniques have evolved for specific analytical tasks, but non-selective preparation methods for screening approaches are rare and often laborious. Another hindrance is a low compatibility between sample preparation and downstream analysis by separation techniques, necessitating further steps in sample preparation.

Capillary electrophoresis coupled to mass spectrometry (CE-MS) is introduced here as a complement to liquid chromatography-MS for the analysis of ionic and ionizable micropollutants. The optimized method uses a non-aqueous background electrolyte of 25 mM NH_4Ac in methanol with a high matrix tolerance when analyzing aqueous samples and biota extracts. The method is able to analyze anionic and cationic compounds in two runs solely by switching the polarity and adjusting the low pressure applied during separation. Compatibility with different sample preparation techniques, evaporative concentration, solid-phase extraction and QuEChERS is demonstrated for aqueous and biota samples. Limits of detections (LODs) in the low µg/l range were reached for aqueous samples and biota extract. Due to relatively low concentrations of matrix components in water samples, it was even possible to detect and quantify neutral compounds transported by the electroosmotic flow. No correlation of LODs with analytes' polarity or charge (at pH 6) was observed in different matrices demonstrating its broad applicability over a large range of $-5.7 \leq \log D_{pH\,6} \leq 5.1$ making it orthogonal to reversed-phase liquid chromatography and hydrophilic interaction liquid chromatography. The quantification of micropollutants in river water was possible after solid-phase extraction, e.g. for the artificial sweetener acesulfame and the commonly prescribed pharmaceutical hydrochlorothiazide.

3.2 Introduction

With the steadily increasing pollution of surface waters due to industrial waste, pharmaceuticals and household chemicals, the occurrence and concentration of environmentally critical substances need to be monitored. As a result, directives and watch lists are implemented by governments and institutions. So far, most micropollutants of intermediate polarity are addressed in state-of-the-art methodology and equipment by gas chromatography and liquid chromatography coupled to mass spectrometry (LC-MS) strategies. However, very polar and especially ionic micropollutants are not included in current monitoring strategies [3]. When looking closer into the Watch List of the Water Framework Directive [164], five non-polar analytes

(log P between 3.8 and 5.4) were recently removed but three analytes were added, among them two rather polar analytes (amoxicillin and ciprofloxacin with log P values of -2.3 and -0.9). The increasing number of polar substances released into the environment and the fact that their degradation products have increased polarity require analytical methods dedicated to these compounds to become implemented into monitoring strategies on a routine basis [3].

Recent trends in separation techniques for polar analytes in environmental water and biota samples were discussed [1, 5, 22]. Whereas hydrophilic interaction liquid chromatography (HILIC) established itself as a complementary approach to reversed-phase liquid chromatography (RPLC) for the analysis of polar compounds [20], mixed-mode liquid chromatography and supercritical fluid chromatography have gained more attention in recent years, as they cover a wider range of analytes' physicochemical properties [92, 95]. On the other hand, ion chromatography (IC) and capillary electrophoresis (CE) are well suited for ionic and ionizable compounds. Whereas the analysis of small molecules using IC-MS is just evolving [6], CE-MS has already demonstrated to be applicable for a broad range of analytes in different matrices regardless of their polarity [142]. Compared to chromatographic separation techniques, CE-MS has a higher matrix tolerance, provides fast measurements and is well suited for the analysis of aqueous samples making it very interesting for the screening of ionizable and charged analytes including transformation products.

The major drawback of CE-MS is its limited loadability. Even when the most efficient on-line enrichment techniques such as large volume sample stacking [14] or transient isotachophoresis [15] are applied, only a few µl can be injected in contrast to chromatographic techniques, where the injection of 100 µl of an aqueous sample is common in non-target screening approaches [165]. Thus, efficient off-line enrichment techniques for charged or ionizable compounds have to be used to reach detection limits relevant in environmental water and biota analysis.

Despite the great success of sample preparation techniques, a non-selective clean-up combined with desirable preconcentration is still difficult to achieve for screening approaches or non-target analysis. Many reviews summarize the possible preconcentration and clean-up strategies such as solid-phase extraction (SPE) [26, 28], QuEChERS [26, 27] or evaporative concentration (EC) [10]. Most methods were optimizedfor downstream LC analysis.

The applicability of CE-MS for the analysis of e.g. pharmaceuticals in environmental samples was already demonstrated about 20 years ago by Ahrer and Buchberger [153], however, the detection limits for four pharmaceuticals were higher than 25 µg/l. Using three extraction steps (liquid-liquid extraction (LLE)-LLE-SPE), detection limits (LODs) were lowered to 55 ng/l, but quantification was no longer possible. The current possibilities and limitations of capillary electrophoresis for the analysis of pharmaceuticals in the environment were critically discussed by Hamdan in 2017 [142]. Although many CE(-MS) methods still barely reach detection limits below 1 µg/l, there are already promising approaches combining CE with different sample preparation methods: Zhang et al. [166] developed an off-line procedure of immunoaffinity extraction

prior to CE-MS for the analysis of eight fluoroquinolones reaching LODs in the medium ng/l range in environmental waters. Wuethrich et al. [167] developed a SPE/CE-MS analysis method for the detection of eight penicillins and sulfonamides with LODs ranging from 5 to 11 ng/l. A more recent example is the approach by Höcker et al. [168], who used CE-MS with an acidic non-aqueous background electrolyte to quantify and find a relatively broad range of strong acids like haloacetic acids and halomethane sulfonic acids in drinking water. Without any enrichment steps, LODs between 30 and 500 ng/l were reached. For biota samples, methods focused on selected analytes in targeted approaches. One example is the determination of biogenic amines in oysters using CE coupled to electrochemiluminescence [169]. So far, most strategies presented, including all steps of the analysis, were selective for either anions or cations. To the best of the authors knowledge, no CE-MS method applicable for both anionic and cationic compounds in biota and environmental samples has evolved.

Thus, the aim of this work was to develop a CE-MS method suitable for the analysis of micropollutants covering a broad polarity range using anionic, neutral and cationic model analytes. Matrix effects and compatibilities of the CE-MS method with different sample preparation techniques (e.g. SPE, QuEChERS and EC) were investigated, when applied to river water and biota samples.
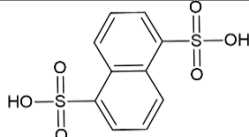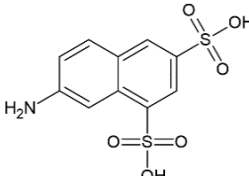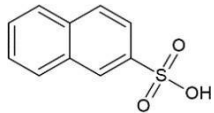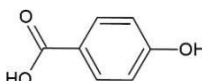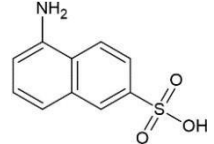
3.3   Materials and methods
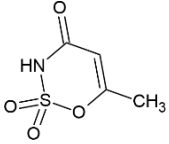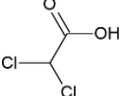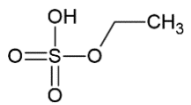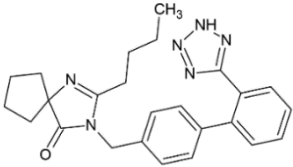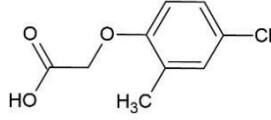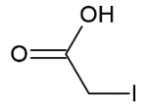
3.3.1   Chemicals
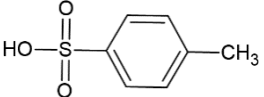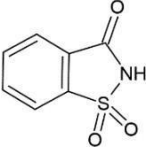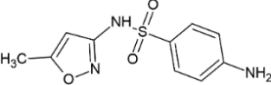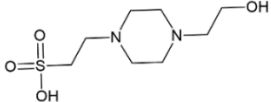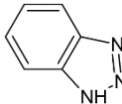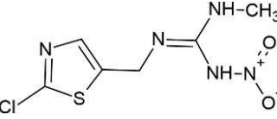
Acetonitrile (MeCN, LC-MS grade), difluoro acetic acid (98%), formic acid (FA, 98%), isopropanol (LC-MS grade), magnesium sulfate (98%), methanol (MeOH, LC-MS grade), sodium chloride (98%) and water (LC-MS grade) were purchased from Sigma-Aldrich (Steinheim, Germany). Acetic acid (HAc, 100%), ammonium acetate (NH₄Ac, 98%) and ammonium hydroxide (NH₄OH, 25% aqueous solution, LC-MS grade) were obtained from Merck (Darmstadt, Germany). Hydrochloric acid (HCl, 32% aqueous solution) was purchased from Fisher Scientific (Waltham, Massachusetts, USA). Monobromo acetic acid (≥ 99%) and trichloro acetic acid (≥ 99.5%) were delivered by Fluka (Buchs, Switzerland), trifluoro acetic acid (99%) by VWR (Darmstadt, Germany). Model analytes and providers are summarized in Table 3-1 together with the chemical structures. 4-Hydroxybenzoic acid-d4 (4-HBA d4), acesulfame-d4 potassium salt (ACE d4), acridine-d9 (ACR d9), dichloro acetic acid-d1 (DCAA d1), metformin-d6 hydrochloride (METF d6), pindolol-d7 (PIND d7), p-toluene-d7-sulfonic acid (p-TSA d7) and saccharin-^{13}C6 (SAC 13C6) were delivered by TRC (Toronto, Canada).
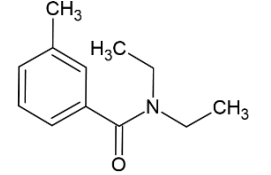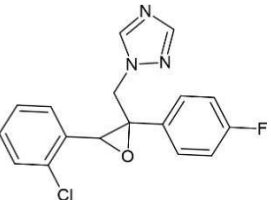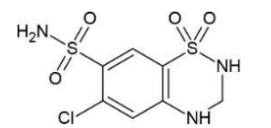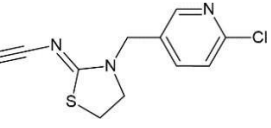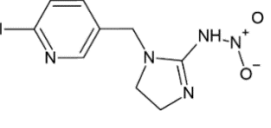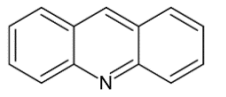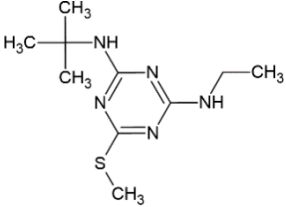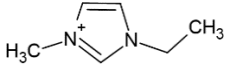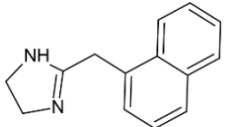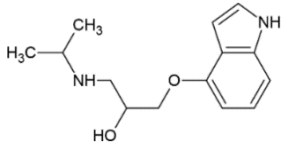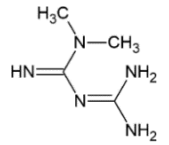
Table 3-1: Model analytes, suppliers thereof and physicochemical properties sorted according to their charge number at pH 6. pK_a, log D values and charge numbers (both pH 6.0) were calculated by Chemicalize provided by ChemAxon (11/11/2020). The column "analysis mode" lists the analysis mode used for each analyte in the final method (see Table 3-2): Analyses of model analytes were conducted using either negative separation polarity in combination with ESI (-) ("negative") or positive separation polarity with ESI (+) ("positive"). For analytes marked with an asterisk *, isotope-labeled standards were available.

analyte	analyte abbrev.	m/z detected	analysis mode	log P	log $D_{pH\,6}$	charge number at pH 6	strong. acidic pK_a	strong. basic pK_a	molecular structure	supplier & purity
1,5-naphthalene disulfonic acid	1,5-NDSA	286.969	negative	1.3	-3.4	-2.0	-2.7			Sigma Aldrich, 97%
7-amino-1,3-naphthalene disulfonic acid	7-A-1,3-NDSA	301.980	negative	-1.6	-4.1	-2.0	-2.8	3.6		Sigma Aldrich, ≥ 98%
2-naphthalene sulfonic acid	2-NSA	207.012	negative	2.1	-0.2	-1.0	-1.8			Sigma Aldrich, ≥ 95%
4-hydroxybenzoic acid	4-HBA	137.024	negative	1.6	-0.2	-1.0	4.4			Fluka, ≥ 98%
5-amino-2-naphthalene sulfonic acid	5-A-2-NSA	222.023	negative	1.1	-0.9	-1.0	-2.2	3.6		Sigma Aldrich, ≥ 95%

analyte	analyte abbrev.	m/z detected	analysis mode	log P	log $D_{pH\,6}$	charge number at pH 6	strong. acidic pKa	strong. basic pKa	molecular structure	supplier & purity
acesulfame *	ACE	161.986	negative	-0.6	-1.5	-1.0	3.0			Sigma Aldrich, ≥ 99%
dichloro acetic acid *	DCAA	126.936	negative	1.1	-2.2	-1.0	2.3			Merck, ≥ 98%
ethyl sulfate	ESU	124.991	negative	-0.5	-2.5	-1.0	-2.1			Sigma Aldrich, ≥ 95%
irbesartan	IRB	429.240	positive	5.4	5.1	-1.0	5.9	4.1		Sigma Aldrich, ≥ 98%
2-methyl-4-chlorophenoxy acetic acid	MCPA	199.017	negative	3.3	-0.2	-1.0	3.4			Sigma Aldrich, ≥ 98%
monoiodo acetic acid	MIAA	184.911	negative	0.7	-2.1	-1.0	3.1			Fluka, 99%

analyte	analyte abbrev.	m/z detected	analysis mode	log P	log $D_{pH\,6}$	charge number at pH 6	strong. acidic pKa	strong. basic pKa	molecular structure	supplier & purity
p-toluene sulfonic acid *	p-TSA	171.012	negative	0.9	-0.7	-1.0	-2.1			Alfa Aesar, 90%
saccharin *	SAC	181.992	negative	0.5	-0.5	-1.0	1.9			Sigma Aldrich, ≥ 98%
sulfamethoxazole	SULFA	252.045	negative	0.8	0.6	-0.4	6.2	2.0		Sigma Aldrich, ≥ 98%
4-(2-hydroxyethyl)-1-piperazine-ethane sulfonic acid	HEPES	239.107	positive	-1.3	-3.1	-0.1	-1.3	7.3		Fluka, 99.5%
1H-benzotriazole	BTA	120.056	positive	1.4	1.3	0.0	9.0	0.2		Sigma Aldrich, 99%
clothianidin	CLO	248.002	negative	0.7	0.5	0.0	15.6	0.4		Sigma Aldrich, ≥ 98%

analyte	analyte abbrev.	m/z detected	analysis mode	log P	log $D_{pH\,6}$	charge number at pH 6	strong. acidic pKa	strong. basic pKa	molecular structure	supplier & purity
N,N-diethyl-m-toluamide	DEET	192.138	positive	2.5	2.5	0.0	-1.0			Sigma Aldrich, ≥ 95%
epoxiconazole	EPO	330.080	positive	3.7	3.7	0.0		2.0		Sigma Aldrich, ≥ 98%
hydrochlorothiazide	HCT	295.957	negative	-0.6	-0.6	0.0	9.1			Sigma Aldrich, ≥ 99%
thiacloprid	THIA	253.032	positive	2.1	2.1	0.0	1.6			Sigma Aldrich, ≥ 98%
imidacloprid	IMI	254.045	negative	1.1	0.5	0.2	9.4	5.3		Sigma Aldrich, ≥ 98%
acridine	ACR	180.081	positive	3.4	3.5	0.6		6.2		Sigma Aldrich, 97%

analyte	analyte abbrev.	m/z detected	analysis mode	log P	log $D_{pH\,6}$	charge number at pH 6	strong. acidic pKa	strong. basic pKa	molecular structure	supplier & purity
terbutryn	TER	242.144	positive	3.7	2.1	0.8	14.3	6.7		Sigma Aldrich, ≥ 98%
1-ethyl-3-methyl-imidazolium	1-E-3-MIM	111.092	positive	-3.1	-3.1	1.0	-	-		Sigma Aldrich, ≥ 95%
naphazoline	NAPHA	211.123	positive	2.2	-0.2	1.0		10.2		Sigma Aldrich, ≥ 98%
pindolol *	PIN	249.160	positive	1.7	-1.4	1.0	14.1	9.7		Sigma Aldrich, 98%
metformin *	MET	130.109	positive	-2.6	-5.7	2.0		12.3		Alfa Aesar, 97%

3.3.2 Q-TOF-MS instrumentation parameters and settings

All analyses were performed using an Agilent CE 7100 capillary electrophoresis (Agilent Technologies, Waldbronn, Germany) interfaced to an Agilent 6550 iFunnel Q-TOF mass spectrometer (Agilent Technologies, Santa Clara, USA) with an electrospray ionization (ESI) source assisted by a sheath liquid interface (Agilent Technologies, Waldbronn, Germany). The composition of the sheath liquid was isopropanol:water (1:1, v/v) with 0.01% FA. The sheath liquid was delivered by a 1260 isocratic pump (Agilent Technologies, Waldbronn, Germany) at a flow rate of 5 µl/min, reached by a split-flow (1:100). The nebulizer pressure was set to 6 psig, and the drying gas flow rate to 11 l/min. Fragmentor voltage was varied to optimize LODs for different analytes between 150 and 400 V in positive and negative polarity. Best overall ionization efficiencies were obtained using –300 V and +400 V for separations in negative and positive analysis mode, respectively. A capillary voltage of $+/−4000$ V, a skimmer voltage of 65 V, and an octopole voltage of 750 V were used. The mass range was set to m/z 50-1000, and the data acquisition rate was 2 spectra/s. Online recalibration during CE-MS analysis was possible by adding 0.2 µmol/l purine, 0.1 µmol/l HP-321 and 0.1 µmol/l HP-921 (all from Agilent Technologies, Waldbronn, Germany) to the sheath liquid. Data analysis was accomplished using MassHunter software (Agilent Technologies, Waldbronn, Germany).

3.3.3 CE instrumentation and settings

The CE separations were carried out using a bare-fused silica capillary (length 60 cm, i.d. 50 µm) from Polymicro Technologies, Phoenix, Arizona.

Table 3-2: Separation conditions and composition of BGEs 1-3 for optimization of the analysis in negative and positive analysis mode. Final BGE separation conditions are listed as BGE final.

BGE	analysis mode (ESI and voltage)	separation voltage	additional pressure	composition
1	negative	+30 kV	30 mbar	20 mM NH$_4$Ac, pH 9
	positive	+30 kV	-	
2	negative	+30 kV	30 mbar	50 mM FA, 55 mM NH$_4$OH, pH 4.5
	positive	-30 kV	30 mbar	
3	negative	-30 kV	60 mbar	50 mM NH$_4$Ac + 3% HAc (v/v) in MeOH
	positive	+30 kV	30 mbar	
final	negative	-30 kV	60 mbar	25 mM NH$_4$Ac + 3% HAc (v/v) in MeOH
	positive	+30 kV	30 mbar	

During method development, three different background electrolytes (BGEs) were used (see Table 3-2 for composition and corresponding CE parameters): BGE 1 was an aqueous basic BGE with 20 mM NH_4Ac at pH 9, BGE 2 an aqueous solution containing 50 mM FA and 55 mM NH_4OH at pH 4.5 and BGE 3 was a non-aqueous buffer made of 50 mM NH_4Ac + 3% HAc (v/v) in MeOH. The final BGE of the optimized method was a mixture of 25 mM NH_4Ac and 3% glacial HAc in MeOH. No measures were taken to remove traces of water present in the buffer components.

If not stated otherwise, samples were injected hydrodynamically by applying a pressure of 100 mbar for 20 s. When injection parameters were varied, the following combinations were used: 75 mbar · 10 s, 100 mbar · 10-30 s. New capillaries were conditioned with BGE for 15 min and flushed between runs for 2 min. The CE capillary was kept at 25 °C during CE runs, and a voltage of + or -30 kV was applied for cation or anion analysis. During separation, additional low pressure was applied depending on the polarity of the measurement and BGE composition (see Table 3-2), if not stated otherwise. The capillary was flushed with air for storage.

3.3.4 Samples and sample preparation

3.3.4.1 Collection of water samples

River water samples were collected in polypropylene vessels at different sites of several rivers (Ammer, Danube, Neckar, Rhine and Steinlach). River samples used in Section 3.4.7 (see also Table 3-3) were collected as follows: X1: 500-2000 m upstream of a wastewater treatment plant (WWTP), X2: several meters upstream of the WWTP, X3: close to the WWTP discharge, X4: 500-2000 m downstream of the WWTP, X5: several km downstream of the WWTP. All samples were filtered with CHROMAFIL Xtra PTFE-45/25 filters (Macherey-Nagel, Düren, Germany) and stored in borosilicate vessels at -20 °C until use. Additionally, a mineral water sample (*M*) was degassed by ultrasonication for 10 min prior to filtration.

3.3.4.2 Stock solutions and spiking

All working solutions of the standards for direct injection were prepared in H_2O. Stock and working solutions were stored at -20 °C before use.

Methanolic stock solutions with a concentration of 20 mg/l containing all analytes were prepared mixing 1 g/l methanolic stock solutions of each analyte. Isotope-labeled standards (ISTD, deuterated and ^{13}C-labeled) and mixtures were prepared and stored in the same way. Samples to be injected without prior enrichment were spiked with the analyte mixtures, to reach a constant ratio of analyte mix:sample of 1:99 (v/v) to keep the methanol content low and constant.

Biota samples were pretreated as described in Sections 3.3.4.5.1 and 3.3.4.6, and the extracts were spiked afterwards. Recoveries for matrix effects were determined comparing the analytes' peak area in spiked (10 µg/l) matrix with the peak areas obtained after the analysis of an aqueous standard. One river water sample (*N1-SPE*, see also Table 3-3) was subjected to SPE (see Section 3.3.4.5.2) after spiking with analyte mix in order to investigate the applicability to real samples.

3.3.4.3 Samples

Different samples were analyzed to demonstrate the broad applicability of the developed NACE-MS method. Table 3-3 lists all samples with information on sample preparation.

Table 3-3: Details on samples used in this work including their origin, sampling date, sample preparation (all aqueous samples were filtered as described in Section 2.4.1 regardless of possible additional sample preparation steps) and spiking concentrations.

sample	sample label	origin/river	sampling date	additional sample preparation (Section)	spiking	referred to in Section
river water	*STL*	Steinlach	02/2019	-	0.1, 0.5, 1, 5, 10, 25, 50, 75, 100, 150, 200 µg/l analyte mix	3.4.5.1, 3.4.5.2
mineral water	*M*	Arnoldi source	07/2019	-	0.1, 0.5, 1, 5, 10, 25, 50, 75, 100 µg/l analyte mix	3.4.5.1, 3.4.5.2
tap water	*T*	University of Tuebingen, Auf der Morgenstelle 18	07/2019	-	0.1, 0.5, 1, 5, 10, 25, 50, 75, 100 µg/l analyte mix	3.4.5.1, 3.4.5.2
river water	*N1*	Neckar, few meters downstream of a WWTP	10/2019	-	0.1, 0.5, 1, 5, 10, 25, 50, 75, 100, 150 and 200 µg/l analyte mix	3.4.5.1, 3.4.5.2
river water	*N1-SPE*		10/2019	SPE Oasis HLB (2.4.4.1.2)	0.001, 0.01, 0.05, 0.1, 0.5, 1 and 5 µg/l analyte mix, **before** SPE	3.4.5.1
river water	*N2*	Neckar, few meters downstream of a WWTP	10/2020	-	1 µg/l ISTD	3.4.6
river water	*N2*		10/2020	SPE Oasis HLB (2.4.4.1.2)	1 µg/l ISTD	3.4.6
river water	*N2*		10/2020	EC (see Section 2.4.4.3)	1 µg/l ISTD	3.4.6

sample	sample label	origin/river	sampling date	additional sample preparation (Section)	spiking	referred to in Section
river water	A1-A5	Ammer	10/2020	-	1 µg/l ISTD	3.4.7
river water	D1-D5	Danube	10/2020	-	1 µg/l ISTD	3.4.7
river water	R1-R5	Rhine	10/2020	-	1 µg/l ISTD	3.4.7
fish	F-SPE	[170]	02/2019	SPE Strata-X-CW (3.3.4.5.1)	0.1, 0.5, 1, 5, 10, 25, 50, 75, 100 µg/l analyte mix, **after** SPE	3.4.5.1, 3.4.5.2
snail	SN-QuE-ChERS	[171]	02/2019	QuEChERS (3.3.4.6)	0.1, 0.5, 1, 5, 10, 25, 50, 75, 100 µg/l analyte mix, **after** QuEChERS	3.4.5.1, 3.4.5.2

3.3.4.4 Sample preparation

3.3.4.5 Solid-phase extraction

Prior to loading the sample onto the SPE column, the cartridge was washed three times with 1 ml MeOH (LC-MS grade) and conditioned three times with 1 ml water (LC-MS grade) for all sorbents.

3.3.4.5.1 Fish extract (sample *F-SPE*)

The following workflow was adapted from [172] to investigate the general compatibility of a biota SPE eluate with the developed NACE-MS method. 100 mg of homogenized juvenile brown trout (*Salmo trutta* f. *fario)* [170] were mixed with 1.5 ml water and vortexed for 30 s. The sample was centrifuged twice at 13000 rpm for 5 min and the supernatant was transferred onto the SPE (Strata-X-CW 33 µm Polymeric Weak Cation, 30 mg, Phenomenex, Torrance, California, USA). The cartridge was washed three times with 1 ml water and the sample was eluted with 1 ml of an acidic MeCN/water mixture (1:1, v/v) + 2% FA (v/v). The eluate was filtered, evaporated to dryness under a stream of nitrogen and afterwards, the residue was redissolved in 300 µl MeOH. Extracts were spiked (see Table 3-3) and the samples were analyzed by NACE-MS.

3.3.4.5.2 River water (sample *N1-SPE*)

For optimized retention of ionic compounds, samples were acidified to pH 1 with HCl (for anions) or alkalized to pH 11 with NH_4OH (for cations). Method development was conducted loading 1 ml acidified or alkalized water sample onto the SPE column (Oasis HLB, 30 mg, Waters, Milford, Massachusetts, USA). The cartridges were washed and the

analytes were eluted under different conditions (see Table S3-4, Section 2.8) to optimize SPE elution. The eluate was evaporated to dryness under a gentle stream of nitrogen, and the concentrated residue was redissolved in 500 µl H_2O.

Optimized conditions for cations were: no washing step after loading and elution with MeOH + 2% FA (v/v). For anions, also no washing step and an elution medium of 5% NH_4OH in MeOH (v/v) was used. 10 ml of the sample *N1-SPE* were loaded onto the SPE column. Quantification of analytes by NACE-MS was conducted via standard addition (for spiking see Table 3-3) as described in Section 6.3.5.

SPE experiments discussed in Section 3.4.6 were conducted as described above, but using 5 ml of sample *N2* spiked with 1 µg/l of ISTD (see Table 3-3), thus a volume enrichment factor of 10 is reached.

3.3.4.6 QuEChERS (sample *SN-QuEChERS*)

We tested if common QuEChERS (Quick, Easy, Cheap, Efficient, Rugged, Safe) biota extracts were compatible with the NACE-MS method. Therefore, 25 mg of Big Ramshorn Snail (*Planorbarius corneus*) [171] homogenate were mixed with 1 ml of a MeCN/water mixture (50:50, v/v) and vortexed for 30 s. 20 mg NaCl and 80 mg dry $MgSO_4$ were added and the mixture was vortexed again for 30 s [2]. Phase separation was supported by centrifugation (15 min, 13000 rpm). 400 µl of the organic MeCN phase were removed and evaporated to dryness under a stream of nitrogen. Finally, the residue was redissolved in 500 µl MeOH. Extracts were spiked and the samples were analyzed by NACE-MS.

3.3.4.7 Evaporative concentration

1 ml of river sample *N2* spiked with 1 µg/l ISTD was evaporated to dryness under a stream of nitrogen and redissolved in 0.1 ml H_2O (volume enrichment factor of 10). Recoveries were determined evaporating 1 ml of the same river sample and reconstituting it with 0.1 ml of a 10 µg/l ISTD aqueous solution (n = 3). All samples were analyzed by NACE-MS. Enrichment factors, matrix effects and theoretical enrichment factors were determined as described in Section 6.3.5.

3.3.5 Data processing and method validation aspects

Extracted ion electropherograms (EIEs) were extracted and evaluated from massprofiles with a mass accuracy of 0.01 m/z using Mass Hunter Qualitative Software (Agilent, V10.0). MassHunter Quantitative Software (V10.1) was used to create calibration curves via the signal areas. LODs and linear range were determined in different matrices using standard addition (see Table 3-3, Table S3-6 and Section 3.3.4.2 for further information) according to DIN 32645. Matrix effects were estimated comparing the recovery from aqueous standards vs. the recovery for analytes to different matrices (tap water, mineral water, river water, fish SPE extract, QuEChERS snail extract) when spiking at a concentration of 10 µg/l. Efficiencies of SPE for the spiked analytes in sample *N2* were calculated via the ratio of the peak areas of each compound obtained for the analyte standards in spiked SPE eluate (10 µg/l) before and after the preconcentration step. Enrichment factors (EF) were calculated dividing the peak area of the ISTD determined after the SPE procedure by the peak area of the spiked untreated sample *N2*. For all spiked ISTD in sample *N2*, matrix effects were determined comparing peak areas of ISTD when

spiked into the SPE eluate with those in an aqueous solution (10 µg/l). Expected enrichment factors (*EF expected*) were determined calculating the product of matrix effect, recovery and the volume enrichment factor (volume sample / final volume extract). EC data were treated in the same way.

All figures were created with Origin 2020 (OriginLab Corporation, Northampton, Massachusetts, USA) and Microsoft Excel 2019 (Microsoft Corporation, Redmond, Washington, USA). Statistical evaluation was conducted using IBM SPSS Statistics 26 (IBM, Armonk, New York, USA).

3.4   Results and discussion

The purpose of this work was to investigate the potential of a CE-MS screening method for a broad range of model analytes present in environmental samples. We aimed at detecting and quantifying model analytes selected in Section 3.4.1 with high selectivity and sufficient detection limits for the analysis of environmental water samples as well as biota samples.

3.4.1 Choice of model analytes

Selection criteria for analytes were: 1) analytes listed in statutory guidelines of water quality (e.g. Directive 2013/39/EU, Commission Implementing Decision (EU) 2015/495, SWISS List on WWTP removal). These regulatory frameworks include mostly pesticides, antibiotics and pharmaceuticals, but also widely used industrial chemicals. 2) Further special analytes were selected which may arise as by-products after treatment of drinking water like halogenated acetic acids (see Guidance on the Biocidal Products Regulation, Volume V, Guidance on Disinfection By-Products, 2017) as well as 3) pharmaceuticals with high prescription rates (for example metformin [173] and hydrochlorothiazide [174]) and 4) representatives for substance classes in processing industry being of relevance also in the environment such as 1*H*-benzotriazole and naphthalene derivatives. The analytes selected have various functional groups (e.g. sulfonamides, sulfonic acids, halogens, carboxylic acids, amines). They differ in polarity, characterized in this study by their $\log$ D at pH 6 (-5.7 (metformin) $\leq \log D_{pH\,6} \leq 5.1$ (irbesartan)), molecular weight (111 (1-ethyl-3-methyl-imidazolium) $\leq$ molecular weight $\leq$ 429 (irbesartan)) and pK_a. Accordingly, analytes are included whose charge is independent of pH (strong acids/bases like ESU or 1-EMIM), which are multiply charged (e.g. 1,5-NDSA, metformin), which are zwitterionic (7-A-1,3-NDSA) or even uncharged in the BGE (for example DEET). The latter will only be transported via the electroosmotic flow (EOF). All parameters are summarized in Table 3-2. With this set of model analytes, it is possible to demonstrate possibilities and limitations of the CE-MS screening method to be developed.

3.4.2 Choice of the BGE

As both anionic and cationic compounds have to be included in the CE-MS screening, either two separate BGEs at very high and very low pH or one BGE applicable to both positively or negatively charged analytes, either in a single or in two separate runs with different polarity are necessary. For the optimization of the BGE, the CE measurements were always conducted twice, one with positive, one with negative ionization mode as

many analytes can be ionized in both ESI modes. A common BGE for both positive and negative analysis mode (including ESI mode and applied voltage, see Table 3-2) requires to make some compromises in selectivity and resolution, but the screening will strongly benefit from shorter analysis times as only short flushing steps before polarity switching are necessary and no hysteresis effects occur. Bare-fused silica capillaries were used to reduce costs.

The first step during method development was the choice of the solvent system (aqueous or non-aqueous), as both have been used successfully in the past [175]. Thus, pre-experiments were conducted with three BGEs common for CE-MS analysis [176, 177] differing in pH and solvent: an aqueous basic BGE 1 at pH 9 (with reverse polarity), an aqueous acidic BGE 2 at pH 4.5, and a non-aqueous BGE 3 with MeOH as solvent (exact compositions see Table 3-2).
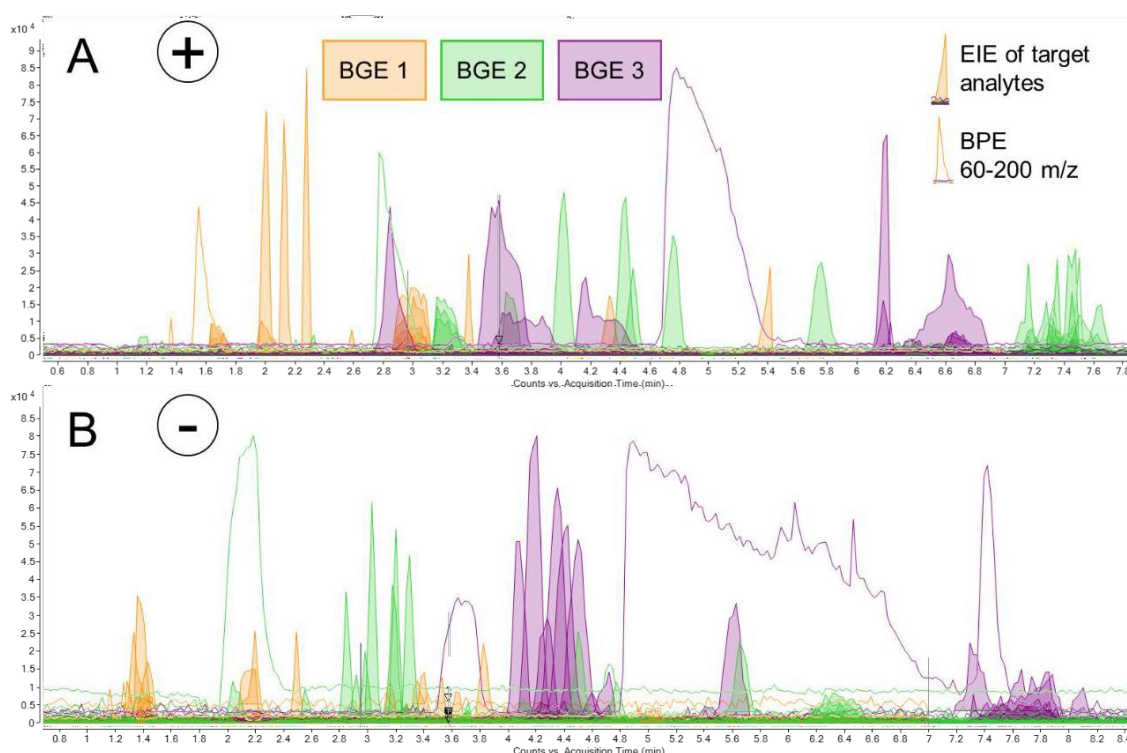
Figure 3-1: EIEs of the analysis of sample N1 spiked with 10 µg/l analyte mix using BGEs 1-3 (see Table 3-2) for A positive and B negative analysis mode. BPEs (m/z 60-200, non-filled lines) were added to judge matrix effects. Injection parameters were 100 mbar · 20 s. Further experimental conditions and analytes see Table 3-2, Sections 3.3.2 and 3.3.3.

Figure 3-1 shows base peak electropherograms (BPEs, 60-200 m/z) and extracted ion electropherograms (EIEs) of cationic and anionic analytes spiked to a river water sample (*N1*, 10 µg/l) for BGEs 1-3. Best peak shapes of cationic analyte signals were obtained for BGE 1; they were worst for BGE 3 as visible from the EIE in Figure 3-1A. For separations in negative analysis mode, an inversed order can be observed. Based on the electropherograms in Figure 3-1, the following parameters were considered for method optimization: 1) sum of relative peak areas (using peak area divided by migration time (MT) for each peak); 2&3) relative standard deviations (RSD) of average peak area and MT (n = 6); 4) analysis time (AT, MT of last detected analyte); 5) migration window

(MW, width of the migration window spanned between the first and last analyte in the electropherogram) divided by AT; 6) sum of electrophoretic resolutions between neighboring peak pairs (called separation power (SP), see [178]) also divided by analysis time and 7) number of detected charged analytes. Dividing MW and SP (Parameters 5&6) by the analysis time is a possibility to highlight superior results whilst maintaining time efficiency.

Figure 3-2 shows a heatmap with the results obtained during the different steps of this method development given as average values of separations in positive and negative analysis mode. Further details are accessible in Section 3.6, (Figure S3-14). The color code was established highlighting best performance with the colors green for highest (sum peak area, MW/AT, SP/AT and sum of charged analytes) and lowest (RSD values and AT) values per column, with red color indicating worst performance.

Ø cationic and anionic	BGE composition		average Σ peak area	Ø RSD of peak areas	Ø RSD of MT	analysis time	migration window/ analysis time (MW/AT)	separation power/ analysis time (SP/AT)	N° charged analytes detected
	electrolyte	solvent							
Step 1 aqueous or nonaqueous	20 mM NH$_4$Ac	H$_2$O	4.5E+05	7.1	1.1	7.8	0.7	7.5E-02	11
	50 mM FA, 55 mM NH$_4$OH	H$_2$O	4.4E+05	7.2	0.4	11.4	0.6	5.6E-02	9.5
	50 mM NH$_4$Ac + 3% HAc	MeOH	7.6E+05	6.2	1.6	9.3	0.6	4.5E-02	9
Step 2 effect of HAc content	50 mM NH$_4$Ac + 1% HAc		6.1E+05	7.2	2.0	10.0	0.6	4.2E-02	9
	50 mM NH$_4$Ac + 3% HAc	MeOH	7.6E+05	6.2	1.6	9.3	0.6	4.5E-02	9
	50 mM NH$_4$Ac + 6.5% HAc		5.7E+05	5.2	0.5	9.6	0.5	3.8E-02	9
	50 mM NH$_4$Ac + 10% HAc		4.8E+05	4.1	0.2	9.7	0.5	3.6E-02	9
Step 3 effect of NH$_4$Ac content	25 mM NH$_4$Ac + 3% HAc		7.7E+05	4.4	1.0	10.1	0.6	4.2E-02	9
	50 mM NH$_4$Ac + 3% HAc	MeOH	7.6E+05	6.2	1.6	9.3	0.6	4.5E-02	9
	75 mM NH$_4$Ac + 3% HAc		6.0E+05	5.4	3.1	9.5	0.6	5.2E-02	9
Step 4 effect of organic solvent	25 mM NH$_4$Ac + 3% HAc	MeOH	7.7E+05	4.4	1.0	10.1	0.6	4.2E-02	9
		MeOH/H$_2$O (75:25, v/v)	1.4E+05	6.1	2.9	16.9	0.6	2.5E-02	9
		MeOH/H$_2$O (50:50, v/v)	1.1E+05	9.2	4.4	17.4	0.7	3.9E-02	9
		MeOH/H$_2$O (25:75, v/v)	1.2E+05	7.3	4.0	17.0	0.7	3.1E-02	9
		H$_2$O	2.7E+05	11.2	2.8	11.2	0.6	4.5E-02	9
		i-PrOH/H$_2$O (25:75, v/v)	7.7E+04	7.6	4.3	23.5	0.8	3.1E-02	9
		MeCN/H$_2$O (25:75, v/v)	2.9E+05	7.3	1.3	12.3	0.6	4.0E-02	9

Figure 3-2: Heat map illustrating the average separation performance over all analytes for negative and positive analysis mode by means of different parameters using twelve different BGEs during the 4 steps of method development (aqueous vs. NACE, effect of HAc content, NH$_4$Ac content and organic solvent). BGE compositions vary in content of salt, acid or type and ratio of organic solvents. The colors code for the performance of the twelve BGEs (ranging from red: lowest performance to green: highest performance). Experimental parameters are listed in Sections 3.3.2 and 3.3.3. The separate values for positive and negative analysis mode can be extracted from Figure S3-14 in Section 3.6.

As seen in Figure 3-2 (first three rows) the sum of peak areas and precision of peak area (average RSD peak area) are superior for BGE 3 for both analysis modes. However, for the other parameters like average RSD MT, separation power / analysis time (SP/AT) and number of charged analytes detected, the use of BGE 3 exhibits inferior results. A closer look into the details (Figure S3-14) reveals that BGE 1 is well suited for cationic analytes, BGE 2 for anions, but both with very poor results for analytes of opposite charge as can be expected. This is not well reflected in the average values (for example 18 anions were detected using BGE 1, but 13 and 12 in BGE 2 and 3).

Using large volume injection, injection parameters (10 · 100 mbar·s) were increased up to 30 · 100 mbar·s (n = 3) to improve sensitivity with acceptable peak shapes at the largest injection plug. The strongest gain in sensitivity by approx. a factor of 3 was observed for BGE 3 (see Figure S3-15).

Matrix effects: For each BGE, matrix effects were determined analyzing different spiked (10 µg/l) water samples (tap water, mineral water and river water) and comparing the peak areas with those of an aqueous standard. Matrix effects were generally low (recoveries between 82-114%, Figure S3-16), only mineral water showed somewhat lower recoveries, especially for cations using BGE 3 (recoveries of 50%).

Trace analysis: To test the BGE's applicability for trace analysis in environmental aqueous samples, a river water sample (*N1*) was spiked with 50 ng/l analyte mix as described in Section 3.3.4.2. All target analytes with signals featuring a signal to noise ratio (S/N ratio) of ≥ 3 are listed in Table S3-5. For this comparison, the possible presence of analytes in the raw sample was neglected. The number of substances detected (out of 28 possible) were 4 (BGE 1) < 9 (BGE 2) < 12 (BGE 3). Especially for anions, BGE 3 was best regarding the number of detected substances and S/N ratios. Again, BGE 2 was well suited for cations with higher S/N ratios than BGE 3, but not suited for anionic analytes as expected from the low pH. For highest analyte coverage, two runs with BGE 2 + 3 would be advantageous, however, at the cost of using two different BGEs.

Summarizing all parameters discussed, BGE 3 and thus NACE was chosen for further method development for combined anion and cation screening as it provided good S/N ratios also at low analyte concentrations, overall good resolution, and the possibility to analyze both cations and anions (in separate runs) within a short overall analysis time. Matrix effects were acceptably low.

3.4.3 Optimization of the NACE method

Having decided for NACE, we further optimized the composition of the BGE with regard to electrolytes and organic solvents (see Figure 3-2) [179]. First, the concentration of HAc in a BGE of 50 mM NH_4Ac was optimized (Step 2 in Figure 3-2). The third step covered the optimization of the NH_4Ac concentration to 25 mM (25-75 mM tested), using the optimal value of 3% HAc. Finally, the type and percentage of organic solvents in hydroorganic BGEs were varied (for details, see Figure S3-14). Beside MeOH (0-100%), amphiprotic i-PrOH and aprotic MeCN were tested as additives in a hydroorganic BGE at ratios ≤ 25% (v/v). At higher ratios excessive migration times or instable currents occurred.

For separations in positive analysis mode, no significant differences in charge state, selectivity and analysis time (p-values > 0.43) were observed when varying the concentration of HAc (1-10%) in a methanolic BGE with 50 mM NH$_4$Ac. For separations in negative analysis mode, only a slight shift of MIAA but not DCAA towards higher migration times was observed with increasing the HAc content. No selectivity changes were observed in contrast to a recent study where the content of NH$_4$Ac was adapted for the analysis of metformin in biota samples [172]. The separation of anions was not affected by the NH$_4$Ac content (see Figure S3-14), so a BGE made of 25 mM NH$_4$Ac + 3% HAc was used, where largest peak areas were observed for cationic analytes.

With the fourth step, effects of the type and content of organic solvents were investigated (using 25 mM NH$_4$Ac + 3% HAc as electrolytes). Despite the influence of organic solvents on pK$_a$ values [180, 181], on the viscosity of BGE and on electrophoretic mobilities, no changes in the number of analytes detected as cations or anions were observed (see Figure 3-2, non-changing values in "N° charged analytes detected"). Due to differences in the electric permittivity, viscosity and ionic strength, the magnitude of the EOF changes [179, 182, 183] and thus the total expected analysis time. Highest analysis times were obtained for hydroorganic solvents with isopropanol and those with 25-75% MeOH content. For the hydroorganic BGE with 25% i-PrOH, high values of MW/AT in combination with a high value of SP/AT indicated a good separation efficiency and a good peak capacity. The same holds true for a BGE with 50% MeOH with shorter analysis time. However, the rather long analysis times compared to pure MeOH or H$_2$O evoke peak broadening caused by longitudinal diffusion and thus increased LODs. Precision of peak areas and migration time proved to be best for the analysis with a BGE based on pure MeOH presumably due to a stable ξ-potential and thus constant EOF.

The unsatisfactory performance of measurements with the pure aqueous BGE (precision of peak areas was 10%) is most likely caused by a reduced ionization efficiency in the ESI source. Improvement could possibly be achieved by adapting the SL composition towards a higher content of organic solvent (not investigated here).

We finally decided to use a fully non-aqueous BGE (25 mM NH$_4$Ac + 3% HAc in 100% MeOH) for fast separations both in negative and positive analysis mode (12.5 min each using voltages of either -30 or +30 kV). Best limits of detection and precision were obtained using positive ionization mode for cation separations at +30 kV and vice versa for anions. Only voltage switching was necessary between separations in positive and negative analysis mode (but no additional flushing). Good separation efficiencies and peak capacities were reached.

3.4.4 Optimization of LODs using SPE

To enable trace analysis in environmental water samples, off-line SPE was optimized for the model analytes investigating its compatibility with the NACE-MS analysis. Oasis HLB cartridges were chosen as a standard solid-phase strategy prior to LC-MS to preconcentrate analytes with a wide polarity range [1, 5, 32]. It enables enrichment of both anions and cations. Best recoveries were obtained without a washing step after sample loading (acidified for anions, alkalized for cations, see Section 3.3.4.5.2) and elution with 1 ml MeOH + 2% FA (v/v) for cations and a solution of 5% NH$_4$OH in MeOH for anions

(see Table S3-4 and Figure S3-13). The eluate is evaporated to dryness under a gentle stream of nitrogen and the sample redissolved in 0.5 ml H_2O. Two sample aliquots of 10 ml of water samples were processed. The eluates were then directly injected (100 mbar · 20 s) for CE-MS analysis.
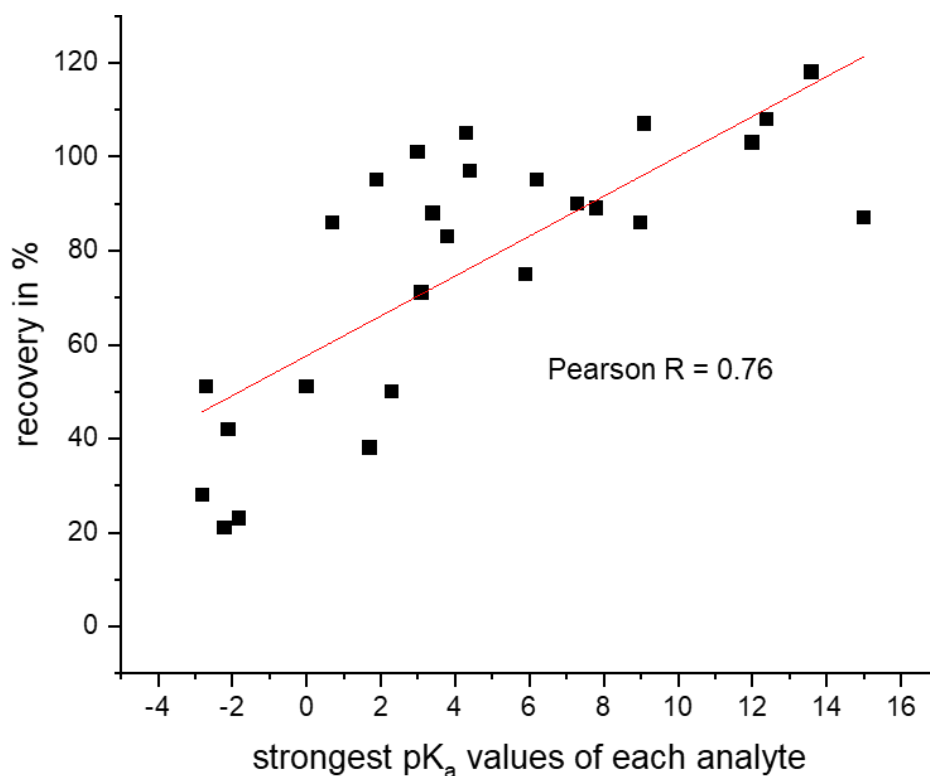
Figure 3-3: Recoveries (listed in Table S3-6) for model analyte obtained with the optimized SPE procedure described in Section 3.3.4.5.2 plotted against their strongest pK_a value. Red line represents the linear fit over all values. For reasons of clarity, corresponding pK_a values of the cation acid were used for basic compounds. The sample was N1-SPE (see Table 3-3), experimental conditions see Sections 3.3.2 and 3.3.3.

Recoveries between 21 and 118% (75% on average) were obtained (see Figure 3-3 and Table S3-6) with a strong correlation (Pearson R = 0.76) between recovery and strongest pK_a values (up to 15) as visible in Figure 3-3. Low recoveries were observed for naphthalene derivates containing a sulfonic acid group (recoveries between 21% (5-A-2-NSA) and 51% (1,5-NDSA) were reached) and further compounds with a permanent charge such as ESU (51%) and 1-E-3-MIM (50%). The optimized SPE step offers satisfactory recoveries (> 60%) for analytes having (corresponding) pK_a values > 3. With increasing charge of the analytes, it is expected that the interaction with the stationary phase is low. For compounds with higher charge numbers, as already mentioned, recoveries decreased with lower pK_a values (and thus degree of ionization), as they cannot be neutralized in the first proto-/deprotonation step for anionic/basic compounds. This leads to enhanced ionic interaction between analyte and stationary phase resulting in low recoveries regardless of subsequent washing/elution steps. Similar loss of charged analytes using this type of stationary phase was also described by Boulard et al. [36]. The

majority of our analytes were preconcentrated and their LODs improved (see Figure 3-4 in Section 3.4.5.1 and Table S3-6). Thus, SPE/NACE-MS is applicable for environmental water samples.

3.4.5 Figures of merit

The developed NACE-MS method was validated for 28 different model analytes spiked at 25 µg/l to the sample *STL* and for further selected samples. The positive and negative ionization mode were used in separate runs. A high precision (n = 12) of the migration time (1.4% RSD on average) and of the peak area (5.3% RSD on average) were reached (see Table S3-6).

3.4.5.1 Limit of detection, linear range and coverage

LODs: LODs and linear range were determined in different matrices (spiked tap water, mineral water, river water, SPE fish extract, QuEChERS snail extract) and summarized in Table S3-6. LODs were 5.1 µg/l on average.
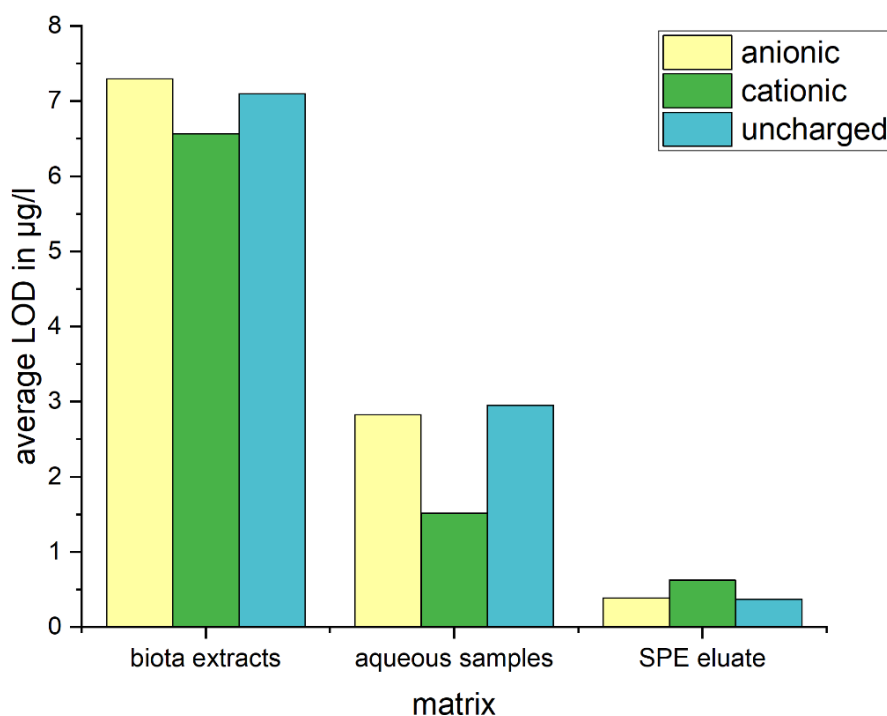
Figure 3-4: Average LODs obtained for the 28 analytes classified by their charge (anionic (n = 12), cationic (n = 6) and uncharged (n = 10)) and the analyzed sample matrix (two biota extracts (samples F-SPE and SN-QuEChERS), four aqueous samples (samples S, M, T and N1) and a river water sample prepared with SPE (N1-SPE, for further information, see Section 3.3.4). LODs were determined as described in Section 6.3.5.

Figure 3-4 shows the LODs obtained for 1) different sample types namely biota extracts, aqueous samples and a river surface sample prepared with SPE and 2) for the 28 analytes grouped by their charge (12 anionic, 6 cationic and 10 neutral analytes (transported via EOF)). 1) *Sample type*: on average, LODs in biota were highest among the different matrices (biota extracts; aqueous samples with river water, mineral/tap water; SPE eluates) for all analytes regardless of their charge state due to more severe quenching

effects by the more complex matrix (see Section 3.4.5.2). The average LOD was 7.1 µg/l. For aqueous matrices, the average LOD was 2.7 µg/l for all analytes detected including neutrals such as DEET or hydrochlorothiazide. 2) *Charge of the analytes*: looking at the ten uncharged analytes only, the average LOD was 4.7 µg/l over all sample matrices and 3.8 µg/l for the 18 charged analytes, with slightly better values for the aqueous samples, though demonstrating no statistic difference (t-test, $\alpha = 0.05$). Consequently, neutral analytes were quantified similar to charged analytes.

Linear range: Linearity reached R² of 0.993 on average for the 28 model analytes. The linear range of this method started at a concentration three times of the LOD (see Table S3-6) and reached 50 µg/l - 100 µg/l and up to 200 µg/l used as the highest calibration level. A second order fit revealed a lower correlation coefficient.

Coverage of NACE-MS: In order to use the NACE-MS method for a non-target-screening, it is important to know its selectivity with regard to the charge of micropollutants in the BGE chosen. The pH of the non-aqueous BGE can be estimated from the theoretical pK_a value of HAc in MeOH, which is 9.7 [181]. Using the Henderson-Hasselbalch equation, we estimate the pK_a value in the non-aqueous BGE to 8.3. In addition, the organic solvent affects the pK_a values of the analytes due to changes in the solvation and stabilization. It is well known, that pK_a values of anions are more strongly affected as anions are less stabilized[181].

In order to predict, which analytes may keep enough charge in the non-aqueous BGE, we plotted the highest aqueous acetic and basic pK_a values of micropollutants (values simulated by Chemicalize provided by ChemAxon (11/11/2020)) against their effective electrophoretic mobility extracted from NACE-MS measurements. In order to obtain a broader view, the set of model analytes was enlarged, see Figure 3-5A and B (data in Table S3-7 and Table S3-8). For anionic compounds, analytes with negative pK_a values in water were not considered as we expect them to be strong acids also in MeOH. Figure 3-5A and B show two electropherograms of all compounds used for the discussion here, also indicating the EOF (t_{eof}). From the migration times (t_{mig}) in Figure 3-5, we calculated effective mobilities as $|\mu_{eff}|$ according to Equation (3-1)

$$|\mu_{eff}| = |\frac{L^2 \cdot (t_{eof} - t_{mig})}{t_{mig} \cdot t_{eof} \cdot V}| \qquad (3-1)$$

using the length L of the capillary (0.6 m) and the applied voltage V of +/-30000 V. The results of $|\mu_{eff}|$ are listed in Table S3-7 and Table S3-8. We chose a value of $|\mu_{eff}| = 1 \cdot 10^{-9}$ m² s^{-1} V^{-1} as a threshold to assign "zero" charge assuming that with the corresponding migration time difference to the EOF of only 0.5 min at least partial comigration with neutral compounds can occur leading to stronger matrix effects. In Figure 3-6, the highest aqueous acidic (black squares) and basic (red squares) pK_a value of each analyte is plotted against $|\mu_{eff}|$ with the threshold indicated as vertical line, differing between cations and anions. Amphoteric compounds with aqueous pI (isoelectric point) values between 6 and 8 will be discussed separately below as they possess acidic and basic functional groups relevant at the chosen pH.
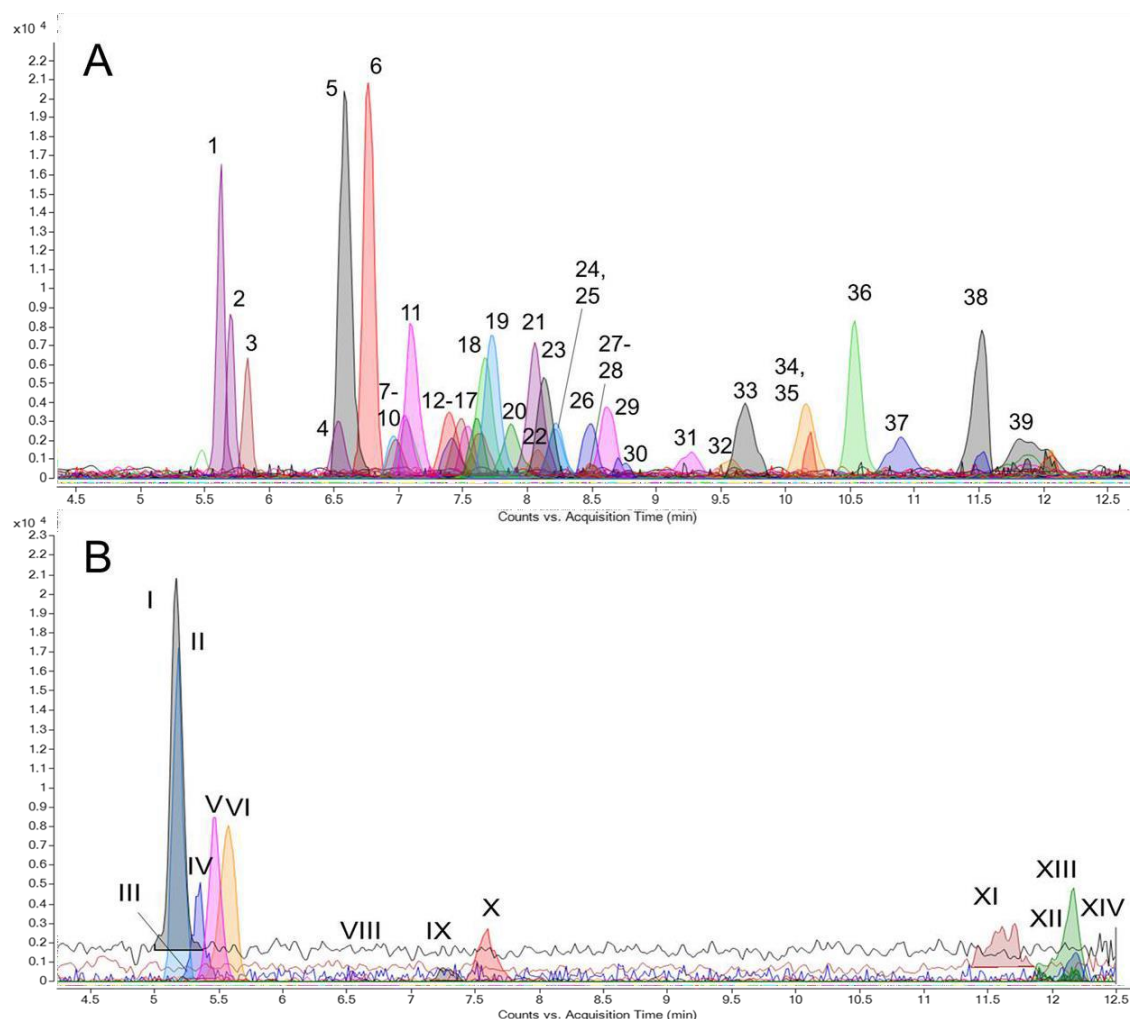
Figure 3-5: A) EIEs of the analysis of an aqueous standard containing the analytes (5 µg/l) listed in Table S3-7. Analysis was performed in positive analysis mode (+30 kV, ESI+). B) EIEs of the analysis of an aqueous standard containing the analytes (10 µg/l) listed in Table S3-8. Analysis was performed in negative analysis mode (-30 kV, ESI-). Further experimental conditions used for both experiments were: 25 mM NH₄Ac with MeOH as solvent, injection parameters: 100 mbar · 20 s and internal pressure was applied A) 30 mbar and B) 60 mbar during separation. For peak identification see Table S3-7 and Table S3-8.

As visible in Figure 3-6A, only 5 of 44 compounds, namely acridine, 4-hydroxybenzoic acid, sulfamethoxazole, 1*H*-benzotriazole and hydrochlorothiazide, are neutral or near-neutral in the pH chosen. For cations, a good negative correlation is visible in Figure 3-6 (t-test, α = 0.05, Pearson R > |0.79|), which is in accordance with the relatively small changes in pK_a values of bases in organic solvents. Metformin with a charge number of 2 in aqueous solution shows a slight offset (see Figure 3-6A, red square at pK_a = 12.3) possibly due to ion-pairing effects. For compounds being anionic in aqueous solution at pH 6, no correlation is visible. Analytes with $pK_a < 4$ appear in a rather small mobility window (in Figure 3-6: $10 \leq \mu_{eff} \leq 22$ vs. $2 \leq \mu_{eff} \leq 19 \cdot 10^{-9}$ m² s⁻¹ V⁻¹). For analytes with $pK_a > 4$, there is a strong shift in migration times with the analytes becoming neutral in the BGE chosen. For example, MCPA, holding a strongest acidic pK_a of 3.1, has a |μ_{eff}| of $10 \cdot 10^{-9}$ m² s⁻¹ V⁻¹ whereas 4-HBA with pK_a of 4.5 is almost exclusively transported by the EOF exhibiting |μ_{eff}| of $1 \cdot 10^{-9}$ m² s⁻¹ V⁻¹. Both molecular structures contain a carboxylic acid group. However, in case of 4-HBA, the carboxylic acid group is attached

directly to the benzene ring, whereas in MCPA it is present at an aliphatic side chain. In general, the different observations for anions vs. cations in MeOH are well in accordance with results published by Sarmini and Kenndler [181]: positively charged compounds experience a similar or only slightly decreased stabilization in pure MeOH as in water, whereas negatively charged analytes are less stabilized. Although there is an average shift of pK_a values of different anionic compounds ((substituted) acetic acids and benzoic acids) of up to 5 units [181, 184], the increase is mostly moderate and strongly depends on the molecular structure. One example for this is the shift of 2-bromoacetic acid and 2-chloroacetic acid from 2.6 (3.1) to 8.1 (7.9) [184] which reverses the order of acidity. As most papers focus on applications, an intense comparison is not possible [179].
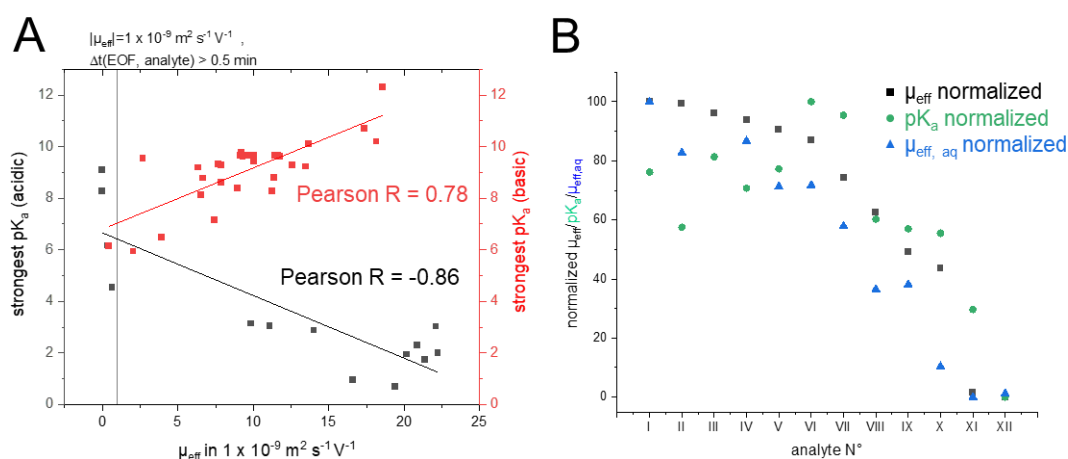

Figure 3-6: A: Strongest acidic (black) and basic (red) pK_a values plotted against $|\mu_{eff}|$. $|\mu_{eff}|$ values for analytes detected in positive analysis mode (red squares) were obtained from the NACE-MS separation of an aqueous standard containing the model analytes listed in Table S3-7, values of analytes represented by black squares were extracted from Table S3-8. Vertical line at $|\mu_{eff}| = 1 \cdot 10^{-9}$ m^2 s^{-1} V^{-1} was defined as threshold: analytes can be expected to be near-neutral and transported mainly by the EOF (migration time difference below 0.5 min). B: normalized (from 0-100) values of μ_{eff} (black), pK_a (green) and $\mu_{eff, aq}$ (blue) used in A and listed in Table S3-8. Deviations between positions of black and green points indicate weaker (pK_a norm. $< \mu_{eff}$ norm.) or stronger (pK_a norm. $> \mu_{eff}$ norm.) destabilization (plus changes in hydrodynamic radius) in comparison with the analytes used here. Selected analytes are indicated: I difluoro acetic acid, II acesulfame, III trichloro acetic acid, IV dichloro acetic acid, V saccharin, VI p-toluene sulfonic acid, VII trifluoro acetic acid, VIII monobromo acetic acid, IX monoiodo acetic acid, X MCPA, XI 4-hydroxybenzoic acid and XII sulfamethoxazole. For further information, see text.

In Figure 3-6B, the different effect of MeOH on pK_a values of acidic compounds was further investigated: the electrophoretic mobilities of the analytes in the non-aqueous BGE and in a corresponding aqueous BGE (μ_{eff}, black squares and $\mu_{eff, aq}$ blue triangles) and their corresponding pK_a values (green circles) were normalized separately (from 0-100) and compared. It can clearly be seen, that the observed, normalized μ_{eff} do not correlate with the normalized pK_a values as visible for the normalized $\mu_{eff, aq}$. This is expected, as the changes in pK_a values strongly depend on the molecular structure (see above).

Due to different shifts in pK_a for acids vs. basic groups, the pI also shifts towards higher values in organic solvents. This is advantageous for a screening by NACE at elevated pH as some compounds will become charged, which would only be included as neutral in an aqueous BGE. Five amphoteric compounds (metoprolol acid, pregabalin, gabapentin,

sulpiride *N*-oxide and ritalinic acid) possessing aqueous pIs between 6.8 and 7.4 demonstrated μ_{eff} between 1.4 and $8.5 \cdot 10^{-9}$ m² s⁻¹ V⁻¹ in NACE. Due to further effects on μ_{eff}, no general trends can be elaborated with the chosen set of model analytes.

As a general conclusion, the method developed here covers a broad range of basic compounds including analytes having pK_a values at about 6 in aqueous solution. Some anion acids can be expected to be transported by the EOF, either due to ion pairing effects leading to neutral analyte-counterion pairs or by shifts in the pK_a values which are too strong, so that the analytes become neutral in the BGE chosen. Further experiments comprising a larger cohort of anionic compounds and changes in the type and concentration of the electrolyte are necessary to fully judge the screening possibilities of the method for anions.

Influences on LODs: We investigated if the methods LODs have a bias with regard to analytes' polarity and charge number using the LODs obtained. In Figure 3-7, the dependence of the LODs on log $D_{pH\,6}$ (aqueous solution at pH 6, simulated data, see Table 3-1) is shown with the analytes grouped according to the charge number ($z > 1.5$; $1.5 \geq z \geq 0.5$; $0.5 > z$) they would have in an aqueous solution at pH 6. This pH corresponds to the estimate analytes' pK_a value (see Figure 3-6) at which they are mainly transported by the EOF in NACE.
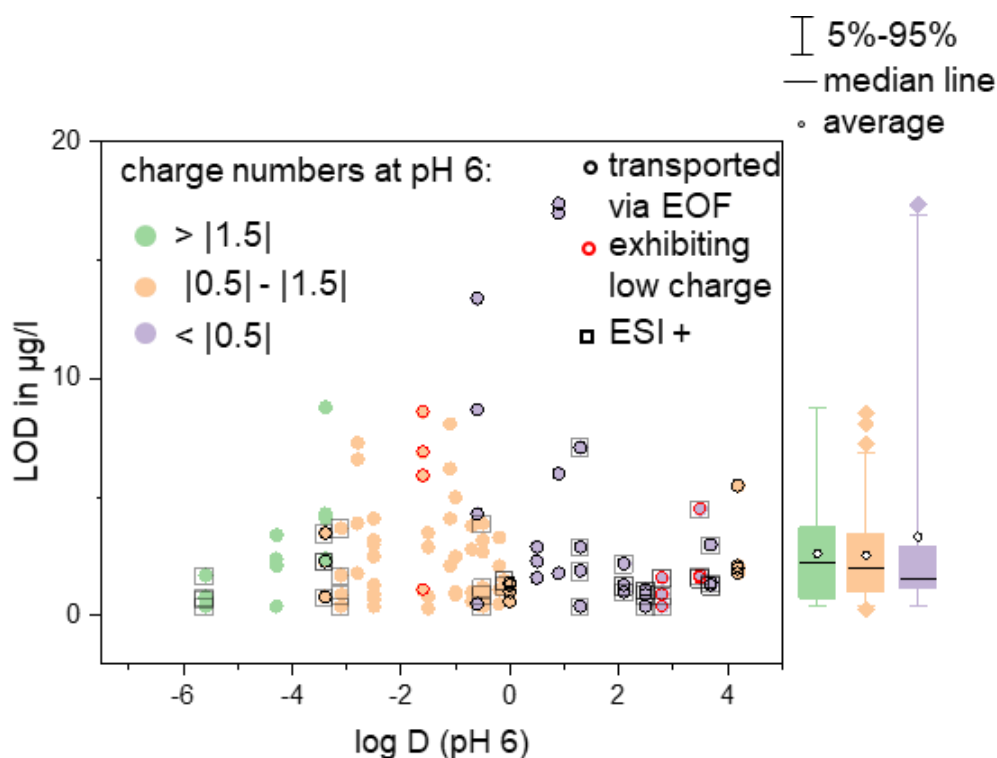
Figure 3-7: Correlation between the LODs determined in the four aqueous sample matrices (samples S, M, T and N1, see also Table S3-6), their corresponding log $D_{pH\,6}$ values and the simulated charge numbers at pH 6 (extracted from Table 3-1). Box-whisker plots on top show distributions of log $D_{pH\,6}$ classified by charge numbers; box-whisker plots on the right show distributions of LOD values classified by charge numbers. Black circles show analytes transported by EOF, red circles mark analytes exhibiting a low charge, namely TERB, ACR and 4-HBA (see also Figure 3-6). Squares indicate analytes detected in ESI+ mode.

However, for anions, we can expect stronger deviations from the charge number present in our experiments. Analytes neutral at pH 6 are indicated by a black circle in Figure 3-7. The analytes TERB, ACR and 4-HBA (red circles) exhibit a low charge demonstrated by migration times close to but smaller than the EOF (see also Figure 3-7).

Ionization efficiency can be seen as the major contributor for good LODs. Several effects have an impact on ionization efficiency, namely polarity, acidity/basicity and finally the comigration with matrix compounds.

Thus, it was investigated whether there is a correlation between LOD and log D values which take ionization into account. Taking a look at Figure 3-7, there seem to be elevated LODs for medium polar analytes. The higher LODs were observed for analytes ionized in negative ESI-mode and only one less polar analyte (IRB) detected in negative mode is present in the model analyte system making it difficult to correlate the parameters. It is thus not clear, whether less polar analytes would have similarly low LODs like IRB or rather higher ones. The latter might be expected, as a lower sensitivity of ESI for less polar compounds is often observed. The addition of formic acid in the SL is favorable for ESI+ [185]. In addition, small, polar compounds might experience reduced ionization efficiencies in ESI as they are not located close to the droplet surface in the aerosol formed [5]. However, this trend was not observed for polar analytes used here.

With regard to the analysis mode, analytes separated and detected in positive analysis mode (+ 30 kV and ESI+, represented by squares in Figure 3-7), exhibited significantly lower LODs compared to separations in negative analysis mode (t-test, $\alpha = 0.05$, average LODs of 1.1 µg/l vs. 3.8 µg/l). It was, however, not further investigated here, whether this effect was caused by general better ionization efficiency in ESI+ mode using this NACE-MS system or it was caused by the combination of separation and ionization polarity.

Though highest LODs were obtained for the neutral analytes HCT and IMI detected in negative analysis mode, the LODs proved independent of the charge number (t-test, $\alpha = 0.05$). It is noteworthy that for the aqueous sample matrices *S*, *M*, *T* and *N1*, compounds with no or very low charge have similar LODs as charged ones. This means that neutral matrix compounds present in river water and transport of analytes by the EOF do not lead to severe quenching effects so that sensitive detection of neutral or near- neutral compounds seems feasible in the low µg/l range. However, the use of isotopically labeled standards may be advantageous for quantitative precision (not investigated here).

3.4.5.2 Matrix effects

Especially using ESI, comigrating matrix components can reduce or enhance the analyte signal intensity [186]. For electro-based separation techniques, the shape of analyte signals is affected by the ionic strength of the BGE vs. the sample as the separation efficiency may be impaired by high salt concentrations. Whereas direct injection was possible for aqueous samples, sample preparation was inevitable for biota samples, as their matrix is more complex. Therefore, the compatibility of two sample preparation techniques developed in-house for the extraction of fish (SPE) and snail (QuEChERS) organisms with NACE-MS were investigated via matrix effects.

1) Matrix load: Figure 3-8 shows the BPEs (60-200 m/z) and EIEs obtained when analyzing the spiked (10 µg/l) samples *STL*, *F-SPE* and *SN-QuEChERS* in positive and negative analysis mode. For comparison, the electropherograms for an aqueous standard are given in Figure 3-8c and d. Ten analytes were transported by the EOF, four of them detected in the negative ionization mode. From the comparison of BPE vs. EIE, we concluded that matrix load is higher in separations of positive polarity than at negative polarity, regardless of sample type and sample preparation (see Figure 3-8a and b). Comparing the BPEs for three matrices *STL*, *F-SPE* and *SN-QuEChERS*, the latter had the highest matrix load. Interestingly, *F-SPE* had largest matrix signals in the positive ionization mode but lowest in negative mode.
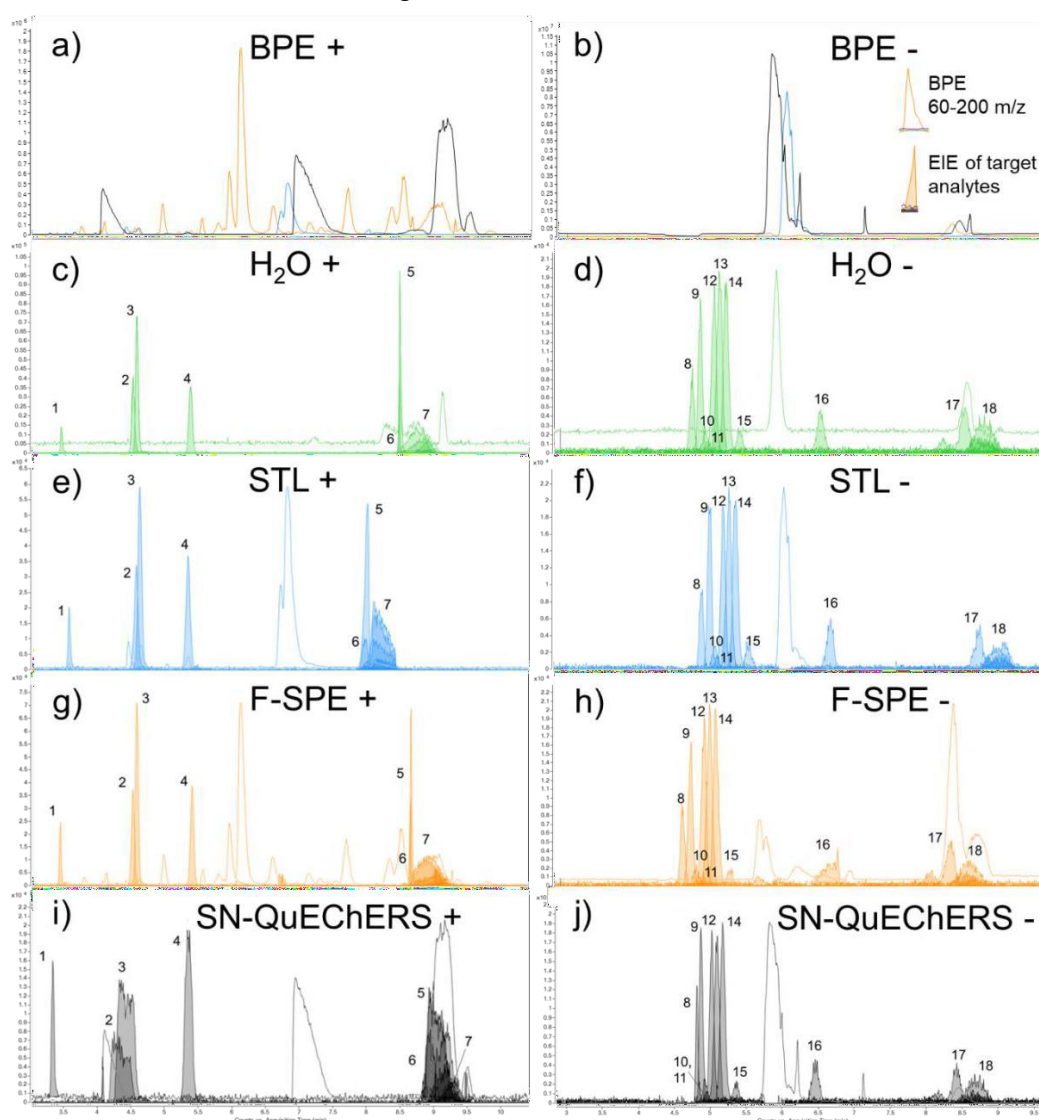
Figure 3-8: BPEs from m/z 60-200 and electropherograms from the NACE-MS analysis of spiked (10 µg/l) samples in positive (a, c, e, g, i) and negative (b, d, f, h, j) analysis mode for all samples (color-coded): a + b: BPE, c + d: LC-MS grade H₂O, e + f: STL, river Steinlach, g + h: F-SPE, fish, and i + j:SN-QuEChERS, snail, see also Table 3-3. BPEs (non-filled) are overlaid in electropherograms c-j and rescaled to highest analyte signals. For separations in positive analysis mode, migration order is as follows: 1) 1-E-3-MIM, 2) METF, 3) NAPHA, 4) PIND, 5) TERB, 6) ACR and 7) EOF containing BTA, DEET, EPO, HEPES, IRB and THIA (n = 12); for separations in negative analysis mode: 8) ESU, 9) ACE, 10) 1,5 NDSA, 11) DCAA, 12) SAC, 13) p-TSA, 14) 2-NSA, 15) 7-A-1,3-NDSA, 16) MCPA, 17) 4-HBA and 18) EOF containing CLO, IMIDA, HCT and SULFA (n = 14). For experimental conditions see Sections 3.3.2 and 3.3.3.

The main interfering factor in environmental water samples was the high salt concentrations and thus conductivity. Highly mobile matrix components, such as inorganic ions Cl^-, Na^+ induced transient isotachophoretic conditions (tITP, see Section 3.4.6) and led to preconcentration but also to migration time changes, especially at higher injection parameters. Interestingly, migration times decreased for cation separation but increased for anion separation (sample *STL*, Figure 3-8e and f). The salt load and its effects strongly differed between the different river waters samples (e.g. sample *N2* from river Neckar in Section 3.4.6).

For most samples, the separation efficiency was preserved relative to the water sample. However, in case of snail extracts using raw QuEChERS extracts, a strong impairment was visible for cation separations. Resolution was lost for compounds 2/3 and 5/6. For metformin (compound 2), similar effects were described before, which were solved by using higher electrolyte concentrations in the NACE-BGE [172]. Clearly, further cleanupis required, e.g. by dispersed solid-phase extraction for these samples. For separations in negative analysis mode, however, no signal deterioration or quenching was observed for the eight analytes possessing highest electrophoretic mobilities, demonstrating the high separation selectivity with less quenching effects especially for analytes with pK_a values > 3 in this analysis mode. In contrast, the signal of MCPA (compound 16, Figure 3-8h), experienced severe peak broadening and showed signs of quenching effects due to comigration with matrix compounds. In case of 4-HBA (compound 17, Figure 3-8h) comigration with a matrix component is observed, too, however without influence on the signal shape. Here, impairment of the ionization efficiency may be expected, as comigration with matrix compounds may occur in all three matrices for other analytes of interest with similar pK_a values.

Neutral matrix compounds were visible in all samples' electropherograms, strongly differing in intensity in both positive and negative ionization mode (Figure 3-8a and b).

2) **Recoveries**: In the second approach, recoveries were determined for the 12 (14) analytes detected in the positive (negative) analysis mode. The compounds were spiked (10 µg/l) to six different samples including *STL*, *F-SPE*, *SN-QuEChERS*, tap water (*T*), mineral water (*M*) and a river water sample which was collected only few meters downstream of a WWTP (*N1*). Figure 3-9 summarizes the average recoveries determined for all analytes in the six samples, differentiating positive (n = 12, red) and negative (n = 14, grey) analysis mode. Average recoveries (calculated using average values marked with a circle in Figure 3-9) of 84% (ranging between 56% and 102%) and 101% (ranging between 85% and 121%) were obtained for analytes detected in positive and negative analysis mode, respectively. As already indicated by the electropherograms, recovery values obtained for the samples *STL*, *F-SPE* and *SN-QuEChERS* were high for negative analysis mode reaching 85 to 97%. In contrast, recoveries were lower reaching only 70% for analytes quantified in positive analysis mode, especially in snail matrix.

Lowest recoveries and thus highest matrix effects were obtained for the mineral water sample *M* with an average recovery of 68% for analytes detected in the positive analysis mode. For analytes using the negative analysis mode, positive matrix effects (average recovery of 121%) were observed in the river water influenced by wastewater for both

charged and neutral analytes. As these positive matrix effects were also present for neutral analytes (see next paragraph), effects from comigration are likely present (see Figure 3-8f, sample *STL*).
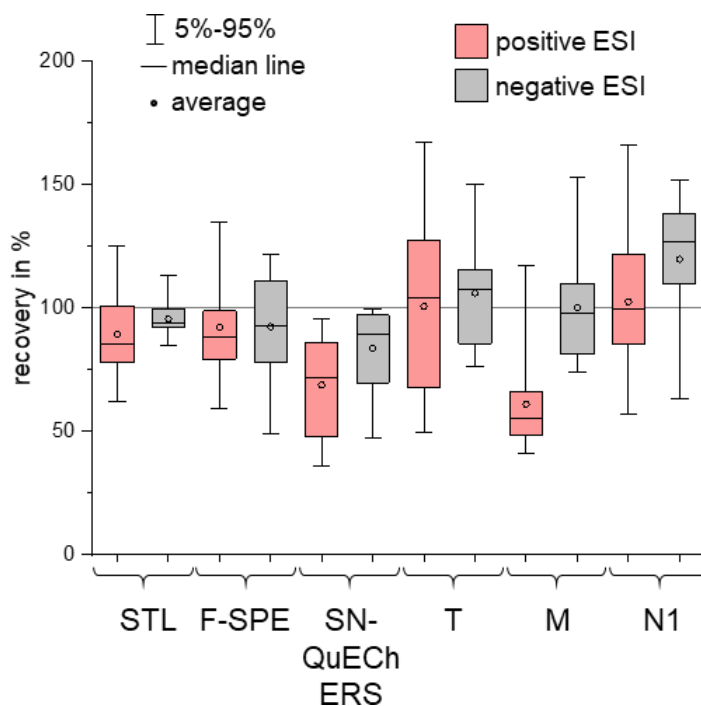
Figure 3-9: Recoveries for all analytes detected in positive (n = 12) and negative (n = 14) analysis (positive and negative ESI) mode (also depicted and listed in Table S3-6) by means of comparing peak areas of the spiked sample (10 µg/l) with those obtained by the analysis of an aqueous sample using LC- MS grade H2O. Vertical line signifies a recovery of 100% (no matrix effects). In addition to the samples STL, F-SPE and SN-QuEChERS shown in Figure 3-8, the recoveries of the samples T, M and N1 are evaluated. For experimental conditions see Sections 3.3.2 and 3.3.3.

We investigated, whether matrix effects were more enhanced for analytes transported by the EOF (see Figure 3-9 for details and Figure S3-17A and B). In general, recoveries of compounds neutral at the BGE chosen were lower by 15% for all sample matrices demonstrating higher matrix effects at both polarities. Recoveries were between 52 and 94% in positive analysis mode (72 to 120% in negative analysis mode). Overall, the recoveries obtained for the negative analysis mode indicated relatively low matrix effects among different environmental and biota samples with recoveries between 72 and 120% even for neutral compounds. Separations in the positive analysis mode, however, showed a stronger dependence on the sample type: recoveries of neutral compounds were reduced by 3-8% (samples *STL* and *N1*) and up to 40% (sample *T*).

3.4.6 Comparison of SPE and EC as sample preparation techniques for aqueous samples prior to NACE-MS

We used a set of model analytes covering a wide range of log $D_{pH\,6}$ values and differing in charge in the non-aqueous BGE to compare the enrichment reached by SPE and EC. Isotopically labeled analytes were spiked, not present in the river water samples. The SPE procedure described in Section 3.3.4.5.2 was followed using 5 ml sample *N2*. Additionally, we preconcentrated 5 ml of sample *N2* using EC by a factor of 10 with final

analyte concentrations of 10 µg/l (see Section 3.3.4.7). We calculated enrichment efficiencies directly from electropherograms using the quotient of the peak areas in the injection solution after the preconcentration method to peak areas obtained analyzing the spiked raw sample. These experimental values were then compared to expected EFs calculated using the product of volume enrichment factor · matrix effect · recovery. Matrix effect and recovery were determined in separate experiments spiking an aqueous sample or the injection solution after EC/SPE cleanup of the river water sample. The electropherograms for the spiked sample *N2* before and after enrichment by SPE or EC are given in Figure 3-10.
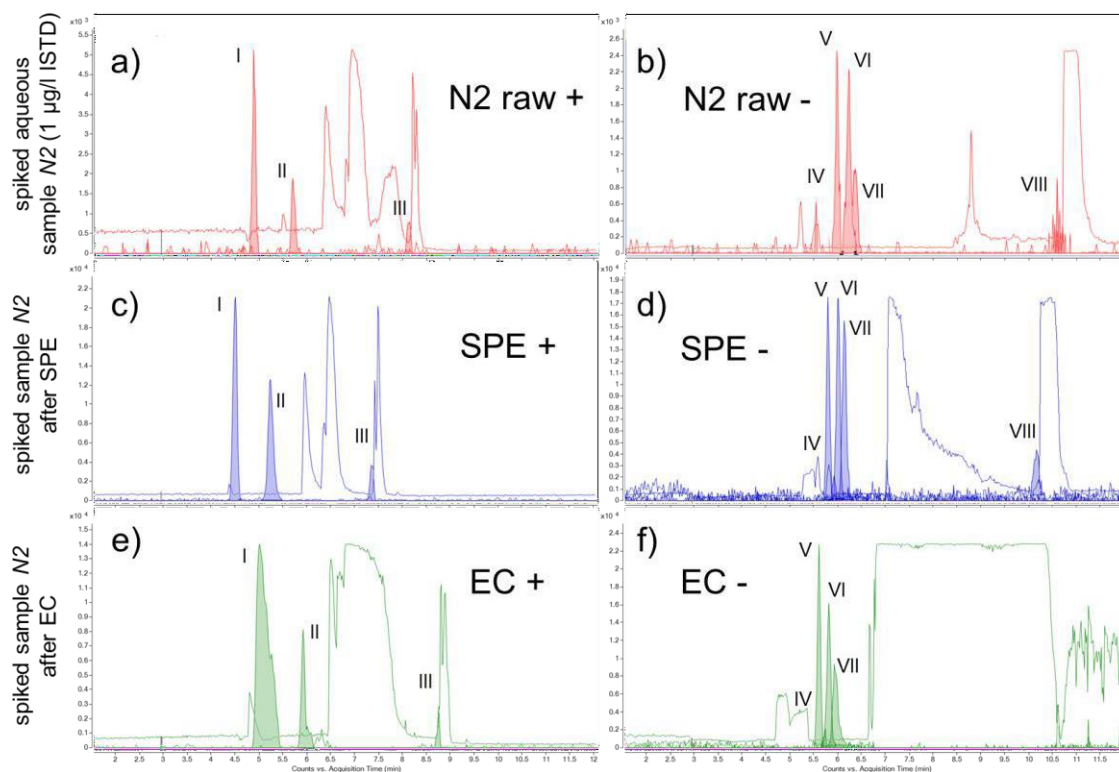
Figure 3-10: EIEs (Roman numerals) of ISTDs and BPEs (scaled to the same intensities) from 50-300 m/z (lines) in positive (left) and negative (right) analysis mode of the NACE-MS method (see Sections 3.3.2 and 3.3.3 for experimental details) of a)&b): spiked (1 µg/l ISTD) aqueous river sample N2, directly injected (see Section 3.3.4.3), c)&d): sample as in a)/b), but preconcentrated with SPE and e)&f): preconcentrated with EC. Spiked ISTD: cations: I) metformin-d6, II) pindolol-d7, III) acridine-d9, and anions: IV) DCAA d1, V) acesulfame-d4, VI) saccharin-^{13}C6, VII) p-TSA d7, VIII) 4-HBA d4 . Details of the SPE procedure are described in Section 3.3.4.5.2, details of the EC procedure in Section 3.3.4.7.

Figure 3-10 shows the BPEs (m/z = 50-300) of the NACE-MS separations using positive and negative analysis modes as well as EIEs of the isotope labeled internal standards which were spiked at a concentration of 1 µg/l to the aqueous river sample. Compared to the raw extract, larger signals for matrix components are visible in the BPE from the SPE extract (see Figure 3-10d) compared to the raw aqueous sample for the negative analysis mode. The signals are due to phosphate ($H_2PO_4^-$, 96.9696 m/z) and sulfate (HSO_4^-, 96.9601 m/z) present in the water sample at elevated concentration, which were also preconcentrated by a factor of 10 using SPE (compare BPE of SPE at 7 min and BPE of raw water sample at 8.8 min). Matrix components neutral in the non-aqueous BGE could not be identified, but MS spectra indicated that SPE was not able to remove the majority of these compounds. However, for the positive analysis mode, the SPE step reduced

background signals, especially in the m/z range of the target analytes (50-300 m/z) compared to the raw water sample.

Using EC, all matrix components were preconcentrated together with the analytes of interest. As a result, very large signals in the negative analysis mode (6.6-10.6 min, Figure 3-10f) were present with sharp boundaries, clearly indicating isotachophoretic (ITP) migration of sulfate and phosphate which act as leading and terminating electrolyte, respectively. Additionally, background noise was visible after the ITP zone. 4-HBA d4 cannot be analyzed after the ITP has passed the detector, presumably due contamination of the ion source by phosphate and sulfate. The prolonged migration in the ITP stack in EC samples reduced the resolution between the analytes *IV-VII*.

In the positive analysis mode, presumably K^+ and Na^+ adducts were present (6.5-8.0 min, Figure 3-10e) evoking tITP phenomena. Strong quenching effects in these migration time ranges are likely as well as reduced resolution for analytes of similar effective electrophoretic mobilities. Two groups of analytes are present differing in the dependence of their effective electrophoretic mobility on the salt matrix and thus on the preconcentration method. Metformin-d6 and pindolol-d7 have high effective electrophoretic mobilities and migrated before potassium (detected as $[KHAc]^+$) and sodium (see Figure 3-10a, c, e, analytes *I* and *II*). Thus, they suffered from destacking phenomena when the sample had a high electric conductivity. Especially after EC enrichment, ionic matrix compounds evoked severe peak broadening (see Figure 3-10e). In contrast, acridine-d9 has a lower effective electrophoretic mobility than potassium and sodium. It became effectively concentrated by tITP as well as other comigrating compounds (see Figure 3-10a, c, e, analyte *III*). In case of SPE eluates, the tITP dissolved during the separation process and acridine-d9 was detected afterwards. In contrast, the higher concentrations of the ionic macro components K^+ and Na^+ in the samples pretreated by EC prolonged the isotachophoretic migration, so that some fronting is observed for acridine-d9 and a lower resolution at the rear end of the ITP. Thus, in samples with even higher salt loads low mobility analytes may be detected still migrating in the ITP stack. Clearly, EC is not well suited for enriching analytes for subsequent NACE-MS analysis.

For separations in negative analysis mode, tITP phenomena can be observed already for the raw water sample. Here, chloride, sulfate and phosphate (detected after analyte *VII*, see Figure 3-10b, d, f) are the major ionic macro components. For analytes *IV-VII,* sample-induced ITP is induced with Cl⁻ as transient leader and sulfate and phosphate as transient terminators. The duration of the tITP depends on the concentrations of these salts and increases from the raw water sample over the SPE eluate to the EC sample. For the latter, the analytes *IV-VII* were released from the ITP stack, however, some matrix components as well as micropollutants with low μ_{eff} can be expected to be kept present in the stack.
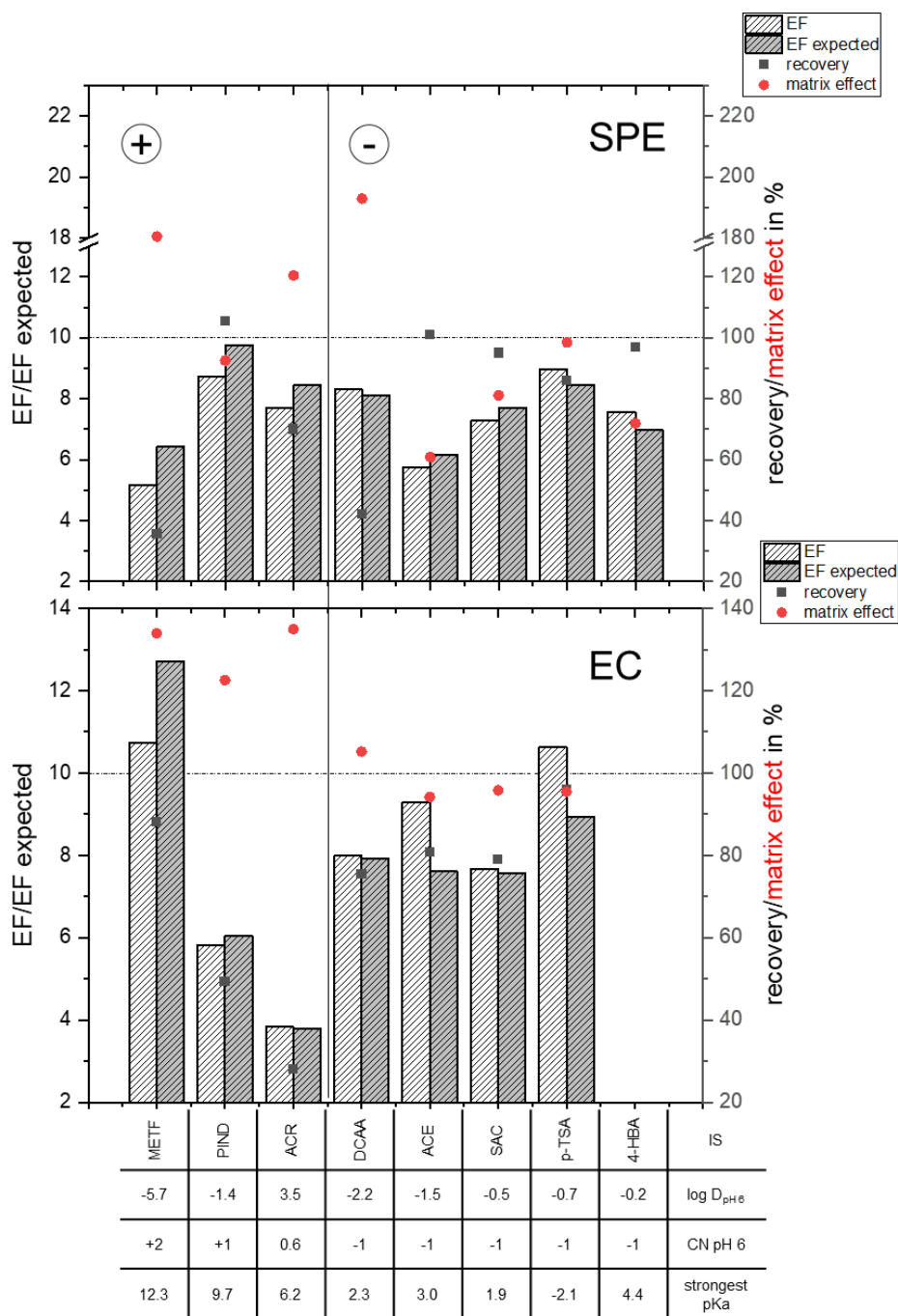
Figure 3-11: Recoveries, matrix effect, experimental EFs and EFs expected calculated from recoveries and matrix effects (for calculations see Section 3.3.5) taking into account the volume reduction by a factor of 10. SPE and EC were used to prepare samples for the analysis of the river water sample N2 spiked with isotope-labeled internal standards (ISTD, 1 µg/l to achieve a final concentration of 10 µg/l after SPE or EC sample preparation). Analytes are sorted according to the migration order in Figure 3-10. Determination of EFs, expected EFs, recovery and matrix effect are described in Sections 3.3.4.5.2 and 3.3.4.7. Horizontal line marks the theoretically achievable EF of 10 if recovery and matrix effects were at 100% each. The vertical line separates cationic and anionic analytes. The table below shows aqueous log $D_{pH\,6}$ values, charge numbers (CN) at pH 6 and each analyte's strongest pK_a value (see Table 3-1).

Figure 3-11 compares the experimental EFs with expected EFs of SPE and EC cleanup steps for the analysis of a river water sample spiked with isotope-labeled internal standards. In both SPE eluates and EC pretreated samples, signals of cations are more strongly affected by the increase of the samples' ionic strength than anions. Higher matrix

effects for cations were observed. Recoveries and EFs were not significantly different between the two sample preparation steps (paired t-test, $\alpha = 0.05$).

For anionic compounds, both SPE and EC reached good EFs for most compounds (7-9 for SPE, 8-10 for EC; excluding acesulfame-d4 in SPE and 4-HBA d4 in EC). However, matrix effects and recovery partly compensated each other.

In general, for both sample preparation strategies, differences in experimental and expected EFs were low, demonstrating that the sample itself has only a small influence on the recovery and the EF. This points to a relatively robust overall method when dealing with different matrices. The differences observed in case of EC sample preparation for the compounds metformin-d6, p-TSA d7 and acesulfame-d4 may be due to salt formation of these permanently charged compounds upon drying and problems in redissolution. The signal of metformin-d6 is strongly impaired in NACE-MS (see Figure 3-10). Metformin-d6 has a very high positive matrix effect, so that experimental EFs > 10 are reached with EC sample preparation. For SPE, the solid phase is not well suited for this compound being doubly charged at neutral pH so that very low recoveries led to an overall experimental EF of only 5.

Using SPE, low recoveries but simultaneously high positive matrix effects (ME > 1) were obtained (especially for metformin-d6 and acridine-d9), whereas for anions, negative matrix effects were compensated by high recovery rates so that overall EFs were > 5 and > 7.4 on average. The low EF of acesulfame-d4 (analyte *V*, Figure 3-10d) can be explained by the high negative matrix effect caused by comigration with the last signal of the first matrix group (see Figure 3-10d, migration time 5.8 min).

For EC, mostly strong positive matrix effects were observed with intermediate to low (pindolol-d7 and especially acridine-d9) recoveries. With these opposing effects, EFs are leveled to similar values in EC and SPE, however, in EC, a stronger dependence on analyte characteristics was observed. Drawbacks when using EC arise for analytes with low effective electrophoretic mobilities such as 4-HBA d4 (analyte *VIII*) as they migrate in the tailing zone of sulfate and phosphate acting as transient terminator just before the EOF signal. Beside quenching by these inorganic ions, also comigration with other matrix components and a lowered resolution due to tITP occur. As a result, these analytes cannot be detected even at elevated concentrations of 10 µg/l. Although the enrichment of sulfate and phosphate also occurs in the SPE pretreated samples, the ITP stack in EC is broader and the ITP does not dissolve completely upon detection. Both recovery and matrix effects but not EFs differ significantly for anionic analytes (paired t-test, $\alpha = 0.05$) using SPE vs. EC as sample pretreatment.

To conclude, the compatibility of both sample preparation techniques with NACE-MS was demonstrated, though with limitations with regard to analyte coverage. It is lower using EC as preconcentration technique especially for anionic analytes than for cationic ones. In both cases, analytes with a medium effective electrophoretic mobility are affected most by matrix effects and detection may be impaired if salt concentrations in the original sample are too high. For SPE, analyte and matrix compounds are preconcentrated simultaneously, but a fraction of inorganic salts is not retained on the SPE column. This enabled the quantification of all model analytes of this study. SPE washing and elution

steps may be further optimized to reduce salt content while maintaining or even increasing the preconcentration of analytes. Overall, SPE showed advantages for the set of model analytes investigated.

3.4.7 *Application to river samples*

Quantification using SPE: Using standard addition, we quantified two micropollutants in river water (sample *N1*) using SPE/NACE-MS: the artificial sweetener acesulfame ACE was detected at a concentration of 1380 ng/l and the commonly prescribed pharmaceutical hydrochlorothiazide (HCT) with high prescription rates at a concentration of 590 ng/l (see Table S3-6). The results were verified using RPLC-MS (C_{18}: 1220 ng/l and 640 ng/l, respectively). Furthermore, the presence of seven other analytes (p-TSA, 2-NSA, SAC, BTA, METF, TERB and DEET) was verified in the river sample, however, concentrations were below LOQ (see Table S3-6 and Section 3.4.4).

Screening approaches: River water samples were collected from three rivers (Danube, Ammer and Rhine) at five different sampling spots each as described in Section 3.3.4.1 taking discharge by wastewater treatment plants (WWTPs) into account. The WWTP's relative population equivalents (PE) provided by the WWTPs were: PE (Rhine) ≈ 10 · PE (Ammer) ≈ 100 · PE (Danube). We thus expected the lowest WW input in the Danube.
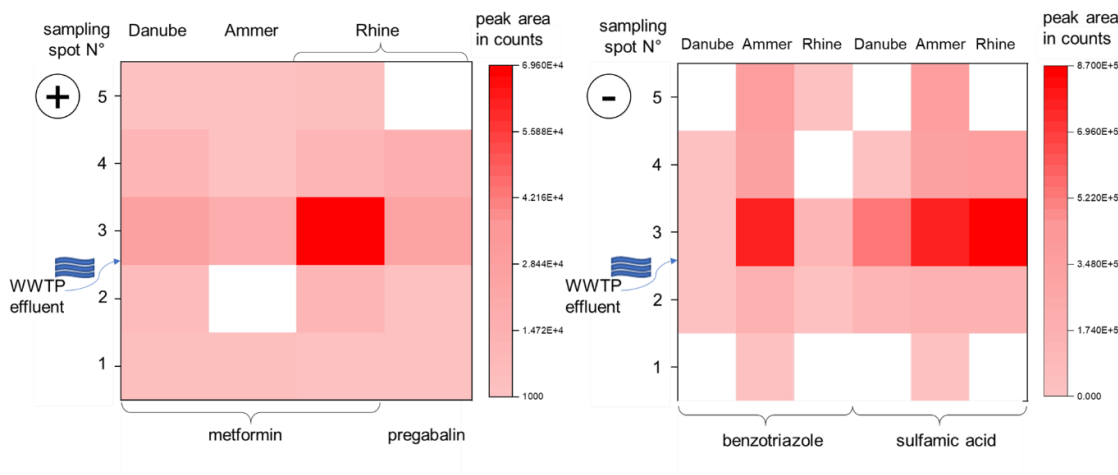
Figure 3-12: Heat map of peak areas of two model analytes (metformin and 1H-benzotriazole) and two suspect analytes (pregabalin and sulfamic acid). Sampling spots 1-5 correspond to the course of the three rivers Danube, Ammer and Rhine (see also Section 3.3.4.1 and Table 3-3) around a WWTP (sampling spot 3 is close to the WWTP discharge). For experimental conditions, see Sections 3.3.2 and 3.3.3.

All 15 samples were directly analyzed using NACE-MS (no sample preconcentration applied) using negative and positive analysis mode. Metformin was identified. Three suspects, the antiepileptic pregabalin [187] (positive analysis mode, migration time = 5.2 min), 1*H*-benzotriazole (negative analysis mode, 10.6 min, transported by EOF) and sulfamic acid (negative analysis mode, migration time = 6.0 min) were found in the majority (85%) of samples. Sulfamic acid is a transformation product of acesulfame, 1*H*-benzotriazole is a common corrosion inhibitor. All compounds are often detected in surface water [39, 188, 189]. In Figure 3-12, their peak areas are plotted in a heat map for the three rivers, indicating the WWTP discharge before sampling spot 3. Concentrations of pregabalin were above the LOD only in the Rhine samples.

For all analytes, peak areas increased when sampling downstream a WWTP and decreased afterwards due to dilution and transformation. It is also possible to differentiate between WWTP of different PEs, as can be seen comparing the peak areas of metformin and sulfamic acid obtained by analyzing samples close to the WWTP effluents of the rivers Rhine and Danube (PE (Rhine) $\approx 100 \cdot$ PE (Danube)).

3.5 Concluding discussion and outlook

The analysis of micropollutants in surface waters and aquatic organisms is still dominated by chromatographic separation techniques and tailor-made sample preparation steps [22, 27]. In our study, we tested if NACE-MS can be an option to analyze charged micropollutants in environmental samples. In metabolomics, CE-MS is already well accepted and established for its high matrix tolerance when analyzing biological matrices, sufficient sensitivity (concentrations in the µg/l range) and the steadily growing data libraries for non-target screening [7, 8]. In environmental analysis, capillary electrophoresis methods are hardly established, as the low environmental concentrations require an even higher sensitivity only achievable after preconcentration of analytes. The compatibility of sample preparation with downstream separation is crucial. Our NACE-MS method was thoroughly validated and its compatibility with sample preparation techniques was demonstrated. It proved to be applicable for the analysis of a broad range of analytes in different types of samples, demonstrating a high versatility and robustness.

In this work, it was possible to establish a NACE-MS method applicable for the analysis of micropollutants (cationic, anionic and non-charged analytes) in environmental water and biota samples. The method showed good reproducibility (RSD values (n = 12) for migration time (1.4% on average) and peak area (5.3% on average)). Average LODs of 4.2 µg/l were reached in aqueous samples and biota extracts. LODs were reduced using off-line SPE sample preparation, though further improvements are necessary. The SPE/NACE-MS method was applied to quantify the artificial sweetener acesulfame and the commonly prescribed pharmaceutical hydrochlorothiazide in river water.

For separations in the negative analysis mode, only minor matrix effects were observed, or they were even positive, when salt concentrations in the sample were not too high (see also Section 3.4.6). With regard to selectivity, discrimination of less acidic compounds ($pK_a > 4$) was observed. For separations in the positive analysis mode, matrix effects appeared to be more distinct, strongly depending on the nature of the particular samples. The matrix effects in aqueous samples were similar to matrix effects obtained in the literature [186]. With the use of internal standards, these effects were minimized and would pave the way for the implementation of NACE-MS for the target analysis of more complex samples, for example QuEChERS extracts of biota samples.

For aqueous samples, the extensive comparison of EC and SPE demonstrated, that both methods are suitable for the enrichment of mobile, charged analytes, but the compatibility with NACE-MS strongly differs: with regard to analytes with lower effective electrophoretic mobility, SPE seems to be the better choice as strong negative matrix effects in EC (see Section 3.4.6) impair their detection. In contrast, the morepronounced matrix removal in SPE increased analyte coverage. Additionally, the higher conformity

between calculated EF and EF for SPE shows its better overall compatibility with NACE-MS analysis. The selectivity of the SPE stationary phase limits coverage. EC may only loose volatile analytes, which may, however, not be covered by NACE-MS anyhow. Analytes of low effective electrophoretic mobilities were discriminated by matrix effects after EC (Section 3.4.6). We conclude that the more time-consuming SPE/NACE-MS method revealed a better sample cleanup with lower co-concentration of ionic macro components acting as transient leaders. SPE/NACE-MS enabled the enrichment and detection of all model analytes used in this section. The LODs improved using SPE (see Section 3.4.4). The current SPE protocol may further be enhanced improving washing steps in order to keep ionic analytes but reduce inorganic salt matrix. Other stationary phases, especially a combination of anion and cation exchange may be tested especially for surface water samples, where enough sample is available compared to biota samples. In contrast to that, the faster EC/NACE-MS method showed limited compatibility with CE-MS due to the preconcentration of ionic macro components. However, the enrichment and analysis of the model analytes chosen in this study was possible.

The method is able to analyze a broad range of analytes covering different physicochemical properties with a common BGE for anions and cations in environmental water samples. Two analytical runs differing in polarity of CE and MS were used with a total analysis time of 30 min. No significant differences between LODs of charged and non-charged analytes as well as between different polarities (using log D) wereobserved (t-test, $\alpha = 0.05$).

The LODs obtained in our study using NACE-MS directly were higher than those reached by Höcker et al. [168] using a slightly different NACE-MS system. Höcker et al. used a more sensitive nanoESI-MS system optimized for anionic analytes only. However, when combined with SPE, the LODs were in a similar range. For the analysis of biota samples, only few and rather specific applications for selected target analytes were presented, e.g. the analysis of the polar antibiotic tetracycline in crucian carp muscle using electrochemiluminescence detection [155] and the analysis of sulfonamides in shrimp, sardine and anchovy with DAD [190]. Both methods reached LODs in the µg/l range. NACE-MS revealed detection limits in the upper ng/l range for the analysis of the anti-diabetic drug metformin in fish extracts without further sample preconcentration [172].

Alternatives for the analysis of ionic and polar compounds are HILIC and IC. For the latter, the combination with MS evolved just recently. Applications for the analysis of small organic micropollutants are evolving fast. The LODs obtained by an IC-MS method developed by Gallidabino et al. [138] were comparable with those reached in the direct NACE-MS method established here (Gallidabino et al.: 1.2 µg/l, in this work 0.4-4.1 µg/l in different matrices, see Table S3-6), despite the strong differences in loadability.

HILIC is capable to analyze a broad range of analytes reaching detection limits in the low ng/l range [21], also in extracts of aquatic organisms [191]. For example, Fauvelle et al. [82] demonstrated LODs of MCPA of 12 ng/l in fresh water. Drawbacks using HILIC can be the reconstitution in organic solvents necessary before analysis to provide sufficient retention, which reduces the enrichment factors achievable [10]. Additionally, long analysis

times are often necessary, as shown by Boulard et al. [36] (-5.7 ≤ log $D_{pH\ 7}$ ≤ 1.0, analysis time of 33 min).

The application to river waters without preceding sample preparation in Section 3.4.7 shows that the NACE-MS method is well applicable for a direct screening at high concentrations of analytes, e.g. metformin (log $D_{pH\ 6}$ = -5.7), pregabalin (-1.3), 1*H*-benzotriazole (1.3) and sulfamic acid (-3.8). Our method comprises aqueous log $D_{pH\ 6}$ values between -5.7 and 5.1, demonstrating that it is rather independent of the polarity of analytes. Only a few chromatographic methods can be found in the literature, comprising such a broad range. For the analysis of these four compounds, several stationary phases were used such as C8 [192], C18 [193] in HPLC or ZIC-HILIC [39] and VDSpher PUR HILIC [194] in HILIC mode, but they were hardly analyzed simultaneously as strong compromises have to be made between selectivity and sensitivity. As long as the concentration of neutral matrix components is not too high, not only charged, but also compounds neutral in the non-aqueous BGE chosen can be analyzed as demonstrated for hydrochlorothiazide and 1*H*-benzotriazole in river water (see Sections 3.4.4 and 3.4.7). Himitations are present when identification of non-charged analytes via MS/MS is desired as migration time is consequently no criterion and increased fragmentation of matrix compounds might occur. Our NACE-MS method offers a fast screening of a broad range of analytes by solely switching polarity (CE and MS) allowing two analytical runs for cations and anions in less than 30 minutes total analysis time. No specific requirements such as coatings or high volumes of chemicals are necessary, demonstrating the simplicity of this method with a low waste production especially with regard to organic solvents. Using internal standards, precise quantification will become possible. If combined with a suitable enrichment method, the NACE-MS method may be used as a complementary analysis technique to RPLC-MS especially applicable for the analysis of ionic and polar compounds. Further research for a more comprehensive sample preparation technique suitable for this system is still necessary, though the first results presented here demonstrate its high potential.

3.6 Supporting information

This Supporting Information provides additional figures and tables complementing the main text. Table S3-4 provides details on the SPE washing and elution conditions investigated during SPE optimization. Figure S3-13 presents average recoveries separately for analytes detected in positive and negative analysis mode with the developed NACE-MS method. Figure S3-14 shows the heat maps separately for positive and negative analysis mode which serve as the basis for the heat map as a complement to Figure 3-2 in the main text. Additional values for migration window and separation power are listed for completeness. Figure S3-15 displays the sum of the relative peak areas (peak area divided by migration time) for the three BGEs 1-3 depending on injection parameters (injection pressure · injection time). Results are depicted for separations in negative (anions) and positive (cations) analysis mode as well as for average values facilitating an overall comparison of the three BGEs. Figure S3-16 summarizes recoveries of analytes spiked at a concentration of 10 µg/l to water samples determined using the three

BGEs 1-3. Table S3-5 provides S/N ratios of detected cationic and anionic analytes using BGE 1-3 analyzing river sample *N1* spiked with 50 ng/l. Table S3-6 complements Figure 3-7 in the main manuscript listing all relevant parameters for model analytes investigated in this work. Figure S3-17 complements the recoveries shown in Figure 3-9 in the manuscript giving additional information on the effects on neutral compounds by grouping results in recoveries of A) non-charged and B) charged analytes. As explained in the manuscript, the model analyte system was extended/varied for a more profound discussion of aspects discussed in Section 3.4.1 Therefore, a standard *PM* from a drinking water facility was analyzed, which consists of a broad range of cationic analytes (5 µg/l). EIEs of 39 of these analytes are depicted in Figure 3-5A. Table S3-7 lists these analytes with additional information. Figure 3-5B depicts electropherograms of analytes detected in NACE-MS in negative analysis mode used for the discussion in Section 3.5.1 which are listed in Table S3-8.

Table S3-4: SPE conditions used to optimize extraction efficiencies of anionic and cationic compounds for Oasis HLB cartridges. According to Section 3.3.4.5.2 in the manuscript, the aqueous samples for anionic detection were acidified to pH 1 using HCl, samples for cationic detection were alkalized to pH 11 using NH$_4$OH. Whereas washing steps were similar for both samples, elution conditions differed for acidic and basic samples.

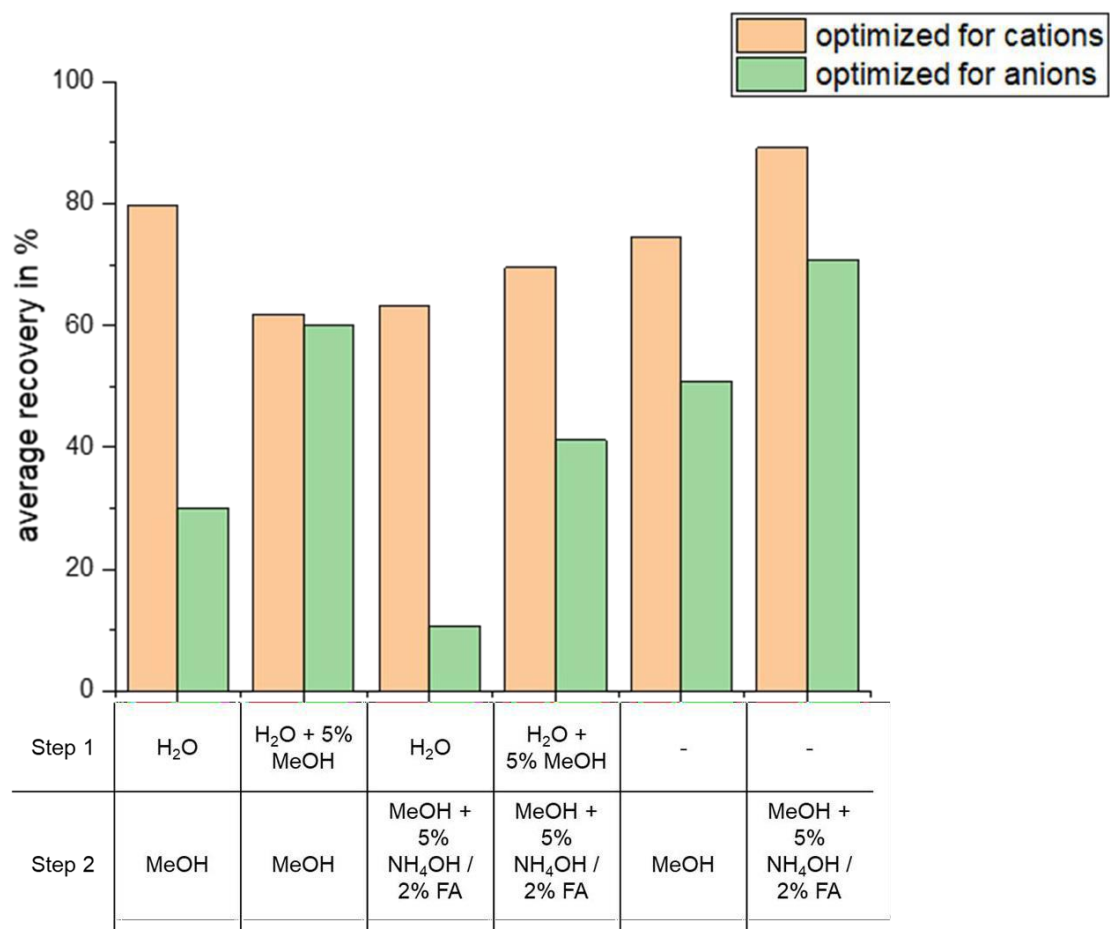| condition N°	wash step	elution conditions	
		anions	**cations**
1	H$_2$O	MeOH	MeOH
2	H$_2$O+ 5% MeOH	MeOH	MeOH
3	H$_2$O	MeOH + 5% NH$_4$OH	MeOH + 2% FA
4	H$_2$O+ 5% MeOH	MeOH + 5% NH$_4$OH	MeOH + 2% FA
5	-	MeOH	MeOH
6	-	MeOH + 5% NH$_4$OH	MeOH + 2% FA

Figure S3-13: Average recoveries obtained for the six different elution conditions in SPE targeting either anionic or cationic compounds listed in Table S3-4 for the analytes detected in positive and negative analysis mode (positive or negative polarity forboth CE separation and MS ionization) with the optimized NACE-MS method. Recoveries were determined according to Section 3.3.4.5.2.

cations

Step	electrolyte	solvent	Σ peak area	Ø RSD of peak areas	Ø RSD of MT	migration window	analysis time	migration window/ analysis time (MW/AT)	separation power	separation power/ analysis time (SP/AT)	N° charged analytes detected
Step 1 aqueous or nonaqueous	20 mM NH₄Ac	H₂O	6.3E+05	3.8	0.7	5.2	7.9	0.7	0.5	6.7E-02	4
	50 mM FA, 55 mM NH₄OH	H₂O	4.3E+05	9.0	0.3	9.3	15.6	0.6	0.5	3.0E-02	6
	50 mM NH₄Ac + 3% HAc	MeOH	4.8E+05	6.4	2.8	6.4	9.5	0.7	0.5	5.8E-02	6
Step 2 effect of HAc content	50 mM NH₄Ac + 1% HAc	MeOH	2.3E+05	8.6	3.8	7.9	11.2	0.7	0.6	5.4E-02	6
	50 mM NH₄Ac + 3% HAc		4.8E+05	6.4	2.8	6.4	9.5	0.7	0.5	5.8E-02	6
	50 mM NH₄Ac + 6.5% HAc		4.4E+05	6.0	0.5	6.4	10.1	0.6	0.5	4.9E-02	6
	50 mM NH₄Ac + 10% HAc		3.5E+05	6.4	0.3	6.2	10.1	0.6	0.5	4.7E-02	6
Step 3 effect of NH₄Ac content	25 mM NH₄Ac + 3% HAc	MeOH	8.7E+05	5.8	1.3	6.8	10.2	0.7	0.5	5.3E-02	6
	50 mM NH₄Ac + 3% HAc		4.8E+05	6.4	2.8	6.4	9.5	0.7	0.5	5.8E-02	6
	75 mM NH₄Ac + 3% HAc		5.2E+05	7.0	5.3	8.7	10.5	0.8	0.8	7.7E-02	6
Step 4 effect of organic solvent	25 mM NH₄Ac + 3% HAc	MeOH	8.7E+05	5.8	1.3	6.8	10.2	0.7	0.5	5.3E-02	6
		MeOH/H₂O (75:25, v/v)	1.3E+05	6.5	4.0	11.5	17.0	0.7	0.6	3.3E-02	6
		MeOH/H₂O (50:50, v/v)	1.4E+05	9.6	5.4	15.9	18.9	0.8	0.9	4.8E-02	6
		MeOH/H₂O (25:75, v/v)	1.2E+05	7.9	5.6	12.7	18.5	0.7	0.6	3.1E-02	6
		H₂O	3.0E+05	10.6	2.1	5.7	9.7	0.6	0.4	4.6E-02	6
		i-PrOH/H₂O (25:75, v/v)	7.1E+04	8.9	6.4	19.6	23.7	0.8	0.9	3.7E-02	6
		MeCN/H₂O (25:75, v/v)	3.2E+05	10.4	0.7	5.9	9.8	0.6	0.5	4.6E-02	6

anions

Step	electrolyte	solvent	Σ peak area	Ø RSD of peak areas	Ø RSD of MT	migration window	analysis time	migration window/ analysis time (MW/AT)	separation power	separation power/ analysis time (SP/AT)	N° charged analytes detected
Step 1 aqueous or nonaqueous	20 mM NH₄Ac	H₂O	2.8E+05	10.5	1.6	5.5	7.6	0.7	0.6	8.4E-02	18
	50 mM FA, 55 mM NH₄OH	H₂O	4.5E+05	5.3	0.5	5.0	7.2	0.7	0.6	8.2E-02	13
	50 mM NH₄Ac + 3% HAc	MeOH	1.0E+06	6.0	0.5	4.1	9.1	0.4	0.3	3.2E-02	12
Step 2 effect of HAc content	50 mM NH₄Ac + 1% HAc	MeOH	9.9E+05	5.7	0.1	3.5	8.8	0.4	0.3	2.9E-02	12
	50 mM NH₄Ac + 3% HAc		1.0E+06	6.0	0.5	4.1	9.1	0.4	0.3	3.2E-02	12
	50 mM NH₄Ac + 6.5% HAc		7.0E+05	4.3	0.5	3.6	9.1	0.4	0.2	2.7E-02	12
	50 mM NH₄Ac + 10% HAc		6.1E+05	1.9	0.2	3.6	9.3	0.4	0.2	2.6E-02	12
Step 3 effect of NH₄Ac content	25 mM NH₄Ac + 3% HAc	MeOH	6.7E+05	3.0	0.7	4.7	10.0	0.5	0.3	3.1E-02	12
	50 mM NH₄Ac + 3% HAc		1.0E+06	6.0	0.5	4.1	9.1	0.4	0.3	3.2E-02	12
	75 mM NH₄Ac + 3% HAc		6.8E+05	3.9	0.9	3.2	8.6	0.4	0.2	2.8E-02	12
Step 4 effect of organic solvent	25 mM NH₄Ac + 3% HAc	MeOH	6.7E+05	3.0	0.7	4.7	10.0	0.5	0.3	3.1E-02	12
		MeOH/H₂O (75:25, v/v)	1.4E+05	5.8	1.9	7.7	16.9	0.5	0.3	1.8E-02	12
		MeOH/H₂O (50:50, v/v)	7.1E+04	8.8	3.4	9.8	15.9	0.6	0.5	3.0E-02	12
		MeOH/H₂O (25:75, v/v)	1.2E+05	6.8	2.3	9.6	15.6	0.6	0.5	3.1E-02	12
		H₂O	2.4E+05	11.7	3.5	8.7	12.8	0.7	0.6	4.4E-02	12
		i-PrOH/H₂O (25:75, v/v)	8.3E+04	6.4	2.3	18.6	23.3	0.8	0.6	2.6E-02	12
		MeCN/H₂O (25:75, v/v)	2.6E+05	4.2	1.9	9.5	14.8	0.6	0.5	3.4E-02	12

Figure S3-14: Heat map illustrating the separation performance for positive and negative polarity by means of different parameters using twelve different BGEs. Compositions vary in content of salt, acid and type and fraction of organic solvent. The colors code for the performance of the twelve BGEs (ranging from red: lowest performance to green: highest performance per BGE/per row). The values presented here serve as basis for the heat map illustrated in Figure 3-2 in the manuscript representing average values. Additionally, values for migration window and separation power are listed for completeness. For further information, see Figure 3-2.
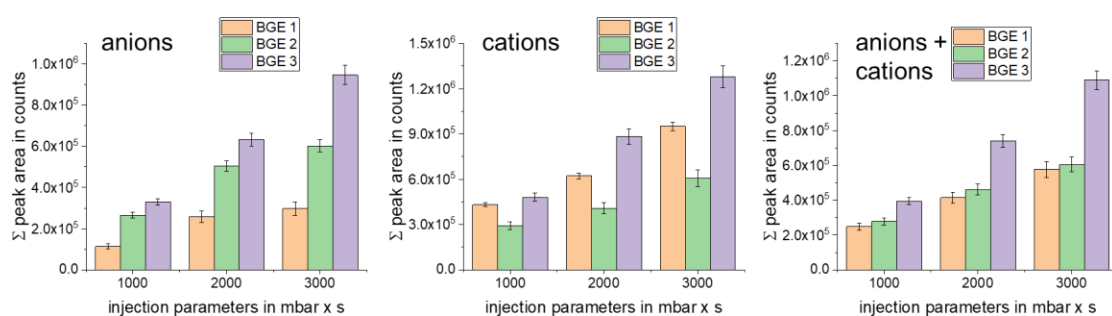
Figure S3-15: Average sum of peak areas from the analysis of 16 anions (4 analytes transported via EOF) and 12 cations (6 analytes transported via EOF) using BGE 1-3 depending on injection parameters in mbar · s. Experimental parameters are listed in Sections 3.3.2 and 3.3.3.
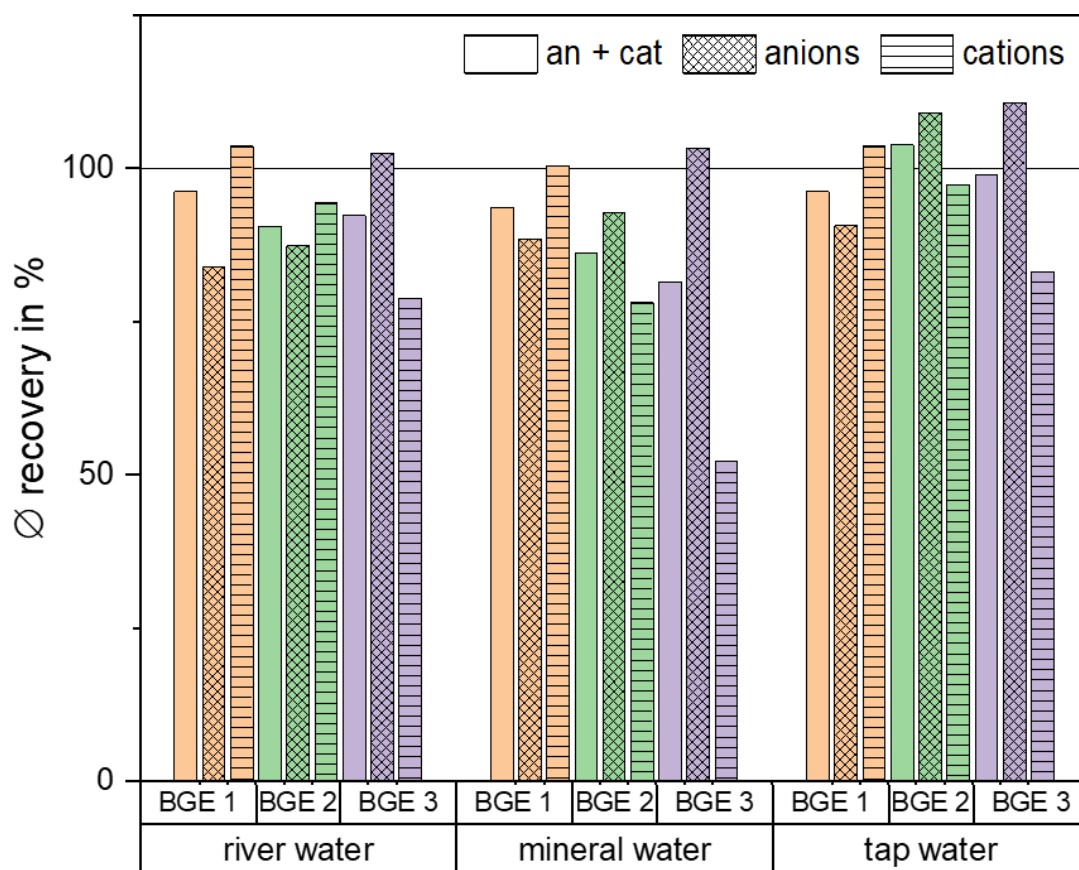
Figure S3-16: Recoveries of analytes spiked at a concentration of 10 µg/l to water samples (tap water, mineral water and river water) determined with the three different BGEs. The recovery was calculated by the ratio of the peak area of each analyte compared to the peak areas of an aqueous standard. Anionic and cationic compounds are grouped according to "analysis mode" in Table 3-1. Experimental parameters are listed in Sections 3.3.2 and 3.3.3.
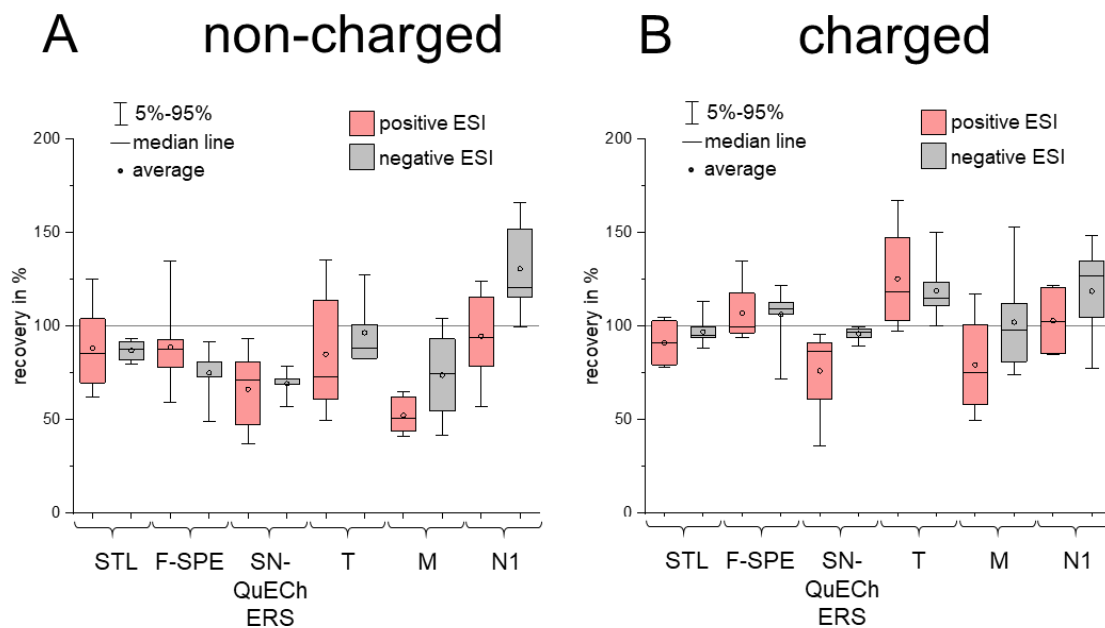
Figure S3-17: Complementary information on recoveries obtained by subdividing the recoveries shown in Figure 3-9 in the manuscript for all analytes detected in positive (n = 12) and negative (n = 14) ESI detection mode for A) non-charged and B) charged analytes. The analytes exhibiting only very low charge (4-HBA, ACR and TERB) were defined as non-charged. For further information, see Figure 3-9 in the manuscript.

Table S3-5: S/N ratios of cationic and anionic analytes using BGE 1-3 (Table 3-2) analyzing sample N1 spiked at 50 ng/l. For experimental conditions, see Sections 3.3.2 and 3.3.3.in the manuscript.

positive analysis mode					negative analysis mode				
analyte	m/z	BGE 1	BGE 2	BGE 3	analyte	m/z	BGE 1	BGE 2	BGE 3
BTA	120	34	30	3	BTA	118	36	4	21
METF	130	5	5	7	ESU	124	3	4	12
TERB	242		10		4-HBA	136			15
PIND	249		27	5	ACE	161			5
THIA	253		7		SAC	181			8
IRB	429		10	13	CLO	248			10
					HCT	295			5
					7-A-1,3-NDSA	301		3	3

Table S3-6: Method validation parameters for the 28 model analytes obtained for different spiked samples (sample spiking was conducted according to Section 3.3.4.2). R², limit of detection (LOD) and linear range were determined according to DIN 32645 with triplicate injection. Separation in the final BGE (see Table 3-2). Injection parameters were 100 mbar · 20 s for all samples. SPE and QuEChERS were used as sample preparation methods for biota samples (fish and snail, for details see Sections 3.3.4.5.1 and 3.3.4.6, respectively). A separate SPE protocol (see Section 3.3.4.5.2) was used for the quantification of analytes in a river water sample (N1).

| | matrix (spiked) | | | | | | | | | | | | | | | | | SPE | | | | |
| | tap water | | | mineral water | | | river water (Steinlach) | | | SPE fish extract | | | QuEChERS snail extract | | | river water (Neckar) | | | river water (Neckar) | | | | |
analyte abbrev.	R^2	LOD in µg/l	lin. range in µg/l	R^2	LOD in µg/l	lin. range in µg/l	R^2	LOD in µg/l	lin. range in µg/l	R^2	LOD in µg/l	lin. range in µg/l	R^2	LOD in µg/l	lin. range in µg/l	R^2	LOD in µg/l	anal. range in µg/l	recovery in %	R^2	LOD in µg/l	lin. range in µg/l	det. conc. in µg/l
1,5-NDSA	0.996	4.3	12-200	0.977	8.8	26-100	0.989	4.1	12-200	0.997	6.9	21-100	0.998	5.2	15-100	0.996	2.4	7-200	51	-			
1-E-3-MIM	0.997	3.7	11-100	0.997	0.9	3-100	0.998	0.4	1-50	0.995	9.8	30-100	0.994	10.9	30-100	0.994	1.7	5-100	51	-			
2-NSA	0.999	1.1	3-200	0.989	3.3	10-100	0.997	0.5	2-50	0.994	8.1	24-100	0.997	2.9	9-100	0.996	2.1	6-200	23	0.992	0.21	0.64-5	< LOQ
4-HBA	0.970	8.6	26-200	0.986	5.9	18-100	0.993	1.1	3-50	0.994	9.5	30-100	0.998	2.4	7-100	0.976	6.9	21-200	97	-			
5-A-2-NSA	0.978	8.1	24-200	0.990	4.1	12-100	0.996	2.1	6-200	-			-			0.982	6.2	18-200	21	-			
7-A-1,3-NDSA	0.999	2.1	6-200	0.994	2.4	7-100	0.998	0.4	1-50	0.975	22.5	60-100	0.997	12.7	39-100	0.994	3.4	10-200	28	-			
ACE	0.993	3.5	11-200	0.999	0.8	2-100	0.999	0.3	1-50	0.996	5.9	18-100	0.999	1.8	6-100	0.994	2.9	9-200	101	0.990	0.37	1.11-5	1.38
ACR	0.996	1.6	5-100	0.996	1.6	5-100	0.998	1.7	5-200	0.994	8.4	25-100	0.994	4.1	12-100	0.973	4.5	15-100	71	0.999	0.15	0.44-5	
BTA	0.975	7.1	-	0.998	1.9	6-100	0.997	0.4	1-50	0.999	2.9	9-100	0.999	4.9	15-100	0.990	2.9	9-150	86	0.999	1.17	-	< LOQ

analyte abbrev.	tap water			mineral water			river water (Steinlach)			SPE fish extract			QuEChERS snail extract			river water (Neckar)			SPE river water (Neckar)				
	R²	LOD in µg/l	lin. range in µg/l	R²	LOD in µg/l	lin. range in µg/l	R²	LOD in µg/l	lin. range in µg/l	R²	LOD in µg/l	lin. range in µg/l	R²	LOD in µg/l	lin. range in µg/l	R²	LOD in µg/l	anal. range in µg/l	reco-very in %	R²	LOD in µg/l	lin. range in µg/l	det. conc. in µg/l
CLO	0.996	2.3	7-100	0.996	2.3	7-100	0.999	1.6	5-200	0.998	6	18-100	0.999	1.9	6-100	0.992	2.9	9-100	118	0.999	0.39	1.17-5	
DCAA	0.996	3.0	9-200	0.997	1.3	4-100	1.00	0.4	1-50	0.987	13.8	42-100	0.998	5.1	15-100	0.989	4.1	12-200	42	0.998	0.15	0.45-5	< LOQ
DEET	0.998	1.1	3-100	0.998	1.1	3-100	0.998	0.4	1-50	0.993	4.9	15-100	0.997	5.8	18-100	0.997	0.9	3-100	87	0.999	0.16	0.47-5	< LOQ
EPO	0.998	1.3	4-100	0.997	1.3	4-100	0.999	1.4	4-200	0.997	10.5	31-100	0.990	14.2	42-100	0.989	3.0	9-100	103	0.999	0.47	1.40-5	
ESU	0.996	2.5	7-200	0.998	0.9	3-100	0.994	0.7	2-50	0.992	9.5	30-100	0.998	4.2	13-100	0.993	3.2	10-200	50	-			
HCT	0.989	13.4	40-200	0.997	4.3	13-100	0.998	0.5	2-50	0.997	5.9	18-100	0.999	4.4	13-100	0.966	8.7	26-200	107	0.998	0.18	0.54-5	0.59
HEPES	0.994	2.3	7-100	0.994	2.3	7-100	0.996	0.8	5-200	0.999	3.3	10-100	0.998	6.5	19-100	0.984	3.5	11-100	-	-			
IMI	0.975	17.4	-	0.973	6.0	18-100	0.997	1.8	5-200	0.998	5.9	18-100	0.969	39.4	-	0.927	17.0	51-200	-	0.997	0.19	0.57-5	
IRB	0.996	2.1	6-100	0.996	1.8	5-100	0.997	2.0	6-100	0.995	12.9	39-100	-			0.960	5.5	16-100	75	-			
MCPA	0.995	5.0	15-200	0.998	0.9	3-100	0.990	1.0	3-50	0.992	12.4	37-100	0.998	5.8	17-100	0.995	2.5	8-200	88	0.997	0.21	0.64-5	
MET	0.999	0.8	2-100	0.999	0.7	2-100	0.998	0.4	1-50	0.998	4.5	15-100	0.985	13.4	40-100	0.993	1.7	5-100	38	0.993	1.04	-	< LOQ
MIAA	0.990	7.3	22-200	0.996	1.8	5-100	0.992	3.9	12-200	-			-			0.984	6.6	20-200	71	0.999	0.03	0.08-5	

analyte abbrev.	tap water			mineral water			river water (Steinlach)			SPE fish extract			QuEChERS snail extract			river water (Neckar)			SPE				
	R²	LOD in µg/l	lin. range in µg/l	R²	LOD in µg/l	lin. range in µg/l	R²	LOD in µg/l	lin. range in µg/l	R²	LOD in µg/l	lin. range in µg/l	R²	LOD in µg/l	lin. range in µg/l	R²	LOD in µg/l	anal. range in µg/l	reco-very in %	R²	LOD in µg/l	lin. range in µg/l	det. conc. in µg/l
NAPHA	0.996	1.5	4-100	0.996	1.5	4-100	-			0.998	4.1	12-100	0.994	5.5	16-100	0.997	1.3	4-100	83	0.999	0.20	0.61-5	
PIN	0.988	2.7	8-100	0.988	3.2	10-100	0.996	0.7	2-50	0.999	1.6	5-100	0.999	2.7	8-100				105	-			
p-TSA	0.996	2.8	89-200	0.998	1.0	3-100	0.997	0.6	2-50	0.998	3.5	10-100	0.997	5.9	18-100	0.992	3.8	11-200	86	0.972	0.63	-	< LOQ
SAC	0.999	1.2	4-100	0.998	0.9	3-100	0.998	0.4	1-50	0.996	4.5	15-100	0.999	3.5	10-100	0.992	3.9	12-200	86	0.984	0.47	1.41-5	< LOQ
SULFA	0.997	1.4	4-100	0.998	1.0	3-100	0.997	0.6	2-50	0.994	6.5	20-100	0.998	7.1	21-100	0.996	1.3	4-100	95	0.997	1.03	-	
TER	0.995	1.6	5-100	0.995	1.6	5-100	0.998	0.4	1-50	0.998	3.2	10-100	0.999	2.1	6-100	0.997	0.9	3-100	90	0.999	0.29	0.86-5	< LOQ
THIA	0.998	1.3	4-100	0.998	1	3-100	0.999	1.3	4-200	0.999	1.4	5-100	0.999	1.9	6-100	0.992	2.2	7-100	108	0.999	0.36	1.08-5	

Table S3-7: List of the model analytes present in the standard PM, *detected in positive analysis mode using the developed NACE-MS system, sorted by effective electrophoretic mobilities* μ_{eff}. *Numbers in the second column are used in Figure 3-5A. Analytes marked with an asterisk * are excluded in the statistical evaluation in Section 3.4.5.1 in the main manuscript. Basic* pK_a, *log D values (pH 6), charge numbers (CN) and isoelectric points (pI) for aqueous solutions were extracted from Chemicalize provided by ChemAxon (11/11/2020).* μ_{eff} *values were calculated according to Equation (3-1) in Section 3.4.5.1 using crotamiton as EOF marker.*

	N°	m/z	MT	basic pK_a value	CN at pH 6	log P	log $D_{pH 6}$	pI	μ_{eff} in 10^{-9} m² s⁻¹ V⁻¹
metformin	1	130.108	5.63	12.3	2.0	-0.9	-5.7		18.59
naphazoline	2	211.123	5.70	10.2	1.0	2.2	-0.2		18.15
amantadine	3	152.143	5.83	10.7	1.0	1.5	-1.6		17.37
fenpropidin	4	274.253	6.53	10.1	1.0	5.4	2.0		13.69
tramadol	5	264.196	6.58	9.2	1.0	2.5	-0.6	11.5	13.46
propamocarb	6	189.160	6.77	9.3	1.0	-1.2	-1.2		12.61
clenbuterol	7	277.087	6.97	9.6	1.0	2.3	-0.8	11.8	11.76
pindolol	8	249.160	7.00	9.7	1.0	1.7	-1.4	11.9	11.64
propranolol	9	260.165	7.05	9.7	1.0	2.6	-0.5	11.9	11.43
prilocaine	10	221.165	7.07	8.8	1.0	2.7	0.0	11.2	11.35
amisulpride	11	370.180	7.09	8.3	1.0	0.3	-2.0	11.2	11.27
sotalol	12	273.127	7.41	9.4	1.0	-0.4	-3.0	9.7	10.06
betaxolol	13	308.222	7.41	9.7	1.0	2.5	-0.6	11.9	10.06
bisoprolol	14	326.233	7.48	9.7	1.0	2.2	-0.9	11.9	9.80
atenolol	15	267.170	7.55	9.7	1.0	0.4	-2.7	11.9	9.56
flecainide	16	415.145	7.62	9.6	1.0	3.2	0.1	11.7	9.31
nadolol	17	310.201	7.65	9.8	1.0	0.9	-2.3	11.6	9.21
acebutolol	18	337.212	7.67	9.7	1.0	1.5	-1.6	11.7	9.14
sulpiride	19	342.148	7.72	8.4	1.0	0.2	-2.0	9.3	8.97
metoprolol acid *	20	268.154	7.87	9.7	0.0	-1.2	-1.2	6.8	8.48
oseltamivir	21	313.212	8.06	9.3	1.0	1.2	-1.7	11.7	7.88
nicotine	22	163.123	8.07	8.6	1.0	1.2	-1.4		7.85
dihydro-codeine	23	302.175	8.13	9.3	1.0	1.5	-1.6	11.7	7.67
trimethoprim	24	291.145	8.21	7.2	1.0	1.3	0.3		7.43
pregabalin *	25	160.133	8.21	10.2	0.0	-1.3	-1.4	7.4	7.43
aminocarb	26	209.129	8.48	4.6	0.0	2.1	2.1	9.7	6.65
sitagliptin	27	408.125	8.48	8.8	1.0	1.3	-1.3		6.65
ketotifen	28	310.126	8.52	8.1	1.0	3.3	1.6	10.2	6.54
codeine	29	300.159	8.60	9.2	1.0	1.3	-1.7	11.5	6.32
clindamycin	30	425.187	8.70	7.6	1.0	1.0	-0.5	9.9	6.05
gabapentin *	31	172.133	9.28	9.9	0.1	-1.3	-1.3	7.4	4.62

	N°	m/z	MT	basic pK$_a$ value	CN at pH 6	log P	log D$_{pH}$ 6	pI	μ$_{eff}$ in 10^{-9} m^2 s^{-1} V^{-1}
imazalil	32	297.056	9.59	6.5	0.7	3.8	3.4		3.92
amisulpride N-oxide *	33	386.174	9.69	3.8	0.0	-0.9	-0.9	8.8	3.71
sulpiride N-oxide *	34	358.143	10.16	3.8	0.0	-0.8	-0.8	7.0	2.75
melamine	35	127.073	10.20	9.6	1.0	-0.6	-2.5		2.68
2,4-dimethyl-chinolin	36	158.096	10.54	5.9	0.5	2.8	2.5		2.04
ritalinic acid *	37	220.133	10.89	10.1	0.0	-0.4	-0.4	7.1	1.43
acridine	38	180.081	11.52	6.2	0.6	3.5	3.1		0.43
crotamiton	39	204.138	11.81	-0.6	0.0	3.1	3.1		0.00

Table S3-8: List of the analytes detected in negative analysis mode using the developed NACE-MS system, sorted by effective electrophoretic mobilities μ_{eff}. Roman numerals in the second column are used in Figure 3-5B. Acidic pK_a, log D values (pH 6), and charge numbers (CN) for aqueous solutions were extracted from Chemicalize provided by ChemAxon (11/11/2020). μ_{eff} values were calculated according to Equation (3-1) in Section 3.4.5.1 using hydrochlorothiazide as EOF marker.

	N°	m/z	MT	acidic pK_a value	CN at pH 6	log P	log $D_{pH\ 6}$	$|\mu_{eff}|$ in E-09 m^2 s^{-1} V^{-1}	$|\mu_{eff,\ aq}|$ in 10^{-9} m^2 s^{-1} V^{-1}
difluoro acetic acid	I	94.995	5.17	2.0	-1.0	0.2	-3.2	22.23	29.80
acesulfame	II	161.987	5.19	3.0	-1.0	-0.6	-1.5	22.10	25.30
trichloro acetic acid	III	160.897	5.29	1.7	-1.0	1.5	-2.0	21.36	
dichloro acetic acid	IV	126.936	5.36	2.3	-1.0	1.1	-2.2	20.88	26.35
saccharin	V	181.992	5.46	1.9	-1.0	0.5	-0.5	20.18	22.39
p-toluene sulfonic acid	VI	171.012	5.58	0.7	-1.0	0.9	-0.7	19.40	22.51
trifluoro acetic acid	VII	112.986	6.05	1.0	-1.0	0.9	-2.6	16.58	18.92
monobromo acetic acid	VIII	136.924	6.56	2.9	-1.0	0.5	-2.6	14.02	13.39
monoiodo acetic acid	IX	184.911	7.26	3.1	-1.0	0.7	-2.1	11.09	13.82
MCPA	X	199.017	7.60	3.1	-1.0	3.3	-0.2	9.86	6.64
4-hydroxybenzoic acid	XI	137.024	11.69	4.5	-1.0	1.6	-0.2	0.65	3.96
sulfamethoxazole	XII	252.045	11.91	6.2	-0.4	0.8	0.6	0.33	4.27
1*H*-benzotriazole	XIII	118.041	12.17	8.3	0.0	1.4	1.3	0.00	0.00
hydrochloro-thiazide	XIV	295.957	12.17	9.1	0.0	-0.6	-0.6	0.00	0.00

4. Development and application of a hydrophilic interaction liquid chromatography mass spectrometry method for the analysis of ionic analytes in environmental samples

4.1 Abstract

In this work, a method development of two new hydrophilic interaction liquid chromatography coupled to mass spectrometry (HILIC-MS) methods complementary to reversed-phase liquid chromatography (RPLC)-MS analysis of polar compounds is described. The HILIC-MS methods were optimized with regard to peak areas, peak symmetry, chromatographic resolution and effects of sample composition. The final methods were: 1) HILIC+, capable to separate 15 basic analytes using 5 mM NH_4OH + 0.1% formic acid (FA) as aqueous eluent and acetonitrile (MeCN) + 0.1% FA as organic eluent and 2) HILIC–, capable to separate 18 acidic analytes using 20 mM NH_4HCO_3 + 0.01% FA as aqueous eluent and MeCN + 0.01% FA as organic eluent. 5% water in samples dissolved in MeCN was found to provide best peak symmetry. Both methods were able to cover analytes with a broad range of physicochemical characteristics (e.g. polarity (-5.6 $\leq$ log $D_{pH\,7.4} \leq$ 4.2) and charge).

The comparison revealed that average limits of detection (300-660 ng/l) were not significantly different between the methods (t-test, α = 0.05). We investigated matrix effects for three sample preparation techniques, solid-phase extraction, electromembrane extraction and field-step electrophoresis. A high matrix tolerance (average matrix effects $\approx$90$\pm$30%) was demonstrated for most of the analytes in these matrices.

4.2 Introduction

The potential of hydrophilic interaction liquid chromatography (HILIC) as a complementary separation technique to reversed-phase liquid chromatography (RPLC) for the analysis of polar compounds has been intensively discussed in the past and HILIC can now be seen as an established analytical technique for this type of analytes [20, 80]. Consequently, many new stationary phases have been developed, most of them based on silica or using a polymer [195]. For silica-bonded stationary phases, different chemical modifications like amide, diol or sulfoalkylbetaine are used. The latter can be assigned to the group of zwitterionic (ZIC) stationary phases. This modification allows to simultaneously separate compounds being anionic or cationic in the eluent chosen. It can be used both for the separation of biomacromolecules such as proteins [196] and for the separation of small molecules, such as pharmaceuticals, metabolites, drugs of abuse and many more as it has recently been reviewed by Erkmen et al. [197].

Unlike most other chromatographic techniques, the interlayer between stationary phase and mobile phase is vital for the HILIC separation process. It is thus crucial to keep the water content above 3% to ensure sufficient hydrophilic partitioning [198]. Other than in for example RPLC, retention of analytes can be traced back to dipole-dipole / hydrogen bonding and to electrostatic interactions, thus adding a second dimension of selectivity.

With regard to the coupling to mass spectrometry (MS), in most cases, lower detection limits (LODs) than in RPLC-MS were observed due to a better compatibility of thehigh organic solvent content and the electrospray ionization (ESI) process [199]. Common buffer electrolytes are ammonium salts of acetate and formate. Ammonium hydroxide or carbonate are also suitable electrolytes, if higher pH values are necessary. Both isocratic and gradient elution are used, with isocratic elution holding the major share. Resolution and analysis time can be influenced by gradient elution increasing polarity or the salt concentration of the mobile phase. However, these higher salt concentrations may impair ionization efficiency when using MS as detection technique. Ion pair reagents such as trifluoroacetic acid, often added in HILIC methods to increase retention of acidic analytes at low pH values [200], should be adjusted carefully -if used- as they can both interfere with the HILIC mechanism and suppress MS signals [201].

With regard to the sample composition, at least 80% organic solvent (in most cases acetonitrile (MeCN)) have to be present in the sample to ensure sufficient retention of hydrophilic analytes. Consequently, this increases LODs as aqueous samples common in environmental analysis have to be diluted. In contrast, good compatibility is given when using sample preparation techniques like liquid-liquid extraction or solid-phase extraction (SPE). Matrix effects can be critical in HILIC especially if high concentrations of inorganic anions and cations are present [202] sometimes necessitating further sample preparation steps. SPE is the most common sample preparation technique for different kind of matrices.

In this study, two more sample preparation techniques were investigated with regard to their ability to remove matrix interferences prior to HILIC analysis: electromembrane extraction (EME) and field-step electrophoresis (FSE). Both techniques have been investigated and described in detail in Chapters 1 and 6 as sample preparation technique for the enrichment of ionic compounds relevant in environmental analysis. The model analyte system was chosen based on previous work (see Chapter 3) covering a broad range of analytes differing in their physicochemical characteristics, e.g. polarity, charge, functional groups.

In this work, we developed two new HILIC-MS methods for the analysis of basic or acidic micropollutants ionizable under the separate conditions. The methods are called HILIC+ and HILIC– using a common zwitterionic stationary phase. Different buffering salts at various concentrations as well as different gradients were tested and optimized in a univariate approach. The main performance criteria were sensitivity, peak symmetry and chromatographic resolution taking into account the fraction of acetonitrile in the sample.
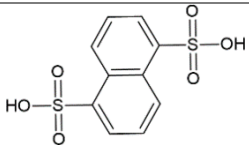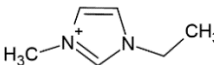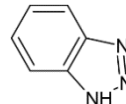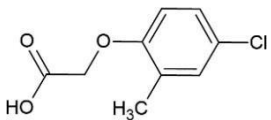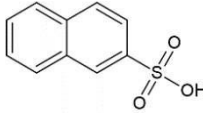
In a second step, we compared the two HILIC methods (HILIC+ and HILIC–) with already existing RPLC-MS methods [2], optimized for bases and acids (RPLC+ and RPLC–). LODs were determined for aqueous standards and spiked river water samples after sample preparation using SPE, EME and FSE. Matrix effects were determined for the resulting eluates or fractions and the raw samples.
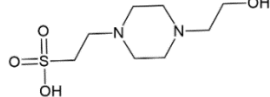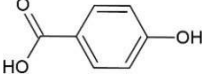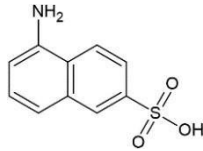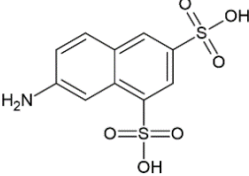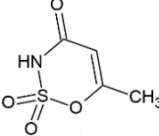
4.3 Materials and methods
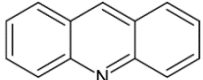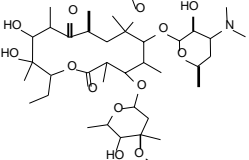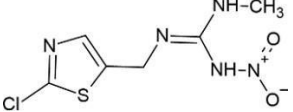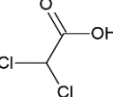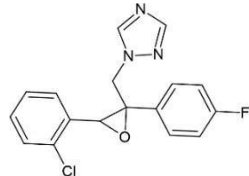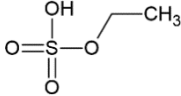
4.3.1 Chemicals
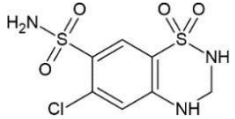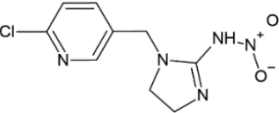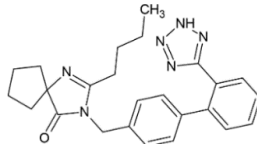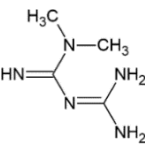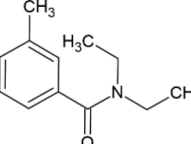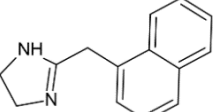
Acetonitrile (MeCN, LC-MS grade), ammonium hydroxide (NH$_4$OH, 25% aqueous solution, LC-MS grade), formic acid (FA, 98%), isopropanol (LC-MS grade), methanol (LC-MS grade), sodium hydroxide (NaOH, $\geq$ 98%), and water (LC-MS grade) were purchased from Sigma-Aldrich (Steinheim, Germany). Hydrochloric acid (HCl, 32% aqueous solution) was obtained from Fisher Scientific (Waltham, Massachusetts, USA). Acetic acid (HAc, 100%), ammonium acetate (NH$_4$Ac, 98%) and ammonium hydrogen carbonate (NH$_4$HCO$_3$, LC-MS grade) were delivered by Merck (Darmstadt, Germany). Suppliers and purity of the model analytes are listed in Table 4-1. Stock solutions (in MeOH) and aqueous working solutions were stored at -20 °C before use.
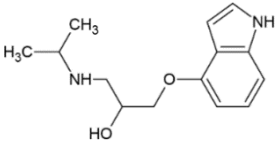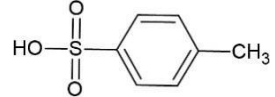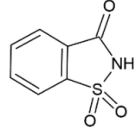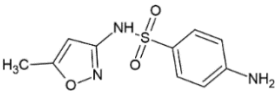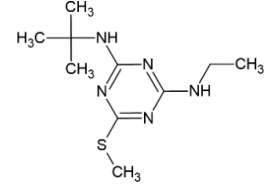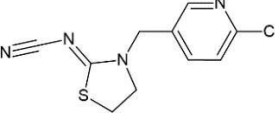
Table 4-1: Model analytes, suppliers thereof and their physicochemical properties sorted alphabetically. pKₐ, log P and log D values (at pH 3 and 7.4, corresponding to the pH of the aqueous eluent in HILIC) were taken from Chemicalize provided by ChemAxon (11/02/2021). "+" or "-" denote, by which methods the analyte was detectable. Methods for bases: RPLC+ and HILIC+ and for acids RPLC- and HILIC- (see Section 4.3.4).

analyte	analyte abbrev.	HILIC / RPLC	m/z detected	log P	log $D_{pH\,3}$	log $D_{pH\,7.4}$	strong. pK_a (acidic)	strong. pK_a (basic)	molecular structure	supplier & purity
1,5-naphthalene disulfonic acid	1,5-NDSA	-	286.969	1.3	-3.4	-3.4	-2.7			Sigma Aldrich, 97%
1-ethyl-3-methyl-imidazolium	1-E-3-MIM	+	111.092	-3.1	-3.1	-3.1	-	-		Sigma Aldrich, ≥ 95%
1*H*-benzo-triazole	BTA	-, +	118.041, 120.056	1.4	1.3	1.3	9.0	0.2		Sigma Aldrich, 99%
2-methyl-4-chlorophenoxy acetic acid	MCPA	-	199.017	3.3	2.3	-1.0	3.4			Sigma Aldrich, ≥ 98%
2-naphthalene sulfonic acid	2-NSA	-	207.012	2.1	-0.2	-0.2	-1.8			Sigma Aldrich, ≥ 95%

analyte	analyte abbrev.	HILIC / RPLC	m/z detected	log P	log $D_{pH\ 3}$	log $D_{pH\ 7.4}$	strong. pK_a (acidic)	strong. pK_a (basic)	molecular structure	supplier & purity
4-(2-hydroxyethyl)-1-piperazine-ethane sulfonic acid	HEPES	-, +	237.092, 239.107	-3.1	-3.1	-3.4	-1.3	7.3		Fluka, 99.5%
4-hydroxy-benzoic acid	4-HBA	-	137.024	1.6	1.3	-1.6	4.4			Fluka, ≥ 98%
5-amino-2-naphthalene sulfonic acid	5-A-2-NSA	-	222.023	1.1	1.0	-1.1	-2.2	3.6		Sigma Aldrich, ≥ 95%
7-amino-1,3-naphthalene disulfonic acid	7-A-1,3-NDSA	-	301.980	-1.6	-2.2	-4.3	-2.8	3.6		Sigma Aldrich, ≥ 98%
acesulfame	ACE	-	161.986	-0.6	-0.8	-1.5	3.0			Sigma Aldrich, ≥ 99%

analyte	analyte abbrev.	HILIC / RPLC	m/z detected	log P	log $D_{pH\,3}$	log $D_{pH\,7.4}$	strong. pK_a (acidic)	strong. pK_a (basic)	molecular structure	supplier & purity
acridine	ACR	+	180.0808	3.4	1.8	3.5		6.2		Sigma Aldrich, 97%
clarithromycin	CLA	+	748.484	3.2	-0.3	1.6	12.5	9.0		Sigma Aldrich, ≥ 98%
clothianidin	CLO	-, +	248.002, 250.016	0.7	0.5	0.5	15.6	0.4		Sigma Aldrich, ≥ 98%
dichloro acetic acid	DCAA	-	126.936	1.1	0.3	-2.5	2.3			Merck, ≥ 98%
epoxiconazole	EPO	+	330.080	3.7	3.7	3.7		2.0		Sigma Aldrich, ≥ 98%
ethyl sulfate	ESU	-	124.991	-0.5	-2.5	-2.5	-2.1			Sigma Aldrich, ≥ 95%

analyte	analyte abbrev.	HILIC / RPLC	m/z detected	log P	log $D_{pH\,3}$	log $D_{pH\,7.4}$	strong. pK_a (acidic)	strong. pK_a (basic)	molecular structure	supplier & purity
hydrochloro-thiazide	HCT	-	295.957	-0.6	-0.6	-0.6	9.1			Sigma Aldrich, $\geq 99\%$
imidacloprid	IMI	-	254.045	0.9	-1.0	0.9	9.4	5.3		Sigma Aldrich, $\geq 98\%$
irbesartan	IRB	-, +	427.225, 429.240	5.4	4.4	4.2	5.9	4.1		Sigma Aldrich, $\geq 98\%$
metformin	MET	+	130.109	-2.6	-5.8	-5.6		12.3		Alfa Aesar, 97%
N,N-diethyl-m-toluamide	DEET	+	192.138	2.5	2.5	2.5	-1.0			Sigma Aldrich, $\geq 95\%$
naphazoline	NAPHA	+	211.123	2.2	-0.2	-0.1		10.2		Sigma Aldrich, $\geq 98\%$

analyte	analyte abbrev.	HILIC / RPLC	m/z detected	log P	log $D_{pH\,3}$	log $D_{pH\,7.4}$	strong. pK_a (acidic)	strong. pK_a (basic)	molecular structure	supplier & purity
pindolol	PIN	+	249.160	1.7	-1.5	-0.5	14.1	9.7		Sigma Aldrich, 98%
p-toluene sulfonic acid	p-TSA	-	171.012	0.9	-0.7	-0.7	-2.1			Alfa Aesar, 90%
saccharin⁻	SAC	-	181.992	0.5	-0.3	-0.5	1.9			Sigma Aldrich, ≥ 98%
sulfa-methoxazole	SULFA	-, +	252.045, 254.059	0.8	0.8	0	6.2	2.0		Sigma Aldrich, ≥ 98%
terbutryn	TER	+	242.144	3.7	0.9	2.8	14.3	6.7		Sigma Aldrich, ≥ 98%
thiacloprid	THIA	+	253.032	2.1	2.0	2.1	1.6			Sigma Aldrich, ≥ 98%

4.3.2 Eluent preparation

Eluents were prepared freshly dissolving the buffer salt in H_2O (see Table 4-2). pH was measured using a pH meter (inoLab pH 7110, Xylem Analytics Germany, WTW, Weinheim, Germany). Eluents containing MeCN were prepared dissolving 0.1 or 0.01% FA or NH_3 to improve ionization efficiency. All eluent compositions used for HILIC+ and HILIC– are listed in Table 4-2. For RPLC-MS separation, a gradient elution using H_2O with 0.1% FA (v/v) (pH 2.7) and MeOH with 0.1% FA (v/v) was accomplished. All eluents were degassed via ultrasonication for 10 min.

Table 4-2: 6 eluent compositions investigated for HILIC+ and 10 eluent compositions for HILIC– within the scope of the HILIC-MS method development. pH values were measured using a pH meter.

HILIC+		HILIC-	
Eluent	**pH**	**Eluent**	**pH**
5 mM NH_4Ac + 0.1% FA	2.95	5 mM NH_4Ac + 0.1% FA	2.95
12.5 mM NH_4Ac + 0.1% FA	3.46	12.5 mM NH_4Ac + 0.1% FA	3.46
20 mM NH_4Ac + 0.1% FA	3.81	20 mM NH_4Ac + 0.1% FA	3.81
5 mM NH_4OH + 0.1% FA	2.99	5 mM NH_4OH + 0.1% FA	2.99
12.5 mM NH_4OH + 0.1% FA	3.43	12.5 mM NH_4OH + 0.1% FA	3.43
20 mM NH_4OH + 0.1% FA	3.90	20 mM NH_4OH + 0.1% FA	3.90
		5 mM NH_4HCO_3 + 0.01% FA	6.70
		12.5 mM NH_4HCO_3 + 0.01% FA	7.00
		20 mM NH_4HCO_3 + 0.01% FA	7.38
		20 mM NH_4HCO_3 + 0.01% NH_3	8.29

4.3.3 Samples and sample preparation

4.3.3.1 Collection and preparation of water samples (*A1* and *N1*)

The source water sample *A1* was collected near the source of the river Ammer close to Herrenberg, Germany. The river water sample *N1* was collected from the river Neckar in Tübingen, a few hundred meters downstream of a wastewater treatment plant (WWTP, 110000 population equivalents, collection in 09/2020). The samples were collected in polypropylene vessels, filtered with a CHROMAFIL Xtra PTFE-45/25 filter (Macherey-Nagel, Düren, Germany) and afterwards stored in a borosilicate vessel at -20 °C before use. The sample *N1 dil.* was prepared using one volumetric part of sample *N1* and four volumetric parts LC-MS grade H_2O. Spiking was conducted afterwards in the same way as described in Section 4.3.3.2.

4.3.3.2 Spiking

Methanolic stock solutions with a concentration of 20 mg/l containing all analytes were prepared using 1 g/l methanolic stock solutions of each analyte. Stock and working solutions were stored at -20 °C before use. Standards (MeCN/H_2O 95:5, v/v for HILIC,

H_2O for RPLC), SPE eluates, EME extracts and FSE matrices were spiked with the analyte mixtures to reach a constant ratio of analyte mix:sample of 1:99 (v/v) to keep the methanol content low and constant. Concentrations in the final samples were 10, 50, 100, 250, 500, 750, 1000 and 2500 ng/l using HILIC-MS and 100, 1000, 5000 and 10000 ng/l using RPLC-MS. For the determination of LODs in matrix, fewer concentration steps were used (100, 500, 1000 and 2500 ng/l for HILIC-MS and 100, 1000, 5000 and 10000 ng/l for RPLC-MS). For the determination of matrix effects, samples *N2* and *N2 dil.* were spiked to reach a final concentration of 1000 ng/l.

4.3.3.3 Solid-phase extraction

To judge possible matrix effects of the SPE procedure, we used a source water sample (*A1*) and spiked the extracts after the SPE procedure (sample *SPE*). For optimized retention of ionic compounds, samples were acidified to pH 1 with HCl (for anions) or alkalized to pH 11 with NH_4OH (for cations). Prior to loading the sample onto the SPE column (Oasis HLB, 30 mg, Waters, Milford, Massachusetts, USA), the cartridge was washed with 3×1 ml MeOH (LC-MS grade) and conditioned with 3×1 ml H_2O (LC-MS grade). The SPE procedure was optimized beforehand (see Chapter 3) indicating highest extraction efficiencies when eluting with MeOH + 2% FA (v/v) for cations or with an elution medium of 5% NH_4OH in MeOH for anions. After loading 5 ml acidified/alkalized source water sample *A1* on the SPE column, elution was conducted without further washing step. The eluate was evaporated to dryness under a gentle stream of nitrogen, the concentrated residue was redissolved in 0.5 ml and spiked with the analyte mix according to Section 4.3.3.2. The composition of the reconstitution solvent was adapted to the subsequent analysis technique (RPLC-MS: H_2O, HILIC-MS: MeCN/H_2O (95:5, v/v)). Analysis of the spiked SPE extracts followed via RPLC-MS and HILIC-MS.

4.3.3.4 Electromembrane extraction

To simulate the composition of EME extracts, aqueous samples (sample *EME*) containing 20 mM NaCl were spiked and prepared as described in Section 4.3.3.2.

4.3.3.5 Field-step electrophoresis

FSE fractions were spiked and analyzed using the two methods HILIC– and RPLC– (sample *FSE*). The protocols for the FSE experiment and sample preparation are described in detail in Chapter 6. In brief, after the FSE experiment, fractions were filtered with CHROMAFIL Xtra PTFE-45/25 filter (Macherey-Nagel, Düren, Germany), pooled (F_{3-5}, see Section 6.3.3.1) and evaporated to dryness under a gentle stream of nitrogen. The concentrated residue was redissolved in the same volume of a proper solvent, if not stated otherwise and spiked with the analyte mix according to Section 4.3.3.2. The composition of the solvent for reconstitution was adapted to the subsequent analysis technique (RPLC-MS: H_2O, HILIC-MS: MeCN/H_2O 95:5, v/v). Analysis of the spiked FSE extracts followed via RPLC– and HILIC–.

4.3.4 LC-MS analysis

For HPLC-MS analysis, a 1260 Infinity LC system coupled to a 6550 iFunnel Q-TOF LC/MS system (Agilent Technologies, Waldbronn, Germany) was used. A jet-stream

electrospray ionization (ESI) source was operated with a nebulizer pressure of 35 psig, a drying gas temperature of 160 °C, a flow rate of 16 l/min and a fragmentor voltage of 360 V. In the positive/negative ionization mode capillary voltage was set to +/-4000 V, skimmer voltage to 65 V and a nozzle voltage to 500 V. The mass range was 40-1000 m/z with a data acquisition rate of 1 spectrum/s. The sheath gas temperature was set to 325 °C with a flow rate of 11 l/min. For internal calibration, solutions of purine and HP0921 (Agilent Technologies, Waldbronn, Germany, m/z = 121.0508, 922.0097) in MeOH/H_2O (95:5, v/v) were used and introduced via a reference nebulizer.

4.3.4.1 C18 Zorbax Eclipse (RPLC-MS)

10 µl aliquots of samples were injected onto a Zorbax Eclipse Plus C18 column (2.1 x 150 mm, 3.5 µm, narrow bore, Agilent Technologies, Waldbronn, Germany). Additionally, a guard column (2.1 x 15 mm, 5 µm, narrow bore, Agilent Technologies, Waldbronn, Germany) was used. For separation, a gradient elution at a flow rate of 0.3 ml/min using A) water and B) methanol, both containing 0.1% FA, was chosen. After 1 min, the initial content of 95% water was decreased to 5% water over 7 min. This mobile phase was kept for another 7 min of 5 % water and then increased over 5 min to 95% water. The same gradient was used for both MS polarities (RPLC+ and RPLC–).

4.3.4.2 SeQuant ZIC-HILIC (HILIC-MS)

5 µl aliquots of samples were injected onto a SeQuant ZIC-HILIC (2.1 x 150 mm PEEK coated, 3.5 µm, 100 Å, Merck, Darmstadt, Germany) for the analysis of polar compounds. In addition, a guard column (2.1 x 20 mm PEEK coated, Merck, Darmstadt, Germany) was placed in front of the column with a coupler.

For separations using positive analysis mode (HILIC+, positive MS polarity), a gradient elution (gradient *95_50*) at a flow rate of 0.3 ml/min using aqueous 5 mM NH_4OH and MeCN, both containing 0.1% FA (v/v), was chosen. The initial content of 95% MeCN was decreased to 50% over 11 min. This mobile phase was kept for one minute and then, the MeCN content increased back to 95% MeCN over 0.5 min. For a proper re-equilibration, this composition was kept for another 11 min before injecting the next sample, leading to a total analysis time of 23.5 min. The re-equilibration step used an increased flow rate of 0.5 ml/min during min 12-19.

For separations using negative analysis mode (HILIC–, negative MS polarity) a gradient elution (gradient *90_40*) at a flow rate of 0.3 ml/min using aqueous 20 mM NH_4HCO_3 and MeCN, both containing 0.01% FA (v/v), was chosen. The initial content of 90% MeCN was decreased to 40% over 15 min. This mobile phase was kept for one minute and then, the acetonitrile fraction was increased to 90% MeCN over 0.5 min. For a proper re-equilibration, this composition was kept for another 8 min before injecting the next sample, leading to a total analysis time of 24.5 min. The re-equilibration step used an increased flow rate of 0.5 ml/min during min 16-22.

A second gradient (*90_80_40*) in negative analysis mode (HILIC–) using different eluent compositions with A) MeCN and B) 20 mM NH_4HCO_3, both containing 0.01% FA (see Table 4-2) was investigated. The MeCN content was decreased from 90% to 80% in 7 min and then to 40% MeCN in another 8 min. This mobile phase was kept for one minute and then, the acetonitrile fraction was increased to 90% MeCN over 0.5 min. For

a proper re-equilibration, this composition was kept for another 8 min before injecting the next sample, leading to a total analysis time of 24.5 min. The re-equilibration step used an increased flow rate of 0.5 ml/min during min 16-22.

Care had to be taken to remove salt deposits in the spray chamber on a daily basis.

4.3.5 Data evaluation and method validation

Extracted ion chromatograms (EICs) were extracted and evaluated from mass profiles with a mass accuracy of 0.01 m/z using Mass Hunter Qualitative Software (Agilent, V10.0). MassHunter Quantitative Software (V10.1) was used to create calibration curves using the peak areas (PAs) and to calculate symmetry values (CSV). LODs were estimated in different matrices using standard addition according to DIN 32645 with α = 0.05.

Chromatographic resolution R between two consecutive peaks was determined via Equation (4-1), using retention times t_1 and t_2 of two neighboring peaks 1 and 2.

$$R(1,2) = \frac{2(t_2 - t_1)}{t_2 + t_1} \tag{4-1}$$

For n peaks, the total chromatographic resolution (TCR) was calculated summing the R values of all pairs of spiked model analytes. TCR was used to judge the selectivity of the chromatographic method.

$$TCR = \sum_{i=2}^{n} R(i-1, i) = \sum_{i=2}^{n} \frac{2(t_i - t_{i-1})}{t_i + t_{i-1}} \tag{4-2}$$

In order to estimate the peak symmetry for all model analytes, we determined the symmetry value of each peak i (CSV$_i$) by the MassHunter Quantitative Software (V10.1). The deviations of 1 (corresponds to symmetric peak) were averaged (average symmetry deviation, ASD) according to Equation (4-3) for n peaks.

$$ASD = \frac{1}{n} \sum_{i=1}^{n} (CSV_i - 1)^2 \tag{4-3}$$

Matrix effects were estimated via the PA of analytes when spiking at a concentration of 1000 ng/l compared to the PA obtained by the analysis of a reference standard.

All figures were created with Origin 2020 (OriginLab Corporation, Northampton, Massachusetts, USA) and Microsoft Excel 2019 (Microsoft Corporation, Redmond, Washington, USA). Statistical evaluation was conducted using IBM SPSS Statistics 26 (IBM, Armonk, New York, USA).

4.4 Results and discussion

4.4.1 HILIC-MS method development

The method development was conducted using an analyte mix containing 15 model compounds detected in positive analysis mode and 18 compounds detectable in negative analysis mode (see Table 4-1) using different eluents, see Section 4.3.2. We focused on three parameters: 1) sensitivity, 2) peak symmetry and 3) resolution between the model

analytes. For a quantitative comparison, average peak areas or peak heights (PAs or PHs) were calculated for each eluent composition (and each gradient in negative analysis mode). Chromatographic resolution (TCR) and average deviations in symmetry (ASD) were calculated according to Equations (4-2) and (4-3) (see Section 4.3.5). A univariate approach was used for the optimization of gradient, buffer type and concentration in eluent as well as sample composition. Results showed that separate methods for acids and bases were advantageous with regard to the performance parameters chosen (for instance compare values of PHs in Table 4-4).

4.4.1.1 Positive analysis mode (HILIC+)

Preliminary experiments proved a gradient starting at 95% of MeCN content decreasing to 50% in 11 min to be as a good starting point. Two different buffer types (NH_4Ac and NH_4OH) and three concentrations (5, 12.5 and 20 mM) thereof were investigated and evaluated with regard to the performance criteria. All results are summarized in Table 4-3, highlighting best performance in green (highest PAs or PHs and TCR values (Equation (4-2)) and lowest values for ASD (Equation (4-3)). TCR values showed no preference towards one buffer composition and were thus not considered further as selection criterion. Values of PAs, PHs and ASD showed no significant differences (t-test, α = 0.05) between the separations with regard to the type of buffer. Comparing these values at concentrations of 5 mM, performance proved best using NH_4OH as buffer. With increasing concentration of salt, the ionization efficiency decreased significantly for all analytes using NH_4OH (but not for NH_4Ac), indicating ion suppression effects or enhanced ion pair formation. Choice was made to further use 5 mM NH_4OH with 0.1% FA as aqueous buffer due to its superior performance with regard to highest sensitivity and peak symmetry.

Table 4-3: Heat map for the eluent optimization of the HILIC+ method. The method was investigated using gradient 95_40 (see Section 4.3.4.2) with regard to the performance criteria (average PAs and PHs, ASD and TCR) using different concentrations (5, 12.5 and 20 mM) and type of salt (NH_4Ac and NH_4OH) in the aqueous eluent. 0.1% FA were added to the aqueous and to the MeCN eluent. Average PAs and PHs were determined using obtained PAs, PHs of the 15 model analytes listed in Table 4-5 by the analysis of a 10 µg/l standard (MeCN/H_2O 95:5, v/v). ASD and TCR values were calculated according to Equations (4-3) and (4-2), respectively (Section 4.3.5). Colors code the performance with highest average PAs, PHs and TCR values as well as lowest ASD values highlighted in green and worst performance in red (column-wise).

conc. in mM	salt	average		ASD	TCR
		PA	PH		
5		1.8E+06	1.6E+05	3.6	1.58
12.5	NH_4Ac	1.8E+06	1.9E+05	2.3	1.56
20		1.9E+06	1.8E+05	2.4	1.55
5		2.8E+06	2.6E+05	2.1	1.59
12.5	NH_4OH	2.2E+06	1.8E+05	3.0	1.55
20		2.1E+06	1.7E+05	2.6	1.55

4.4.1.2 Negative analysis mode (HILIC–)

Preliminary experiments indicated that starting the gradient with 90% MeCN (gradient *90_40*, see Section 4.3.4.2) was the best starting point for further method development. As ionization efficiencies were inacceptable for analytes detected in negative analysis mode using any of the three eluents chosen in HILIC+ (see Section 4.4.1.1), a fourth, more basic eluent composition was investigated: NH_4HCO_3 was chosen using 0.01% FA as additive (resulting in pH values between 6.7-7.4, see Table 4-2). The gradient was slightly modified (gradient *90_80_40*, see Section 4.3.4.2) in order to reach acceptable resolution for the stereoisomers 1,5-NDSA and 2,6-NDSA (see Section 4.3.2). The corresponding chromatograms are shown in Figure 4-1. The slow gradient of 10% per 7 min using gradient *90_80_40* (compared to the steady gradient of 10% per 3 min using gradient *90_40*) results in stronger retention for the four polar analytes 1,5-NDSA, 2,6-NDSA, 7-A-1,3-NDSA and HEPES. However, the increase in resolution was accompanied by a significant reduction (almost factor of 2) in PHs (see also Table 4-4). With regard to a broader screening, we preferred the method with better LODs enabling to quantify 18 acidic analytes.
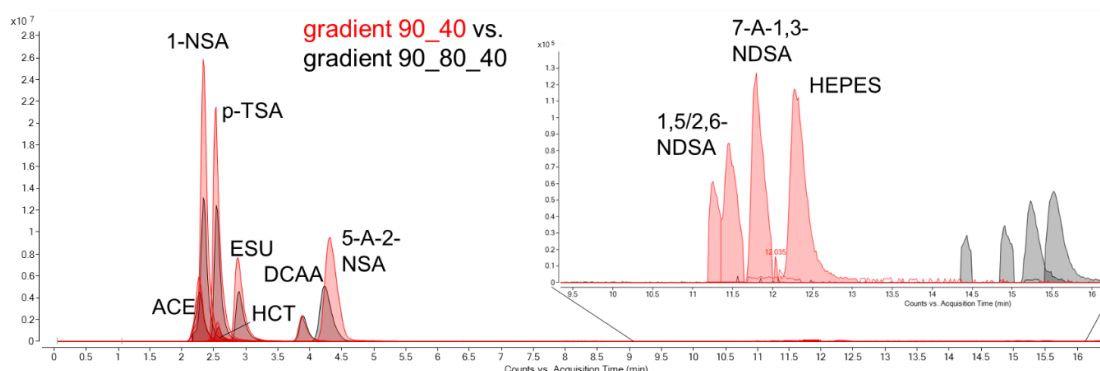
Figure 4-1: EICs obtained by using the two different gradients 90_40 (red chromatograms) and 90_80_40 (black chromatograms) during method development of HILIC–. The gradients used are further described in the text and in Section 4.3.4.2. Analyte concentration and sample composition was 10000 ng/l and MeCN/H$_2$O 95:5 (v/v), respectively. Injection volume was 5 µl. For better clarity, only EICs of selected analytes listed in Table 4-1 are shown.

From Figure 4-1 and Table 4-4, it can be seen that highest sensitivity is obtained using the eluent with NH_4HCO_3 and 0.01% FA, predominantly due to the elevated pH of the eluent, which promotes the ionization of the acidic compounds. A higher pH values was not applicable with regard to the advised pH range of the stationary phase material. No significant trends with regard to symmetry (ASD values) and resolution (TCR values) were observed. With the exception of a few elution conditions (5 mM NH_4Ac and 5/12.5 mM NH_4OH using the gradient *90_80_40*), symmetry and resolution were acceptable for the eluent compositions investigated here.

With regard to the sensitivity in general, as can be seen in Figure 4-1, there is a noticeable shift towards lower sensitivities for analytes with higher retention, probably caused by the higher H_2O content in the eluent composition impairing ionization efficiency. We tried to further enhance LODs especially for the analytes with strong retention on the stationary phase adding ammonia, known to increase ionization of acidic analytes in HILIC [203]. However, even a small concentration (0.01%) added led to a strong decrease in retention for most of the analytes and was not further investigated.

Finally, for HILIC– the elution was made mixing an aqueous buffer with 20 mM NH_4HCO_3 + 0.01% FA using a gradient starting at 90% MeCN + 0.01% FA decreasing to 40% in 16 min. This method provided the highest sensitivity among all buffer compositions investigated here (see Table 4-4).

Table 4-4: Heat map for the eluent and gradient optimization of the HILIC– method. Two gradients were investigated with regard to their performance (average PAs, PHs, ASD and TCR) using different salt type (NH_4HCO_3, NH_4Ac and NH_4OH) and concentrations (5, 12.5 and 20 mM) in the aqueous eluent. Additionally, FA was added to the aqueous and organic eluent at a percentage of 0.01% FA for NH_4HCO_3 and 0.1% FA for the other three salts. PAs and PHs were determined from the PAs and PHs of the 18 analytes listed in Table 4-6 using data from the injection of a standard in MeCN/H_2O 95:5, (v/v) at a concentration of 10 µg/l. ASD and TCR values were calculated according to Equations (4-3) and (4-2), respectively (Section 4.3.5). Color coded the performance with highest average PA, PH and TCR values as well as lowest ASD values highlighted in green and worst performance in red (column-wise).

gradient	conc. in mM	eluent buffer salt	average		ASD	TCR
			PA	PH		
90_80_40	5	NH_4HCO_3	8.1E+06	5.0E+05	2.3	0.53
	12.5		8.0E+06	4.9E+05	1.3	0.62
	20		3.5E+07	2.1E+06	1.5	0.65
	5	NH_4Ac	2.0E+06	2.0E+05	3.3	0.36
	12.5		1.4E+06	1.6E+05	3.4	0.74
	20		5.0E+06	5.2E+05	1.2	0.46
	5	NH_4OH	3.0E+06	3.0E+05	2.9	0.35
	12.5		6.6E+06	6.4E+05	6.3	0.45
	20		3.9E+06	3.8E+05	1.6	0.45
90_40	5	NH_4HCO_3	9.4E+06	5.6E+05	1.2	0.55
	12.5		2.3E+07	1.4E+06	3.0	0.64
	20		6.5E+07	3.7E+06	1.2	0.66
	5	NH_4Ac	7.6E+05	8.0E+04	1.3	0.70
	12.5		2.9E+06	3.4E+05	1.1	0.53
	20		3.9E+06	4.3E+05	1.1	0.46
	5	NH_4OH	2.0E+06	2.0E+05	2.6	0.74
	12.5		6.1E+06	6.1E+05	2.0	0.56
	20		2.2E+06	2.0E+05	2.2	0.45

4.4.1.3 Sample composition

Sample composition is described as an important parameter in HILIC separations as too high contents of H_2O in the sample could reduce retention of polar target analytes and impact peak shapes [204]. We investigated the impact of the fraction of water in the sample solution between 1 and 10% on the separation by the HILIC+ and HILIC– method. Results are shown in Figure 4-2A and B. As expected, the best performance was observed for lowest H_2O content of 1% for both HILIC methods. Whereas HILIC+ was robust with regard to the H_2O content between 1 and 5%, the separation efficiency decreased with an increase to 5% H_2O especially for analytes with low retention when using HILIC–. Further increasing the H_2O content from 5 to 10% revealed lower retention times for all model analytes. In case of HILIC+, this was accompanied by a significant decrease in separation efficiency (see for instance the signal of NAPHA at RT 5.5, Figure 4-2A) and

the appearance of peak splitting [205] (see for instance signals of PIND, 1-E-3-MIM and METF, Figure 4-2A).
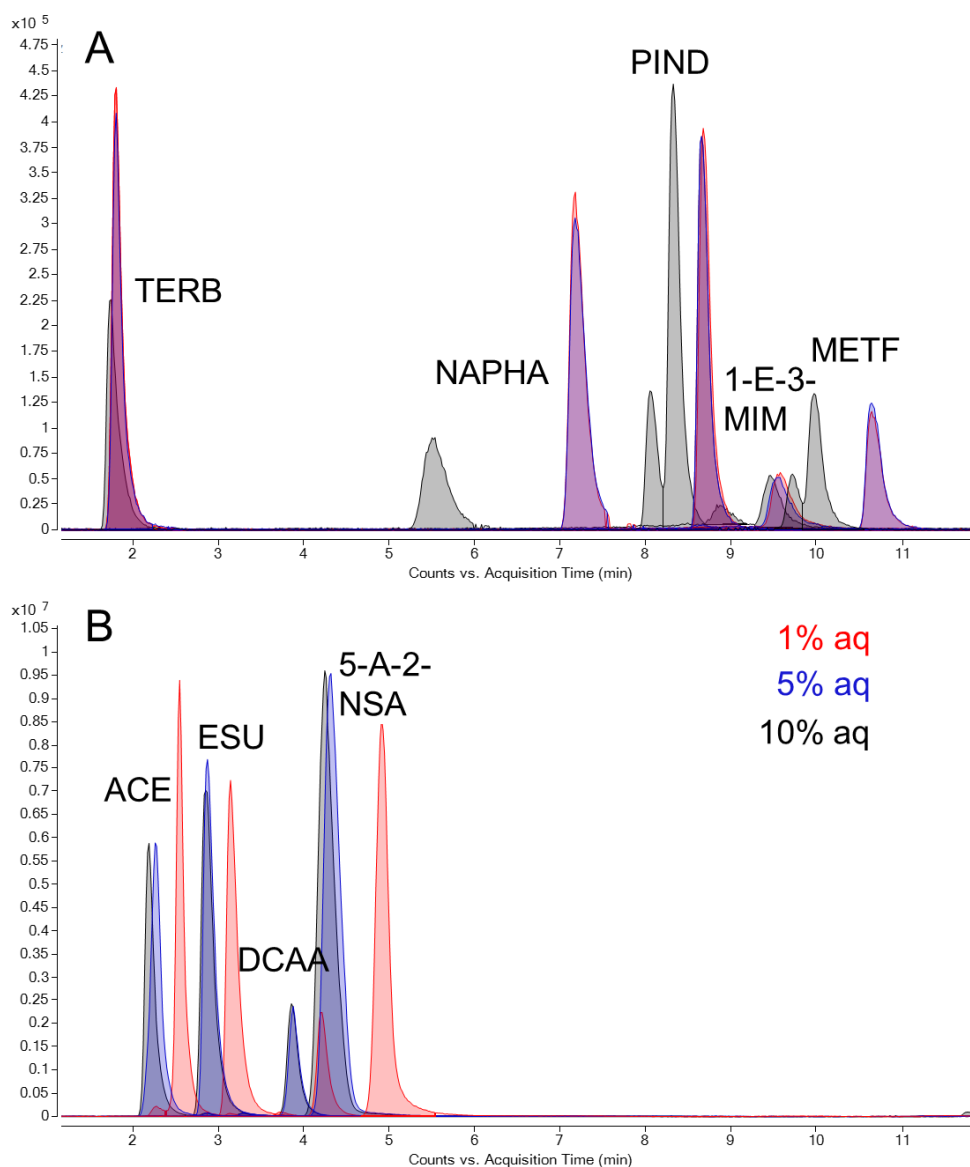
Figure 4-2: EICs demonstrating the effect of sample composition: H_2O content of 1% (red), 5% (blue) and 10% (black) on A: HILIC+ and B: HILIC– separations. For clarity, only EICs of selected analytes are depicted. Concentrations of analytes were 1 µg/l and 10 µg/l for A and B, respectively. The injection volume was 5 µl. For further details on gradients and instrumental parameters see Section 4.3.4.

Concluding, there is a strong dependence on the composition of the sample and care has to be taken that the water content does not exceed 5%. This means a strong dilution by a factor of 20, impairing LODs.

4.4.2 Method validation

Both HILIC methods developed here and the RPLC methods were validated with regard to sensitivity (LOD), precision (migration time and peak areas) and matrix effects for different sample preparation techniques (all parameters discussed in Section 4.4.2.1). We also discuss the orthogonality of the HILIC- and RPLC-MS methods (Section 4.4.2.2).

4.4.2.1 LOD, reproducibility and matrix effect

The results from the validation experiments described in Section 4.3.3.1 are listed in Table 4-5 and Table 4-6. LODs in MeCN/H_2O (95:5, v/v) were determined using a calibration curve for both HILIC-MS methods and in H_2O for RPLC-MS according to DIN 32645 (α = 0.05) (see Section 4.3.3.2). LODs were determined for samples *SPE*, *EME* (only HILIC-MS) and *FSE* (only for negative analysis mode) (see Section 4.3.3).

Taking a look at the results of experiments conducted in positive analysis mode in Table 4-5, the average LODs (determined as described in Section 4.3.5) range from 260 to 460 ng/l using HILIC+ and from 660 to 1010 ng/l for RPLC+. The precision of RT (n = 3, analyte concentration 2500 ng/l) was 0.2% (0.2%) and for PA 0.6% (1.8%) for HILIC+ (RPLC+), demonstrating very good reproducibility for both LC-MS methods.

The results for the negative analysis mode (see Table 4-6), revealed average LODs ranging from 560 to 770 ng/l with HILIC– and from 600 to 1160 ng/l for RPLC–. Average retention time precision was high for both methods (0.4% and 0.2% for HILIC– and RPLC–) and also for peak area with 3.4% and 2.0%, see Table 4-5 and Table 4-6. Whereas RPLC– and RPLC+ reached similar LODs, the positive analysis mode was more sensitive for HILIC+ than for HILIC–.

As some analytes have very high or low LODs such as BTA, IMIDA, IRB and 1,5-NDSA (see Table 4-5 and Table 4-6), we also compared the median between the sample preparation techniques and the type of LC separation. For HILIC– and HILIC+, similar median LODs over all sample preparation techniques were obtained (ca. 200-400 ng/l). For RPLC-MS, these values were between 560 and 850 ng/l. This shows that RPLC is less sensitive than HILIC, but a comparable sensitivity for both polarities is present.

Table 4-5: Retention time with precision and LODs in different matrices using HILIC+ and RPLC+ for 15 model analytes detected in positive analysis mode (see Table 4-1 for analytes abbreviations). Relative standard deviations (RSDs) were determined using a 10000 ng/l standard solution. Injection volumes were 5 and 10 µl for HILIC+ and RPLC+, respectively. Method parameters are given in Section 4.3.4. Spiking of the blank samples and matrix samples SPE eluate and EME was conducted as described in Section 4.3.3.2. n.d.: not detected. For further information, see text.

	retention time and precision (n = 3)						LODs from calibration curves in matrix				
	HILIC+			RPLC+			LOD blank		LOD in matrix in ng/l		
analyte	RT in min	RSD in %		RT in min	RSD in %		MeCN	H$_2$O	SPE eluate		EME
		RT	PA		RT	PA	HILIC	RPLC	HILIC	RPLC	HILIC
1-E-3-MIM	9.51	0.09	0.03	1.70	0.15	0.36	181	229	68	424	117
ACR	3.04	0.01	0.51	8.87	0.03	0.31	163	672	1241	1398	118
BTA	1.97	0.02	0.12	8.89	0.16	7.17	39	489	92	854	516
CLARI	7.49	0.35	0.55	11.11	0.05	3.45	141	752	756	1999	n.d.
CLOTH	1.87	0.01	0.31	9.24	0.06	0.23	119	550	141	884	24
DEET	1.75	0.05	1.16	11.45	0.02	0.37	440	66	177	303	359
EPOXI	1.73	0.55	0.19	12.30	0.02	0.04	430	920	742	1010	262
HEPES	12.57	0.14	1.00	1.70	0.89	2.03	600	885	n.d.	522	n.d.
IRB	2.45	0.02	1.60	11.62	0.10	2.20	766	1279	1345	4169	26
METF	10.42	0.00	0.47	1.63	0.67	0.96	453	884	331	522	192
NAPHA	7.12	0.01	0.08	8.94	0.16	2.10	49	894	367	591	150
PIND	8.16	0.11	0.42	7.99	0.03	3.40	505	180	281	429	773
SULFA	1.85	0.45	0.23	8.97	0.22	1.67	363	851	20	865	155
TERB	2.00	0.05	0.03	11.61	0.02	0.83	562	814	739	348	199
THIA	1.78	0.43	2.47	9.96	0.03	1.17	356	401	145	874	512
average		0.15	0.61		0.17	1.75	344	658	460	1013	262
median							363	752	306	854	192

Table 4-6: *Retention time with precision and LODs in different matrices using HILIC– and RPLC– for 18 model analytes detected in negative analysis mode (see Table 4-1 for analytes abbreviations). RSD values were determined using a 10000 ng/l standard solution. Injection volumes were 5 and 10 µl for HILIC– and RPLC–, respectively. Method parameters are given in Section 4.3.4. Spiking of the blank samples and matrix samples SPE eluate, EME and FSE was conducted as described in Section 4.3.3.2. n.d.: not detected. For further information, see text.*

analyte	retention time and precision (n = 3)						LODs from calibration curves in matrix						
	HILIC–			RPLC–			LOD blank		LOD in matrix in ng/l				
	RT in min	RSD in %		RT in min	RSD in %		MeCN	H₂O	SPE eluate		EME	FSE	
		RT	PA		RT	PA	HILIC	RPLC	HILIC	RPLC	HILIC	HILIC	RPLC
1,5- NDSA	14.96	0.65	12.48	1.75	0.00	3.25	768	1221	3430	975	1573	505	210
2-NSA	2.26	0.31	1.86	9.50	0.09	0.41	12	210	658	331	550	515	731
4-HBA	3.40	0.97	3.77	8.13	0.11	0.66	673	310	707	572	n.d.	1073	500
5-A-2-NSA	4.26	0.90	1.18	2.86	0.60	1.57	293	730	195	6200	n.d.	1101	1788
7-A-1,3-NDSA	15.28	0.04	0.83	1.91	0.47	1.01	398	422	293	3477	1796	462	781
ACE	2.22	0.30	2.86	3.45	0.30	0.42	17	444	356	311	105	359	570
BTA	1.83	0.12	7.78	8.86	0.10	3.33	3806	712	243	330	n.d.	295	486
CLOTH	1.87	0.35	1.00	9.23	0.09	1.06	339	190	253	601	30	232	684
DCAA	3.30	0.23	4.67	2.42	0.02	0.83	433	531	n.d.	n.d.	276	2351	803
ESU	2.87	0.23	1.33	1.92	0.08	2.75	202	961	378	1633	162	423	755
HCT	2.49	0.28	4.45	6.77	0.12	3.28	324	931	621	1087	238	251	875
HEPES	15.50	0.27	2.72	1.59	0.51	2.40	500	748	748	434	n.d.	362	562
IMIDA	1.73	0.61	0.81	9.18	0.10	4.10	2229	673	234	309	114	456	463
IRB	1.81	n.d.	n.d.	11.62	0.07	0.78	66	502	2914	1545	179	265	442
MCPA	2.71	0.26	5.32	11.63	0.00	0.60	184	637	n.d.	632	2349	1886	562
p-TSA	2.53	0.62	0.49	7.38	0.12	4.08	240	140	459	471	301	439	363
SAC	2.47	0.28	4.46	6.90	0.12	3.08	210	598	265	372	112	310	540
SULFA	1.92	0.35	2.10	8.94	0.00	2.80	447	835	597	503	17	233	507
average		0.40	3.42		0.16	2.02	619	600	772	1164	557	640	646
median							332	618	419	572	209	431	562

As no significant differences in LODs were observed (t-test, $\alpha = 0.05$), matrix effects can be expected to be low. This hypothesis was verified in a second set of experiments by determining matrix effects for all model analytes in three spiked samples *EME*, *SPE* and *FSE* and for comparison in a spiked (diluted) river water sample *N1*. Average matrix effects are presented in Figure 4-3A and B. As expected, very low matrix effects with average values ranging between 75 and 125% were obtained. This indicates an overall high matrix tolerance for both RPLC-MS and HILIC-MS which can also be seen in Figure 4-3B, exhibiting similar matrix tolerance for both methods (average matrix effects $\approx 90 \pm 30\%$). One exception was found for the spiked SPE eluate analyzed using RPLC– with an average matrix effect of 50%, which is highest among the negative matrix effects. This correlates well with the rather high average LODs of 1164 ng/l observed for the model analytes. The small positive matrix effects observed for the sample *N1* are expected to come from micropollutants identical to the model analytes or comigrating substances with very similar mass in the original water sample.
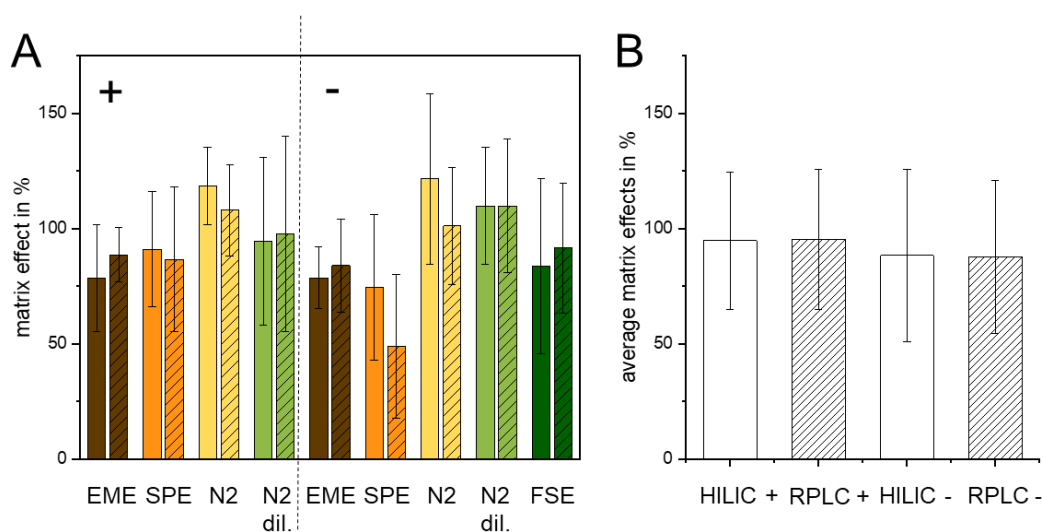

Figure 4-3: A: Average matrix effects obtained after analyzing spiked (1000 ng/l) matrices with and without sample preparation (EME, SPE, N2, N2 dil. and FSE, see Section 4.3.3) with HILIC+ or RPLC+ and HILIC– or RPLC–. Comparison of PAs of samples vs. PAs of a standard analyte mix (MeCN/H$_2$O 95:5 (v/v) and H$_2$O for HILIC and RPLC, respectively). Plain bars correspond to HILIC analysis, striped bars to RPLC methods. B depicts the average matrix effects over all matrices grouped according to HILIC and RPLC as well as the analysis mode. For details on methodical parameters, see Sections 4.3.4.1 (RPLC) and 4.3.4.2 (HILIC).

High LODs of individual analytes are either related to ion suppression for early eluting analytes (BTA and IMIDA using HILIC-MS, 7-A-1,3-NDSA and 5-A-2-NSA using RPLC-MS) or insufficient precision of the peak area using HILIC-MS (e.g. for 1,5-NDSA). As the retention mechanism involves polarity and charge, there was no correlation between LOD values and the log $D_{pH7.4}$ values, retention time of the model analytes or with matrix effects. A further optimization aspect would be to increase retention times in the two HILIC methods in order to increase both orthogonality and minimize ion suppression caused by coeluting analytes and matrix compounds (see also Section 4.4.2.2).

With regard to HILIC-MS, care has to be taken if concentrations of salt in the samples exceed the concentrations investigated here, as this might have an impact on retention of analytes (interaction of charged matrix compounds with the stationary phase). The at least 10-fold dilution used for samples containing high salt concentrations (pure river water sample, EME extract with 20 mM NaCl) reduced the impact of these charged matrix ions. However, in other preliminary experiments (results not shown) using higher concentrations and a different type of salt (100 mM $NaClO_4$ in $MeCN/H_2O$ 90:10, v/v), stronger ion suppression effects and an impact on retention was observed.

The LODs obtained in this study are higher than those reported in the literature: eleven out of 430 compounds analyzed in water and wastewater in a study conducted by Robles-Molina et al. [186] were identical to the model analytes here. Using polarity switching ESI-MS with RPLC separation, LODs between 0.1 and 59.9 ng/l were achieved for CLOTH, CLARI, DEET, HCT, IMIDA, MCPA, METF, PIND, SULFA, TERB and THIA. The stationary phase and eluents were very similar to the ones applied here, but column dimensions were 4.6 x 50 mm, 1.8 µm (instead of 4.6 x 150 mm used in this study). Differences in the gradient chosen and especially higher injection volume (20 µl instead of 10 µl) can be observed. However, an SPE preconcentration step by a factor of 200 can be identified as major reason for the lower LODs by Robles-Molina et al. [186]. Higher injection volumes may also improve LODs. For example, Nürenberg et al. [206] used 100 µl in a method similar to the one presented here.

Different HILIC methods using a zwitterionic stationary phase reached LODs between 1 and 10 ng/l for analytes investigated here (METF, MCPA, ACE, SAC, and CLARI) [28, 39, 82, 207]. However, all of these methods used a SPE step prior to LC-MS separation with preconcentration factors between 2 [39] and 67 [82]. Future work will try to increase the preconcentration factor for all sample preparation techniques applied here, see also Chapter 1 and 6.

4.4.2.2 Complementarity between HILIC-MS and RPLC-MS

We investigated if the HILIC methods provided a complementary separation selectivity to the RPLC-MS method for the analysis of polar compounds. Figure 4-4A and C show the chromatograms of a standard solution using HILIC-MS (red) and RPLC-MS (black). With its better LODs (see Figure 4-4 and Section 4.4.2.1), HILIC is more suitable for trace analysis of polar compounds. However, some deterioration of peak shapes is visible with tailing in HILIC+ for all analytes as well as fronting and general peak broadening for polar to very polar analytes (RT of 8 min or lower) using RPLC–. Orthogonality was reached in a sense that overall resolution in HILIC was good for analytes with low retention due to a higher separation efficiency whereas the opposite was observed for RPLC-MS.
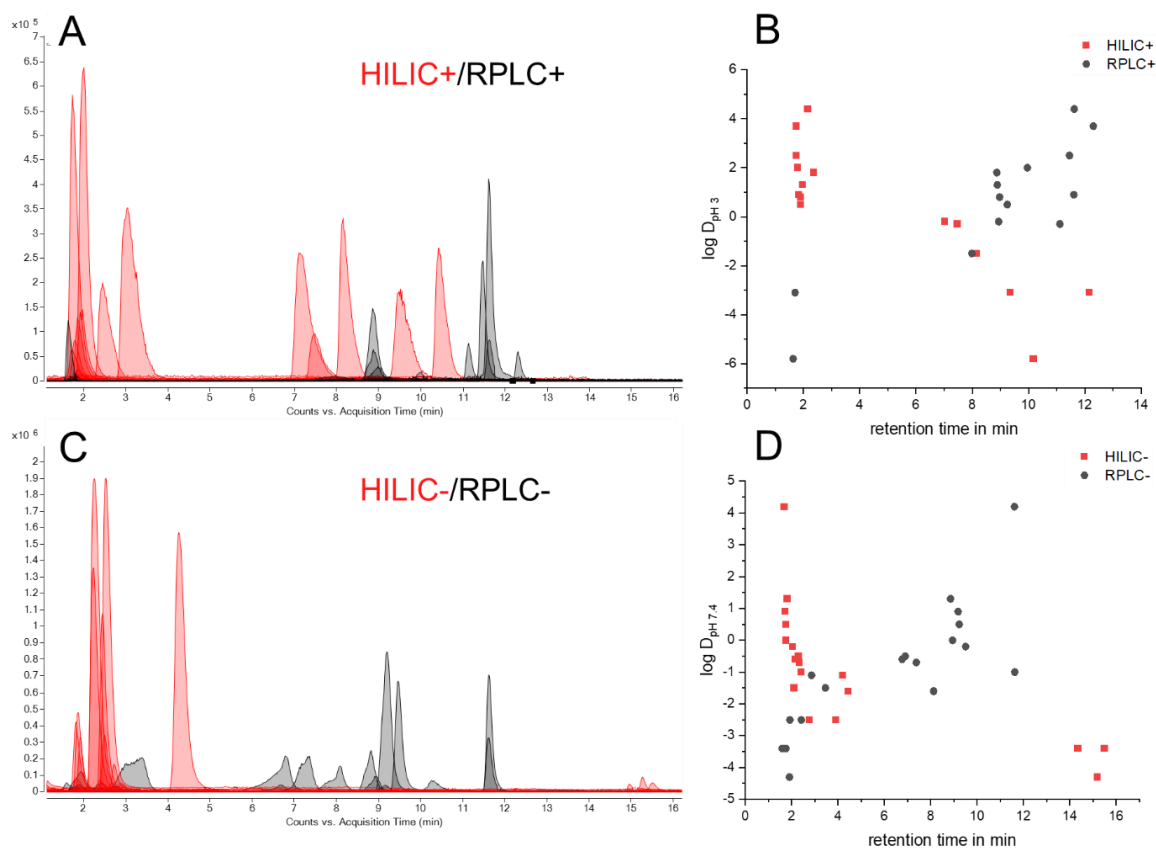
Figure 4-4: Chromatograms of separations of a standard solution (A: 1000 ng/l, C: 10000 ng/l) in A) positive and C) negative analysis mode using HILIC+/– (red) and RPLC+/– (black) as separation methods (for gradient and injection conditions see Sections 4.3.4.1 and 4.3.4.2). Correlation of B) log $D_{pH\ 3.0}$ and D) log $D_{pH\ 7.4}$ with retention time.

Figure 4-4B and D correlate the log $D_{pH\ 3}$ or log $D_{pH\ 7.4}$ values with retention time to demonstrate the separation complementarity of the two LC-MS methods. All chromatographic methods demonstrate a good correlation between retention time and log D values (Pearson R values between 0.70 and 0.88) with HILIC– showing lowest correlation. For RPLC, lowest polarity values of analytes still demonstrating retention are approx. at a log $D_{pH\ 3/7.4}$ value of -2, demonstrating a broad application range. This indicates that the RPLC method used here is optimized for medium polar compounds, as the average RPLC methods rather cover analytes possessing log D values down to 0-2 [1]. Sufficient retention is achieved for most analytes with log $D_{pH\ 3}$ values ≤ 0 using HILIC+ and for most analytes with log $D_{pH\ 7.4}$ values ≤ -1 using HILIC–. The retention of very polar analytes (log $D_{pH\ 7.4}$ values between 0 and -2.5) is very low and very high for only slightly more polar analytes (log $D_{pH\ 7.4}$ ≤ -3), so further improvement is advisable for analytes in this polarity range.

Concluding, both methods can be used complementarily for the analysis of micropollutants with a broad range of polarities, though some limitations in the analysis of anionic compounds are observed. Further method optimization will focus on improving the analysis of very polar anionic compounds, starting with a different stationary phase better suited for the analysis of anionic compounds. This would indicate the usage of two different stationary phases and result in long equilibration steps to cover

a wide range of analytes. Another possibility might be a stationary phase with both ionic and polar interactions. With this, a broader analyte range could be covered by simply changing elution conditions. As the same stationary phase can be used, one might even be able to allow direct sequential separation of both ionic and polar compounds by for example double injection with a suitable elution protocol. For this, the Raptor Polar X stationary phase (Restek, Bad Homburg, Germany) [208] recently developed seems promising. To the best of our knowledge, such an approach is not yet applied in HILIC screening methods but rather compromises are made with regard to an overall sufficient coverage for all analytes in a single run.

4.5 Conclusion

After optimizing buffer type and concentration as well as the gradient, two HILIC-MS methods (HILIC+ and HILIC−) were implemented complementary to already existing RPLC-MS methods (RPLC+ and RPLC−). Average LODs of 340 and 620 ng/l were reached using the developed HILIC+ and HILIC− methods and 660 and 600 ng/l using RPLC+ and RPLC−. All four methods were successfully applied to the analysis of the model analytes in spiked sample matrices without and with sample preparation techniques like SPE, EME and FSE. A high matrix tolerance for the majority of the analytes (average matrix effects ≈ 90±30%) was demonstrated. The sample composition proved crucial for the two HILIC methods with significant impact of the water content on retention and for some analytes also on peak shape and intensities. This limits the LODs reached as aqueous samples require high dilution to become compatible with HILIC separation. As separations using the HILIC− method exhibited low retention of polar and very high retention for very polar compounds, further optimization is advisable, for example by using a different stationary phase.

5. Development of an electromembrane extraction setup and method for the extraction and preconcentration of organic micropollutants from environmental waters

5.1 Abstract

For the analysis of micropollutants in environmental water samples, an efficient sample enrichment is required as mostly low analyte concentrations are present. For analytes of low and medium polarity, this can well be accomplished using solid-phase extraction, but there is a lack of methods to preconcentrate analytes of high polarity and especially charged or ionizable analytes. Electromembrane extraction (EME) was shown to efficiently preconcentrate analytes by the electromigration from the donor solution with the sample to the acceptor solution across a suitable membrane. Since its introduction 15 years ago, EME has experienced great progress with regard to selectivity of the membrane, instrumental setups or applications with a focus on analyzing biological fluids.

Within the scope of this work, a new flow-through cell consisting of two polyetherether ketone chambers and a 3D-printed sample channel combined with bubbleless electrodes was developed. A model analyte system containing basic and acidic compounds covering a broad range of functional groups (e.g. sulfonamides, sulfonic acids, halogens, carboxylic acids, amines) and polarity ($-7.7 \leq \log D_{pH\,5} \leq 2.4$) was used to demonstrate simultaneous extraction of anions and cations and to optimize the process of EME. Polymer inclusion membrane compositions were varied with regard to high average extraction efficiencies for all model analytes, offering broad analyte coverage. In terms of reaching high enrichment factors whilst maintaining reproducibility, the whole EME setup was reviewed with regard to magnitude of applied current/voltage, extraction time and handling of the whole EME process.

With the optimized membranes and setup, the three experimental parameters flow rate, current magnitude and extraction time were further investigated using a Box-Behnken-Design. A thorough comparison between compatibilities of different separationmethods (reversed-phase liquid chromatography coupled to mass spectrometry (MS), hydrophilic interaction liquid chromatography-MS and capillary electrophoresis-MS) and possible matrix effects was conducted. As a final step, the EME system was applied to the extraction of the target analytes from a (diluted) river water sample to investigatematrix removal and preconcentration effects.

5.2 Introduction

The efficient analysis of ionic and polar micropollutants experiences increasing attention in environmental studies. As already discussed in Chapter 3, capillary electrophoresis coupled to mass spectrometry (CE-MS) is an interesting tool for the analysis of such charged compounds. The major drawback of CE-MS is its limited loadability. Even when the most efficient on-line enrichment methods are applied, only a few µl can be injected

in contrast to chromatographic techniques, where the injection of 100 µl of an aqueous sample is common in non-target screening [81]. Thus, efficient enrichment techniques for charged or ionizable compounds have to be developed. For this, we aimed at using electromembrane extraction (EME) to preconcentrate ionic and ionizable micropollutants. A major focus is to broaden the selectivity of EME for screening purposes and to reach sufficient recoveries also for polar analytes.

Interest has grown in microextraction techniques with analyte enrichment due to their reduced consumption of organic solvents, the small sample volumes needed and their overall lower operational costs and shorter extraction times. Liquid-liquid extraction can be performed classically by shaking or ultrasonication. In electroextraction, an electric field is applied to accelerate the extraction of charged analytes [209]. It was already applied in the early 90ies with a focus on analytes enrichment in recent years [210]. In 2014, Yamini et al. [211] showed a steady increase in the number of publications concerning electroextraction since 1992. Recently, EME gained more and more attention, well reflected in the number of very recent reviews [13, 212-215]. In EME, a membrane separates donor and acceptor solution to provide a higher selectivity. It was first introduced by Pedersen-Bjergaard and Rasmussen in 2006 [12] using a supported liquid membrane (SLM) between an aqueous sample and the aqueous acceptor solution. Generally, in EME using SLM, charged species migrate in an electric field from the sample solution across the SLM into the acceptor solution. The SLM consists of a base polymer (often polypropylene) which is dipped into an organic solvent, chosen to act as an ion-pair reagent (e.g. 2-nitrophenyl octyl ether (NPOE); di-(2-ethylhexyl) phosphoric acid, DEHPA) [216]. This strategy has two benefits: (1) by using a smaller volume of the acceptor solution compared to the donor solution, enrichment of the analytes is possible with (2) a simultaneous clean-up from non-charged matrix compounds. A high matrix tolerance and compatibility with common analytical techniques like liquid chromatography, gas chromatography and CE have already been demonstrated [75], most of them using CE and reversed-phase liquid chromatography (RPLC) [213]. Hydrophilic interaction liquid chromatography (HILIC) was rarely applied, although its application increased in the last few years with a general shift in EME applications to more polar compounds [214, 217]. However, for HILIC, dilution of the aqueous acceptor solution by at least a factor of 5 with acetonitrile (MeCN) is necessary to have sufficient analyte retention and acceptable peak shapes during the separation [217].

Conditions favorable to reach high extraction efficiencies for analytes, often investigated in designs of experiments, can also be suitable to extract ionic matrix components such as inorganic ions. This can severely impact the following separation and detection. The salt content in the acceptor solution after enrichment is most critical for downstream analysis. In addition, matrix components enriched by EME may coelute or comigrate with the target analytes. Positive and negative matrix effects overlay differences in enrichment factors (EFs) making the use of ratios of peak areas to calculate EFs critical [218]. Determining EFs at different concentrations [219] or generating a calibration curve in the targeted concentration range [220] are practices to minimize these effects. Many EME setups proved stable and gave reproducible results, also for samples with a high

matrix load. Matrix effects strongly depend on sample composition and conductivity so they should be investigated carefully during method optimization to discriminate them from enrichment effects. However, during optimization of EME parameters, compositions of acceptor solutions change due to different selectivity of the membrane, varying magnitude of the electric field or extraction time. In most cases, using the same (validated) separation method for the analysis of the acceptor solution is enough to balance possible matrix effects, still being able to elaborate significant parameters. Possible matrix effects may be estimated by simulating extreme conditions of EME or spiking the analytes to an EME blank.

Since the first application in 2006, the membrane type and composition were optimized to fine-tune enrichment efficiency and selectivity [221]. Membranes were used both in the form of hollow fibers [76, 220, 222-228] or as flat membranes [219, 221, 229-233]. In 2014, Koruni et al. [76] presented a simultaneous extraction of both acidic and basic drugs over a broad range of polarities using two SLMs of different composition. Three years later, Mamat and See [228] used a similar approach for the enrichment of both cationic and anionic herbicides across two hollow polymer inclusion membranes (PIMs). Bubbleless electrodes enabled applying higher voltages of up to 3000 V without instabilities caused by bubble formation due to electrolysis. [228] The extraction of larger sample volumeswas reached using flow-through cells with either SLMs [222, 234] or PIMs [229, 230] in various applications. EME in a chip format was successfully conducted in 2010 by Petersen et al. [235] with an SLM. In 2018, Zarghampour et al. [232] presented a dual on-chip EME device with a single-compartment microfluidic device. Using two different SLMs, it was possible to extract diclofenac as an acidic analyte and nalmefene as a basic analyte from human urine samples.

Improving the extraction efficiencies of highly-polar analytes is of growing interest in EME research [214] as the polarity of the SLMs published so far limited the log D range of substances that can be transferred. If the polarity of the SLM solvent is too high, leaking into the aqueous sample phase is more likely. Thus, different approaches have been investigated to improve mass transfer of polar analytes through the SLM such as using less polar organic additives. For example, by using nitrophenyl pentyl ether instead of NPOE, 45 polar basic metabolites with $-5.0 \leq \log D_{pH\ 5} \leq 0.2$ were extracted with recoveries ranging from 10 to 90% [236]. With ion pairing reagents like DEHPA, bulk sample complexation was induced so that eight polar bases with $\log D_{pH\ 5}$ values in the range of -5.7 to -0.6 were extracted with recoveries > 40% [217]. Most work was accomplished using basic analytes, preconcentration of polar acidic compounds was rarely investigated. In one example, a polar acrylic nanostructured support was used instead of common polypropylene sheets to facilitate carrier-mediated transport for acidic compounds through membranes made using Aliquat 336 and 1-octanol. For four polar acidic compounds with $\log D_{pH\ 5}$ values between -2.3 and -0.2, recoveries between 60 and 85% were reached [237].

Recoveries of 34% to 81% were reached by Román-Hidalgo et al. [238] using a PIM instead of an SLM, when enriching nonsteroidal anti-inflammatory drugs and other highlypolar acidic drugs ($\log D_{pH\ 5}$ values between -2.9 and 1.4). PIMs were developed as an
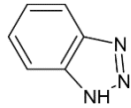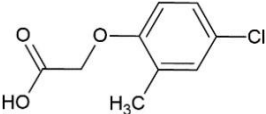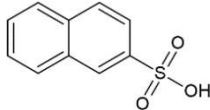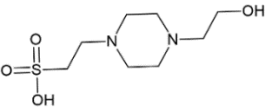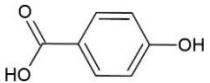
alternative to SLMs to increase mechanical robustness of the membrane, reduce the tendency of components leaching into donor or acceptor solution and to be able to store the membranes for a longer time [239]. SLMs are still used in the majority of EME setups, but the number of studies with PIMs increased [219, 228, 230, 238, 240]. With PIMs, the successful extraction of basic and acidic polar compounds such as propane sulfonate [231] (log $D_{pH\,5}$ -2.8), tetraethylammonium [231] (log $D_{pH\,5}$ -2.5), nicotinic acid [238] (log $D_{pH\,5}$ -2.9) and hippuric acid [238] (log $D_{pH\,5}$ -2.8) was achieved. In this study, we focus on micropollutants, which are not well covered by current analytical methods. We want to enrich analytes of broad log D range in order to have a relatively low selectivity for downstream analysis using non-target screening. In order to simultaneously extract cations and anions from environmental water samples, a dual EME flow-through cell is envisaged. Inspired by the flow-through cell design of Zarghampour et al. [232], we developed a cell made of polyether ether ketone (PEEK) with a bubbleless electrode adapted from the study by Mamat and See [228], which allows to apply a higher field strength. For optimization, the composition of PIMs, content and pH of the donor and acceptor solutions as well as instrumental parameters (bubbleless electrode, dual flow- through cell, length/diameter of capillaries connecting acceptor cell and bubbleless electrode) were considered.
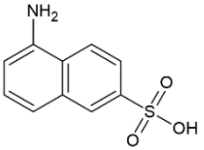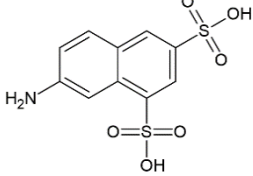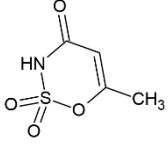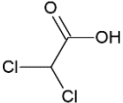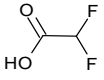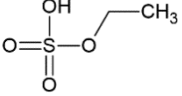
5.3 Materials and methods

5.3.1 Chemicals

2-fluorophenyl 2-nitrophenyl ether (FPNE, ≥ 98%), 2-nitrophenyl octyl ether (NPOE, 98%), acetonitrile (MeCN, LC-MS grade), cellulose triacetate (CTA), di-(2-ethylhexyl) phosphoric acid (DEHPA, 97%), formic acid (FA, 98%), iodoacetic acid-2-^{13}C (MIAA 13C), isopropanol (LC-MS grade), methanol (MeOH, LC-MS grade), sodium chloride (NaCl, ≥ 99.8%), sodium hydroxide (NaOH, ≥ 98%), tris (2-ethylhexyl) phosphate (TEHP, 97%) and water (LC-MS grade) were purchased from Sigma-Aldrich (Steinheim, Germany). Aliquat 336 (90%) was obtained from Alfa Aesar (Haverhill, Massachusetts, USA), dichloromethane (DCM, HPLC grade) and hydrochloric acid (HCl, 32% aqueous solution) from Fisher Scientific (Waltham, Massachusetts, USA). Acetic acid (HAc, 100 %), ammonium acetate (NH$_4$Ac, 98 %), ammonium hydrogen carbonate (NH$_4$HCO$_3$, LC-MS grade) and venlafaxine-d6 hydrochloride (VENLA d6) were obtained from Merck (Darmstadt, Germany). 4-Hydroxybenzoic acid-d4 (4-HBA d4), acesulfame-d4 potassium salt (ACE d4), acridine-d9 (ACR d9), dichloro acetic acid- d1 (DCAA d1), metformin-d6 hydrochloride (METF d6), pindolol-d7 (PIND d7), p- toluene-d7-sulfonic acid (p-TSA d7) and saccharin-^{13}C6 (SAC 13C6) were delivered by TRC (Toronto, Canada). Isotope-labeled standards were all of analytical grade or higher. Suppliers and purity of the model analytes are listed in Table 5-1a and b. Stock solutions (in MeOH) and working solutions (aqueous) were stored at -20 °C before use.

Table 5-1a): Model analytes, suppliers thereof and their physicochemical properties sorted alphabetically and grouped into anions (Table 5-1a) and cations (Table 5-1b). pK_a, log D values and charge numbers (both pH 5.0, the pH value of an aqueous standard solution) were taken from Chemicalize provided by ChemAxon (11/02/2021). For analytes marked with an asterisk * isotope-labeled standards were available, resulting in a total number of 23 anionic and 15 cationic analytes included in this study.

analyte	analyte abbrev.	m/z detected	log P	log $D_{pH\ 5}$	charge number at pH 5	strongest pK_a (acidic)	strongest pK_a (basic)	molecular structure	supplier & purity
1*H*-benzotriazole	BTA	118.041	1.4	1.3	0.0	9.0	0.2		Sigma Aldrich, 99%
2-methyl-4-chlorophenoxy acetic acid	MCPA	199.017	3.3	0.8	-1.0	3.4			Sigma Aldrich, ≥ 98%
2-naphthalene sulfonic acid	2-NSA	207.012	2.1	-0.2	-1.0	-1.8			Sigma Aldrich, ≥ 95%
4-(2-hydroxyethyl)-1-piperazine-ethane sulfonic acid	HEPES	239.107	-3.1	-3.1	0.0	-1.3	7.3		Fluka, 99.5%
4-hydroxybenzoic acid *	4-HBA	137.024	1.6	0.6	-0.8	4.4			Fluka, ≥ 98%

analyte	analyte abbrev.	m/z detected	log P	log D$_{pH\,5}$	charge number at pH 5	strongest pK$_a$ (acidic)	strongest pK$_a$ (basic)	molecular structure	supplier & purity
5-amino-2-naphthalene sulfonic acid	5-A-2-NSA	222.023	1.1	-0.3	-1.0	-2.2	3.6		Sigma Aldrich, ≥ 95%
7-amino-1,3-naphthalene disulfonic acid	7-A-1,3-NDSA	301.980	-1.6	-3.5	-2.0	-2.8	3.6		Sigma Aldrich, ≥ 98%
acesulfame *	ACE	161.986	-0.6	-1.5	-1.0	3.0			Sigma Aldrich, ≥ 99%
dichloro acetic acid *	DCAA	126.936	1.1	-1.6	-1.0	2.3			Merck, ≥ 98%
difluoro acetic acid	DFAA	94.995	0.2	-2.7	-1.0	2.0			Sigma Aldrich, ≥ 98%
ethyl sulfate	ESU	124.991	-0.5	-2.5	-1.0	-2.1			Sigma Aldrich, ≥ 95%
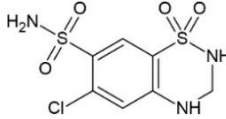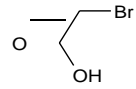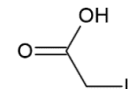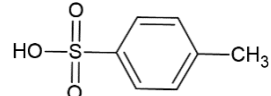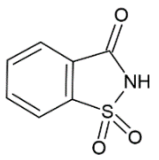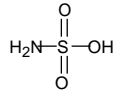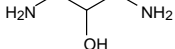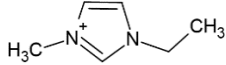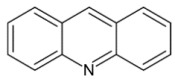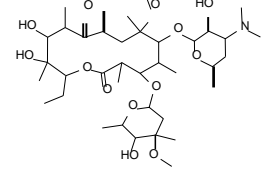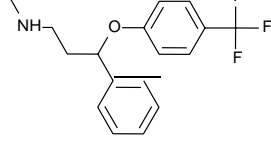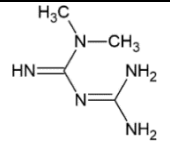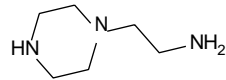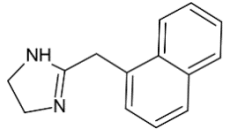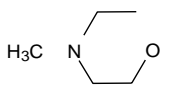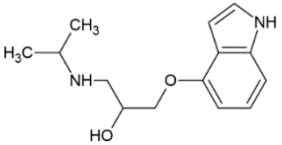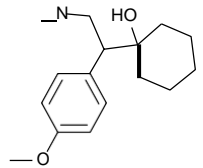
analyte	analyte abbrev.	m/z detected	log P	log D$_{pH\,5}$	charge number at pH 5	strongest pK$_a$ (acidic)	strongest pK$_a$ (basic)	molecular structure	supplier & purity
hydrochlorothiazide	HCT	295.957	-0.6	-0.6	0.0	9.1			Sigma Aldrich, ≥ 99%
mono bromo acetic acid	MBAA	136.924	0.5	-1.8	-1.0	2.6			Fluka, ≥ 99%
monoiodo acetic acid *	MIAA	184.911	0.7	-1.2	-1.0	3.1			Fluka, 99%
p-toluene sulfonic acid *	p-TSA	171.012	0.9	-0.7	-1.0	-2.1			Alfa Aesar, 90%
saccharin *	SAC	181.992	0.5	-0.5	-1.0	1.9			Sigma Aldrich, ≥ 98%
sulfamic acid	SULAC	95.976	-1.4	-3.8	-1.0	-1.8			Sigma Aldrich, 99.3%

Table 5-1b: List of cationic model analytes. For further information, see Table 5-1a.

analyte	analyte abbrev.	m/z detected	log P	log $D_{pH\,5}$	charge number at pH 5	strongest pK_a (acidic)	strongest pK_a (basic)	molecular structure	supplier & purity
1,3-diamino-2-propanol	1,3-DA-2-PRO	91.087	-2.1	-7.7	2.0	14.6	9.6		Alfa Aesar, 97%
1-ethyl-3-methyl-imidazolium	1-E-3-MIM	111.092	-3.1	-3.1	1.0	-	-		Sigma Aldrich, ≥ 95%
acridine *	ACR	180.081	3.4	3.5	0.6		6.2		Sigma Aldrich, 97%
clarithromycin	CLA	748.484	3.2	-0.1	1.0		9.0		Sigma Aldrich, ≥ 98%
fluoxetine	FLX	310.141	4.2	0.9	1.0		9.8		Sigma Aldrich, ≥ 98%

analyte	analyte abbrev.	m/z detected	log P	log $D_{pH\,5}$	charge number at pH 5	strongest pK$_a$ (acidic)	strongest pK$_a$ (basic)	molecular structure	supplier & purity
metformin *	MET	130.109	-2.6	-5.7	2.0		12.3		Alfa Aesar, 97%
N-aminoethyl piperazine	N-AEP	130.134	-1.1	-7.4	1.0		9.6		Sigma Aldrich, 99%
naphazoline	NAPHA	211.123	2.2	-0.2	1.0		10.2		Sigma Aldrich, ≥ 98%
N-methyl morpholine	NMP	102.091	0	-2.5	1.0		7.5		Sigma Aldrich, 99%
pindolol *	PIN	249.160	1.7	-1.4	1.0	14.1	9.7		Sigma Aldrich, 98%
venlafaxine*	VENLA	278.212	2.7	-0.6	1.0		8.9		Sigma Aldrich, ≥ 98%

5.3.2 Samples and sample preparation

5.3.2.1 Acceptor solutions

10 mM HCl and NaOH acceptor solutions were prepared daily using 1 M stocksolutions and were then degassed for 5 min at 120 mbar. After ultrasonication for 5 min, the acceptor solutions were put on ice. Before each experiment, the acceptor cell at the anode was filled with 10 mM NaOH and the acceptor cell at the cathode with 10 mM HCl using 1 ml syringes (B. Braun Melsungen AG, Melsungen, Germany) connected to bare-fused silica capillaries (length 20 cm, i.d. 200 µm; Polymicro Technologies, Phoenix, Arizona, see Sections 5.3.3.3 and Figure 5-1, VI).

5.3.2.2 Samples for EME

Methanolic stock solutions containing all analytes with a concentration of 20 mg/l were prepared mixing 1 g/l methanolic stock solutions of each analyte. Isotope-labeled standards (ISTD, deuterated and ^{13}C-labeled) and mixtures thereof were prepared and stored in the same way at -20° C. In order to keep the methanol content low and constant, samples to be used for the EME experiments were spiked with the analyte mixtures to reach a constant ratio of analyte mix:sample of 1:99 (v/v). The final concentrations are given in the text. All samples were degassed for 10 min using ultrasonication before drawing up the sample into a 50 ml syringe (polypropylene and polyethylene, Henke-Sass Wolf, Tuttlingen, Germany) for injection into the EME setup.

5.3.2.3 Sample preparation of acceptor solutions for downstream analysis

Acceptor solutions were injected directly for RPLC-MS and NACE-MS analysis. For HILIC-MS, a further 10-fold dilution with MeCN was necessary to provide sufficient retention. For this, 10 µl of each acceptor solution were mixed with 90 µl MeCN priorto HILIC-MS analysis.

5.3.2.4 River water sample

The water sample $N2$ was collected from the river Neckar in Tübingen, a few hundred meters downstream of a wastewater treatment plant (WWTP, 110000 population equivalents, collection in 09/2020). The sample was collected in a polypropylene vessel, filtered with a CHROMAFIL Xtra PTFE-45/25 filter (Macherey-Nagel, Düren, Germany) and then stored in a borosilicate vessel at -20 °C before use. The sample $N2/H_2O$ $1:4$ was prepared diluting sample $N2$ 1:4 (v/v) with LC-MS grade H_2O. Then, spiking and ultrasonication was conducted in the same way as described for aqueous samples in Section 5.3.2.2.

5.3.3 EME setup

In the following, we use the attributes anionic and cationic with regard to the charge of the analytes relevant in the extraction process (for example, the anionic acceptor solution contains anions, the anionic membrane transports anions).

5.3.3.1 Membrane preparation

Base polymer (CTA), plasticizer (TEHP/FPNE/NPOE) and ionic carrier (Aliquat 336/DEHPA) were dissolved in 5 ml DCM in a 5 ml volumetric flask by stirring

for 30 min. Due to the high viscosity of Aliquat 336, the required amount added was weighed for higher precision. The solutions were poured into a metal casting mold containing four circular cavities (Ø 8 cm each, see Section 5.3.3.3 and Figure 5-1, I and II) and finally covered with a petri dish to ensure slow evaporation of DCM. The obtained PIMs were stored in aluminum foil until further use. Final compositions for PIMs were 25 mg CTA, 8.2 µl TEHP and 18.1 µl DEHPA (40/22/38, m%) for cationic and 25 mg CTA, 4.9 µl FPNE, 6.1 µl NPOE and 13.3 mg Aliquat 336 (49/12.5/12.5/26, m%) for anionic membranes (see also Table 5-2).

5.3.3.2 Membrane optimization

To optimize the membrane composition, different ratios of base polymer (CTA), plasticizer (TEHP) and ionic carrier (Aliquat 336/DEHPA) were investigated based on optimized compositions published before [219, 229]. Our experiments were conducted using a cell with two chambers separated by the corresponding membrane (for anions with Aliquat 336 or cations with DEHPA) [241]. 0.1 mM NaClO$_4$ solution was used as electrolyte and a positive/negative potential of 100 V was applied for 10 min. Recoveries of the extraction of selected compounds from Table 5-1 (cations: 1-E-3-MIM, CLA, METF and PIND; anions: 2-NSA, 7-A-1,3-NDSA, ACE, DCAA, ESU, MIAA, p-TSA and SAC) were determined using NACE-MS (see Section 5.3.4.2) via the compounds' peak areas determined for solutions in the acceptor cells at t = 10 min compared to those in the donor cell at t = 0 min.

5.3.3.3 Flow-through cell

The flow-through cell consisted of two PEEK blocks (see Figure 5-1, IV) containing both an acceptor channel with a total volume of 105 µl and 112 µl for the anionic and cationic acceptor cell (named with regard to the charge of the analytes in the cell). Each block was covered with the corresponding membrane (Figure 5-1, II) which was adhered with a double-sided adhesive tape (3M 468MP, 3M Deutschland, Neuss, Germany). A 3D-printed separation layer (thermoplastic polyurethane, Figure 5-1, VIII) was pressed between the two membranes, resulting in a sample channel surrounded by the 3D-printed piece, the PEEK blocks and the membrane. The area of the sample channel is identical to the area of the acceptor channel, thus the maximum surface area (80 mm²) between sample solution and acceptor solution was used during electroextraction. The sample was introduced through one of the PEEK blocks by a syringe pump (LA-100, Landgraf Laborsysteme, Langenhagen, Germany, Figure 5-1, VII) and is guided out of the same PEEK block into waste (Figure 5-1, IX). Due to electrolysis and bubble formation at electrodes, the bubbleless electrode approach of Mamat and See [228] was transferred to our setup: each acceptor channel was connected via a PEEK capillary (length 20 mm, ID 0.25 mm; TechLab, Braunschweig, Germany) with a 3D-printed outlet buffer vessel (Figure 5-1, V) made of polylactide. The outlet buffer vessels were stirred with a magnetic stirrer and platinum electrodes inserted, connected to high voltage sources (Figure 5-1, III). Different currents or voltages were applied for different time intervals using a DC high voltage source 2290E-5 (Keithley Instruments, Cleveland, Ohio, USA). After the experiment, acceptor solutions were collected in the 100 µl vials by flushing the

acceptor channel with air and subsequently analyzed via RPLC-MS, HILIC-MS and/or NACE-MS.
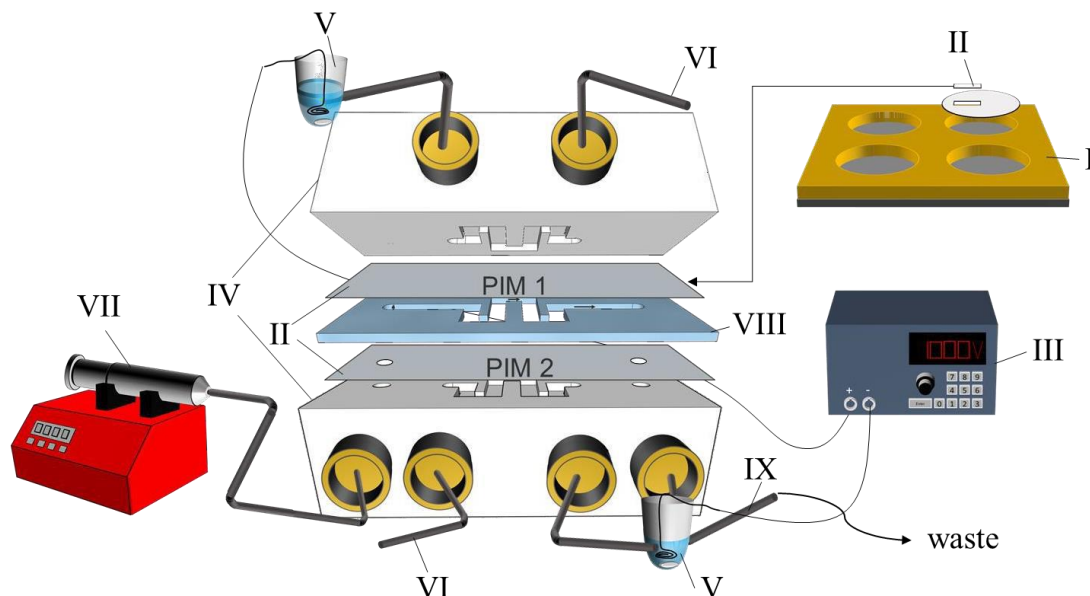
Figure 5-1: Setup of the EME flow-through cell applied in the workflow described in Figure 5-2. I: casting mold for PIM preparation, II: PIM for anions and cations, III: DC high voltage source, IV: PEEK blocks containing acceptor solutions, V: bubbleless electrode vessel containing magnetic stirring bar and Pt electrode, VI: acceptor solution inlet connected to a 1 ml syringe via a bare-fused silica capillary, VII: syringe pump, VIII: 3D-printed sample channel and IX: sample outlet to waste. Detailed information on type of material or manufacturer can be gathered from Sections 5.3.1 and 5.3.3.

5.3.4 *Chromatographic and electrophoretic separation techniques*

5.3.4.1 LC-MS analysis

For HPLC-MS analysis, a 1260 Infinity LC system coupled to a 6550 iFunnel Q-TOF LC/MS system (Agilent Technologies, Waldbronn, Germany) was used. A jet-stream electrospray ionization (ESI) source was operated with a nebulizer pressure of 35 psig, a drying gas temperature of 160 °C, a flow rate of 16 l/min and a fragmentor voltage of 360 V. In the positive/negative ionization mode, the capillary voltage was set to +/-4000 V, the skimmer voltage to 65 V and the nozzle voltage to 500 V. The mass range was 40-1000 m/z with a data acquisition rate of 1 spectrum/s. The sheath gas temperature was set to 325 °C with a flow rate of 11 l/min. For internal calibration, solutions of purine and HP0921 (Agilent Technologies, Waldbronn, Germany, m/z = 121.0508, 922.0097) in MeOH/water (95/5) were used and sprayed via a reference nebulizer.

5.3.4.1.1 RPLC-MS (C18)

Aliquots of 2 µl sample were injected onto a Zorbax Eclipse Plus C18 column (2.1 x 150 mm, 3.5 µm, narrow bore, Agilent Technologies, Waldbronn, Germany). Additionally, a guard column (2.1 x 15 mm, 5 µm, narrow bore, Agilent Technologies, Waldbronn, Germany) was used. For separation, a gradient elution at a flow rate of 0.3 ml/min using water and MeOH, both containing 0.1% FA (v/v), was chosen. After 1 min, the initial content of 95% water was decreased to 5% water over 7 min. This mobile phase was kept for another 7 min and then, the water content was increased to

95% over 5 min. The same gradient was used for both anionic and cationic acceptor solutions, solely switching MS polarity.

5.3.4.1.2 HILIC-MS (ZIC-HILIC)

Aliquots of 5 µl sample were injected onto a SeQuant ZIC-HILIC (2.1 x 150 mm PEEK coated, 3.5 µm, 100 Å, Merck, Darmstadt, Germany) for the analysis of polar compounds. In addition, a guard column (2.1 x 20 mm PEEK coated, Merck, Darmstadt, Germany) was put in front of the column with a coupler.

The detection of analytes in the anionic acceptor solution was accomplished using negative ionization mode for MS detection. A gradient elution at a flow rate of 0.3 ml/min using aqueous 20 mM NH_4HCO_3 and MeCN, both containing 0.01% FA (v/v), was chosen. The initial content of 90% MeCN was decreased to 40% over 15 min. This mobile phase was kept for one minute and then, the acetonitrile fraction was increased to 90% MeCN over 0.5 min. For a proper re-equilibration, this composition was kept for another 8 min before injecting the next sample, leading to a total analysis time of 24.5 min. The re-equilibration step used an increased flow rate of 0.5 ml/min during min 16-22.

The detection of analytes in the cationic acceptor solution was accomplished using positive ionization mode for MS detection. A gradient elution at a flow rate of 0.3 ml/min using aqueous 5 mM NH_4OH and MeCN, both containing 0.1% FA (v/v), was chosen. The initial content of 95% MeCN was decreased to 50% over 11 min. This mobile phase was kept for one minute and the MeCN content then increased back to 95% MeCN over 0.5 min. For a proper re-equilibration, this composition was kept for another 11 min before injecting the next sample, leading to a total analysis time of 23.5 min. The re-equilibration step used an increased flow rate of 0.5 ml/min during min 12-19.

5.3.4.2 NACE-MS analysis

All NACE-MS analyses were performed using an Agilent CE 7100 capillary electrophoresis (Agilent Technologies, Waldbronn, Germany) interfaced to an Agilent 6550 iFunnel Q-TOF mass spectrometer (Agilent Technologies, Santa Clara, USA) with an ESI source assisted by a sheath liquid interface (Agilent Technologies, Waldbronn, Germany). The composition of the sheath liquid was 50% isopropanol in water (v/v) with 0.01% FA (v/v). The sheath liquid was delivered by a 1260 isocratic pump (Agilent Technologies, Waldbronn, Germany) at a flow rate of 5 µl/min, delivered by a split-flow (1:100). The nebulizer pressure was set to 6 psig, and the drying gas flow rate to 11 l/min. Fragmentor voltage was set to +400/–300 V. A capillary voltage of +/−4000 V, a skimmer voltage of 65 V, and an octopole voltage of 750 V were used. The mass range was set to m/z 40-1000, and the data acquisition rate was 2 spectra/s. Online recalibration during NACE-MS analysis was possible by adding 0.2 µmol/l purine, 0.1 µmol/l HP-321 and 0.1 µmol/l HP-921 (all from Agilent Technologies, Waldbronn, Germany) to the sheath liquid. Data analysis was accomplished using MassHunter software (Agilent Technologies, Waldbronn, Germany).

CE separations were carried out using a bare-fused silica capillary (length 65 cm, i.d. 50 µm; Polymicro Technologies, Phoenix, Arizona). The non-aqueous background electrolyte (BGE) was a mixture of 25 mM NH_4Ac and 3 % HAc in MeOH. Samples

were injected hydrodynamically by applying a pressure of 100 mbar for 20 s. New capillaries were conditioned with BGE for 15 min and flushed between runs for 2 min. The CE capillary was kept at 25 °C during CE runs, and a voltage of +/-30 kV was applied. The capillary was kept in BGE upon storage.

5.3.5 Final protocol of the EME experiments

For the EME preconcentration, the protocol presented in Figure 5-2 was established.

Before experiment
- Manufacturing of PIMs in casting mold and slow evaporation over night
- Preparation of acceptor and sample solutions
- Cutting-out templets from adhesive tapes

Preparation of flow through cell
- Mounting templet from adhesive tape on each PEEK chamber
- Fixating PIMs on adhesive tape
- Carefully flushing acceptor solution to check for leakages
- Fixating 3D-printed sample channel separation layer on one of the PEEK chambers
- Housing both PEEK chambers and sample channel in a fixture and screwing tightly
- Starting to pump sample through channel using the syringe pump
- Flushing acceptor channels and filling electrode vessels
- Placing electrodes into the two acceptor vessels
- Starting magnetic stirrer and apply constant voltage or constant current

During the experiment
- Recording current and voltage application
- Checking for inconsistencies (leakages, voltage interruptions, …)

After the experiment
- Switching off recording unit, high voltage source, magnetic stirrer and syringe pump
- Pressure-assisted sampling of acceptor solutions into a sample vial via rinsing acceptor channel using a 1 ml syringe filled with air
- For NACE-MS and RPLC-MS analysis: direct injection
- For HILIC-MS: 10-fold dilution with MeCN prior to injection

Figure 5-2: Typical workflow of an EME experiment.

5.3.6 Data evaluation and method validation

Extracted ion chromatograms (EICs) were extracted and evaluated from mass profiles with a mass accuracy of 0.01 m/z using Mass Hunter Qualitative Software (Agilent, V10.0). EFs were calculated dividing the peak area of analyte signals (PA_{acc})determined after the EME procedure in the acceptor cells by the peak area determined for the spiked but untreated sample (PA_{sample}). For the determination of recoveries Rec in %, the volume ratio of the acceptor (V_{acc}) vs. the sample volume (V_{sample}) was considered, leading to Equation (5-1):

$$Rec = \frac{PA_{acc}}{PA_{sample}} \cdot \frac{V_{acc}}{V_{sample}} \cdot 100\% = EF \cdot \frac{V_{acc}}{V_{sample}} \cdot 100\% \qquad (5\text{-}1)$$

V_{acc} was determined by weighing the liquid in the two acceptor channels to be 0.105 ml and 0.112 ml for anionic and cationic acceptor solutions. V_{sample} can be calculated using flow rate · extraction time for each experiment. In case a stagnant sample solution was sampled, the volume in the sample channel was estimated based on the dimensions of the meander structure in the 3D-printed separation layer resulting in an effective sample volume of approximately 150 µl. The volume factor corresponds to the reciprocal value of the volume ratio and defines the maximum possible values of EF.

Matrix effects caused by salt concentrations were estimated via the recovery of analytes when spiking at a concentration of 5 µg/l (10 µg/l for NACE-MS) to an aqueous solution of 25 mM NaCl (for HILIC-MS diluted 10-fold with MeCN, thus 0.5 µg/l and 2.5 mM NaCl) compared to the recovery using aqueous reference standards without salt. For this, the corresponding peak areas of the analytes $PA_{25\ mM\ NaCl}$ and $PA_{standard}$ were used. Positive ($> 100\%$) and negative ($< 100\%$) matrix effects (ME) were defined by Equation (5-2):

$$ME = \frac{PA_{25\ mM\ NaCl}}{PA_{standard}} \cdot 100\% - 100\% \qquad (5\text{-}2)$$

All figures were created with Origin 2020 (OriginLab Corporation, Northampton, Massachusetts, USA) and Microsoft Power Point 2019 (Microsoft Corporation, Redmond, Washington, USA). 3D sketches of the flow-through cell were designed using SketchUp (Trimble Inc., Sunnyvale, California, USA). Statistical evaluation was conducted using IBM SPSS Statistics 26 (IBM, Armonk, New York, USA). The Box-Behnken-Design was created and evaluated using the Freeware Develve (Velp, The Netherlands).

5.4 Results and discussion

5.4.1 Investigation of selected parameters

The intention of this work was to establish a reproducible EME setup using rather non-selective PIMs to enable the simultaneous extraction and enrichment of a broad range of model analytes from aqueous samples into the cationic and anionic acceptor solutions. Several preliminary studies were conducted to optimize the flow-through cell. The following parameters were considered: membrane composition, current vs. voltage control, composition of acceptor solutions, flow rate for the sample, and analyte concentration range. In a final step, a Box-Behnken-Design (BBD) was used to investigate dependence of recoveries and EFs from the three parameters extraction time, flow rate and current (see Section 5.4.3) determined to be crucial for the EME.

5.4.1.1 Membrane composition

As a central part of the extraction step, several PIM compositions were investigated based on results in the literature. Four main aspects were addressed: 1) broad analyte coverage and thus low selectivity towards the polarity of analytes, 2) mechanical stability, 3) reproducibility of the manufacturing process, and 4) good precision in extraction

efficiencies. The starting point was the work of See and Hauser [231], where the effect of PIM compositions on extraction efficiencies of several model analytes was investigated. The use of CTA as mechanically robust base polymer could already be demonstrated in an earlier work of Schmidt-Marzinkowski et al. [230]. In the first set of experiments, TEHP was used as plasticizer for both anionic and cationic membranes. Ionic carriers were Aliquat 336 and DEHPA for anionic and cationic membranes, respectively. We investigated a wide range of membrane compositions using a simplified experimental setup with only two cells and sulfonic acid derivates and quaternary ammonium compounds as model analytes and not the flow-through cell. From these experiments, we chose three membrane compositions for anionic and cationic modes each for their good mechanical stability (see Table 5-2, PIM N° 1-6). The number of model analytes was enlarged (see Table 5-1 and Section 5.3.3.2). We obtained average recoveries (n = 3) of 27-68% (see Table 5-2). The experiments showed that at least 50 mg of PIM matrix were required when filling the trays of 8 mm in diameter in cationic membranes, which was double the amount reported by See and Hauser [231]. It was crucial to evaporate DCM very slowly by covering the casting mold with a petri dish. The production of anionic membranes containing Aliquat 336 was easier and stable membranes were obtained already with 25 mg (see PIM N°4, Table 5-2) without the necessity of slow DCM evaporation. The reason for the different behavior lies in the different abilities of DEHPA and Aliquat 336 to interact with the base polymer CTA as thoroughly elaborated by Pereira et al. [242]. An interesting alternative to manufactured cationic PIMs might be a commercial polyether sulfone membrane (3M MicroPES Flat Membrane 1F EL, 3M Deutschland, Neuss, Germany). Preliminary EME experiments using this membrane offered a high extraction efficiency with high precision (88 ± 3%) for the extraction of quaternary ammonium compounds [241]. However, with the relatively thick membrane (110 µm), analytes may become trapped and poor extraction efficiencies may evolve at low concentrations.

In general, extraction efficiencies decrease with increasing thickness of the PIM [229]. The relatively higher relative standard deviations (RSD) values for PIMs N° 1 (cationic) and N° 4 (anionic) listed in Table 5-2 were expected, as only 50 and 25 mg total mass were used for their production and the manufacturing process still exhibited reproducibility problems. The average extraction efficiencies and precision were sufficient using the cationic PIM N° 2, which was implemented into the flow-through cell. For the extraction of anions, the membranes were further optimized as extraction efficiencies were below 50% on average. Using membranes N° 5 as a starting point, we added different amounts of the plasticizers TEHP, FPNE and/or NPOE to produce membranes N° 7-9 (see Table 5-2) [243]. As these new PIMs were solely used in the flow-through cell and no stagnant experiments were conducted, determined recoveries were lower due to the applied flow rate (see also discussion in Section 5.4.4). However, taking a look at Table 5-2, the recoveries were at least doubled compared to PIM N° 5. With regard to mechanical stability and homogeneity we finally chose PIM N° 8 for further experiments.

Table 5-2: PIM compositions investigated for the extraction of cationic (PIM N° 1-3) and anionic analytes (PIM N° 4-9). If not stated otherwise, PIM N° 2 and 8 were used during the following EME experiments in the flow cell. Recoveries listed under "two cell compartment" were determined using the two-compartment cell described in Section 5.3.3.2 and recoveries listed under "flow-through cell" according to Section 5.3.3.3 (extraction current of 150 µA, flow rate of 0.3 ml/min and extraction time 15 min) and Equation (5-1) in Section 5.3.6.

PIM N°	base polymer	ionic carrier		two cell compartment	flow-through cell	plasticizer		
	CTA in mg (%)	DEHPA in µl (m%)	Aliquat 336 in mg (m%)	av. rec. ± av. RSD in % (n = 3)	av. rec. in %	TEHP in µl (m%)	FPNE in µl (m%)	NPOE in µl (m%)
cationic membranes								
1	19 (37)	23.3 (44)		68 ± 27		10.9 (19)		
2	25 (40)	18.1 (38)		60 ± 7		8.2 (22)		
3	30 (50)	10.9 (17)		62 ± 16		20.7 (33)		
anionic membranes								
4	19 (74)		3.8 (16)	47 ± 21		2.7 (10)		
5	25 (50)		17.5 (35)	47 ± 9	11	8.2 (15)		
6	30 (50)		25.0 (43)	27 ± 13		4.3 (7)		
7	25 (46)		13.3 (24)	-	25		12.5 (30)	
8	25 (49)		13.3 (26)	-	27		4.9 (12.5)	6.1 (12.5)
9	25 (49)		13.3 (26)	-	24	4.6 (8.3)	3.2 (8.3)	4.1 (8.3)

We experimentally verified that diffusion of analytes through the PIMs (without applying an electric field) can be neglected. It was also investigated whether the membrane could be reused by repeating EME experiments with the same membranes but a blank sample. The acceptor solutions were analyzed and strong memory effects were observed with all model analytes detected in the anionic and cationic acceptor solutions [244]. Thus, for all experiments conducted here, new membranes were used before each EME run.

5.4.1.2   Current vs. voltage control

We varied the inner diameter of the PEEK capillaries connecting cell and acceptor solutions from 130-250 µm. With this small instrumental change, it was possible to apply extraction voltages between 500-1500 V while keeping the current below 150 µA. Preliminary results indicated higher extraction efficiencies at lower extraction voltages possibly due to the smaller inner diameter which hindered a fast transport of extracted ions to the acceptor vials. Clearly, not all parameters are well understood in EME. In the literature, mainly voltage-controlled setups are used [212] and no or little information about resulting currents is provided. Our preliminary experiments with an aqueous standard showed higher reproducibility using voltage control, well in accordance with preferences described in the literature. However, all further experiments were conducted in constant-current mode. Voltage and current control and the understanding of related effects become vital, when real samples strongly differing in conductivities are to be extracted by EME [213]. Current-controlled EME proved superior in our experiments when analyzing diluted river water samples as a higher reproducibility was observed, similar to the literature [236, 245, 246]. Additionally, Rahmani et al. [247] demonstrated that current patterns and precision of extraction efficiencies are correlated.

5.4.1.3   Analyte concentration range

One of the goals was to improve detection limits using EME for analyte enrichment prior to NACE-MS. The following settings were chosen based on our preliminary experiments: spiked aqueous samples (10, 50, 100 and 500 ng/l); current-controlled EME at 400 µA for 20 min using PIM N° 2 and N° 5 (see Table 5-2). In order to investigate the precision of the procedure, isotopically labeled standards of some of the model analytes (see Table 5-1) were added at a concentration of 10 µg/l. Exemplarily, the results of the analyte METF and its isotopically labeled standard METF d6 are shown in Figure 5-3. An increase in signal areas of METF (red dots) with and without using EME for enrichment can be observed. The increase is almost linear for METF with NACE-MS ($R^2 = 0.9927$) but somewhat lower using EME/NACE-MS with $R^2 = 0.9864$ (see Figure 5-3).

Regarding extraction efficiencies, first of all, the small differences between the standard and its isotopologue at low concentrations were well within the standard deviation of the EME/NACE-MS method. Similar EEs were obtained for METF and METF d6, albeit the concentration of METF varied whereas the concentration of METF d6 was constantly high with 10000 ng/l. This demonstrates that the concentration dependence of EFs is low. However, whereas EFs were similar (RSD = 12%) with about 4 for the spiking levels 10, 100 and 500 ng/l, they were strongly elevated (factor of 2.5) for both METF and METF-d6 at 50 ng/l, pointing to an outlier with impairments of the EME process (for example instabilities in EME step or memory effects). Obviously, the internal standard can be used for corrections in this case. Excluding the value of 50 ng/l would result in a R^2 value of 0.9970, demonstrating high linearity. The increase in sensitivity can be quantified by comparing the slopes of the two calibration curves, resulting in a 4-fold higher sensitivity using the EME/NACE-MS setup.
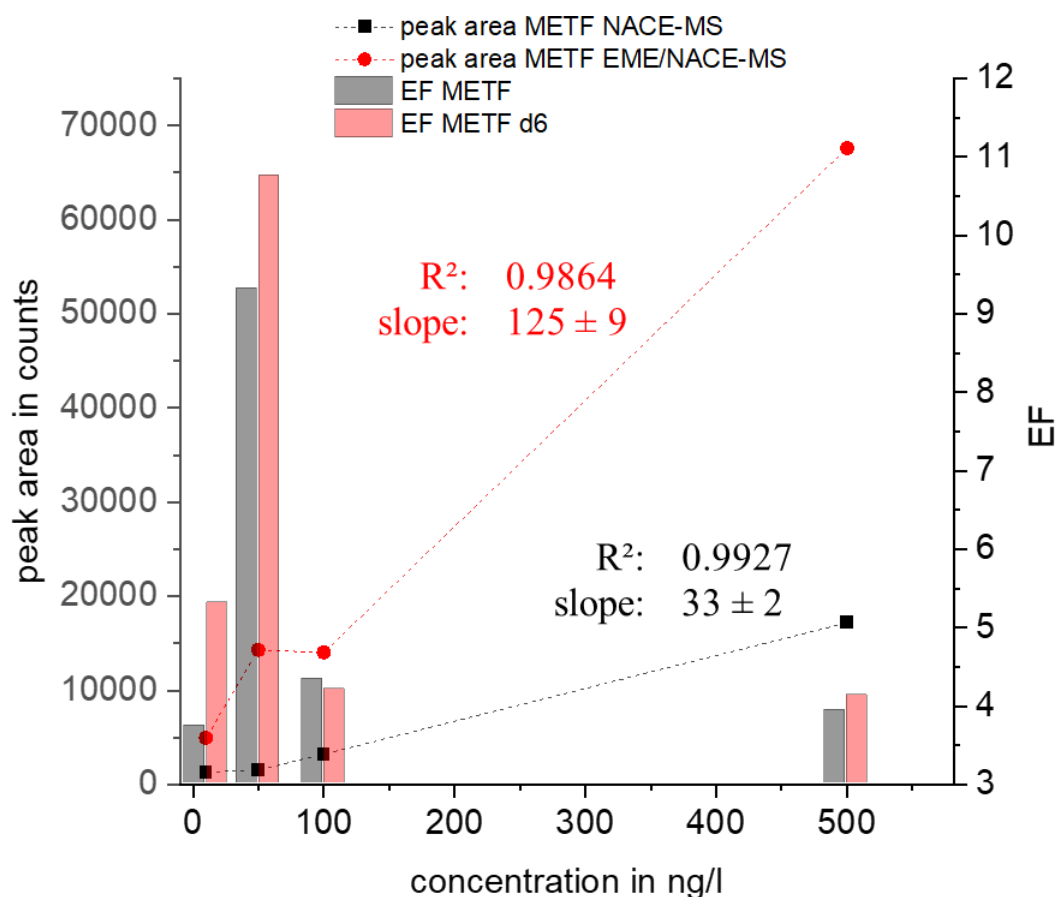
Figure 5-3: Peak areas of METF without (black squares) and with EME (red dots) prior to NACE-MS analysis of spiked (10, 50, 100 and 500 ng/l) aqueous samples. The bars show EFs (see Section 5.3.6) of METF (grey) and METF d6 (red). METF d6 was spiked at a concentration of 10000 ng/l in all samples analyzed here. R² and slope values were obtained via linear regression. EME conditions: 400 µA extraction current, 20 min extraction time, 0.3 ml/min flow rate. NACE-MS analysis was conducted as described in Section 5.3.4.2.

For the majority of anionic analytes, EFs between 1 and 3 only and with a low reproducibility were obtained, due to the inferior performance of the PIM N° 5 [244]. As a consequence, a broader spiking range at slightly higher concentrations (100, 250, 500, 750 and 1000 ng/l) was chosen for a second set of experiments to qualitatively investigate the improvement of sensitivity using the EME setup. Whereas the concentration of MIAA and DFAA was below the detection limit (LOD) when using NACE-MS only for spiking concentrations of 1000 ng/l, the analytes were well detectable in the EME acceptor solution from extracting a sample at a concentration of 250 ng/l. SULAC was even detectable in the sample spiked with 100 ng/l after EME preconcentration demonstrating great potential also for anions, despite the requirement for some further improvements.

5.4.2 Compatibility with separation methods and matrix effects

To investigate the general compatibility of our EME setup with different separation methods, acceptor solutions were analyzed with NACE-MS, RPLC-MS using a C18 stationary phase and also HILIC-MS (using a ZIC-HILIC stationary phase) as the target analytes were mostly polar. We chose an intermediate concentration of the model analytes

in an aqueous sample of 5 µg/l, sufficiently high relative to the LOD but small enough to prevent overloading of the separation system. The LODs of analytes in NACE-MS were mostly < 2 µg/l without EME. Overloading in RPLC was avoided using low injection volumes. A compromise had to be made for the HILIC method: best separation efficiency was determined by injecting samples with a water fraction of 5%, which would require a 20-fold dilution, resulting in concentrations of 100 ng/l. We finally diluted only 1:10 with MeCN (MeCN/H$_2$O ratio of 90:10, v/v) as the peak shapes were still acceptable.

Two similar, but slightly different EME experiments (200 µA, 25 min, 0.4 ml/min vs. 200 µA, 30 min, 0.35 ml/min) were conducted as described in Section 5.3.5. Figure 5- 4A-F depicts the chromatograms (A-D) and electropherograms (E, F) for the analysis of the acceptor solutions (red lines) using the second EME condition (200 µA, 30 min, 0.35 ml/min). The black lines correspond to the aqueous reference sample which was used for the EME experiment. All analytes present exhibited an increase in peak areas using EME as sample preparation technique. Especially for the analysis of the cationic acceptor solution using RPLC-MS detector saturation was observed for several analytes, resulting in lower apparent EFs calculated (see below).
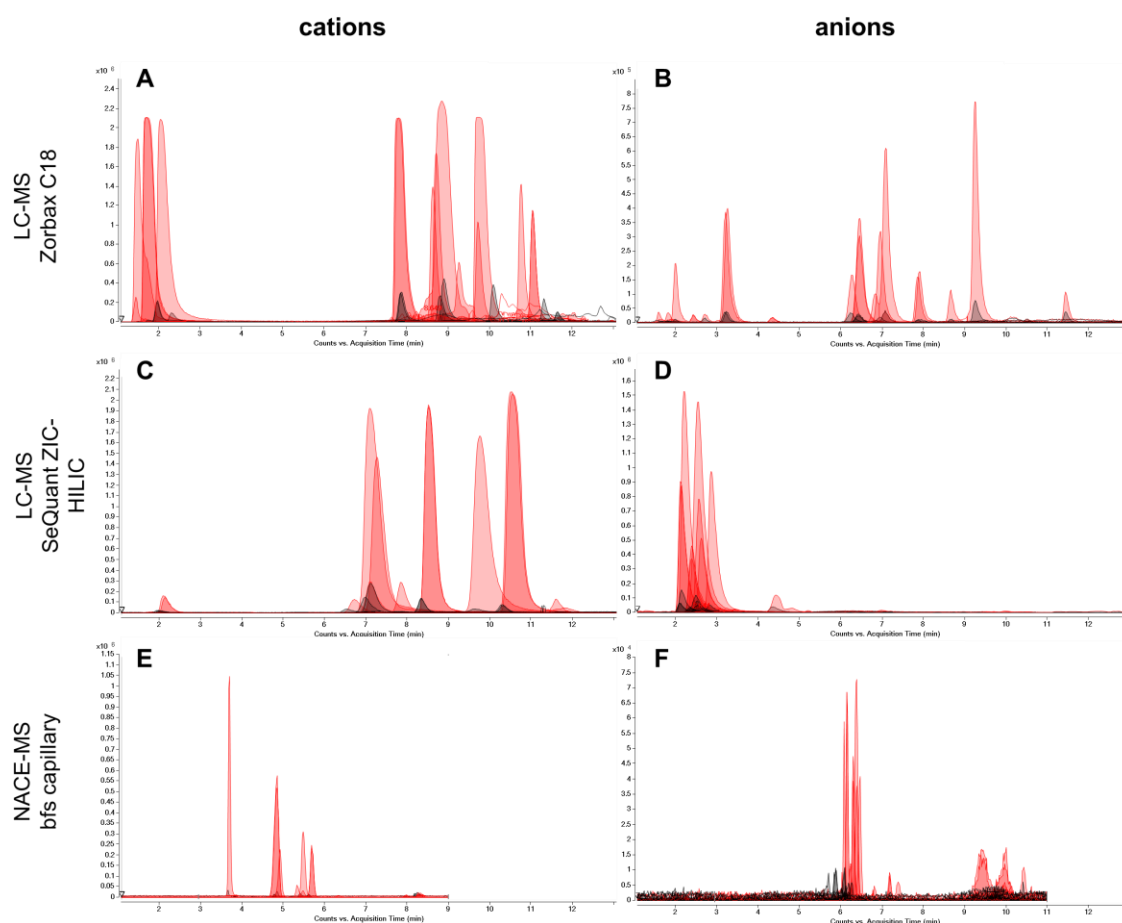
Figure 5-4: Chromatograms (A-D) and electropherograms (E, F) of the analysis of the positive and negative acceptor solutions (red filled lines) obtained after conducting an EME experiment using 200 µA extraction current, 30 min extraction time and a flow rate of 0.35 ml/min. RPLC-MS (A, B), HILIC-MS (C, D) and NACE-MS (E, F) were used as described in Sections 5.3.4.1.1, 5.3.4.1.2 and 5.3.4.2, respectively. Black filled lines correspond to the aqueous sample before the EME sample preparation step. Bfs: bare-fused silica.

Figure 5-5A-D shows the EFs calculated according to Section 5.3.6 using RPLC-, HILIC- and NACE-MS for analyte quantification in the cationic (Figure 5-5A and C) and anionic (Figure 5-5B and D) acceptor solutions. The EFs are sorted according to the log D values of the analytes at the pH 5 of the aqueous sample. Additionally, positive/negative matrix effects (see Section 5.3.6, Equation (5-2)) were determined via the ratio of peak areas obtained for an spiked aqueous standard (0.5 µg/l for HILIC-MS, 5 µg/l for RPLC-MS and 10 µg/l for NACE-MS) with and without the addition of NaCl to the acceptor solution to simulate enriched salt matrix. Results are displayed in Figure 5-5E and F for cationic and anionic acceptor solutions. It has to be mentioned, that not all values (EFs and matrix effects) could be determined with sufficient precision as some LODs were not met. In the following, only general trends are elaborated.
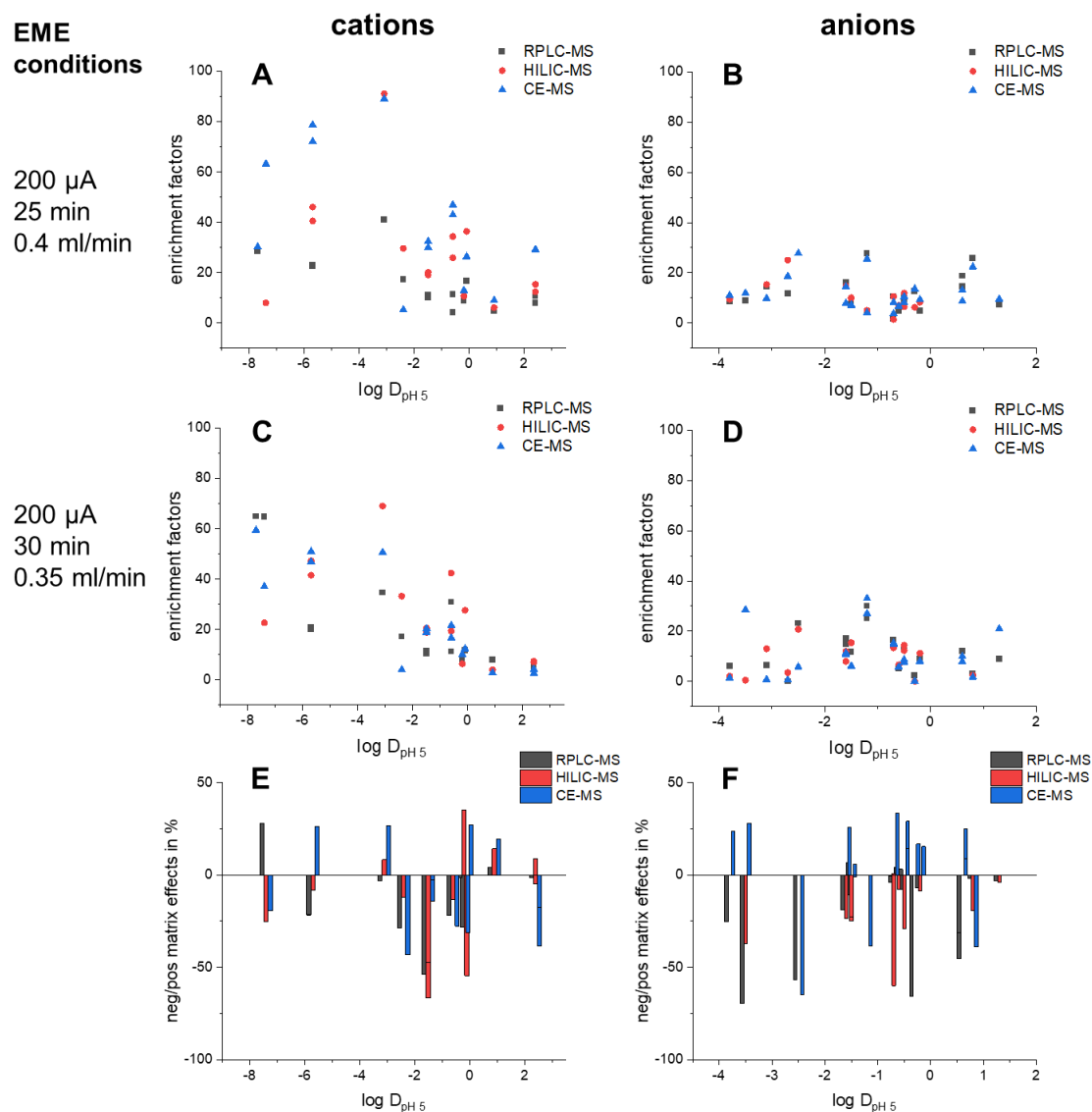
Figure 5-5: Enrichment factors (calculated as described in Section 5.3.6) obtained sorted according to the analytes' log $D_{pH\,5}$ values (Table 5-1) for two different EME experiments analyzing the acceptor solutions (A, C: positive acceptor solutions, B, D: negative acceptor solutions) with RPLC-MS (black squares), HILIC-MS (red dots) and NACE-MS (blue triangles). E and F depict the matrix effects calculated by Equation (5-2) in Section 5.3.6 for the model analytes in a 25 mM NaCl solution (for HILIC-MS 10-fold dilution with MeCN, thus 2.5 mM NaCl) compared to an aqueous solution. Analyses of the acceptor solutions (A-D) and the spiked standards (E and F) were conducted as described in Section 5.3.4.

Taking a look at the graphs A-D in Figure 5-5, significantly higher EFs were obtained for cations compared to anions in both EME experiments. Average EFs ranged from 5 (ACR d9) to 74 (1-E-3-MIM) with an average EF of 26 for all 15 cationic model analytes. For the 23 anions, EFs ranged between 2 (MCPA) and 31 (MIAA) with an average EF of 12 in both EME experiments. The differences in EFs between anions and cations were not significant (paired t-test, α = 0.05), demonstrating a broad coverage achieved by both PIMs.

A lower precision of EF values was observed for cations than for anions (37% RSD vs. 20%) mostly due to differences of EFs determined by RPLC compared to results by HILIC or CE. Some of these differences can be explained by overloading of the column with sample in RPLC-MS analysis. This is depicted exemplarily in Figure 5-4A for the analysis of the acceptor solutions using the same EME conditions as in Figure 5-5C and D. As saturation is reached, the EFs gained are lower for eight analytes (1-E-3-MIM, METF (d6), VENLA (d7), PIND (d7) and NAPHA with log $D_{pH\,5}$ of -3.1, -5.7, -0.2, -1.5 and -0.6, respectively). As for the EFs themselves, precision was independent of the analytes' polarity. Another reason for the differences in EFs is matrix effects in the downstream analysis method. Thus, matrix effects ME were calculated according to Equation (5-2) and were summarized in Figure 5-5E and F. In both detection modes, matrix effects were present without significant correlation between detection polarity and polarity of analytes (log $D_{pH\,5}$ values). Whereas in positive detection mode both positive and negative matrix effects were observable for all three separation methods, positive matrix effects were solely observed for NACE-MS in negative detection mode. The reason for this is not yet identified and needs further research. Only for a few analytes, the EFs correlated with the type and magnitude of the matrix effect: for instance, the EFs determined for NMP (log $D_{pH\,5}$ = -2.4 Figure 5-5E) and 7-A-1,3-NDSA (log $D_{pH\,5}$ =-3.5, Figure 5-5F) correlate with the order and magnitude of positive and/or negative matrix effects. However, for most analytes no such pattern was present, indicating that each analyte behaved differently with regard to the EME experiments and the subsequent separation technique. Matrix effects will thus depend on the selectivity of the separation method chosen. Adjusted EFs may be obtained upon the determination of matrix effects when spiking acceptor solutions after a blank EME experiment.

Within the scope of these experiments, it was possible to demonstrate the compatibility with all three separation techniques. Attention needs to be paid to analytes showing high matrix effects, which may impair the determination of EFs, complicating comparative analysis and method optimization.

5.4.3 Box-Behnken-Design

Optimal operation conditions for EME of river water samples were considered [147, 234, 248]. As investigating each parameter individually is laborious and time consuming, we chose Box-Behnken-Design (BBD) as a more efficient chemometric approach compared to a three-level full factorial design [249]. It avoids combinations of extreme values of all factors: combinations of high current/voltage with high flow rates and long extraction times were difficult to apply producing run failures.

The BBD design is summarized in Table 5-3. We analyzed the acceptor solutions with NACE-MS and RPLC-MS to obtain a more comprehensive view on enrichment and matrix effects (see Section 5.4.2). The starting method for the BBD was current-control at 200 µA for 15 min with a flow rate of 0.3 ml/min.

Table 5-3: BBD for the optimization of current, time and flow rate for the EME experiment using the flow-through cell. Blocks correspond to experiments on day 1 and day 2. Starting point 0 was an EME experiment with 200 µA extraction current (first position), 15 min time (second position) and a flow rate of 0.3 ml/min (third position). Spiked analyte concentration in the sample was 5 µg/l. The design was planned using the freeware Develve (Develve, Velp, The Netherlands). Results for EF and Rec are given for the cationic and anionic cell differentiating between the values obtained from RPLC vs. NACE-MS analysis. Values are average values for 23 and 15 analytes in the anionic and cationic acceptor cells, respectively (see Table 5-1). For further information, see text.

Block	Box Behnken Design	current in µA	time in min	flow rate in ml/min	average EF (Rec) in cationic acceptor cell		average EF (Rec) in anionic acceptor cell	
					RPLC-MS	NACE-MS	RPLC-MS	NACE-MS
1	000	200	15	0.3	6.3 (22.9)	9.2 (23.0)	3.4 (7.9)	6.8 (15.4)
1	−−0	100	5	0.3	1.5 (9.2)	2.0 (12.0)	1.2 (5.8)	1.4 (16.7)
1	+−0	300	5	0.3	2.3 (22.0)	2.5 (18.6)	1.6 (12.3)	3.4 (24.5)
1	−+0	100	25	0.3	11.3 (18.6)	13.4 (20.1)	11.8 (19.3)	19.9 (17.7)
1	++0	300	25	0.3	14.1 (14.5)	9.1 (13.5)	5.0 (6.0)	7.9 (7.1)
1	0−−	200	5	0.2	1.4 (6.8)	2.1 (27.4)	0.4 (2.4)	1.2 (47.6)
1	000	200	15	0.3	11.3 (31.7)	10.8 (27.5)	7.2 (18.7)	14.8 (44.0)
2	0−+	200	5	0.4	1.4 (9.1)	2.2 (7.1)	1.0 (7.5)	4.1 (12.5)
2	0+−	200	25	0.2	11.3 (31.7)	19.9 (42.2)	10.0 (27.6)	16.1 (37.7)
2	0++	200	25	0.4	18.0 (23.0)	37.9 (38.8)	12.0 (12.3)	15.6 (22.1)
2	−0−	100	15	0.2	3.1 (15.7)	5.0 (15.6)	3.2 (15.6)	3.6 (24.8)
2	−0+	100	15	0.4	6.4 (13.7)	7.8 (13.3)	14.2 (34.5)	15.0 (37.9)
2	+0−	300	15	0.2	8.0 (38.4)	10.9 (43.8)	5.5 (21.1)	8.1 (29.4)
2	+0+	300	15	0.4	5.8 (15.3)	6.8 (11.5)	10.4 (18.7)	11.8 (25.5)
2	000	200	15	0.3	6.0 (18.3)	10.0 (25.6)	7.7 (18.7)	7.2 (23.5)

An aqueous solution containing 5 µg/l of the analytes listed in Table 5-1 served as sample solution. The goal was to optimize EFs and recoveries (Rec) for both anionic and cationic extraction steps. For this, the three parameters current, time and flow rate were reduced (marked as "−")/increased (marked as "+")/maintained (marked as "0") independently for each experiment (see Table 5-3, column "Box Behnken Design"). The parameter range was determined in preliminary studies and was set between 150 and 250 µA for current, 15 and 25 min for time and 0.2 and 0.4 ml/min for flow rate. The results using RPLC-MS and NACE-MS are listed in Table 5-3. EFs and Rec were calculated as described in Section 5.3.6, Equation (5-1) for each analyte; the average values over all analytes are given in Table 5-3 for anionic and cationic acceptor solutions and RPLC-MS vs. NACE-MS.

During these experiments, volume factors between 9 (5 min, 0.2 ml/min) and 90 (25 min, *0.4* ml/min) were investigated. They define the maximum enrichment factors that can be reached in the EME experiment. We calculated average EFs over all 38 analytes, separately for analytes detected in anionic (23) and cationic (15) acceptor cells. Whereas EFs determined in cationic acceptor cells correspond well to these volume factors using both RPLC-MS and NACE-MS, this was not observed for the enrichment of anions.

The center point conditions (marked as "000") are used three times in the BBD (see Table 5-3). The average EFs (Rec) of these three experiments in cationic acceptor cells were 7.9 (24.3) and 10.0 (25.4) using RPLC-MS and NACE-MS. For anionic acceptor cells, average EFs (Rec) of 6.1 (15.1) and 9.6 (27.6) were obtained for RPLC-MS and NACE-MS. RSD values ranged between 23 and 43% with one exception: average EFs obtained in cationic cell by NACE-MS showed a lower variance (6.5%), however, calculation of RSD values for each analyte individually resulted in an average RSD value of 35%. Taking a look at the average EFs and Rec values, they differ from 2 to 29% between the two separation methods used. Though some deviations might have their origin in the differing compatibility with separation methods already discussed in Section 5.4.2, these values are still within the overall RSD values obtained using RPLC-MS and NACE-MS, indicating insufficient reproducibility of the EME setup.

We compared the results obtained in the BBD for average values and for the analytes individually and also for NACE-MS vs. RPLC-MS. Statistical significance was defined for p-values lower than 0.05. Figure 5-6A and B show two heat maps of all p-values for the 23 anionic compounds and 15 cationic compounds using EF values (Figure 5-6A) and Rec values (Figure 5-6B), highlighting significant factors and interactions in red.

Taking a look at the profile of the heat maps in Figure 5-6A comparing EFs determined by RPLC-MS vs. NACE-MS, the overall profile of the heat maps is rather similar, when considering the high RSD values of 35% mentioned earlier. EFs were significantly different when changing extraction times for 11 out of 15 cationic analytes and 20 out of 22 anionic analytes using RPLC-MS and 10 and 11 analytes quantified by NACE-MS.

Calculated Rec values according to Equation (5-1) are normalized to differences in flow rate and extraction time. Though high values of Rec are preferable, a compromise is often made between high volume factors and acceptable values of Rec to keep enrichment times short. With the normalization, the heatmap profile in Figure 5-6B changes compared to

the EF maps. This is expected, as the adjustment of the EF values by the volume factors of each experiments sets the focus directly on the extraction process through the membrane rather than the whole EME process. Only for a few analytes, the Rec values depend on the factors of the BBD. Possible reasons for this are 1) the low reproducibility of the EME process (RSD values of 35% averaged over all analytes) and 2) the limited robustness of the membrane preparation process which can result in high variations between different membrane batches.
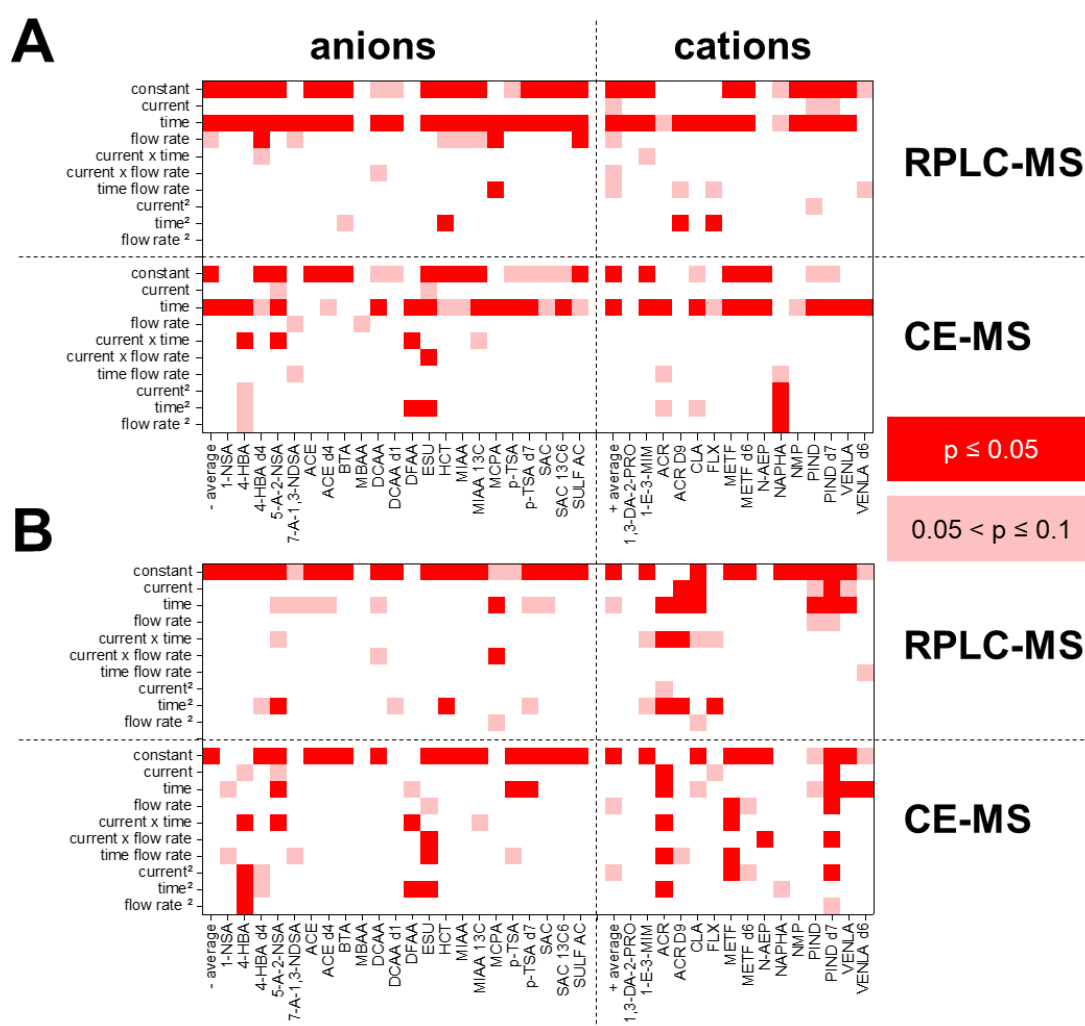
Figure 5-6: Heat map showing significant p-values (red, $p \leq 0.05$, determined with Develve) for the factors current, time, flow rate and interactions thereof by using EFs (Figure A) and Rec (Figure B) values obtained by analyzing each acceptor solution of the BBD (see Table 5-3) using RPLC-MS and NACE-MS. Average values (values listed in Table 5-3, marked here as "- average" and "+ average") and values for each analyte individually (abbreviations see Table 5-1) were reviewed. RPLC-MS analysis was conducted according to Section 5.3.4.1.1, NACE-MS according to Section 5.3.4.2. For further information, see Table 5-3 and text.

Figure 5-7A-F shows the response surfaces for EF values (A, C and E) and Rec values (B, D and F) for the three analytes 4-HBA, 5-A-2-NSA and DFAA, showing a significant dependence on the interaction of current and time. All three anionic analytes possess different functional groups and a different molecular backbone (log $D_{pH\,5}$ values between -2.7 and 0.6) and are thus representative for the general performance of the EME process.

The values were obtained by NACE-MS analysis. Similar shapes of the response surfaces are visible for EF and Rec.

BBD: EF   BBD: Rec.
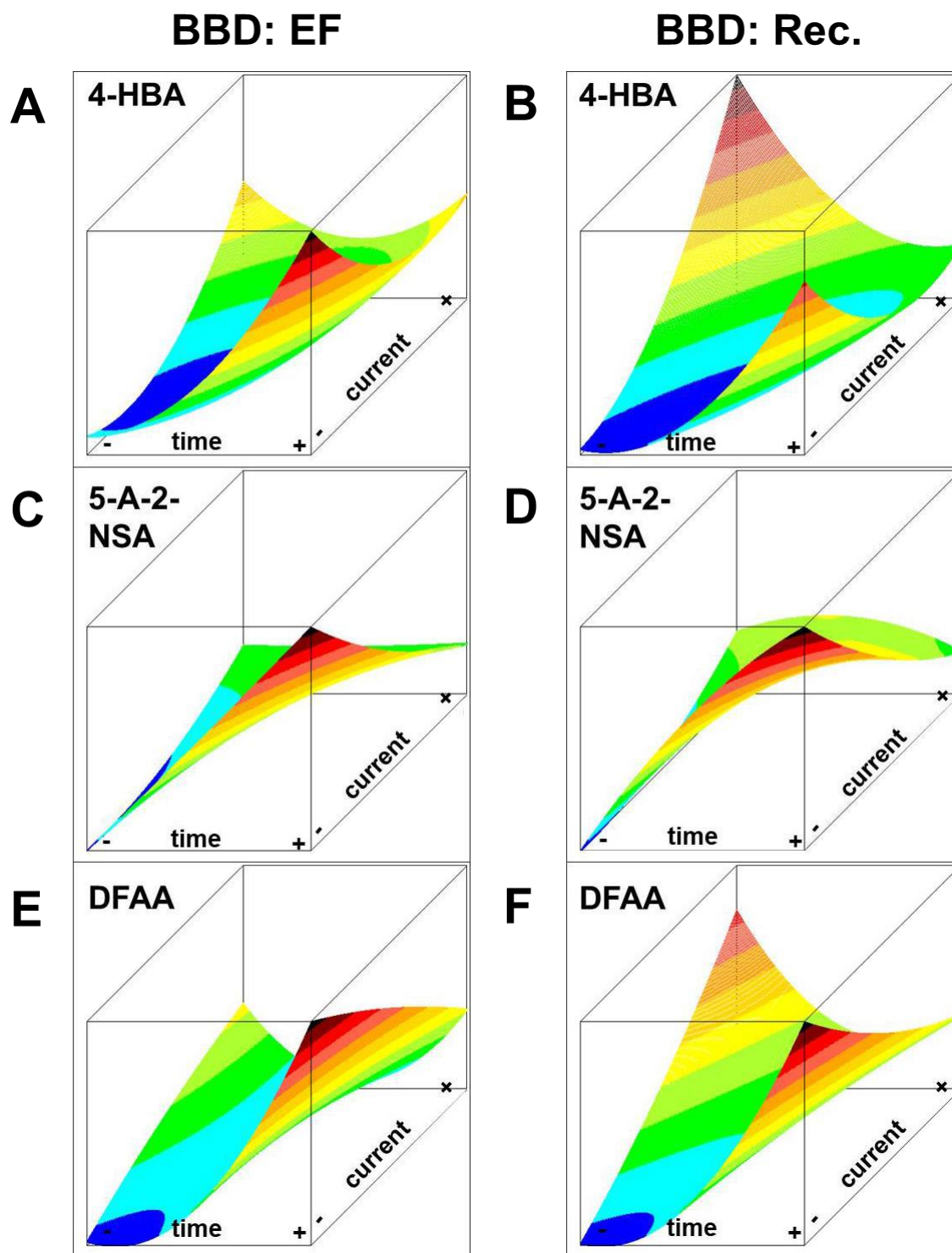
Figure 5-7: Response surface graphs for selected analytes using the BBD with EF (A, C, E) and Rec values (B, D, F) depending on factors time and current (interaction significant, see Figure 5-6) for the three anionic analytes 4-HBA, 5-A-2-NSA and DFAA. Results are based on NACE-MS (see Section 5.3.4.2). For further information, see Table 5-3 and text.

For all three analytes, high extraction times combined with low currents were favorable for obtaining high EF values. A second maximum in the response surfaces was present at short extraction times but high currents. This maximum was more pronounced for Rec

values as can be seen in the response surface graphs of Rec for 4-HBA and DFAA (Figure 5-7B and D). This demonstrates the possible differences between EFs and Rec values due to the correction of the Rec values by the volume factor. The results indicated good extraction recoveries using short extraction times and high currents. However, as expected, higher flow rates did not compensate short extraction times completely (see also discussion in Section 5.4.4). An overall lower volume factor resulted in lower EF values. Thus, a compromise would have to be made with lower extraction efficiencies but overall higher EFs. Additionally, with the exception of the Rec values of 4-HBA (p = 0.960) and DFAA (p = 0.065), higher extraction times (positive coefficients) proved to be significant. No significant dependence of EFs on the factors in the BBD was obtained for cations. Looking at Rec values, only the two analytes ACR and METF showed a significant dependence on current · time. Figure 5-8A-D shows the response surfaces for METF and ACR both for NACE-MS and RPLC.
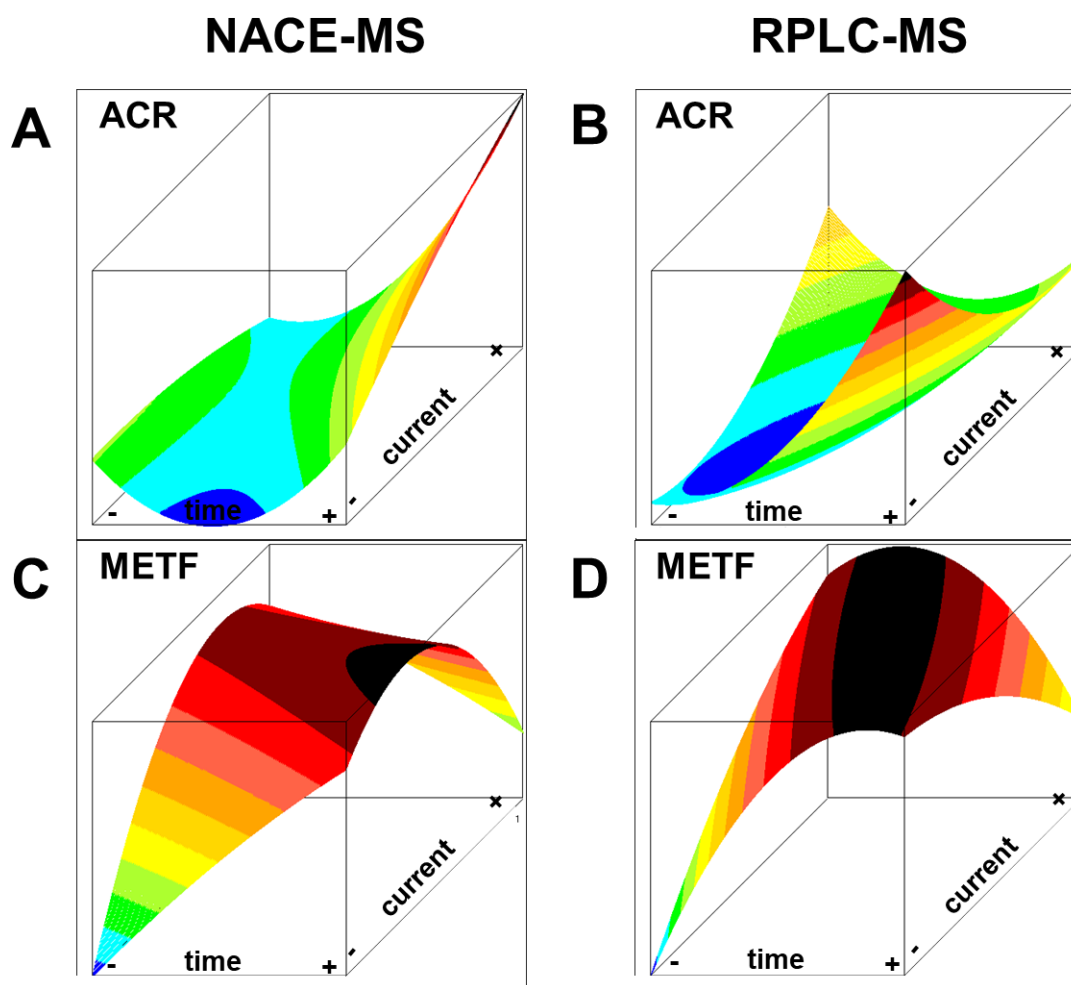
Figure 5-8: Response surfaces of the BBD for Rec values in correlation with the factors time and current, which proved to show significant interaction (see Figure 5-6) for the two cationic analytes ACR and METF. For quantification, NACE-MS (Figures A and C, see also Section 5.3.4.2) and RPLC-MS (Figure B and D, see also Section 5.3.4.1.1) were used. In Figure D the dependence of time and current for METF is shown, but no significant correlation was obtained for this interaction (p-value of 0.16). For further information, see Table 5-3 and text.

For the two analytes ACR and METF (Figure 5-8A and C), the factors current and time have a different impact on extraction efficiencies: highest enrichment efficiencies for METF were obtained close to the center point of the BBD, whereas for ACR, highest recoveries were reached at the corners of the BBD. Presumably, this is due to the different charge states as METF is doubly charged whereas ACR (basic pK_a value of 6.2) is probably not fully ionized at the pH of the EME experiments. In addition, polarities differ strongly between these two analytes (log $D_{pH\,5}$ values of -5.7 (METF) and 2.4 (ACR)) which is relevant for the transport through the membrane. Comparing the response surfaces obtained using NACE-MS vs. those obtained by RPLC-MS (Figure 5-8A and B), different optimal conditions prevail. For NACE-MS analysis, high current and high extraction time provide highest Rec values, whereas for RPLC analysis, low currents and long extraction times should be combined. This discrepancy underlines the impact of matrix effects mentioned in Section 5.4.2, which may overlay effects in the EME process itself. Looking further into detail, it appears that in NACE-MS analysis, ACR migrates close to the EOF and matrix effects caused by differing salt concentrations in the sample are more likely. However, further information and comparisons with more analytes would be necessary for a clearer distinction between effects due to enrichment vs. matrix components.

The evaluation of this Box-Behnken-Design leads to five major conclusions: 1) Time seems to be a significant parameter for most analytes. 2) Differentiating between values of EF and Rec allows to validate the system with regard to its overall performance including the downstream analysis, but also the efficiency of the transport through the membrane itself, which is important for membrane optimization. 3) Using different separation methods is an interesting tool to validate the developed EME setup and its optimization as matrix effects may superimpose those from the EME process. 4) The EME-system developed reveals high enrichment factors for cationic analytes, whereas improvements are needed to enhance the extraction of anionic compounds. 5) The reproducibility of the system has to be improved.

5.4.4 Application to river water sample & stagnant vs. flow sample introduction

The EME protocol using the parameters optimized in Section 5.4.3 was followed with spiked river water as sample. As long extraction times proved significant to obtain higher EFs, the analytes were enriched for 30 min. It is known that high salt concentrations in samples (as present in most environmental waters) can affect the extraction of target analytes, so we tested if diluting the samples aids extraction. Additionally, it was of interest, if the presence of a sample flow affects the recoveries of different analytes.

We compared the results for the river water samples (*N2*) with those of a 1:4 diluted river water sample (*N2*/H_2O 1:4 v/v) and an aqueous standard. For all three samples, EME experiments were performed 1) under a constant flow rate and 2) at stagnant conditions. A high flow rate of 0.35 ml/min was chosen to reach a high volume factor. Recoveries were determined as described in Section 5.3.6 using NACE-MS.

All results are summarized in Figure 5-9A-C for anionic analytes and D-F for cationic analytes sorted by their log $D_{pH\,5}$ values. Recoveries (Rec values) were compared for

constant flow (Figure 5-9A and D) vs. a stagnant sample solution (Figure 5-9C and F). For better comparison, Figure 5-9B and E use the average values of both settings with error bars.
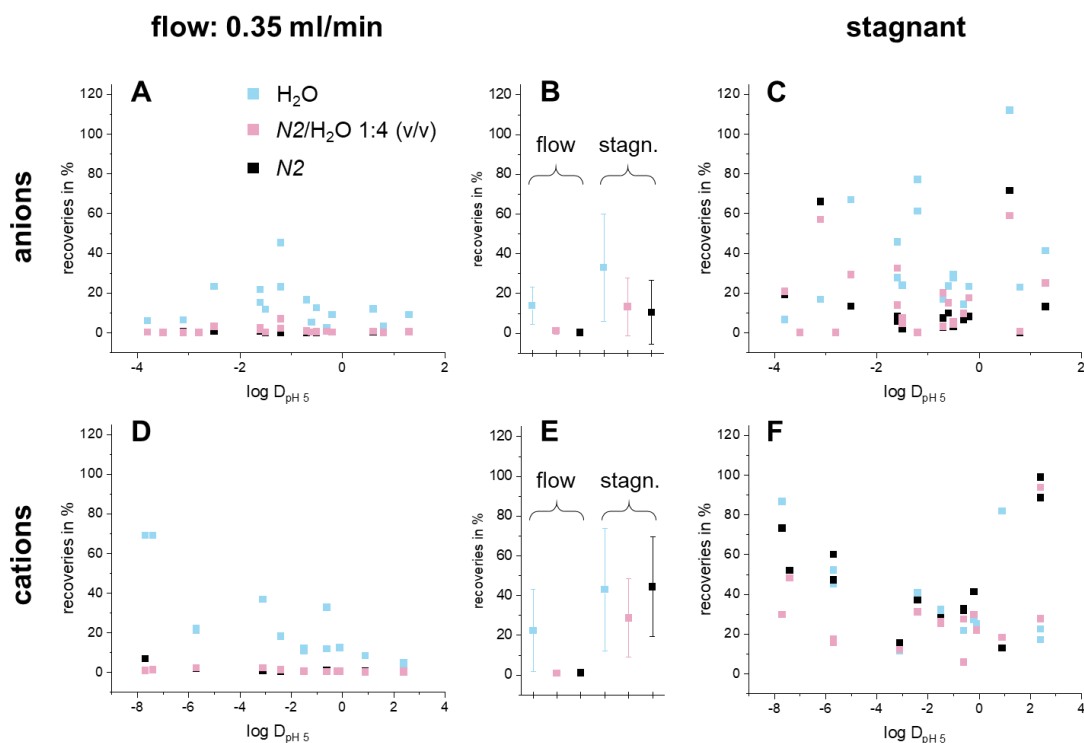
Figure 5-9: Recoveries in dependence of the log D_{pH5} values (Rec values, see Equation (5-1) in Section 5.3.6) for all anions (A-C) and cations (D-F) with mean values given in B and E. For each sample, one experiment was conducted using a flow rate of 0.35 ml/min (Figures A and D) and one using stagnant conditions (Figures C and F). B and E show the average Rec values for the three matrices under a steady flow and stagnant conditions. EME experiments with samples spiked with the analytes at a concentration of 5 µg/l. Blue: aqueous solution, black: river water sample N2, red: 5-fold dilution of river water sample N2. Analytes are listed in Table 5-1. All EME experiments were conducted at a constant current of 200 µA for 30 min. Analytes were quantified in the acceptor solutions by NACE-MS (see Section 5.3.4.2).

In average, extraction recoveries were similar for anionic and cationic compounds when operating the EME experiment under a constant flow rate of 0.35 ml/min. When switching to a stagnant solution, a similar improvement in extraction recoveries was observed for anions and cations. Recoveries in spiked diluted and original river samples depended on the way of sample introduction: for EME experiments operating with flow, recoveries decreased drastically for anions and cations when using (diluted) river water samples. Under stagnant EME conditions, recoveries improved significantly (t-test, $\alpha = 0.05$) only for cations in both diluted and original river water samples. Only slightly better recoveries were obtained for anionic compounds.

5.4.5 Concluding discussion

Several reasons account for the increase in recoveries when switching to a stagnant solution: First, target analytes can reach the membrane without having to counteract fluidic forces caused by the sample flow. Aranda-Merino et al. [250] showed, for example, that recoveries of non-steroidal anti-inflammatory drugs in an aqueous sample decreased when increasing the flow rates. Second, when ions of high electrophoretic mobility are

present in the sample at higher concentrations, as it is often the case in real samples, these charged matrix ions compete with the target analytes as is commonly observed for electrokinetic injection in capillary electrophoresis [251]. High salt concentrations in the sample were reported to influence recoveries of target analytes in the EME [252]. Third, the differences in conductivities of sample and acceptor solution define the electric field strength, directly influencing the migration of ions across the EME membrane. Often, the ion balance [253] is discussed, defined as the ratio between the total concentration of ions in the sample and the total concentration of ions in the acceptor solution to influence the EF. For samples with higher conductivities the adaption of acceptor solutions to higher conductivities and thus decreasing the difference in conductivities have been reported to provide higher extraction efficiencies and thus higher EFs [254].

A possible explanation for the differences we observed between cationic and anionic analytes was given by Nasrollahi et al. [255]. By measuring the impedance of an EME setup, the authors discussed effects suppressing the analyte migration caused by the addition of different types of salt. Experiments showed that for cationic analytes the interference mainly derive from the proton despite that all other cations investigated (K^+, Na^+, Li^+) possess significantly smaller positive free energy of transfer through the membrane. For anionic compounds, however, anions like Cl^- or NO_3^- exhibited a lower positive free energy of transfer and had a strong influence on the time dependence of the sample solutions' resistance and double layer capacitance. Though these results were established for an SLM and strongly depend on the membrane composition, they are well in accordance with the results observed in the experiments of our study: for cationic analytes, the major interference seems to be the competition with other positively charged matrix compounds. This effect decreases significantly when using a stagnant solution. Instead of a continuous delivery of competing matrix ions with high mobility which upholds the developed transient saturation of the membrane, this transient state dissolved over time. Consequently, target analytes can migrate through the membrane, resulting in similar recoveries as when using an aqueous standard. Thus, for cationic analytes, increased recoveries (and thus EFs) might be achieved with an optimized ratio between flow rate and extraction time. For anionic compounds, the change in the sample solutions' resistance over time caused by Cl^- or NO_3^- (or in case of the river water sample sulfate and phosphate) is stronger than in the cationic system. Possibly, increasing the extraction time under stagnant conditions can aid in resolving transient electrokinetic effects due to e.g., transient isotachophoresis or transient saturation of the membrane by these highly mobile inorganic ions. Hansen et al. [253] thoroughly investigated the effect of ion balance on the EFs at constant pH. They clearly showed that at high salt concentration, ion pairing becomes important in the SLM, leading to reduced extraction efficiencies. As the local electric field strength depends on the composition of sample and acceptor solution and the local conditions in the membrane [253], it strongly changes during the EME experiment, especially under stagnant condition.

One possibility to improve our EME process, might be an increase of the pH in the anionic acceptor solution (pH > 7) and a decrease in the cationic acceptor solution (pH < 7) to assure that the pH drop across the membrane does not evoke destacking phenomena towards the acceptor side. Care has to be taken not to lose analytes migrating further to

the bubbleless electrode and not to have a mismatch of relative conductivities in the sample vs. acceptor solution. A free choice of the composition of the acceptor solution is not possible, as downstream analysis may suffer from the high ionic matrix load as discussed in Section 5.4.2.

Experiments using analytes with higher and lower electrophoretic mobilities than the inorganic salts may aid in further understanding the underlying transient electrokinetic phenomena. Basic understanding would thus be gained when looking at all chemical parameter in the sample and acceptor solution: type of ions, pH and concentration/conductivity. These parameters are often investigated but a stronger focus on the electrophoretic mobility of the ions is required.

5.5 Conclusion and outlook

In this work, a new EME setup using a flow-through cell for the simultaneous enrichment of 15 cationic and 22 anionic analytes covering a wide range of polarities (-7.7 $\leq \log D_{pH\,5} \leq 2.4$ and $-3.5 \leq \log D_{pH\,5} \leq 1.3$ for cationic and anionic analytes, respectively) was established. The high analyte coverage shows that PIM compositions were successfully optimized either in a stagnant, two compartment test cell or directly in a flow-through cell. By implementing bubbleless electrodes, the system proved to be robust over a wide range of EME conditions, varying the parameters voltage (100-4000 V), flow rate (stagnant up to 0.5 ml/min) and extraction time (up to 30 min so far). The versatility of the setup, for example switching connecting PEEK capillaries to reduce the voltage (current) whilst increasing the applied extraction current (voltage) allowed to study the influence of the electric field strength across the membrane over a wide range. In addition, the volume of the sample channel can easily be adapted by simply changing the height of the 3D-printed sample compartment.

We demonstrated, that by optimizing all parameters in a BBD using RPLC- and NACE-MS for downstream analysis, EME effects may be superimposed by matrix effects. Comparing extraction efficiencies with recoveries and results for different quantification methods, these effects can be distinguished. Improvements in sensitivity for the EME/NACE-MS system were achieved for both cationic and anionic compounds using long extraction times reaching average EFs of 20 and 40 for anionic and cationic compounds, respectively.

The application of the optimized EME protocol to spiked river samples showed that high concentrations of (inorganic) salts reduced recoveries especially under conditions of sample flow, where these highly mobile matrix ions are constantly delivered to the membrane and compete with the analytes in the transport through the membrane. A stagnant sample solution showed better recoveries, even for a non-diluted river sample. Further optimization is thus necessary with regard to combinations of flow rate and time, the composition of the membranes and the relative conductivities and salt loads of sample vs. acceptor solutions. Adjusting the pH value of the acceptor solutions may aid in improving extraction efficiencies. We expect thinner membranes to enhance the transport of highly mobile ions through the membrane preventing saturation effects and reduce the bias regarding effective electrophoretic mobilities. The same positive impact can be

expected, when the area of the membrane covered by the electric field is increased, for example by applying the electric field over the compete meander structure of the flow cell.

To conclude, a promising dual EME flow-through cell compatible with chromatographic and electrophoretic separation techniques was established, though further adjustments are needed for the application of real samples. Our EME/NACE-MS setup was applicable to analytes with a wide range of physicochemical characteristics and may aid in reaching a non-target preconcentration for ionic analytes in environmental matrices.

6. Validation of field-step electrophoresis as clean-up step for the analysis of environmental water samples

6.1 Abstract

In environmental analysis, sample preparation is often necessary as concentrations of micropollutants are low and matrix compounds might interfere with their detection. Especially for ionic and ionizable analytes, both suitable sample preparation and quantification strategies by separation techniques coupled to mass spectrometry are still scarce. Accordingly, the development of new sample preparation techniques ideally with a broad analyte coverage is of great interest.

In this work, a new sample preparation technique for ionizable micropollutants and their transformation products is introduced for environmental sciences: we developed a field-step electrophoresis (FSE) as sample clean-up step for micropollutants in river water. The FSE system (triethylamine and acetic acid at pH 10) was able to preconcentrate 15 acidic model analytes (pK_a from -2.2 to 9.1) present in aqueous samples in two fractions. Simultaneously, it removed highly mobile matrix compounds including inorganic ions such as sulfate and chloride. The fractions could either be directly injected for downstream analysis by reversed-phase liquid chromatography (RPLC) or capillary electrophoresis coupled to mass spectrometry (MS) or further processed by evaporative preconcentration with subsequent reconstitution in an organic solvent suitable for separation methods like hydrophilic interaction chromatography. The FSE/RPLC-MS method exhibited high quantitative precision (relative standard deviations of model analytes' peak areas between 3 and 6%). The system was successfully applied to a spiked river water sample and performance was compared with common solid-phase extraction and evaporative concentration procedures, demonstrating a low selectivity and thus high coverage. Analyzing FSE fractions of a river water sample using non-target screening by RPLC-MS revealed a strong reduction in matrix load especially at low retention times. 17 compounds present in the relevant FSE fraction were identified by retention time, exact mass and mass spectrum. Suspect screening by FSE/RPLC-MS was further facilitated using the additional information on the selectivity for anionic compounds.

6.2 Introduction

The steadily increasing pollution of surface waters by industrial waste, pharmaceuticals and household chemicals demands for governmental regulations. For this, sufficient analytical workflows should be available to control these regulations and identify new risks. Since most micropollutants in aqueous samples are present at trace levels (ng/l to µg/l range), separation techniques alone often do not reach the required detection limits (LODs), and they can be utilized only when sample enrichment is applied [26-29]. The main objectives of sample preparation are the removal of matrix compounds and analyte preconcentration. The method should provide a high precision and sufficient analyte recoveries. For screening purposes, the preconcentration method needs a low selectivity and ideally no bias towards different physicochemical properties. Most work has been done using solid-phase extraction (SPE) [26, 28]

or evaporative concentration (EC) [10], but mostly sample preparation steps are optimized for selected (groups of) analytes [5].

Recently, we compiled a list of 455 compounds previously detected in water and biota analysis from various research articles [1]. Among these compounds, 70% of the analytes were charged at pH 7, with 70% of them possessing a charge number $\leq$ -0.5 (values were simulated by Chemicalize provided by ChemAxon (11/02/2021)). As a result, even focusing solely on charge (negative charge in our study) as a selectivity criterion could result in a broad analyte coverage of analytes present in environmental samples. In addition, transformation often results in acidic functional groups, for example by hydroxylation at aromatic structures, so transformation products can be included. In this work, we want to transfer methods of free flow electrophoresis (FFE), often applied in protein analysis to environmental science, using the specific mode field-step electrophoresis (FSE). It was first introduced by Wagner and Kessler in 1983 [17] as a new method for preparative protein isolation. The basic principle is discussed shortly, for further information, see [16]. FSE uses a flat chamber, which can be filled with different electrolytes and the sample using parallel injection ports along the upper side. Other than in common field zone electrophoresis, the separation buffer is not uniform across the separation chamber. Instead, the chamber is filled with two parallel bands of buffers strongly differing in their conductivity. The sample itself is introduced as a broad stream along the low-conductivity section. The electric field is applied perpendicular to the buffer and sample flow in such a way that (in our case negatively) charged analytes migrate to the high-conductivity section. Reaching it, the effective electrophoretic mobility of the charged analytes is reduced – stacking at the interface between the high- and low-conductivity buffer takes place. The preconcentrated analytes can be sampled at the end of the separation chamber in different fractions.

The FSE principle offers several advantages for the analysis of environmental water samples: the fractionation provides the possibility to remove neutral and positively charged compounds, but also fast inorganic anions may be removed as they are collected in different fractions when the focusing time and conductivity steps are optimized. Additionally, high volumes of aqueous samples can be introduced and fractions collected continuously providing preconcentration from large sample volumes. In combination with volatile FSE media, enrichment factors can be improved by evaporation of fractions and reconstitution in small volumes. Depending on the subsequent separation method, an orthogonal separation mechanism is possible, for example, if chromatographic separation is used.

In this study, the potential of FSE as clean-up and preconcentration step for environmental water samples was investigated and validated using different separation techniques coupled to mass spectrometry (MS) in order to demonstrate the compatibility with two liquid chromatography (LC)-MS methods (reversed-phase liquid chromatography (RPLC) and hydrophilic interaction liquid chromatography (HILIC)-MS as complementary chromatographic approaches [20]) and capillary electrophoresis (CE)-MS [142].

Additionally, a non-target screening was conducted to evaluate potential interferences with the FSE media throughout the identification process.

6.3 Materials and methods

6.3.1 Chemicals

1*H*-benzotriazole (BTA $\geq$ 98%), 2-methyl-4-chlorophenoxy acetic acid (MCPA $\geq$ 98%), 2-naphthalene sulfonic acid (2-NSA, $\geq$ 95%), 5-amino-2-naphthalene sulfonic acid (5-A-2- NSA, $\geq$ 95%), acesulfame (ACE, $\geq$ 99%), acetonitrile (MeCN, LC-MS grade), ethyl sulfate (ESU, $\geq$ 95%), formic acid (FA, 98%), hydrochlorothiazide (HCT, $\geq$ 99%), isopropanol (LC- MS grade), methanol (MeOH, LC-MS grade), saccharin (SAC, $\geq$ 98%), sulfamethoxazole (SULFA, $\geq$ 98%), sulfamic acid (SULAC, 99.3%), triethylamine (TEA, $\geq$ 99.5%) and water (LC-MS grade) were purchased from Sigma-Aldrich (Steinheim, Germany). Acetic acid (HAc, 100 %), ammonium acetate (NH$_4$Ac, 98%), ammonium hydroxide (NH$_4$OH, 25% aqueous solution, LC-MS grade) and dichloro acetic acid (DCAA, $\geq$ 98%), were obtained from Merck (Darmstadt, Germany). 4-(2-hydroxyethyl)-1-piperazine-ethane sulfonic acid (HEPES, 99.5%), 4-hydroxybenzoic acid (4-HBA, $\geq$ 98%) and umbelliferone (UMBE, 99%) were delivered by Fluka (Buchs, Switzerland). p-Toluene sulfonic acid (p-TSA, 90%) was purchased from Alfa Aesar (Haverhill, Massachusetts, USA), hydrochloric acid (HCl, 32% aqueous solution) from Fisher Scientific (Waltham, Massachusetts, USA). Acetic acid (100 %) for FSE was delivered by Carl Roth (Karlsruhe, Germany). 4-Hydroxybenzoic acid-d4 (4-HBA d4), acesulfame-d4 potassium salt (ACE d4), dichloro acetic acid-d1 (DCAA d1), saccharin-^{13}C6 (SAC ^{13}C6) and p-toluene-d7-sulfonic acid H$_2$O (p-TSA d7) were delivered by TRC (Toronto, Canada).

6.3.2 Workflow of the off-line FSE/LC-MS and off-line FSE/CE-MS measurements

For a better overview, the principle workflow of FSE with subsequent analysis by LC or CE is presented in Figure 6-1 and will be further explained in the following sections. Aqueous standards or river water spiked with model analytes and isotope-labeled standards (Step **1**, Figure 6-1, see Sections 6.3.3.2 and 6.3.3.4) were continuously injected for 25 min for FSE separation (Step **2**, see Section 6.3.3.5) into the low-conductivity buffer as a broad zone. Five fractions (**F₁-F₅**, corresponding to Fractions 55-59 on the 96-dwell plate) were collected which sample around the preconcentration zone between the high and low-conductivity buffer zones. Due to stacking, the original sample zone of anionic analytes was narrowed. The fractions were then prepared for the subsequent analysis step according to Section 6.3.3.3 (Steps **3**-**6**) or for preconcentration by evaporation and reconstitution. Final analysis (Step **7**) was conducted using CE-MS (Section 6.3.4.2), HILIC-MS (Section 6.3.4.1.2) or RPLC-MS (Section 6.3.4.1.1) for the first set of experiments (**Exp. 1**). In a second set (**Exp. 2**), analytes were spiked at different concentrations and isotope-labeled standards were added. Fractions from **Exp. 2** were analyzed using RPLC-MS. Steps **2-5** were identical for all experiments. For reconstitution, see Section 6.3.3.3.

workflow
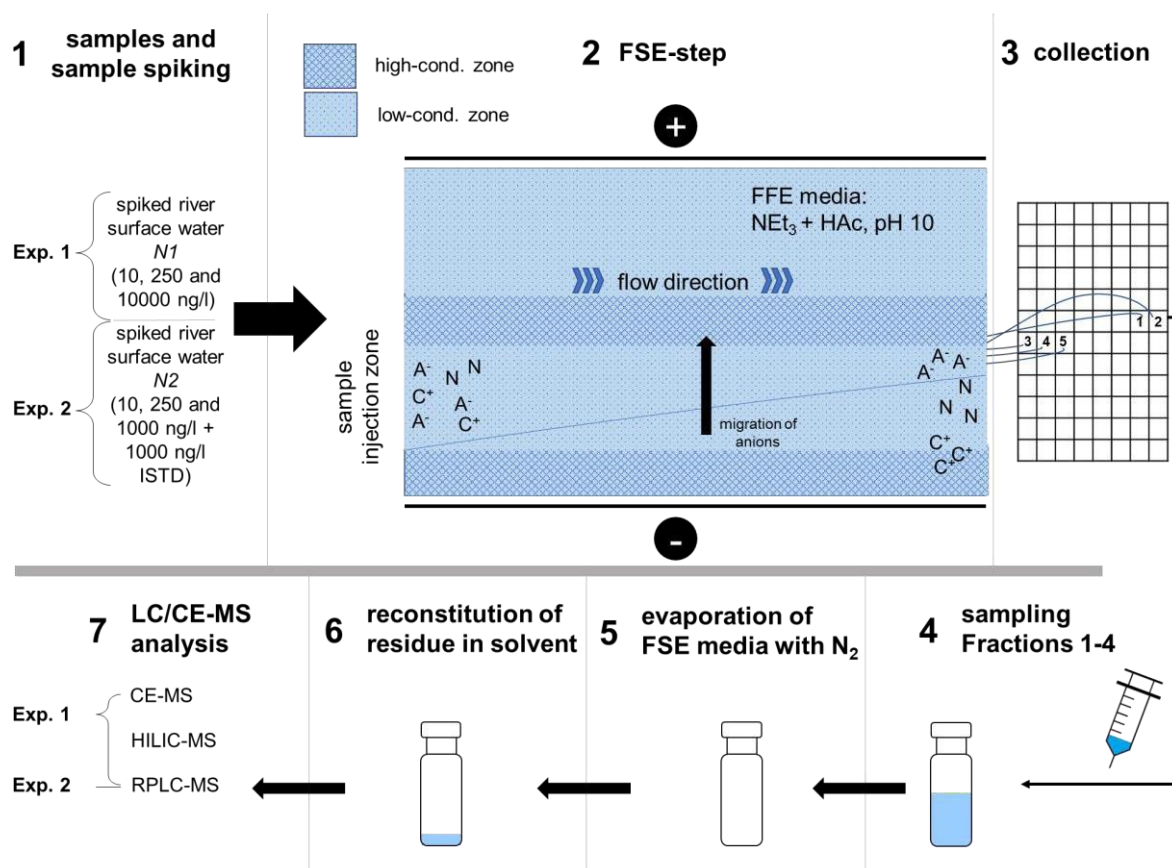
Figure 6-1: Typical workflow of the off-line FSE/LC-MS and off-line FSE/CE-MS experiments used here. High-conductivity zone: 250 mM TEA + HAc, pH 10.3, low-conductivity zone: 15 mM TEA + HAc, pH 10.3. A⁻: anionic compounds, C⁺: cationic compounds, N: neutral compounds. For explanation, see text.

6.3.3 Samples and sample preparation

6.3.3.1 Collection of river water

Two river water samples *N1* and *N2* were collected from the river Neckar in Tübingen, a few hundred meters downstream of a wastewater treatment plant (WWTP, 110000 population equivalents) in February and September 2020. Samples were collected in polypropylene vessels, filtered with a CHROMAFIL Xtra PTFE-45/25 filter (Macherey-Nagel, Düren, Germany) and stored in a borosilicate vessel at -20 °C before use.

6.3.3.2 Preparation of solutions

Methanolic stock solutions with a concentration of 20 mg/l containing all analytes (see Table 6-1) were prepared using 1 g/l methanolic stock solutions of each analyte. Isotope-labeled standards (ISTD, deuterated and/or ^{13}C-labeled) were prepared and stored in the same way. Standards in water (for CE and RPLC) or MeCN (for direct HILIC analysis) and FSE matrices were spiked with the analyte and ISTD mixtures, to reach a constant ratio of analyte mix:sample of 1:99 to keep the methanol content low and constant. Stock and working solutions were stored at -20 °C before use.

6.3.3.3 Treatment of FSE fractions

After the FSE experiments, selected fractions were filtered via CHROMAFIL Xtra PTFE-45/25 filters (Macherey-Nagel, Düren, Germany), pooled if necessary and evaporated to dryness under a gentle stream of nitrogen. The concentrated residue was redissolved in the same volume of a proper solvent, if not stated otherwise. The type of solvent was adapted to the subsequent analysis technique (RPLC-MS and CE-MS: H_2O, HILIC-MS: MeCN/H_2O (95:5, v/v)).

6.3.3.4 Spiking for determination of LODs and matrix effects

Blank FSE fractions (FSE experiment using LC-MS grade H_2O as sample) were spiked to estimate the method LODs and matrix effects. In preliminary experiments, fractions **F₁**-**F₁₀** around the stacking zone were investigated to determine fraction resolution, demonstrating that Fractions **F₃** and **F₄** hold the major share of model analytes. Thus, these fractions situated directly at the boundary between the two buffers of different conductivity were collected (Fractions **F₃** and **F₄**, see Section 6.3.2) as well as neighboring fractions (**F₁**, **F₂** and **F₅**). They were evaporated to dryness under a gentle stream of nitrogen after filtration. Depending on the task, fractions were pooled (for example Fractions **F₃**-**F₅**, called **F₃₋₅**). Spiking concentrations had to be adapted to the downstream analysis: HILIC-MS: 10, 100, 500, 1000 and 2500 ng/l; RPLC-MS: 100, 1000, 5000 and 10000 ng/l; CE-MS: 1000, 10000, 50000 and 100000 ng/l. Matrix effects were determined by comparing peak areas of the analytes in the FSE fraction vs. the peak areas obtained from the analysis of an aqueous standard, directly injected. Concentrations of the aqueous standard were 500, 1000 and 10000 ng/l for HILIC-MS, RPLC-MS and CE-MS, respectively.

LODs of RPLC-MS were estimated by spiking model analytes (10, 250, 1000 and 2500 ng/l) to H_2O, the river sample *N2* and a pooled blank Fraction **F₃₋₄** (*H_2O-blank*, **Exp. 2**, narrowed down by a factor of 10, see Figure 6-1 and Section 6.3.2). For the comparison of FSE preconcentration capabilities with SPE and EC (see Section 6.4.6), 500 µl of the pooled Fraction **F₃₋₄** of **Exp. 2** (see Figure 6-1) was evaporated to dryness as described. Reconstitution followed in 50 µl LC-MS grade H_2O (thus volume reduction by a factor of 10) and samples were analyzed using RPLC-MS.

6.3.3.5 FSE experiments

FSE separations were conducted at 10 °C using the following conditions and media: the experiments were run in a horizontal separation using a 0.2 mm spacer for the separation channel. A flow rate of approx. 330 ml/h was used in combination with a voltage of 600 V, which resulted in a current of approx. 90 mA. The FSE chamber was filled with a high- and low-conductivity buffer made of 250 mM and 15 mM TEA, both titrated to pH 10.3 using acetic acid. Samples were perfused into the separation chamber in the low-conductivity buffer zone at 12.7 ml/h. Residence time in the separation chamber was 25 min. Fractions were collected (collection rate of 3.4 ml/h) in polypropylene microtiter plates, numbered 1 (anode) through 96 (cathode).

The FSE experiments were conducted in two experimental blocks using sample *N1* in **Exp. 1** and sample *N2* in **Exp. 2**, see Figure 6-1. In **Exp. 1**, we used the blank sample *N1* (*N1-blank*), and *N1* spiked with analytes at concentrations of 10, 250 and 10000 ng/l (labeled *N1-10/250/10000 ng/l*) to cover a wide concentration range and enable the analysis using HILIC

but also CE-MS with its higher LODs in the µg/l range. **Exp. 2** was conducted for subsequent target and non-target screening by RPLC-MS: sample *N2* was injected for FSE directly *(N2)*, or spiked at concentrations of 10, 250 and 1000 ng/l (*N2-10/250/1000 ng/l*), for downstream RPLC-MS. Additionally, an aqueous sample (spiked at 250 ng/l, *H2O-250 ng/l*) was subjected to FSE and used as a reference. In **Exp. 2.**, ISTDs were spiked at a concentration of 1000 ng/l before FSE experiments. A system blank was obtained injecting LC-MS grade H_2O for FSE fractionation (*H2O-blank*).

6.3.3.6 SPE procedure

For optimal retention of anionic compounds, 5 ml of sample *N2* (spiked with concentrationsof 10, 250 and 1000 ng/l of analyte mix and additionally 1000 ng/l ISTD mix in all samples) were acidified to pH 1 with HCl. Prior to loading, the cartridge (30 mg Oasis HLB, Waters, Eschborn, Germany) was washed three times with 1 ml MeOH (LC-MS grade) and conditioned three times with 1 ml water (LC-MS grade). Highest extraction efficiencies for model analytes (see Table 6-1) were reached using an elution medium of 5% NH_4OH in MeOH without washing steps after loading (see Chapter 3 for SPE optimization). The eluate was evaporated to dryness under a gentle stream of nitrogen, and the concentrated residue was redissolved in 0.5 ml H_2O and the sample injected for RPLC-MS analysis.

6.3.3.7 EC procedure

1 ml of river sample *N2* (spiked with concentrations of 10, 250 and 1000 ng/l of analyte mix and additionally 1000 ng/l ISTD mix in all samples) was evaporated to dryness under a stream of nitrogen and redissolved in 0.1 ml H_2O. All samples were analyzed by RPLC-MS.

6.3.4 Chromatographic and electrophoretic separation techniques

6.3.4.1 LC-MS analysis

For information on RPLC-MS used for non-target screening (referred to as *RPLC-NTS*, Section 6.4.7), all information is given in [256], though some relevant points will be mentioned here. The stationary phase used was the same as described in Section 6.3.4.1.1. Instead of the TripleTOF5600 as described, a x500R-System (Q-TOF) was used. In addition to 95 µl sample, 5 µl of a mix containing 16 isotope-labeled internal standard (IS) were injected. [256]

For all other RPLC-MS and HILIC-MS analysis, a 1260 Infinity LC system coupled to a 6550 iFunnel Q-TOF LC/MS system (Agilent Technologies, Waldbronn, Germany) was used. A jet-stream electrospray ionization (ESI) source was operated with a nebulizer pressure of 35 psig, a drying gas temperature of 160 °C, a flow rate of 16 l/min and a fragmentor voltage of 360 V. In the negative ionization mode, the capillary voltage was set to 4000 V, skimmer voltage to 65 V and the nozzle voltage to 500 V. The mass range was 40-1000 m/z with a data acquisition rate of 1 spectrum/s. The sheath gas temperature was set to 325 °C with a flow rate of 11 l/min. For internal calibration, solutions of purine and HP0921 (Agilent Technologies, Waldbronn, Germany, m/z = 121.0508, 922.0097) in MeOH/water (95/5) were used and sprayed via a reference nebulizer.

6.3.4.1.1　RPLC-MS

10 µl aliquots of the processed samples were injected onto a Zorbax Eclipse Plus C18 column (2.1 x 150 mm, 3.5 µm, narrow bore, Agilent Technologies, Waldbronn, Germany) for the analysis of compounds of medium polarity. Additionally, a guard column (2.1 x 15 mm, 5 µm, narrow bore, Agilent Technologies, Waldbronn, Germany) was used. For separation, a gradient elution at a flow rate of 0.3 ml/min using A) water and B) MeOH, both containing 0.1% FA (v/v), was chosen. After 1 min, the initial content of 95% water was decreased to 5% water over 7 min. This mobile phase was kept for another 7 min and then, the water content was increased to 95% over 5 min.

6.3.4.1.2　HILIC-MS

5 µl aliquots of the processed samples were injected onto a SeQuant ZIC-HILIC (2.1 x 150 mm polyether ether ketone (PEEK) coated, 3.5 µm, 100 Å, Merck, Darmstadt, Germany) for the analysis of polar compounds. In addition, a guard column (2.1 x 20 mm PEEK coated, Merck, Darmstadt, Germany) was put in front of the column with a coupler. For separation, a gradient elution at a flow rate of 0.3 ml/min using A) aqueous 20 mM NH_4HCO_3 and B) MeCN, both containing 0.01% FA (v/v), was chosen. The initial content of 90% MeCN was decreased to 40% water over 15 min. This mobile phase was kept for 1 min and the MeCN content was increased to 90% over 0.5 min. To ensure full re-equilibration, this composition was kept for another 8 min before injecting the next sample, leading to a total analysis time of 24.5 min. The re-equilibration step used an increased flow rate of 0.5 ml/min during min 16-22.

6.3.4.2　CE-MS analysis

The CE separations were carried out using a polyvinyl alcohol (PVA) coated capillary (length 60 cm, i.d. 50 µm) from Agilent Technologies, Waldbronn, Germany. The aqueous BGE was optimized for anion analysis and contained 20 mM NH_4Ac, pH 9 (see also Chapter 3). Samples were injected hydrodynamically by applying a pressure of 100 mbar for 20 s. New capillaries were conditioned with BGE for 15 min and flushed before and between runs with BGE for 2 min. The CE capillary was kept at 25 °C during CE runs. A separation voltage of -30 kV was applied. During the separation, an additional low pressure of 30 mbar was applied. The capillary was flushed with air for storage.

All CE-MS analyses were performed using an Agilent CE 7100 capillary electrophoresis (Agilent Technologies, Waldbronn, Germany) interfaced to the Agilent 6550 iFunnel Q-TOF mass spectrometer as for RPLC-MS but with an electrospray ionization (ESI) source assisted by a sheath liquid interface (Agilent Technologies, Waldbronn, Germany). The composition of the sheath liquid was isopropanol:water (1:1, v/v) with 0.01% FA (v/v). The sheath liquid was delivered by a 1260 isocratic pump (Agilent Technologies, Waldbronn, Germany) at a flow rate of 5 µl/min, delivered by a split-flow (1:100). The nebulizer pressure was set to 6 psig, and the drying gas flow rate to 11 l/min. The fragmentor voltage was set to –300 V. A capillary voltage of −4000 V, a skimmer voltage of 65 V, and an octopole voltage of 750 V were used. The mass range was set to m/z 40-1000. The data acquisition rate was 2 spectra/s. Online recalibration during CE-MS analysis was possible by adding 0.2 µmol/l purine, 0.1 µmol/l HP-321 and 0.1 µmol/l HP-921 (all from Agilent Technologies, Waldbronn, Germany) to the sheath liquid.

6.3.5 Data processing and method validation aspects

Extracted ion chromatogram (EICs) traces were extracted and evaluated from mass profile data with a mass accuracy of 0.01 m/z using Mass Hunter Qualitative Software (Agilent, V10.0). S/N ratios used in Section 6.4.6 were also calculated using Qualitative Software. MassHunter Quantitative Software (V10.1) was used to create calibration curves. The linear range was determined via the signal areas (not signal height). LODs were determined in different matrices using standard addition (see Section 6.3.3.4 for further information) according to DIN 32645 (α = 0.05). Matrix effects were estimated comparing the recovery of analytes when spiking at a concentration of 1000 ng/l for RPLC-MS, 500 ng/l for HILIC-MS and 10000 ng/l for CE-MS to different blank FSE fractions (*H_2O-blank*, see Section 6.3.3.5) to the recovery using aqueous standards. Enrichment factors (EFs) were calculated by dividing the peak area of each analyte signal obtained from the analysis of the FSE fractions by the peak area of analytes in the spiked original sample used for injection into FSE. Fractions with the highest analyte concentration are referred to as fraction$_{MAX}$ for each analyte (see Section 6.4.4). For the non-target screening in Section 6.4.7, the ratio was determined using peak heights of suspects and internal standards (IS) instead of peak areas. The term volume enrichment factor (VEF) corresponds to the enrichment factor theoretically achieved if an analyte is preconcentrated in one fraction only. The ratio of sample rate (12.7 ml/h) and fraction collection rate (3.4 ml/h) leads to a VEF of 3.7, when injecting for 25 min.

Data were evaluated with Origin 2020 (OriginLab Corporation, Northampton, USA) and Microsoft Excel 2019 (Microsoft Corporation, Redmond, Washington, USA). Statistical evaluation was conducted using IBM SPSS Statistics 26 (IBM, Armonk, New York, USA).

6.4 Results and discussion

6.4.1 Study design
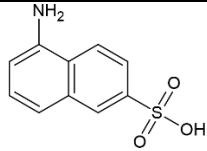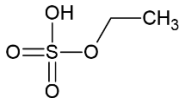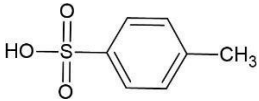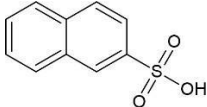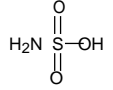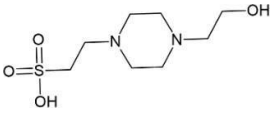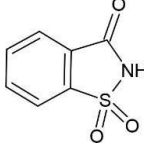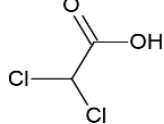
In this work, the potential of FSE as a sample clean-up step for aqueous samples was investigated and validated. The idea of using FSE was to preconcentrate anionic species in only a few fractions. As a first step (**Exp. 1**, see Figure 6-1), a river water sample *N1* spiked with model analytes (10, 250 and 10000 ng/l) was fractionated using FSE and specific fractions were analyzed with RPLC-MS, HILIC-MS and CE-MS to investigate their compatibility with FSE. RPLC-MS performed best and was used for subsequent experiments. The performance of FSE sample pretreatment was evaluated in a second set of experiments (**Exp. 2**, see Figure 6-1) by the comparison with common SPE and EC sample preparation using the river water sample *N2* spiked with model analytes (10, 250 and 1000 ng/l) and isotope-labeled internal standards (1000 ng/l).
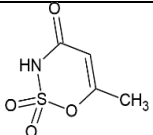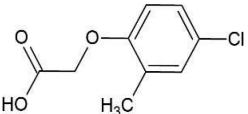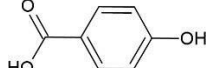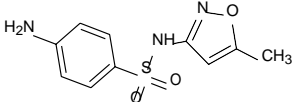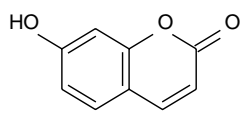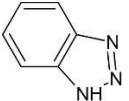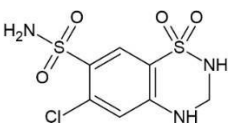
6.4.2 Model analyte system

20 model analytes, five of them with an isotopologue used as ISTD (marked with an asterisk * in Table 6-1) were chosen due to the broad range of physicochemical characteristics covered: the analytes differed in their functional groups (e. g. sulfonamides, sulfonic acids, (halogenated) carboxylic acids, amines), and thus polarity (-3.1 (HEPES) $\leq$ log P $\leq$ 2.4 (MCPA)) and acidity

(-2.2 (5-A-2-NSA) $\leq$ pK$_a$ $\leq$ 9.1 (HCT)) as can be seen in Table 6-1. For polarity, we considered log D at pH 10 according to the pH in the FSE experiments. The log D$_{pH\ 10}$ range was from -4.0 (HEPES) to 0.1 (BTA). The analytes were spiked to two river water samples *N1* and *N2* and analyzed by the off-line combination of FSE with RPLC-, HILIC- and CE-MS.

*Table 6-1: Model analytes and their physicochemical properties sorted according to lowest (acidic) pK$_a$. pK$_a$ and log D values were simulated by Chemicalize provided by ChemAxon (11/02/2021). For analytes marked with an asterisk * an isotopically labeled internal standard was available.*

analyte abbrev.	analyte	log P	log D$_{pH\ 10}$	strong. acidic pK$_a$	molecular structure	detected in FSE fraction(s) (fraction$_{Max}$ in bold)
5-A-2-NSA	5-amino-2-naphthalene sulfonic acid	1.1	-1.1	-2.2		**4**
ESU	ethyl sulfate	-0.1	-2.5	-2.1		**3**
p-TSA *	p-toluene sulfonic acid	1.7	-0.7	-2.1		**4**
2-NSA	2-naphthalene sulfonic acid	2.1	-0.2	-1.8		**4**
SULAC	sulfamic acid	-1.4	-3.8	-1.8		**2**
HEPES	4-(2-hydroxyethyl)-1-piperazine ethane sulfonic acid	-3.1	-4	-1.3		**4**
SAC *	saccharin	0.5	-0.5	1.9		**4**
DCAA *	dichloro acetic acid	1.1	-2.5	2.3		**3**, 4

analyte abbrev.	analyte	log P	log $D_{pH\ 10}$	strong. acidic pK_a	molecular structure	detected in FSE fraction(s) (fraction$_{Max}$ in bold)
ACE *	acesulfame	-0.6	-1.5	3.0		**3**, 4
MCPA	2-methyl-4-chlorophenoxy acetic acid	2.4	-1.1	3.4		**4**
4-HBA *	4-hydroxybenzoic acid	1.3	-2.7	4.4		**3**
SULFA	sulfamethoxazole	0.8	-0.2	6.2		**4**
UMBE	umbelliferone	1.5	-0.4	7.8		**4**
BTA	1*H*-benzotriazole	1.3	0.1	9.0		**4**
HCT	hydrochloro-thiazide	-0.6	-1.7	9.1		**4**

6.4.3 Compatibility and orthogonality of FSE with common subsequent separation techniques

The compatibility with three different separation techniques was investigated, namely RPLC-MS, HILIC-MS and CE-MS (for details, see Section 6.3.4). We looked at matrix effects, method LODs of the separation method as well as the orthogonality in separation between the FSE step and the subsequent separation technique. A direct injection of FSE fractions was possible for all methods but some disturbances and instabilities during the measurements were observed, probably caused by TEA in the FSE fractions from the FSE electrolytes. Thus, as we chose volatile components for the FSE media, fractions were evaporated to dryness and reconstituted as described in Figure 6-1 (Steps **5**&**6**). We investigated the impact of FSE media after evaporation and reconstitution on RPLC-MS, HILIC-MS and CE-MS. Matrix effects (see Section 6.3.5) were between 80 and 110% on average, but slightly elevated in CE-MS for single analytes such as DCAA and SAC, possibly due to some remaining FSE electrolytes or effects of transient ITP. Good compatibility of FSE sample preparation with chromatographic techniques was observed with negligible matrix effects (100% on average). Method LODs were lowest for separations using HILIC (0.10-0.25 µg/l) < RPLC (0.6-0.8 µg/l) and highest for CE-MS (3-17 µg/l). FSE proved well compatible with HILIC and RPLC separation as matrix effects were negligible and method LODs did not increase relative to reference standards.

We investigated if a bias with regard to analyte polarity or pK_a values was induced in FSE and judged the orthogonality of preparative FSE vs. downstream analytical separation. Figure 6-2 presents the retention or migration times of the analytes detected in the fractions and in the raw water sample for comparison. Polarity and pK_a values were color-coded.

The general profile of the analytes' retention time (RT) / migration time (MT) in each analysis method is demonstrated by the reference "raw sample" and compared to RT/MT of analytes present in the FSE fractions. As expected, selectivity is mainly dictated by polarity for chromatographic separations (low retention of polar compounds using non-polar C18 phase as well as low retention of non-polar compounds using the polar ZIC-HILIC phase). For chromatographic separations, no correlation between fractionation and elution order of the analytes is present, which is best visible in the broad distribution of retentions times in Fraction **F4** covering analytes with a broad range of polarities and pK_a values. However, we want to stress that Fractions **F2** and **F3** contain most of the early eluting analytes. But clearly, the number of analytes eluting close to the void volume was reduced by FSE, which will aid in reducing matrix effects. For CE, the migration order is primarily influenced by pK_a values of the analytes defining the analytes' charge. As pH values of the FSE media (pH 10) and the BGE of CE-MS (pH 9) were similar, there was a high correlation of fractionation with CE separation. But despite this correlation, the number of comigrating analytes is still clearly reduced.

Though analyses using HILIC-MS offered lowest method LODs, RPLC was used for further validation, as all 15 model analytes were detected at high resolution (see Figure 6-2) and sufficient sensitivity. With HILIC-MS, only 13 analytes were detected as method LODs of DCAA and BTA were too high in the concentration range chosen.
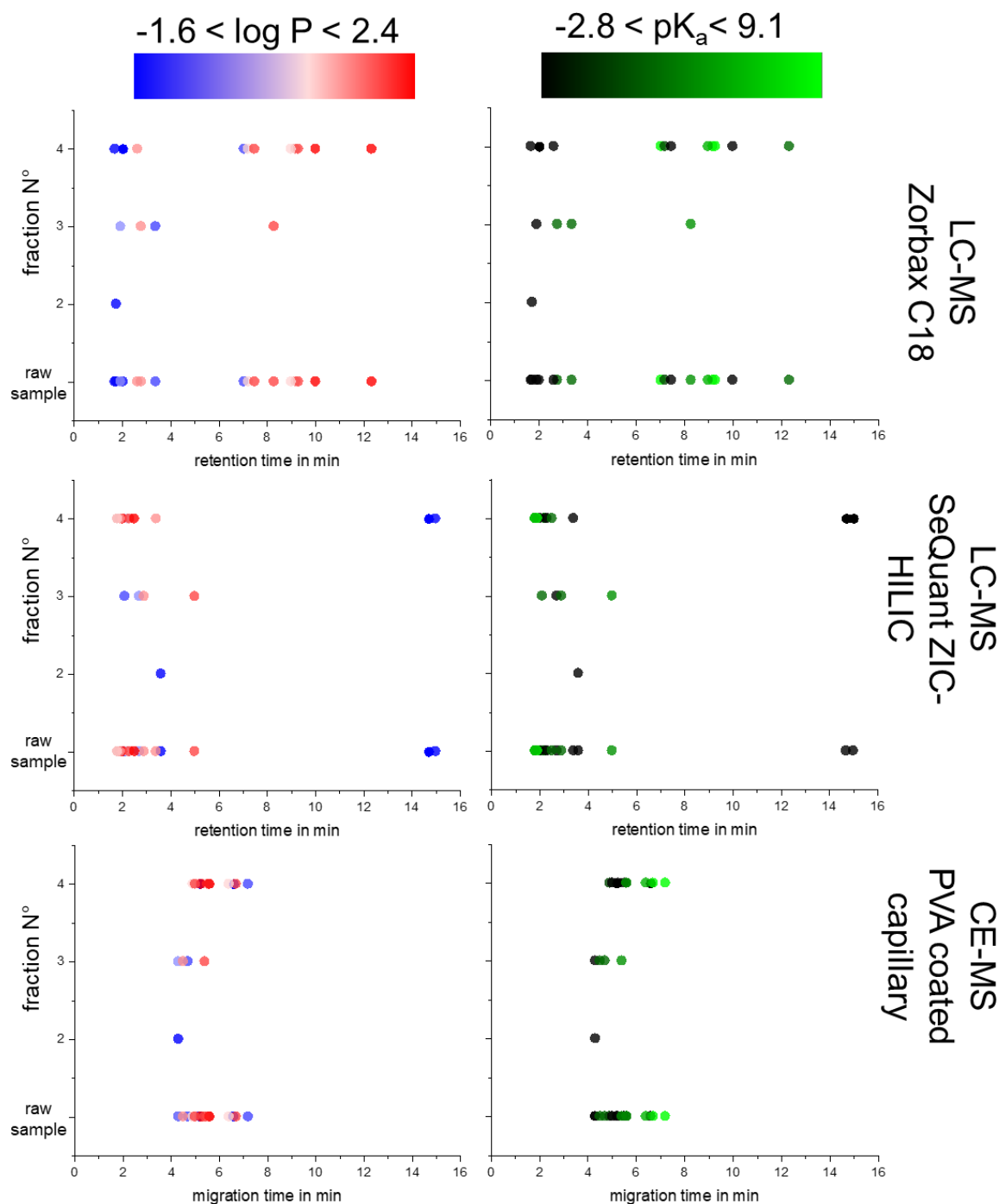
*Figure 6-2: Differences in selectivity of Fractions **F₂-F₄** and the three separation methods (RPLC, HILIC and CE). Circles represent analytes detected in their specific fraction$_{MAX}$ (FSE separation) or in the raw sample (for comparison) plotted with their retention (chromatographic separation) or migration time (CE separation). The color code refers to polarity or pK$_a$ values. With HILIC-MS, BTA and DCAA were not detected. The analysis methods were conducted as described in Sections 6.3.4.1.1 (RPLC-MS), 6.3.4.1.2 (HILIC-MS) and 6.3.4.2 (CE-MS).*

6.4.4 FSE fractionation and reproducibility

Analytes were preconcentrated at the boundary between high- and low-conductivity buffer leading to very few fractions with an elevated concentration of the analytes. This was achieved injecting samples into the FSE system at a flow rate of 12.7 ml/h over 25 min (total sample

volume of approx. 5 ml) and collecting fractions of approx. 1.5 ml at a collection rate of 3.4 ml/h.

For the river water sample spiked with model analytes at a concentration of 10000 ng/l, all 15 model analytes were detected by LC-MS and CE-MS in at least one of the FSE Fractions **F₂**-**F₄** and sometimes in 2 fractions (see Table 6-1). Having in mind the wide range of polarities (-3.1 ≤ log P ≤ 2.4) and acidities (-2.2 ≤ pKₐ ≤ 9.1), this demonstrates that FSE fractionation is solely selective with regard to (anionic) charge, so a large analyte coverage was reached. As the FSE experiment was performed at pH 10, this premise is realized even for less acidic compounds, e.g. HCT (pKₐ = 9.1). We calculated the ratios of peak areas from chromatograms at the concentration level of 10000 ng/l from FSE fraction$_{MAX}$ (fraction with the maximum analyte concentration) vs. the spiked raw water sample. Ratios were between 0.4 and 1.8, demonstrating that both enrichment and matrix effects have to be considered. Dividing these values by the *VEF* of 3.7 of the FSE fractionation (see Section 6.3.5) analyte recoveries were between 11 and 50% in single fractions. Looking at the analyte recovery over all fractions, we also calculated the peak area ratios for analytes in the fractions (sum of peak area, when the analyte was present in several fractions) vs. the ones in the unprocessed sample. These ratios were in the range of 0.6 to 2.3, leading to FSE recovery values between 16 and 70%. Low ratios < 1 evolve, when analyte losses occurred or matrix effects in the analysis of one of the samples were present. It is also possible, that the analytes spread over more fractions but their concentration was below LOD in these fractions. The relatively small difference between total EFs of all fractions (0.6-2.3) and EFs of each fraction$_{MAX}$ (0.4-1.8) showed that analytes do not spread over more than two FSE fractions.
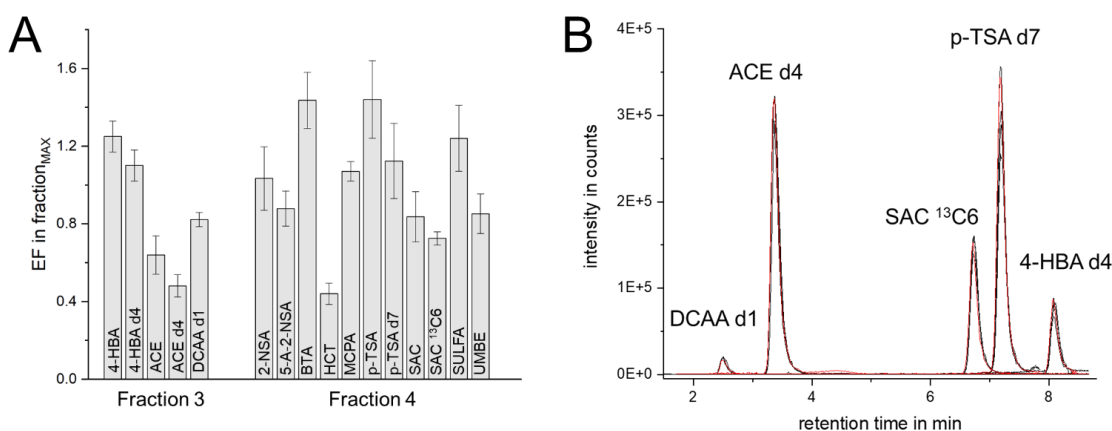
*Figure 6-3: A: Average relative enrichment factors of analytes in the fraction$_{MAX}$ obtained after FSE separation relative to the peak area of the original spiked water samples (directly injected) for 16 of the 20 analytes, calculated from RPLC-MS analysis. For model analytes, EFs of the FSE experiments N1-250/10000 ng/l and N2- 250/1000 ng/l were considered (n = 4). For the ISTDs, results from **Exp. 2** (N2, N2-10/250/1000 ng/l and H₂O- 250 ng/l, thus n = 5) are plotted. EFs of ESU, DCAA and HEPES could not be determined due to insufficient LODs in fractions and/or reference sample. For SULAC, concentrations were too high in the original samples to calculate EFs. B: EICs of the five spiked (1000 ng/l in each sample) isotope-labeled analytes from the RPLC-MS analysis of FSE fraction$_{MAX}$ (Fraction **F₃**: DCAA d1, ACE d4 and 4-HBA d4; Fraction **F₄**: SAC ¹³C6 and p-TSA d7) in **Exp. 2** (see Figure 6-1 and Section 6.3.3.5). Fractions of all five samples (N2, N2-10/250/1000 ng/l, H₂O- 250 ng/l) were prepared as described in Section 6.3.3.3 and analyzed with RPLC-MS (see Section 6.3.4.1.1). The obtained EICs of ISTDs were overlaid in this graph.*

Fraction$_{MAX}$ is Fraction **F₄** for most analytes, only two analytes (DCAA and ACE) were present in Fractions **F₃** and **F₄** (ratios of peak areas **F₃/F₄** DCAA 70:30 and ACE 60:40). Figure 6-3A exemplarily shows the average EFs in the Fractions **F₃** and **F₄** of 16 of the 20 model analytes which were detected at all three concentration levels. EFs of analytes and isotope-labeled counterparts were similar for 4-HBA, ACE and p-TSA (paired t-test, $\alpha = 0.05$, for SAC a p-value of 0.027 was obtained). The average relative EFs in Fractions **F₃** and **F₄** are 0.86 and 1.01. For analytes missing, the concentrations in either the raw water sample or in the fraction did not fall into the linear range (see legend in Figure 6-3). The error bars reveal average relative average deviations (RSDs) of 9 and 12% for analytes' peak areas in the two fractions. As these values were calculated from the results of two separate FSE experiments and their consecutive LC-MS analysis using two different spiked river water samples *N1* and *N2* within a time interval of over half a year, these deviations indicate a good robustness of the overall method. A further discussion is presented in Section 6.4.5. As ISTDs were added at a concentration of 1000 ng/l to all river water samples (*N2*) and a water sample (LC-MS grade) in **Exp. 2**, we used these samples to determine reproducibility. The fractions were analyzed using RPLC-MS and highest concentrations of the ISTDs were detected in Fractions **F₃** and **F₄** (Fraction **F₃**: DCAA d1, ACE d4 and 4-HBA d4; Fraction **F₄**: SAC ^{13}C6 and p-TSA d7; see also Table 6-1). Figure 6-3B shows the EICs of the analyses of these fractions for all five samples. Clearly, the FSE method offers high reproducibility for different samples (pure H₂O and river water). It is also visible that matrix effects were low for this set of analytes as water and river water samples showed very similar results (see red EICs of sample *H₂O-250 ng/l* in Figure 6-3). The RSD values were between 3 and 6% over the whole analytical process (see Figure 6-1).

6.4.5 *Influence of FSE media on LODs*

Blank pooled Fraction **F₃₋₄** was preconcentrated by a factor of 10 and afterwards spiked (pretreatment and spiking see Section 6.3.3.4). RPLC-MS analysis was conducted to investigate the influence of the FSE electrolytes on LODs. The LODs were compared with those determined by RPLC-MS of the spiked river water sample (before FSE) and for an aqueous standard solution. The results of these experiments are listed in Table 6-2. LODs differed significantly in aqueous solution, river water and FSE fractions (paired t-test, $\alpha = 0.05$). Though slight impairment might be present for the FSE extract (70% in average higher matrix effects in FSE fractions vs. 90% on average in the raw river water sample, see Table 6-2), no significant difference was observed. Linearity (R^2) also proved independent of sample type for all three matrices.

As expected, both the river water matrix and the FSE media revealed higher LODs. FSE media were 10 times preconcentrated by evaporation and reconstitution, so matrix effects by FSE electrolytes were considered low compared to the enrichment of analytes reached by stacking.

Table 6-2: LODs and R² values determined for the 15 model analytes (sorted by acidic pK_a values, see Table 6-1) obtained by calibration curves in sample N2 (standard addition, spiked concentrations 10, 250, 1000 and 2500 ng/l) and pooled Fraction F_{3-4} of H_2O-blank (narrowed down by a factor of 10). Matrix effects were determined by comparing peak areas of the spiked samples (1000 ng/l) with peak areas obtained in aqueous standards (see Section 6.3.5). n.d.: not determined, if not at least 3 calibration points were present.

matrix / analyte	aqueous standard		spiked river water *N2*			pooled Fraction F_{3-4} 1:10 (v/v) of H_2O-blank		
	R^2	LOD in ng/l	R^2	LOD in ng/l	matrix effect in %	R^2	LOD in ng/l	matrix effect in %
5-A-2-NSA	0.999	74	0.999	2	89	0.996	438	56
ESU	0.999	178	0.999	95	87	0.999	38	30
p-TSA	0.999	133	0.999	228	105	n.d.	n.d.	n.d.
2-NSA	0.999	72	0.999	88	99	0.999	362	99
SULAC	0.999	292	n.d.	n.d.	n.d.	n.d.	n.d.	n.d.
HEPES	0.999	259	n.d.	n.d.	1	0.999	15	30
SAC	0.999	50	0.999	197	104	0.999	191	87
DCAA	0.999	350	0.973	1422	81	0.990	711	163
ACE	0.999	142	0.999	165	73	0.999	292	86
MCPA	0.999	387	n.d.	n.d.	96	n.d.	n.d.	62
4-HBA	n.d.	n.d.	n.d.	n.d.	44	n.d.	n.d.	n.d.
SULFA	0.999	240	n.d.	n.d.	145	0.939	1791	42
UMBE	0.999	37	0.999	94	90	0.999	46	49
BTA	0.999	61	0.999	73	155	0.999	240	104
HCT	0.999	76	0.999	68	91	0.999	339	26
average	0.999	168	0.996	381	90	0.992	406	70

6.4.6 Comparison of FSE/RPLC-MS with common SPE and EC

We compared the sample preparation by FSE with the common techniques evaporative concentration and solid-phase extraction. For SPE, Oasis HLB cartridges were chosen as an accepted standard in LC-MS approaches for a wide polarity range of analytes [5]. The general procedure was similar for all three sample preparation techniques: a preconcentration factor of 10 was chosen by volume reduction. The detailed protocols are given in Section 6.3.2. Figure 6-4 shows the RPLC-MS chromatograms (EICs of analytes) of the spiked river water sample *N2-10 ng/l* before (Figure 6-4A) and after sample preparation by B) FSE, C) SPE and D) EC.
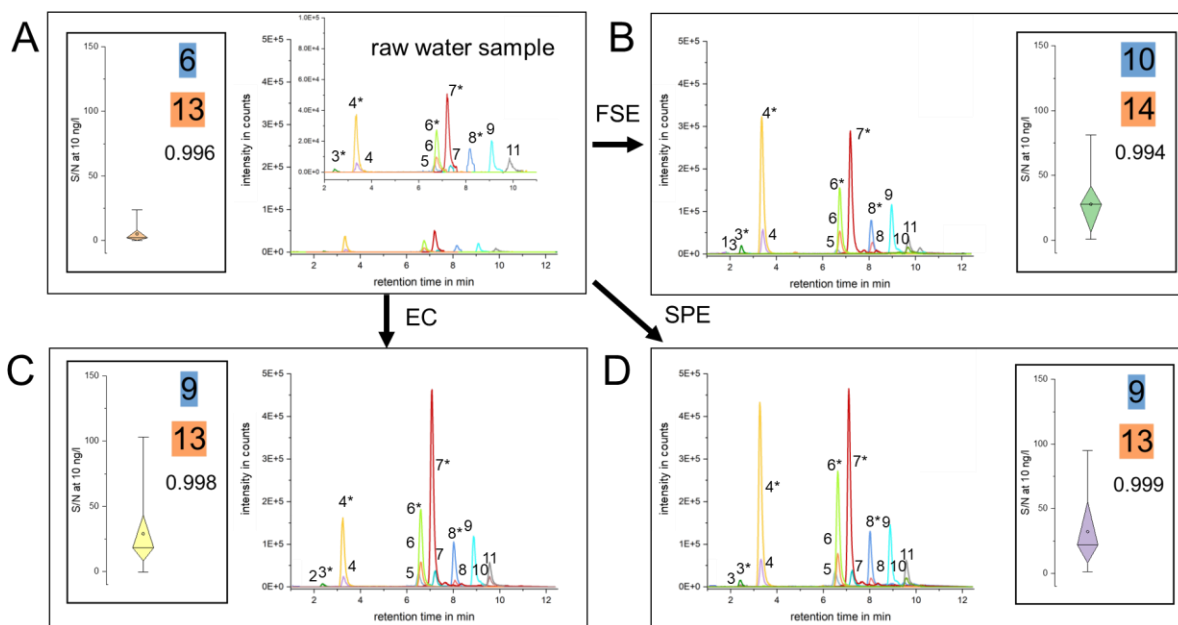
Figure 6-4: Chromatograms obtained by RPLC-MS analysis (see Section 6.3.4.1.1) of A: the raw sample N2- 10 ng/l, B: of the FSE Fractions F₃₋₄ (see Sections 6.3.3.4 and 6.3.3.5), C: of the SPE extract (see Section 6.3.3.6) and D: of the EC reconstituted solution (see Section 6.3.3.7). The inserts show a) blue: the information on the number of analytes detected at a concentration of 10 ng/l, b) orange: the number of analytes detected at a concentration of 1000 ng/l and c) the R² values of the calibration curves as a mean for all analytes, and d) Box- whisker plots with the median (line) and average S/N (points) at a concentration of 10 ng/l (thus solely counting model analytes, but not ISTD). The signal identification is: 1) HEPES, 2) ESU, 3) DCAA, 4) ACE, 5) HCT, 6) SAC, 7) p-TSA, 8) 4-HBA, 9) BTA, 10) UMBE and 11) 2-NSA. Numbers marked with an asterisk * indicate the isotope-labeled standards (spiked at 1000 ng/l in raw sample N2). SULAC was excluded, as elution close to void volume led to strong quenching effects (see also Table 6-2) for all three sample preparation methods. For further information, see text.

Selectivity & Sensitivity: Comparing the chromatograms, similar intensities relative to the raw sample can be observed. ACE d4 (Peak 4*) is interesting as it seems to be better enriched by FSE and SPE relative to e.g. p-TSA (Peak 7) but not by EC, where even a (relative) reduction in intensity was visible. Possibly, ionization suppression by matrix effects was present for the river water sample after EC enrichment.

Clearly, all sample preparation methods provided an increase in sensitivity, visible by the higher peak intensities, the higher S/N ratio at 10 ng/l and the higher number of analytes detected already for samples spiked with model analytes at 10 ng/l. This is indicated by the number of analytes detected (blue numbers in Figure 6-4), which increased almost equally for all three

enrichment techniques. The increase of S/N values proved significant by a factor of approx. 6 for all three sample preparation techniques (paired t-test, $\alpha = 0.05$).

Looking at single analytes, 2-NSA, ACE, BTA, HCT, p-TSA and SAC can be detected in all four samples at a spiked concentration of 10 ng/l. Their LODs were > 10 ng/l (see Table 6-2), so we expect some of these compounds already present in the river water. Signals of 4-HBA and UMBE increased after all three sample preparation steps investigated here and became detectable even at the lowest spiked concentration of 10 ng/l (before preconcentration at 250 ng/l). Results were similar for all sample preparation techniques for SULFA, MCPA and 5-A-2-NSA, as they were detected in all samples at spiked concentrations $\geq$ 250 ng/l. In contrast, ESU, HEPES and DCAA, were enriched to different extents. SULAC was excluded due to inconclusive results in RPLC-MS analysis. The analyte ESU becomes detectable after preconcentration only at higher concentrations ($\geq$ 250 ng/l) using the EC and FSE procedure. Using SPE, a decrease in peak area compared to the original sample was observed caused by the poor retention of the ionic compound on the SPE sorbent (see Chapter 3, Section 3.3.4.5.2). For the analyte DCAA, enrichment was observed for all three sample preparation steps. Strongest quenching effects were present after EC, probably caused by the enrichment of matrix compounds. Preconcentration of DCAA was effective in SPE and FSE, as it was detected when spiking at 10 ng/l after both SPE and FSE. The analyte HEPES could only be quantified after FSE. We do not know, why this analyte could not be detected after SPE or EC. Possible reasons are ionization quenching by matrix components (see Section 6.4.3), or a strong positive bias in the enrichment process either in FSE or negative bias in SPE and EC. However, a further, more profound investigation with more model analytes has to be conducted to fully understand all parameters influencing the FSE fractionation.

Our results indicate that improvement in sensitivity was achieved using all three sample preparation steps. The newly established FSE step showed some bias regarding analytes' charge state, though less pronounced as the bias of SPE's regarding analytes' polarity. The analyte loss is expected to be higher compared to EC, as the latter will only loose volatile components or analytes which are difficult to redissolve after evaporation. However, the FSE step offers several advantages: the efficient salt removal increases the loadability of samples which is advantageous compared to EC, where high salt concentrations of the samples can be seen as its major limitation, leading to strong matrix effects caused by their simultaneous preconcentration. Due to the fractionation process, large concentration differences in the sample are not critical and overloading, as sometimes present in SPE, is prevented. The abandonment of organic solvents is favorable and FSE shows high potential for automation. Finally, FSE and RPLC-MS were orthogonal in their separation process, and matrix effects were clearly lowered (see Section 6.4.3).

6.4.7 Applicability of FSE as sample clean-up step for non-target screening of acidic compounds

Fractions F_1 and F_4 and the spiked river sample from **Exp. 2** were analyzed with the established *RPLC-NTS* method (see Section 6.3.4.1) optimized for the non-target screening of micropollutants in environmental waters. Two aspects important for non-target screening were investigated, namely matrix removal and the use of charge as an additional identification criterion to verify suspects and minimize false-positive results.

Removal of matrix components

Figure 6-5A and B show the total ion chromatograms (TICs) of the river water sample *N2* and fractions thereof in positive and negative ESI mode. The comparison of the TIC mass traces for both polarities revealed a significant decrease in the intensity of the matrix components eluting close to or in the void volume caused by e.g. (inorganic) salts and very polar neutrals when comparing the TIC of the raw sample vs. Fraction F_4 (Sample *N2*) holding the major share of charged analytes.

Panel C (ESI+):

RT in min	IS	H₂O	N2	F₁	F₄
2.00	melamin d6	1.0	0.8	0.0	0.4
2.17	metformin d6	1.0	0.6	0.0	0.7
5.37	sotalol d6	1.0	1.0	0.5	0.9
6.05	hydrochlorothiazide 13C,d2	1.0	0.2	0.2	0.4
6.12	lidocaine d10	1.0	1.0	0.5	0.9
6.36	benzotriazole d4	1.0	0.9	0.6	1.0
7.26	chloridazon d5	1.0	0.9	0.2	0.7
8.42	sulfadimethoxine d6	1.0	1.0	0.4	0.5
9.46	irbesartan d4	1.0	0.9	0.9	1.0
10.48	diuron d6	1.0	1.0	0.5	0.9
10.95	darunavir d9	1.0	1.2	0.8	1.0
11.54	bicalutamide d4	1.0	1.0	0.6	1.0
11.58	propazine d6	1.0	1.0	0.4	0.9
12.3	azoxystrobin d4	1.0	0.9	0.7	0.9
13.81	fipronil 13C2,15N2	1.0	0.9	0.7	0.9
14.57	diazinon d10	1.0	1.0	0.7	1.0

Panel D (ESI-):

RT in min	IS	H₂O	N2	F₁	F₄
5.35	sotalol d6	1.0	0.8	0.6	0.9
6.04	hydrochlorothiazide 13C,d2	1.0	0.8	0.8	1.0
6.31	benzotriazole d4	1.0	0.7	0.6	0.7
7.25	chloridazon d5	1.0	0.7	0.6	0.8
8.38	sulfadimethoxine d6	1.0	0.8	0.7	0.9
9.45	irbesartan d4	1.0	0.9	0.8	0.9
10.44	diuron d6	1.0	0.9	0.8	0.9
10.93	darunavir d9	1.0	0.8	0.8	0.9
11.5	bicalutamide d4	1.0	0.9	0.8	1.0
13.8	fipronil 13C2,15N2	1.0	0.9	0.8	1.0

Figure 6-5: TICs of a blank sample (LC-MS grade H_2O, spiked with IS, green lines), of the river water (samples N2-250 ng/l and N2-1000 ng/l, blue lines) spiked with the model analytes as well as the TICs for the FSE fractions (F_1, of sample N2-250/1000 ng/l (black lines) and F_4 of N2 (red lines)) in both positive (A, C) and negative (B, D) ESI polarity. In positive ESI polarity, the EIC of TEA is additionally visualized as purple line. C and D show a heat map containing the peak heights of the spiked IS normalized to 1 (color code from red to green) in the different matrices (H_2O, N2, F_1 and F_4). For all analyses, the RPLC-NTS method mentioned in Section 6.3.4.1 was used. All samples were diluted one-fold.

In FSE, neutral compounds remained in the sample zone but were not preconcentrated at the stacking boundary. Only compounds in the sample stream directed to Fractions F_3 and F_4 were

recovered for subsequent RPLC-MS analysis. Cationic compounds will migrate away from the stacking boundary and anions of high electrophoretic mobility, e.g. the inorganic anions chloride, phosphate and sulfate, often present at high concentrations in environmental samples will cross the stacking boundary and will not be present in the fractions of interest, when the migration path in FSE is long enough. Obviously, sample cleanup using FSE was successful in reducing the number of matrix components, as intensities in Fraction F_4 decreased significantly compared to the raw sample. The only exception was the TIC of Fraction F_1 analyzed in the positive ionization mode. Here, the maximum of the TIC signal at the beginning of the chromatogram is at higher retention times. TEA, the cation in the FSE electrolytes, was identified as major contributor to this maximum as can be seen by the EIC of TEA at m/z 102.128 in Figure 6-5A. The elevated amount compared to F_4 is expected, as F_1 is collected in the high-conductivity zone which contains an approx. 17-fold higher TEA concentration compared to the low-conductivity zone which is sampled in F_4.

Additionally, Figure 6-5C and D depict two heat maps coding the suppression of internal standards (IS) spiked to every sample just before *RPLC-NTS* analysis in both ESI modes, referenced to pure water (peak heights were used). Matrix interferences were acceptable in positive ESI mode and were clearly reduced upon FSE sample preparation in negative ESI mode. The heat maps reveal the matrix effects for the different analytes in the river water sample and the two Fractions F_1 and F_4: in positive ESI mode (Figure 6-5C), matrix effects were significantly higher when detecting analytes of the IS in Fraction F_1 (paired t-test, $\alpha = 0.05$). Effects did not differ between the original sample *N2* and F_4, demonstrating the good compatibility of the FSE media in the relevant fraction. Compared to the aqueous river water sample, the negative ESI mode (Figure 6-5D) revealed stronger matrix effects. However, they were smaller for F_4, when compared to the river water sample *N2*.

Consequently, the reduction of coelution increased information on sample composition and might facilitate identification via MS/MS.

Non-target screening

Already in the TIC traces of Fraction F_4, an increase in intensity and number of distinct signals was observed for both ESI polarities (see Figure 6-5A and B). A closer evaluation of the data using libraries revealed 26 suspects based on retention time and exact mass. The suspects are listed in Table 6-3 and some of their EICs are depicted in Figure 6-6. Suspect analytes in Fraction F_4 were not detected in Fraction F_1 in the high-conductivity buffer zone. Instead, they were enriched by factors between 0.9 and 15.2 (see ratio F_4/sample in Table 6-3). The suspects were looked at in more detail considering the criteria of FSE of anionic charge and a VEF of 3.7. For some analytes, EFs > 3.7 were observed which cannot result solely from FSE preconcentration (see for instance adipic acid, Figure 6-6, N°6, Table 6-3). Matrix effects and low precision when concentrations are close to the LOD are expected to evoke this inconsistency. Some suspects (see for instance the analytes levetiracetam and genistein in Table 6-3) exhibited ratios of peak heights in F_4 to the ones in the original sample of over 100, indicating false-positive results (which was corroborated by their MS/MS spectra).

18 (70%) of the analytes in Table 6-3 have a (simulated) negative charge number ($\leq$ -0.2) at pH 10, which is the selection criterion for the FSE sample preparation step. 13 of these were verified by MS/MS, e.g. valsartan acid and candesartan (see Figure 6-7 1a-c and 2a-c and

Figure legend). In addition to that, using MS/MS, potential (negatively charged) suspect compounds demonstrating too high EFs of ≥ 140 could be falsified (see MS/MS spectrum genistein in Figure 6-7, 3b and c). Four neutral suspects (diphenylamine, *N*-ethylaniline, benzoguanamine and venlafaxine, see Table 6-3) were verified using MS/MS.
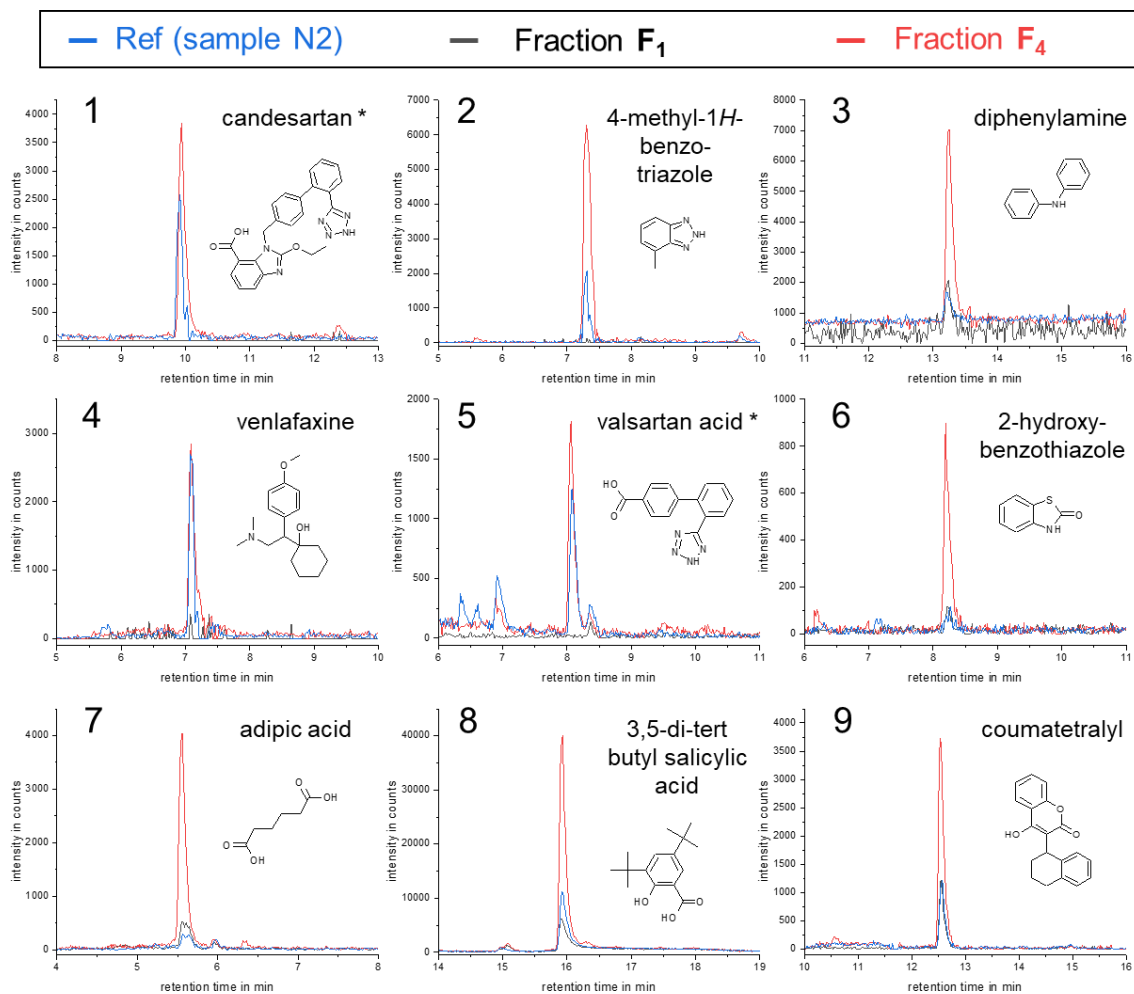
Figure 6-6: EICs of selected suspects in the sample N2 (blue lines) and the Fractions F_1 (black lines) and F_4 (red lines) (confirmed by their MS/MS spectra including their molecular structures) listed in Table 6-3 using RPLC-NTS. For analytes marked with an asterisk *, MS/MS spectra are depicted exemplarily in Figure 6-7. For details on RPLC-NTS method parameters, the reader is referred to [256].

The ratio of 0.9 for the analyte venlafaxine corresponds well with the FSE mechanism: neutral analytes can reach the Fraction F_4, though with a concentration reduced compared to the original sample due to widening of the sample flow by a factor of approx. 4 (sample flow rate of 12.7 ml/min vs. fraction collection rate of 3.4 ml/min). However, the other ratios seem very high. For *N*-ethylaniline, the combination of lack of charge and high ratio suggests a false- positive result. Other neutral suspects with too high enrichment factors were classified as false- positives using MS/MS (e.g. levetiracetam and dimefuron). Consequently, the increased selectivity by charge strongly aids in suspect screening.
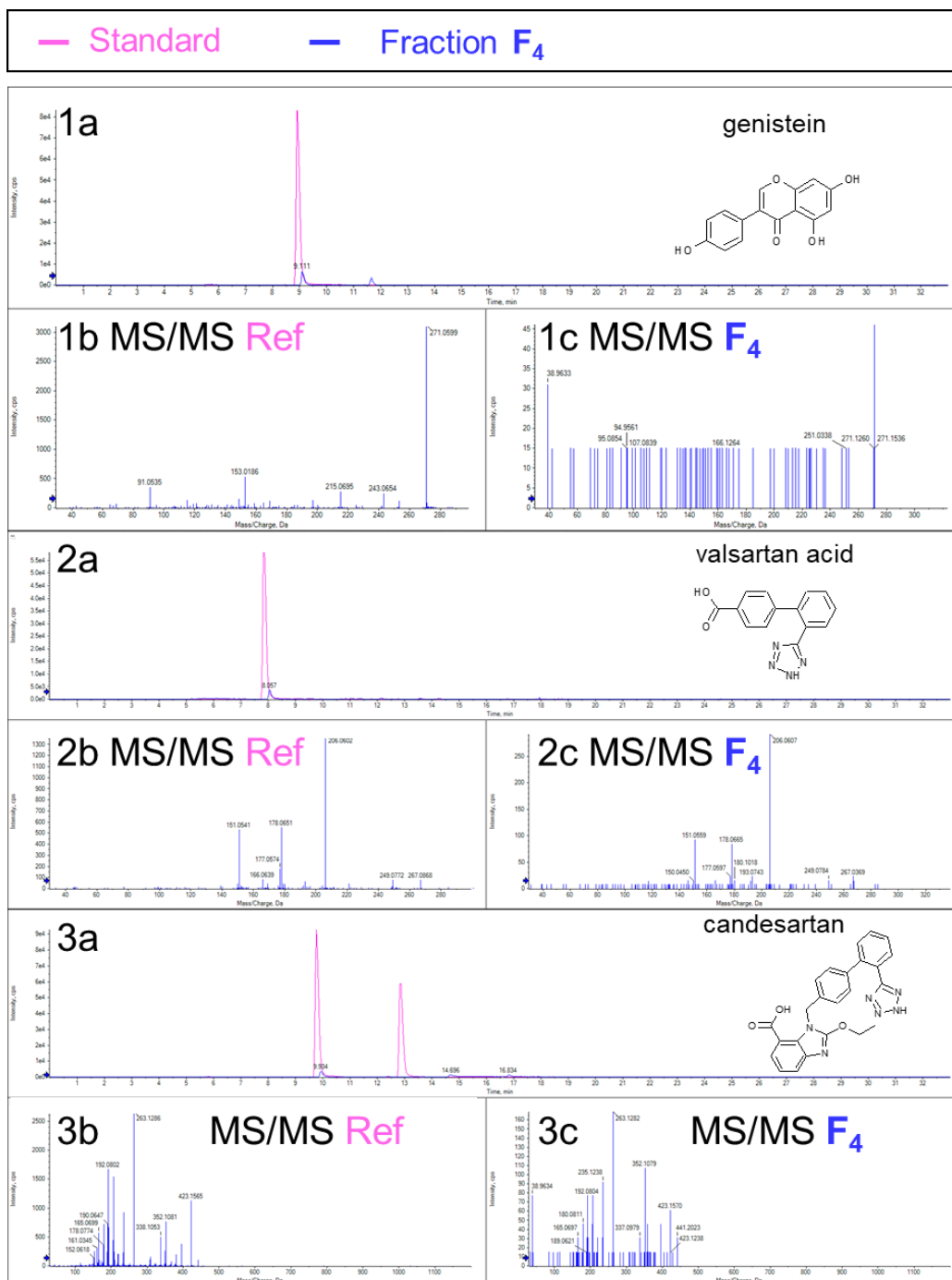
Figure 6-7: EICs of the suspects genistein (1, not verified), valsartan acid (2, verified by MS/MS) and candesartan (3, verified by MS/MS) also listed in Table 6-3. EICs of reference standard (pink) and suspect in Fraction F_4 are shown in 1a, 2a and 3a).MS/MS spectra of the suspects are given in 1b, 2b and 3b from the reference standard (5 µg/l) and in 1c, 2c and 3c from Fraction F_4. Comparison of MS/MS spectra to reference spectra falsified suspect genistein and verified suspects valsartan acid and candesartan. For details on RPLC-NTS method parameters, the reader is referred to [256].

FSE is able to capture transformation products, as can be seen by the suspect valsartan acid (Figure 6-6, N°5, Table 6-3) as the transformation product of valsartan. We want to stress that analyte polarity was not decisive for an analyte to be covered by FSE as log $D_{pH\,10}$ values of preconcentrated analytes ranged from -6.6 (adipic acid) to 1.5 (3,5-di-tert butylsalicylic acid). Thus, different substance classes were covered, also visible by the different molecular structures shown in Figure 6-6.

*Table 6-3: List of suspect compounds in ESI+ and ESI– obtained after analyzing Fraction **F₄** (sample N2) by RPLC-NTS. Three analytes were detected in both ESI polarities in separate runs. Column "MS/MS conf." reveals the confirmation by MS/MS (n – no, y – yes and o – no MS/MS spectra recorded). Strongest acidic and basic pK$_a$ values, charge number and log P values as well as log D values at pH 10 (log D$_{pH 10}$) were simulated by Chemicalize provided by ChemAxon (11/02/2021). Analytes are sorted according to their charge number at pH 10. Last three columns list the ratios of peak heights of analytes in Fraction **F₄** vs. the peak heights in the original sample N2 (that is, the enrichment efficiency) in ESI+ and ESI- mode as well as the peak number in the EICs depicted in Figure 6-6.*

MS polarity	suspect analyte	MS/MS conf.	RT in min	strong. acidic pK$_a$	strong. basic pK$_a$	charge number at pH 10	log P	log D$_{pH 10}$	peak height ratio **F₄**/ sample ESI+	peak height ratio **F₄**/ sample ESI-	peak N° Figure 6-6
ESI+	genistein	n	9.1	6.6		-3.0	3.1	-1.8	140.3		
	candesartan	y	10.0	3.5	1.5	-2.0	5.3	0.2	1.5		1
	ciclopirox	y	5.2	6.8		-1.0	2.2	-0.1	11.3		
	dimethachlor CGA 354742 (dimethachlor ESA)	o	7.0	-0.8		-1.0	1.2	-1.1	70.3		
	5-methyl-1-*H*-benzotriazol; 4-methylbenzotriazole	y	7.4	9.1	0.5	-0.9	1.8	0.8	3.8		2
	3-phenylphenol; 4-phenylphenol	n	11.0	9.9		-0.6	3.3	3.0	249.2		
	rac *N,O*-didesmethyl venlafaxine	n	6.0	10.3	9.7	-0.2	1.7	1.7	5.8		
	diphenylamine	y	13.3		0.8	0.0	3.4	3.4	7.1		3
	N-ethylaniline	y	5.6		4.9	0.0	1.8	1.8	270.9		
	1,3-diisopropylurea	n	6.9	15.7	-1.3	0.0	0.6	0.6	32.6		
	levetiracetam	n	5.5		-1.6	0.0	-0.6	-0.6	227.5		
	benzoguanamine	y	5.8	15.6	7.0	0.0	1.8	1.8	17.5		
	3-[*N*-n-butyl *N*-acetyl]aminopropionic acid-ethyl ester	n	9.7		-1.3	0.0	1.0	1.0	70.5		
	venlafaxine	y	7.1	14.4	8.9	0.0	2.7	2.7	0.9		4
ESI+/ ESI-	valsartan acid	y	8.1	4.0	-1.5	-2.0	3.2	-2	1.2	1.4	5
	2-hydroxybenzothiazole	y	8.2	11.3	-1.3	-1.0	2.5	0.9	7.6	8.4	6
	L-phenylalanine	y	5.3	2.5	9.5	-0.8	-1.2	-1.8	8.6	49.7	
ESI-	adipic acid	y	5.6	3.9		-2.0	0.5	-6.6		15.2	7
	1*H*-benzotriazole	y	6.4	9.0	0.2	-1.0	1.3	0.1		0.6	
	3-hydroxybenzaldehyde; 4-hydroxybenzaldehyde	y	6.7	7.3		-1.0	1.4	-0.7		3.7	
	p-toluene sulfonic acid	y	5.7	-2.1		-1.0	1.7	-0.7		2.3	
	benzothiazolesulfonic acid	y	6.2	-2.8		-1.0	-0.3	-0.4		3.1	
	3,5-di-tert butyl salicylic acid	y	15.9	2.8		-1.0	5.1	1.5		3.5	8
	coumatetralyl	y	12.5	5.6		-1.0	3.8	1.0		3.3	9
	difenoxuron	o	10.2	14.0		0.0	2.7	2.7		2.3	
	dimefuron	n	11.1	12.9		0.0	3.4	3.4		3.4	

6.5   Conclusion and outlook

A new sample preparation method for the analysis of ionizable micropollutants in surface waters based on free flow electrophoresis was presented. It used a step mode preconcentration by stacking analytes at the boundary between a high- and low-conductivity buffer. This step mode FFE, called FSE, proved suitable for the focusing of a broad range of acidic analytes with pK_a values of up to 10. Model analytes spiked into FSE samples were recovered in mostly one, rarely two fractions. FSE media were chosen to be volatile and a good compatibility of the dried and reconstituted fractions with downstream analysis by RPLC-, HILIC- and CE-MS was demonstrated, with best overall performance using FSE/RPLC-MS for the model analytes investigated here. The orthogonality of the chromatographic separation processes and the electrophoretic FSE step helped to largely reduce matrix effects especially for early eluting compounds in RPLC. Chromatographic analysis of river water and fractions thereof showed that the intensity of matrix components eluting in the void volume was strongly reduced especially in negative ESI polarity. Clearly, inorganic salts, (polar) neutral and cationic compounds were removed by FSE. The FSE sample preparation was selective for anions with a charge number > -0.2 in the FSE medium, but no dependence regarding pK_a or polarity was observed otherwise. The comparison of the performance with established sample preparation techniques in water analysis like SPE and EC demonstrated the potential of FSE for the analysis of micropollutants in river water and showed its broad coverage and capability to increase S/N ratios by a factor of up to 6.

The FSE/RPLC-MS procedure had a high precision (RSD peak areas 3-6%). With the current parameters for FSE and subsequent sample preparation, the volume preconcentration is low and mostly relative enrichment factors close to 1 were often observed (see Figure 6-3A). Compared to the achievable enrichment factor of 3.7 (see Section 6.3.5), loss of analyte during fractionation is evident. For example, it is possible, that high mobility analytes cross the stacking boundary and thus leave the stack before sampling the fractions. Further factors are possible interferences by remaining FSE electrolytes and sensitivity losses for analytes spreading over more than one fraction, but also possible matrix effects in the direct analysis of the river water sample may be relevant. Tuning flow vs. separation velocity in FSE has to be improved in future investigations in order to increase loadability: 5 times higher sample flow rates are possible to achieve better preconcentration during fractionation. Further enrichment can be reached by narrowing down the fractions after FSE separation, which is feasible as the FSE electrolytes were volatile. In contrast to direct evaporative concentration of environmental samples, FSE separation removes critical salt matrix components whereas they become enriched in EC. After evaporation, reconstitution in a suitable solvent is possible, which avoids dilution of the fraction for HILIC separations, where 80% MeCN should be present for injection.

FSE was shown for the first time to be an interesting tool for screening applications in environmental analysis, especially when bearing in mind that transformation products in the environment have a higher acidity than their parent compounds. A proof of concept

for non-target screening was presented resulting in 17 suspects identified by retention time and MS/MS spectra in the relevant FSE fraction with only very minor interferences of the FSE electrolytes with the subsequent non-target screening. The additional selectivity criterion of charge by FSE proved to be useful in excluding false-positive results. Future work will develop FSE sample preparation methods for basic analytes. An application to sea water with its very high salinity is envisaged.

7. Conclusive discussion

Optimization of sample preparation and downstream analysis is necessary to cover a broad range of analytes for environmental monitoring strategies. The compatibility between sample preparation and the subsequent analysis step is of great importance, as otherwise analytes will be lost, a strong bias is introduced in e.g. analyte enrichment, or quantification is impaired by matrix effects. Adapting both steps to each other helps to obtain a broad analyte coverage and precise information on the sample composition. Orthogonality between sample preparation and subsequent analysis technique might contribute to reducing matrix effects. The analysis of micropollutants in environmental samples lacks methodology suitable for polar and ionizable compounds, so that their fate and relevance, especially for many transformation products, remain to be elucidated.

In this thesis, new **separation methods** for the analysis of, in particular, polar and ionizable compounds were developed based on electromigrative and chromatographic separation mechanisms: 1) The new non-aqueous capillary electrophoresis mass spectrometry (NACE-MS) method proved to be applicable for the analysis of a broad range of analytes in different sample types including mineral and river water as well as biota after QuEChERS extraction. These applications demonstrate high matrix tolerance and high precision. Detection limits (LODs) in the low µg/l range were reached without preconcentration. Solely by switching polarities between two runs of one sample, the method managed to analyze both cations and anions as a common background electrolyte was used for both polarities. The method also proved suitable for the analysis of neutral compounds in river water samples. With a preceding solid-phase extraction (SPE) step, quantification of the artificial sweetener acesulfame and the commonly prescribed pharmaceutical hydrochlorothiazide in river water was possible. The NACE-MS method was successfully applied for screening purposes demonstrating the capability to differentiate the degree of contamination when sampling along rivers before and after wastewater treatment plants as well as between the three rivers investigated. No bias to analytes' polarity was observed, which demonstrates the method's potential for non-target screening as a complementary strategy to common reversed-phase liquid chromatography (RPLC)-MS non-target screening. Future work will focus on the optimization of the ionization conditions at the CE-MS electrospray ionization interface, starting with an optimization of the sheath liquid composition.

2) Chromatographic separations were established using two different stationary phases for separation by RPLC-MS and hydrophilic interaction liquid chromatography (HILIC)-MS. One RPLC-MS and two HILIC-MS methods, optimized for either anions and cations, were examined. Optimized methods showed LODs in the medium ng/l range and low matrix effects of $\approx$ 90±30% on average for the majority of the analytes. The sample composition proved crucial for the two HILIC methods with significant impact of the water content on retention and for some analytes also on separation efficiency and signal intensities. This limited the LODs reached, as aqueous samples required five-fold dilution to become compatible with HILIC separation. As separations using the HILIC method for anionic analytes exhibited low retention of polar and very high retention for very polar

compounds, further optimization is advisable, especially by using a different stationary phase.

In addition to the separation methods presented here, two new **sample preparation** strategies were developed in this work: 1) an electromembrane extraction (EME) setup and method using a flow-through cell for the simultaneous enrichment of both cationic and anionic analytes and 2) a new field-step electrophoresis (FSE) protocol for the fractionation of charged analytes. For both strategies, the analytes' charge was the only prerequisite and decisive for selectivity. Using EME, cationic and anionic analytes were extracted simultaneously in a dual flow cell, whereas only anionic compounds were looked at using FSE.

With the EME setup, analytes possessing a wide range of polarities from $-7.7 < \log D_{pH\,5} < 2.4$ were covered after optimizing the membrane compositions, which illustrates that EME can be broadened from common target to non-target analysis. Using RPLC-MS and NACE-MS for the analysis of acceptor solutions demonstrated the importance of considering matrix effects when evaluating EME effects. This is crucial for a deeper understanding of basic EME principles. The developed setup allowed to study salt effects when extracting analytes from environmental waters, though further development is required. The membrane thickness should be further decreased, and the membrane manufacturing process should become better reproducible by automation. Then, the EME setup can be considered for a non-target approach in environmental water samples.

The FSE step was optimized for anions and proved suitable for the focusing of a broad range of acidic analytes with pK_a values of up to 10 in not more than two fractions, showing no bias with regard to polarity. FSE was more compatible with RPLC-MS than with NACE-MS. FSE/RPLC-MS was applied to river water samples revealing a high precision (relative standard deviations of peak areas between 3 and 6%). FSE/RPLC-MS showed broad analyte coverage, which was reached as the content of inorganic salts and polar neutral analytes was strongly reduced and succeeded in identifying anions eluting early. A comparison with common sample preparation techniques like SPE and evaporative concentration (EC) proved the potential of FSE to become implemented for non-target screening approaches, possible also for samples of high contents of inorganic salts such as seawater. Contrary to the EME method, solely acidic compounds will be focused, and a second fractionation would be necessary for basic analytes.

The extensive evaluation of sample preparation steps and their **compatibility** with downstream separation techniques in this work allows a concluding discussion:

Selectivity: The four sample preparation steps differ strongly in their selectivity or coverage: for SPE, selectivity is strongly limited by the analytes' polarity and also by their charge, depending on the type of sorbent. EC shows the highest coverage, as only volatile analytes may become lost and some drawbacks might occur due to incomplete redissolution. For EME and FSE, the analytes' charge is the primary selectivity criterion. However, for EME, the coverage may be reduced to a certain extent by the selectivity of the analyte transfer through the membrane. The results of this thesis show that a fine-tuning of the membrane composition allows to increase the analyte coverage. Both EME

and FSE proved to be promising sample preparation methods for non-target screening as demonstrated in model applications.

Good compatibility with regard to selectivity was shown for all combinations of sample preparation and separation techniques coupled to MS. Orthogonality in separation proved advantageous, especially when using FSE/RPLC-MS. Chromatographic analysis of river water and its FSE fractions thereof showed that the intensity of compounds eluting in the void volume was strongly reduced, particularly in the case of compounds detected in negative ESI polarity. Presumably, highly mobile anionic compounds, polar neutral as well as cationic compounds were removed by the FSE step.

Compatibility with micropollutant analysis: Whereas for SPE, EC, and FSE, analyte enrichment takes place during reconstitution in lower volumes compared to the original sample volume, the enrichment in EME occurs directly during the EME process with a low volume of the acceptor solution. This gives rise to a large number of parameters (e.g. sample flow rate, applied current, etc.) which can be fine-tuned for optimal recovery and enrichment compared to the SPE and EC procedure. In FSE, further improvement of enrichment efficiencies is possible, e.g. by increasing the sample load. Adaptations with respect to the salt content can easily be made.

As FSE media were chosen to be volatile, SPE, EC, and FSE enabled solvent exchange after evaporation facilitating compatibility with downstream analysis by RPLC-, HILIC- and CE-MS. For EC, limitations with regard to incomplete redissolution of all analytes might have to be considered due to the enrichment of inorganic salts. Solely for EME, so far, no solvent exchange has been possible, and thus the sensitivity is limited here if combined with HILIC-MS.

The sensitivity of separation methods was improved using all four sample preparation procedures with respect to LODs reached in published studies. NACE-MS on its own was not sensitive enough for the direct analysis of river water, but by using EME/NACE-MS, sensitivity was increased reaching LODs in the medium ng/l range.

Matrix effects: Matrix interferences especially caused by high salt concentrations in the sample were the major factor limiting EME preconcentration. For SPE, an adaptation of the elution protocol was able to at least partially remove matrix compounds, which becomes especially important if high volume preconcentration factors are targeted. FSE media may have to be adapted if higher salt concentrations are present in the sample to ensure proper stacking conditions. So far, no interferences have been observed, and FSE has proved to be particularly valuable in the reduction of matrix, demonstrating great potential with its high matrix tolerance towards sample composition as well as downstream analysis. For EC, matrix effects become relevant in reconstitution and downstream analysis, which limit enrichment when the salt content is high.

Concluding, two new sample preparation methods compatible with newly developed chromatographic and electromigrative separation techniques were established, validated, and their performance was assessed with regard to matrix tolerance, LODs, and analyte coverage. The results of this thesis demonstrate the high potential of using charge as selectivity criterion for both sample preparation (EME and FSE) and separation (NACE-MS). In particular, EME/NACE-MS and FSE/RPLC-MS showed promise for the analysis

of ionic and ionizable micropollutants, since they cover a broad polarity range in different environmental samples. This was exemplified in the successful analysis of micropollutants and a non-target screening in river water samples was presented as proof-of-concept application. The results obtained may serve as a base for future developments and improvements and contribute to closing the analytical gap that exists in the analysis of ionizable polar micropollutants in environmental sciences.

8. References

1. Knoll, S.; Rösch, T.; Huhn, C., Trends in sample preparation and separation methods for the analysis of very polar and ionic compounds in environmental water and biota samples. *Anal Bioanal Chem* **2020,** *412* (24), 6149-6165.

2. Wicht, A.-J. Development and application of new analytical methods based on chromatographic and electrophoretic separations to assess the environmental behavior of anthropogenic pollutants and their uptake in fungi and chironomids. PhD thesis, Universität Tübingen, 2018.

3. Reemtsma, T.; Berger, U.; Arp, H. P.; Gallard, H.; Knepper, T. P.; Neumann, M.; Quintana, J. B.; Voogt, P., Mind the gap: persistent and mobile organic compounds- water contaminants that slip through. *Environ Sci Technol* **2016,** *50* (19), 10308-10315.

4. Krauss, M.; Singer, H.; Hollender, J., LC-high resolution MS in environmental analysis: from target screening to the identification of unknowns. *Anal Bioanal Chem* **2010,** *397* (3), 943-951.

5. Zahn, D.; Neuwald, I. J.; Knepper, T. P., Analysis of mobile chemicals in the aquatic environment-current capabilities, limitations and future perspectives. *Anal Bioanal Chem* **2020,** *412* (20), 4763-4784.

6. Stoll, D. R., Pass the salt: Evolution of coupling ion-exchange separations and mass spectrometry. *LCGC Europe* **2019,** *32* (8), 405-409.

7. Zhang, W.; Ramautar, R., CE-MS for metabolomics: Developments and applications in the period 2018-2020. *Electrophoresis* **2021,** *42* (4), 381-401.

8. Drouin, N.; Pezzatti, J.; Gagnebin, Y.; Gonzalez-Ruiz, V.; Schappler, J.; Rudaz, S., Effective mobility as a robust criterion for compound annotation and identification in metabolomics: Toward a mobility-based library. *Anal Chim Acta* **2018,** *1032*, 178-187.

9. Kern, S.; Fenner, K.; Singer, H. P.; Schwarzenbach, R. P.; Hollender, J., Identification of transformation products of organic contaminants in natural waters by computer-aided prediction and high-resolution mass spectrometry. *Environ Sci Technol* **2009,** *43* (18), 7039-7046.

10. Mechelke, J.; Longree, P.; Singer, H.; Hollender, J., Vacuum-assisted evaporative concentration combined with LC-HRMS/MS for ultra-trace-level screening of organic micropollutants in environmental water samples. *Anal Bioanal Chem* **2019,** *411* (12), 2555-2567.

11. Koke, N.; Zahn, D.; Knepper, T. P.; Fromel, T., Multi-layer solid-phase extraction and evaporation-enrichment methods for polar organic chemicals from aqueous matrices. *Anal Bioanal Chem* **2018,** *410* (9), 2403-2411.

12. Pedersen-Bjergaard, S.; Rasmussen, K. E., Electrokinetic migration across artificial liquid membranes. New concept for rapid sample preparation of biological fluids. *J Chromatogr A* **2006,** *1109* (2), 183-190.

13. Drouin, N.; Kubáň, P.; Rudaz, S.; Pedersen-Bjergaard, S.; Schappler, J., Electromembrane extraction: overview of the last decade. *TrAC Trends Anal Chem* **2019,** *113*, 357-363.

14. Quesada-Molina, C.; Olmo-Iruela, M. d.; García-Campaña, A. M., Analysis of cephalosporin residues in environmental waters by capillary zone electrophoresis with off-line and on-line preconcentration. *Anal Methods* **2012,** *4* (8), 2341-2347.

15. Timerbaev, A. R.; Hirokawa, T., Recent advances of transient isotachophoresis-capillary electrophoresis in the analysis of small ions from high-conductivity matrices. *Electrophoresis* **2006,** *27* (1), 323-340.

16.   Weber, P. J. A.; Weber, G.; Eckerskorn, C.; Schneider, U.; Posch, A., 10 Free-flow isoelectric focusing. In *Separation Science and Technology*, Garfin, D.; Ahuja, S., Eds. Academic Press: Cambridge, 2005; Vol. 7, pp 211-245.

17.   Wagner, H.; Kessler, R., Free flow field step focusing-a new method for preparative protein isolation. In *Electrophoresis '82*, Stathakos, D., Ed. De Gruyter: Berlin, Boston, 2019; pp 303-312.

18.   Richardson, M. L.; Bowron, J. M., The fate of pharmaceutical chemicals in the aquatic environment. *J Pharm Pharmacol* **1985**, *37* (1), 1-12.

19.   Reemtsma, T.; Berger, U.; Arp, H. P. H.; Gallard, H.; Knepper, T. P.; Neumann, M.; Quintana, J. B.; Voogt, P. d., Mind the gap: persistent and mobile organic compounds - water contaminants that slip through. *Environ Sci Technol* **2016**, *50* (19), 10308-10315.

20.   van Nuijs, A. L.; Tarcomnicu, I.; Covaci, A., Application of hydrophilic interaction chromatography for the analysis of polar contaminants in food and environmental samples. *J Chromatogr A* **2011**, *1218* (35), 5964-5974.

21.   Salas, D.; Borrull, F.; Fontanals, N.; Marcé, R. M., Hydrophilic interaction liquid chromatography coupled to mass spectrometry-based detection to determine emerging organic contaminants in environmental samples. *TrAC Trends Anal Chem* **2017**, *94*, 141-149.

22.   Schmidt, T. C., Recent trends in water analysis triggering future monitoring of organic micropollutants. *Anal Bioanal Chem* **2018**, *410* (17), 3933-3941.

23.   Zhang, Q.; Yang, F.-Q.; Ge, L.; Hu, Y.-J.; Xia, Z.-N., Recent applications of hydrophilic interaction liquid chromatography in pharmaceutical analysis. *J Sep Sci* **2017**, *40* (1), 49-80.

24.   Zahn, D.; Reemtsma, T.; Berger, U.; Knepper, T. P., Quellen und Verbreitung persistenter und mobiler organischer Stoffe in Roh- und Trinkwasser. *Vom Wasser* **2019**, *117* (4), 125-129.

25.   Bicker, W.; Lämmerhofer, M.; Lindner, W., Mixed-mode stationary phases as a complementary selectivity concept in liquid chromatography–tandem mass spectrometry-based bioanalytical assays. *Anal Bioanal Chem* **2008**, *390* (1), 263-266.

26.   Wasik, A.; Kot-Wasik, A.; Namiesnik, J., New trends in sample preparation techniques for the analysis of the residues of pharmaceuticals in environmental samples. *Curr Anal Chem* **2016**, *12* (4), 280-302.

27.   Núñez, M.; Borrull, F.; Pocurull, E.; Fontanals, N., Sample treatment for the determination of emerging organic contaminants in aquatic organisms. *TrAC Trends in Anal Chem* **2017**, *97*, 136-145.

28.   Rossmann, J.; Schubert, S.; Gurke, R.; Oertel, R.; Kirch, W., Simultaneous determination of most prescribed antibiotics in multiple urban wastewater by SPE-LC-MS/MS. *J Chromatogr B* **2014**, *969*, 162-170.

29.   David, V.; Galaon, T.; Bacalum, E., Sample enrichment by solid-phase extraction for reaching parts per quadrillion levels in environmental analysis. *Chromatographia* **2019**, *82* (8), 1139-1150.

30.   Ribeiro, C.; Ribeiro, A. R.; Maia, A. S.; Goncalves, V. M.; Tiritan, M. E., New trends in sample preparation techniques for environmental analysis. *Crit Rev Anal Chem* **2014**, *44* (2), 142-185.

31.   Armenta, S.; Garrigues, S.; de la Guardia, M., Green analytical chemistry. *TrAC Trends Anal Chem* **2008**, *27* (6), 497-511.

32.   Fontanals, N.; Marce, R. M.; Borrull, F., On-line solid-phase extraction coupled to hydrophilic interaction chromatography-mass spectrometry for the determination of polar drugs. *J Chromatogr A* **2011**, *1218* (35), 5975-5980.

33.   Gomez, M. J.; Petrovic, M.; Fernandez-Alba, A. R.; Barcelo, D., Determination of pharmaceuticals of various therapeutic classes by solid-phase extraction and liquid

chromatography-tandem mass spectrometry analysis in hospital effluent wastewaters. *J Chromatogr A* **2006,** *1114* (2), 224-233.

34. Barron, L.; Tobin, J.; Paull, B., Multi-residue determination of pharmaceuticals in sludge and sludge enriched soils using pressurized liquid extraction, solid phase extraction and liquid chromatography with tandem mass spectrometry. *J Environ Monit* **2008,** *10* (3), 353-361.

35. Huerta, B.; Jakimska, A.; Gros, M.; Rodriguez-Mozaz, S.; Barcelo, D., Analysis of multi-class pharmaceuticals in fish tissues by ultra-high-performance liquid chromatography tandem mass spectrometry. *J Chromatogr A* **2013,** *1288*, 63-72.

36. Boulard, L.; Dierkes, G.; Ternes, T., Utilization of large volume zwitterionic hydrophilic interaction liquid chromatography for the analysis of polar pharmaceuticals in aqueous environmental samples: benefits and limitations. *J Chromatogr A* **2018,** *1535*, 27-43.

37. Chau, H. T. C.; Kadokami, K.; Ifuku, T.; Yoshida, Y., Development of a comprehensive screening method for more than 300 organic chemicals in water samples using a combination of solid-phase extraction and liquid chromatography-time-of-flight-mass spectrometry. *Environ Sci Pollut Res Int* **2017,** *24* (34), 26396-26409.

38. Carneiro, M. C.; Puignou, L.; Galceran, M. T., Comparison of silica and porous graphitic carbon as solid-phase extraction materials for the analysis of cationic herbicides in water by liquid chromatography and capillary electrophoresis. *Anal Chim Acta* **2000,** *408* (1-2), 263-269.

39. Scheurer, M.; Sacher, F.; Brauch, H. J., Occurrence of the antidiabetic drug metformin in sewage and surface waters in Germany. *J Environ Monit* **2009,** *11* (9), 1608-1613.

40. Köke, N.; Zahn, D.; Knepper, T. P.; Frömel, T., Multi-layer solid-phase extraction and evaporation-enrichment methods for polar organic chemicals from aqueous matrices. *Anal Bioanal Chem* **2018,** *410* (9), 2403-2411.

41. Rodriguez-Mozaz, S.; Lopez de Alda, M. J.; Barcelo, D., Advantages and limitations of on-line solid phase extraction coupled to liquid chromatography-mass spectrometry technologies versus biosensors for monitoring of emerging contaminants in water. *J Chromatogr A* **2007,** *1152* (1-2), 97-115.

42. Huntscha, S.; Singer, H. P.; McArdell, C. S.; Frank, C. E.; Hollender, J., Multiresidue analysis of 88 polar organic micropollutants in ground, surface and wastewater using online mixed-bed multilayer solid-phase extraction coupled to high performance liquid chromatography-tandem mass spectrometry. *J Chromatogr A* **2012,** *1268*, 74-83.

43. Cai, Q.; Zhang, L.; Zhao, P.; Lun, X.; Li, W.; Guo, Y.; Hou, X., A joint experimental-computational investigation: Metal organic framework as a vortex assisted dispersive micro-solid-phase extraction sorbent coupled with UPLC-MS/MS for the simultaneous determination of amphenicols and their metabolite in aquaculture water. *Microchem J* **2017,** *130*, 263-270.

44. He, Z.; Liu, D.; Zhou, Z.; Wang, P., Ionic-liquid-functionalized magnetic particles as an adsorbent for the magnetic SPE of sulfonylurea herbicides in environmental water samples. *J Sep Sci* **2013,** *36* (19), 3226-3233.

45. Luo, Y. B.; Shi, Z. G.; Gao, Q.; Feng, Y. Q., Magnetic retrieval of graphene: extraction of sulfonamide antibiotics from environmental water samples. *J Chromatogr A* **2011,** *1218* (10), 1353-1358.

46. Arthur, C.; Pawliszyn, J., The principle and application of solid-phase micro-extraction (SPME). *Anal Chem* **1990,** *62*, 2145-2148.

47.   Li, J.; Wang, Y.-B.; Li, K.-Y.; Cao, Y.-Q.; Wu, S.; Wu, L., Advances in different configurations of solid-phase microextraction and their applications in food and environmental analysis. *TrAC Trends Anal Chem* **2015,** *72*, 141-152.

48.   Souza-Silva, É. A.; Jiang, R.; Rodríguez-Lafuente, A.; Gionfriddo, E.; Pawliszyn, J., A critical review of the state of the art of solid-phase microextraction of complex matrices I. Environmental analysis. *TrAC Trends Anal Chem* **2015,** *71*, 224-235.

49.   Piri-Moghadam, H.; Ahmadi, F.; Pawliszyn, J., A critical review of solid phase microextraction for analysis of water samples. *TrAC Trends Anal Chem* **2016,** *85*, 133-143.

50.   Aresta, A.; Bianchi, D.; Calvano, C. D.; Zambonin, C. G., Solid phase microextraction--liquid chromatography (SPME-LC) determination of chloramphenicol in urine and environmental water samples. *J Pharm Biomed Anal* **2010,** *53* (3), 440-444.

51.   López-Blanco, M. C.; Cancho-Grande, B.; Simal-Gándara, J., Comparison of solid-phase extraction and solid-phase microextraction for carbofuran in water analyzed by high-performance liquid chromatography–photodiode-array detection. *J Chromatogr A* **2002,** *963* (1-2), 117-123.

52.   Balakrishnan, V. K.; Terry, K. A.; Toito, J., Determination of sulfonamide antibiotics in wastewater: a comparison of solid phase microextraction and solid phase extraction methods. *J Chromatogr A* **2006,** *1131* (1-2), 1-10.

53.   Suarez, B.; Santos, B.; Simonet, B. M.; Cardenas, S.; Valcarcel, M., Solid-phase extraction-capillary electrophoresis-mass spectrometry for the determination of tetracyclines residues in surface water by using carbon nanotubes as sorbent material. *J Chromatogr A* **2007,** *1175* (1), 127-132.

54.   Zhou, Q.; Xiao, J.; Wang, W., Comparison of multiwalled carbon nanotubes and a conventional absorbent on the enrichment of sulfonylurea herbicides in water samples. *Anal Sci* **2007,** *23* (2), 189-192.

55.   Carasek, E.; Morés, L.; Merib, J., Basic principles, recent trends and future directions of microextraction techniques for the analysis of aqueous environmental samples. *Trends Environ Anal Chem* **2018,** *19* (July), e00060.

56.   Soares da Silva Burato, J.; Vargas Medina, D. A.; de Toffoli, A. L.; Vasconcelos Soares Maciel, E.; Mauro Lancas, F., Recent advances and trends in miniaturized sample preparation techniques. *J Sep Sci* **2020,** *43* (1), 202-225.

57.   Yang, L.; Said, R.; Abdel-Rehim, M., Sorbent, device, matrix and application in microextraction by packed sorbent (MEPS): A review. *J Chromatogr B* **2017,** *1043*, 33-43.

58.   Pereira, J. A. M.; Goncalves, J.; Porto-Figueira, P.; Figueira, J. A.; Alves, V.; Perestrelo, R.; Medina, S.; Camara, J. S., Current trends on microextraction by packed sorbent - fundamentals, application fields, innovative improvements and future applications. *Analyst* **2019,** *144* (17), 5048-5074.

59.   Saracino, M. A.; Lazzara, G.; Prugnoli, B.; Raggi, M. A., Rapid assays of clozapine and its metabolites in dried blood spots by liquid chromatography and microextraction by packed sorbent procedure. *J Chromatogr A* **2011,** *1218* (16), 2153-2159.

60.   Morales-Cid, G.; Cardenas, S.; Simonet, B. M.; Valcarcel, M., Fully automatic sample treatment by integration of microextraction by packed sorbents into commercial capillary electrophoresis-mass spectrometry equipment: application to the determination of fluoroquinolones in urine. *Anal Chem* **2009,** *81* (8), 3188-3193.

61.   Prieto, A.; Schrader, S.; Moeder, M., Determination of organic priority pollutants and emerging compounds in wastewater and snow samples using multiresidue protocols on the basis of microextraction by packed sorbents coupled to large volume injection gas

chromatography–mass spectrometry analysis. *J Chromatogr A* **2010,** *1217* (38), 6002-6011.

62.	Rezaee, M.; Assadi, Y.; Milani Hosseini, M. R.; Aghaee, E.; Ahmadi, F.; Berijani, S., Determination of organic compounds in water using dispersive liquid-liquid microextraction. *J Chromatogr A* **2006,** *1116* (1-2), 1-9.

63.	Sajid, M.; Alhooshani, K., Dispersive liquid-liquid microextraction based binary extraction techniques prior to chromatographic analysis: A review. *TrAC Trends Anal Chem* **2018,** *108*, 167-182.

64.	Nojavan, Y.; Kamankesh, M.; Shahraz, F.; Hashemi, M.; Mohammadi, A., Ion pair-based dispersive liquid-liquid microextraction followed by high performance liquid chromatography as a new method for determining five folate derivatives in foodstuffs. *Talanta* **2015,** *137*, 31-37.

65.	Vazquez, M. M.; Vazquez, P. P.; Galera, M. M.; Garcia, M. D., Determination of eight fluoroquinolones in groundwater samples with ultrasound-assisted ionic liquid dispersive liquid-liquid microextraction prior to high-performance liquid chromatography and fluorescence detection. *Anal Chim Acta* **2012,** *748*, 20-27.

66.	Sereshti, H.; Khorram, P.; Nouri, N., Recent trends in replacement of disperser solvent in dispersive liquid-liquid microextraction methods. *Sep Purif Rev* **2018,** *48* (2), 159-178.

67.	Bruzzoniti, M. C.; Checchini, L.; De Carlo, R. M.; Orlandini, S.; Rivoira, L.; Del Bubba, M., QuEChERS sample preparation for the determination of pesticides and other organic residues in environmental matrices: a critical review. *Anal Bioanal Chem* **2014,** *406* (17), 4089-4116.

68.	Anastassiades, M.; Scherbaum, E.; Bertsch, D. In *Validation of a simple and rapid multiresidue method (QuEChERS) and its implementation in routine pesticide analysis*, MGPR Symposium: Aix en Provence, France, 2003.

69.	Kachhawaha, A. S.; Nagarnaik, P. M.; Jadhav, M.; Pudale, A.; Labhasetwar, P. K.; Banerjee, K., Optimization of a modified QuEChERS method for multiresidue analysis of pharmaceuticals and personal care products in sewage and surface water by LC-MS/MS. *J AOAC Int* **2017,** *100* (3), 592-597.

70.	Cerqueira, M. B. R.; Guilherme, J. R.; Caldas, S. S.; Martins, M. L.; Zanella, R.; Primel, E. G., Evaluation of the QuEChERS method for the extraction of pharmaceuticals and personal care products from drinking-water treatment sludge with determination by UPLC-ESI-MS/MS. *Chemosphere* **2014,** *107*, 74-82.

71.	Braganca, I.; Placido, A.; Paiga, P.; Domingues, V. F.; Delerue-Matos, C., QuEChERS: a new sample preparation approach for the determination of ibuprofen and its metabolites in soils. *Sci Total Environ* **2012,** *433*, 281-289.

72.	Berlioz-Barbier, A.; Baudot, R.; Wiest, L.; Gust, M.; Garric, J.; Cren-Olive, C.; Bulete, A., MicroQuEChERS-nanoliquid chromatography-nanospray-tandem mass spectrometry for the detection and quantification of trace pharmaceuticals in benthic invertebrates. *Talanta* **2015,** *132*, 796-802.

73.	Núñez, M.; Borrull, F.; Fontanals, N.; Pocurull, E., Determination of pharmaceuticals in bivalves using QuEChERS extraction and liquid chromatography-tandem mass spectrometry. *Anal Bioanal Chem* **2015,** *407* (13), 3841-3849.

74.	Lopes, R. P.; Reyes, R. C.; Romero-Gonzalez, R.; Vidal, J. L.; Frenich, A. G., Multiresidue determination of veterinary drugs in aquaculture fish samples by ultra high performance liquid chromatography coupled to tandem mass spectrometry. *J Chromatogr B* **2012,** *895-896*, 39-47.

75.	Oedit, A.; Ramautar, R.; Hankemeier, T.; Lindenburg, P. W., Electroextraction and electromembrane extraction: advances in hyphenation to analytical techniques. *Electrophoresis* **2016,** *37* (9), 1170-1186.

76.   Koruni, M. H.; Tabani, H.; Gharari, H.; Fakhari, A. R., An all-in-one electro-membrane extraction: development of an electro-membrane extraction method for the simultaneous extraction of acidic and basic drugs with a wide range of polarities. *J Chromatogr A* **2014,** *1361*, 95-99.

77.   Drouin, N.; Rudaz, S.; Schappler, J., Sample preparation for polar metabolites in bioanalysis. *Analyst* **2017,** *143* (1), 16-20.

78.   Oertel, R.; Neumeister, V.; Kirch, W., Hydrophilic interaction chromatography combined with tandem-mass spectrometry to determine six aminoglycosides in serum. *J Chromatogr A* **2004,** *1058* (1), 197-201.

79.   Valette, J. C.; Demesmay, C.; Rocca, J. L.; Verdon, E., Separation of tetracycline antibiotics by hydrophilic interaction chromatography using an amino-propyl stationary phase. *Chromatographia* **2004,** *59* (1), 55-60.

80.   Nguyen, H. P.; Schug, K. A., The advantages of ESI-MS detection in conjunction with HILIC mode separations: Fundamentals and applications. *J Sep Sci* **2008,** *31* (9), 1465-1480.

81.   Seitz, W.; Schulz, W.; Weber, W. H., Novel applications of highly sensitive liquid chromatography/mass spectrometry/mass spectrometry for the direct detection of ultra-trace levels of contaminants in water. *Rapid Commun Mass Spectrom* **2006,** *20* (15), 2281-2285.

82.   Fauvelle, V.; Mazzella, N.; Morin, S.; Moreira, S.; Delest, B.; Budzinski, H., Hydrophilic interaction liquid chromatography coupled with tandem mass spectrometry for acidic herbicides and metabolites analysis in fresh water. *Environ Sci Pollut Res Int* **2015,** *22* (6), 3988-3996.

83.   Hayama, T.; Yoshida, H.; Todoroki, K.; Nohta, H.; Yamaguchi, M., Determination of polar organophosphorus pesticides in water samples by hydrophilic interaction liquid chromatography with tandem mass spectrometry. *Rapid Commun Mass Spectrom* **2008,** *22* (14), 2203-2210.

84.   Kovalova, L.; McArdell, C. S.; Hollender, J., Challenge of high polarity and low concentrations in analysis of cytostatics and metabolites in wastewater by hydrophilic interaction chromatography/tandem mass spectrometry. *J Chromatogr A* **2009,** *1216* (7), 1100-1108.

85.   van Nuijs, A. L.; Tarcomnicu, I.; Simons, W.; Bervoets, L.; Blust, R.; Jorens, P. G.; Neels, H.; Covaci, A., Optimization and validation of a hydrophilic interaction liquid chromatography-tandem mass spectrometry method for the determination of 13 top-prescribed pharmaceuticals in influent wastewater. *Anal Bioanal Chem* **2010,** *398* (5), 2211-2222.

86.   Sordet, M.; Bulete, A.; Vulliet, E., A rapid and easy method based on hydrophilic interaction chromatography coupled with tandem mass spectrometry (HILIC-MS/MS/MS) to quantify iodinated X-ray contrast in wastewaters. *Talanta* **2018,** *190*, 480-486.

87.   Lindner, U.; Lingott, J.; Richter, S.; Jiang, W.; Jakubowski, N.; Panne, U., Analysis of gadolinium-based contrast agents in tap water with a new hydrophilic interaction chromatography (ZIC-cHILIC) hyphenated with inductively coupled plasma mass spectrometry. *Anal Bioanal Chem* **2015,** *407* (9), 2415-2422.

88.   Gago-Ferrero, P.; Schymanski, E. L.; Bletsou, A. A.; Aalizadeh, R.; Hollender, J.; Thomaidis, N. S., Extended suspect and non-target strategies to characterize emerging polar organic contaminants in raw wastewater with LC-HRMS/MS. *Environ Sci Technol* **2015,** *49* (20), 12333-12341.

89.   dos Santos Pereira, A.; David, F.; Vanhoenacker, G.; Sandra, P., The acetonitrile shortage: is reversed HILIC with water an alternative for the analysis of highly polar ionizable solutes? *J Sep Sci* **2009,** *32* (12), 2001-2007.

90.   Hendrickx, S.; Adams, E.; Cabooter, D., Recent advances in the application of hydrophilic interaction chromatography for the analysis of biological matrices. *Bioanalysis* **2015,** *7* (22), 2927-2945.

91.   Pilařová, V.; Plachká, K.; Khalikova, M. A.; Svec, F.; Nováková, L., Recent developments in supercritical fluid chromatography – mass spectrometry: Is it a viable option for analysis of complex samples? *TrAC Trends Anal Chem* **2019,** *112*, 212-225.

92.   Bieber, S.; Greco, G.; Grosse, S.; Letzel, T., RPLC-HILIC and SFC with mass spectrometry: polarity-extended organic molecule screening in environmental (water) samples. *Anal Chem* **2017,** *89* (15), 7907-7914.

93.   West, C., Current trends in supercritical fluid chromatography. *Anal Bioanal Chem* **2018,** *410* (25), 6441-6457.

94.   Ordonez, E. Y.; Benito Quintana, J.; Rodil, R.; Cela, R., Computer assisted optimization of liquid chromatographic separations of small molecules using mixed-mode stationary phases. *J Chromatogr A* **2012,** *1238*, 91-104.

95.   Walshe, M.; Kelly, M. T.; Smyth, M. R.; Ritchie, H., Retention studies on mixed-mode columns in high-performance liquid chromatography. *J Chromatogr A* **1995,** *708* (1), 31-40.

96.   Kazarian, A. A.; Nesterenko, P. N.; Soisungnoen, P.; Burakham, R.; Srijaranai, S.; Paull, B., Comprehensive analysis of pharmaceutical products using simultaneous mixed-mode (ion-exchange/reversed-phase) and hydrophilic interaction liquid chromatography. *J Sep Sci* **2014,** *37* (16), 2138-2144.

97.   Zhang, L.; Dai, Q.; Qiao, X.; Yu, C.; Qin, X.; Yan, H., Mixed-mode chromatographic stationary phases: Recent advancements and its applications for high-performance liquid chromatography. *TrAC Trends Anal Chem* **2016,** *82*, 143-163.

98.   Sykora, D.; Rezanka, P.; Zaruba, K.; Kral, V., Recent advances in mixed-mode chromatographic stationary phases. *J Sep Sci* **2019,** *42* (1), 89-129.

99.   Strege, M. A.; Stevenson, S.; Lawrence, S. M., Mixed-mode anion-cation exchange/hydrophilic interaction liquid chromatography-electrospray mass spectrometry as an alternative to reversed phase for small molecule drug discovery. *Anal Chem* **2000,** *72* (19), 4629-4633.

100.   Mashige, F.; Ohkubo, A.; Matsushima, Y.; Takano, M.; Tsuchiya, E.; Kanazawa, H.; Nagata, Y.; Takai, N.; Shinozuka, N.; Sakuma, I., High-performance liquid chromatographic determination of catecholamine metabolites and 5- hydroxyindoleacetic acid in human urine using a mixed-mode column and an eight- channel electrode electrochemical detector. *J Chromatogr B* **1994,** *658* (1), 63-68.

101.   Bicker, W.; Lammerhofer, M.; Lindner, W., Determination of chlorpyrifos metabolites in human urine by reversed-phase/weak anion exchange liquid chromatography-electrospray ionisation-tandem mass spectrometry. *J Chromatogr B* **2005,** *822* (1-2), 160-169.

102.   Ferguson, P. L.; Iden, C. R.; Brownawell, B. J., Analysis of nonylphenol and nonylphenol ethoxylates in environmental samples by mixed-mode high-performance liquid chromatography–electrospray mass spectrometry. *J Chromatogr A* **2001,** *938* (1-2), 79-91.

103.   Lara-Martin, P. A.; Gomez-Parra, A.; Gonzalez-Mazo, E., Development of a method for the simultaneous analysis of anionic and non-ionic surfactants and their carboxylated metabolites in environmental samples by mixed-mode liquid chromatography-mass spectrometry. *J Chromatogr A* **2006,** *1137* (2), 188-197.

104.   Gao, L.; Shi, Y.; Li, W.; Ren, W.; Liu, J.; Cai, Y., Determination of organophosphate esters in water samples by mixed-mode liquid chromatography and tandem mass spectrometry. *J Sep Sci* **2015,** *38* (13), 2193-2200.

105. Montes, R.; Aguirre, J.; Vidal, X.; Rodil, R.; Cela, R.; Quintana, J. B., Screening for polar chemicals in water by trifunctional mixed-mode liquid chromatography-high resolution mass spectrometry. *Environ Sci Technol* **2017,** *51* (11), 6250-6259.

106. Montes, R.; Rodil, R.; Cela, R.; Quintana, J. B., Determination of persistent and mobile organic contaminants (PMOCs) in water by mixed-mode liquid chromatography-tandem mass spectrometry. *Anal Chem* **2019,** *91* (8), 5176-5183.

107. González-Mariño, I.; Estevez-Danta, A.; Rodil, R.; Da Silva, K. M.; Sodre, F. F.; Cela, R.; Quintana, J. B., Profiling cocaine residues and pyrolytic products in wastewater by mixed-mode liquid chromatography-tandem mass spectrometry. *Drug Test Anal* **2019,** *11* (7), 1018-1027.

108. Small, H.; Stevens, T. S.; Bauman, W. C., Novel ion exchange chromatographic method using conductimetric detection. *Anal Chem* **1975,** *47* (11), 1801-1809.

109. Wei, D.; Wang, X.; Wang, N.; Zhu, Y., A rapid ion chromatography column-switching method for online sample pretreatment and determination of l-carnitine, choline and mineral ions in milk and powdered infant formula. *RSC Adv* **2017,** *7* (10), 5920-5927.

110. Muhammad, N.; Guo, D.; Zhang, Y.; Intisar, A.; Subhani, Q.; Qadir, M. A.; Cui, H., Online clean-up setup for the determination of non-fluorescent acidic pharmaceutical drugs in complex biological samples. *J Chromatogr A* **2019,** *1126-1127*, 121708.

111. Luo, X.; Chen, L.; Zhao, Y., Simultaneous determination of three chloroacetic acids, three herbicides, and 12 anions in water by ion chromatography. *J Sep Sci* **2015,** *38* (17), 3096-3102.

112. Zakaria, P.; Bloomfield, C.; Shellie, R. A.; Haddad, P. R.; Dicinoski, G. W., Determination of bromate in sea water using multi-dimensional matrix-elimination ion chromatography. *J Chromatogr A* **2011,** *1218* (50), 9080-9085.

113. Gyparakis, S.; Diamadopoulos, E., Formation and reverse osmosis removal of bromate ions during ozonation of groundwater in coastal areas. *Sep Sci Technol* **2007,** *42* (7), 1465-1476.

114. Chen, Z.; Megharaj, M.; Naidu, R., Determination of bromate and bromide in seawater by ion chromatography, with an ammonium salt solution as mobile phase, and inductively coupled plasma mass spectrometry. *Chromatographia* **2007,** *65* (1-2), 115-118.

115. Evenhuis, C. J.; Buchberger, W.; Hilder, E. F.; Flook, K. J.; Pohl, C. A.; Nesterenko, P. N.; Haddad, P. R., Separation of inorganic anions on a high capacity porous polymeric monolithic column and application to direct determination of anions in seawater. *J Sep Sci* **2008,** *31* (14), 2598-2604.

116. Nojavan, S.; Bidarmanesh, T.; Memarzadeh, F.; Chalavi, S., Electro-driven extraction of inorganic anions from water samples and water miscible organic solvents and analysis by ion chromatography. *Electrophoresis* **2014,** *35* (17), 2446-2453.

117. Liu, J.-M.; Liu, C.-C.; Fang, G.-Z.; Wang, S., Advanced analytical methods and sample preparation for ion chromatography techniques. *RSC Adv* **2015,** *5* (72), 58713-58726.

118. Teh, H. B.; Li, S. F., Simultaneous determination of bromate, chlorite and haloacetic acids by two-dimensional matrix elimination ion chromatography with coupled conventional and capillary columns. *J Chromatogr A* **2015,** *1383*, 112-120.

119. Pacholec, F.; Eaton, D. R.; Rossi, D. T., Characterization of mixtures of organic acids by ion-exclusion partition chromatography-mass spectrometry. *Anal Chem* **1986,** *58* (12), 2581-2583.

120.   Karu, N.; Dicinoski, G. W.; Hanna-Brown, M.; Haddad, P. R., Determination of pharmaceutically related compounds by suppressed ion chromatography: II. Interactions of analytes with the suppressor. *J Chromatogr A* **2012,** *1224*, 35-42.

121.   Pantsar-Kallio, M.; Manninen, P. K. G., Speciation of halogenides and oxyhalogens by ion chromatography-inductively coupled plasma mass spectrometry. *Anal Chim Acta* **1998,** *360* (1-3), 161-166.

122.   Jansons, M.; Pugajeva, I.; Bartkevics, V., Evaluation of selected buffers for simultaneous determination of ionic and acidic pesticides including glyphosate using anion exchange chromatography with mass spectrometric detection. *J Sep Sci* **2019,** *42* (19), 3077-3085.

123.   Wouters, S.; Haddad, P. R.; Eeltink, S., System design and emerging hardware technology for ion chromatography. *Chromatographia* **2016,** *80* (5), 689-704.

124.   Eghbali, H.; Bruggink, C.; Agroskin, Y.; Pohl, C. A.; Eeltink, S., Performance evaluation of ion-exchange chromatography in capillary format. *J Sep Sci* **2012,** *35* (24), 3461-3468.

125.   Wang, J.; Schnute, W. C., Optimizing mass spectrometric detection for ion chromatographic analysis. I. Common anions and selected organic acids. *Rapid Commun Mass Spectrom* **2009,** *23* (21), 3439-3447.

126.   Pröfrock, D.; Prange, A., Inductively coupled plasma-mass spectrometry (ICP-MS) for quantitative analysis in environmental and life sciences: a review of challenges, solutions, and trends. *Appl Spectrosc* **2012,** *66* (8), 843-868.

127.   Sacher, F.; Raue, B.; Brauch, H. J., Analysis of iodinated X-ray contrast agents in water samples by ion chromatography and inductively-coupled plasma mass spectrometry. *J Chromatogr A* **2005,** *1085* (1), 117-123.

128.   Aga, D. S.; Thurman, E. M.; Yockel, M. E.; Zimmerman, L. R.; Williams, T. D., Identification of a new sulfonic acid metabolite of metolachlor in soil. *Environ Sci Technol* **1996,** *30* (2), 592-597.

129.   Profrock, D.; Prange, A., Compensation of gradient related effects when using capillary liquid chromatography and inductively coupled plasma mass spectrometry for the absolute quantification of phosphorylated peptides. *J Chromatogr A* **2009,** *1216*(39), 6706-6715.

130.   Axelsson, B. O.; Jornten-Karlsson, M.; Michelsen, P.; Abou-Shakra, F., The potential of inductively coupled plasma mass spectrometry detection for high-performance liquid chromatography combined with accurate mass measurement of organic pharmaceutical compounds. *Rapid Commun Mass Spectrom* **2001,** *15* (6), 375-385.

131.   Bettmer, J.; Montes Bayon, M.; Encinar, J. R.; Fernandez Sanchez, M. L.; Fernandez de la Campa Mdel, R.; Sanz Medel, A., The emerging role of ICP-MS in proteomic analysis. *J Proteomics* **2009,** *72* (6), 989-1005.

132.   Prange, A.; Pröfrock, D., Chemical labels and natural element tags for the quantitative analysis of bio-molecules. *J Anal At Spectrom* **2008,** *23* (4), 432.

133.   Michalski, R., *Application of IC-MS and IC-ICP-MS in environmental research.* John Wiley & Sons, Hoboken, New Jersey: 2016.

134.   Reyes, L. H.; Mar, J. L.; Rahman, G. M.; Seybert, B.; Fahrenholz, T.; Kingston, H. M., Simultaneous determination of arsenic and selenium species in fish tissues using microwave-assisted enzymatic extraction and ion chromatography-inductively coupled plasma mass spectrometry. *Talanta* **2009,** *78* (3), 983-990.

135.   Christison, T.; Madden, J. E.; Rohrer, J. *Determination of cationic polar pesticides in homogenized fruit and vegetable samples using IC-HRAM MS*; Thermo Fisher: Sunnyvale, CA, USA, 2019.

136.   Michalski, R., Ion chromatography applications in wastewater analysis. *Separations* **2018,** *5*, 16.

137.   Kurz, A.; Bousova, K.; Beck, J.; Schoutsen, F.; Bruggink, C.; Kozeluh, M.; Kule, L.; Godula, M., Routine analysis of polar pesticides in water at low ng/L levels by ion chromatography coupled to triple quadrupole mass spectrometer. *Thermo Scientific* **2017**.

138.   Gallidabino, M. D.; Hamdan, L.; Murphy, B.; Barron, L. P., Suspect screening of halogenated carboxylic acids in drinking water using ion exchange chromatography - high resolution (Orbitrap) mass spectrometry (IC-HRMS). *Talanta* **2018,** *178*, 57-68.

139.   Gallidabino, M. D.; Irlam, R. C.; Salt, M. C.; O'Donnell, M.; Beardah, M. S.; Barron, L. P., Targeted and non-targeted forensic profiling of black powder substitutes and gunshot residue using gradient ion chromatography - high resolution mass spectrometry (IC-HRMS). *Anal Chim Acta* **2019,** *1072*, 1-14.

140.   Ali, I.; Alharbi, O. M. L.; Marsin Sanagi, M., Nano-capillary electrophoresis for environmental analysis. *Environ Chem Lett* **2015,** *14* (1), 79-98.

141.   Bol'shakova, D. S.; Amelin, V. G., Determination of pesticides in environmental materials and food products by capillary electrophoresis. *J Anal Chem* **2016,** *71* (10), 965-1013.

142.   Hamdan, I. I., Capillary electrophoresis in the analysis of pharmaceuticals in environmental water: A critical review. *J Liq Chrom Relat Tech* **2017,** *40* (3), 111-125.

143.   Altria, K. D.; Elder, D., Overview of the status and applications of capillary electrophoresis to the analysis of small molecules. *J Chromatogr A* **2004,** *1023* (1), 1-14.

144.   Herrera-Herrera, A. V.; Hernandez-Borges, J.; Borges-Miquel, T. M.; Rodriguez-Delgado, M. A., Dispersive liquid-liquid microextraction combined with nonaqueous capillary electrophoresis for the determination of fluoroquinolone antibiotics in waters. *Electrophoresis* **2010,** *31* (20), 3457-3465.

145.   Horciciak, M.; Masar, M.; Bodor, R.; Danc, L.; Bel, P., Trace analysis of glyphosate in water by capillary electrophoresis on a chip with high sample volume loadability. *J Sep Sci* **2012,** *35* (5-6), 674-680.

146.   Krishna Marothu, V.; Gorrepati, M.; Vusa, R., Electromembrane extraction - a novel extraction technique for pharmaceutical, chemical, clinical and environmental analysis. *J Chromatogr Sci* **2013,** *51* (7), 619-631.

147.   Tabani, H.; Fakhari, A. R.; Zand, E., Low-voltage electromembrane extraction combined with cyclodextrin modified capillary electrophoresis for the determination of phenoxy acid herbicides in environmental samples. *Anal Methods* **2013,** *5* (6), 1548.

148.   Herrera-Herrera, A. V.; Ravelo-Perez, L. M.; Hernandez-Borges, J.; Afonso, M. M.; Palenzuela, J. A.; Rodriguez-Delgado, M. A., Oxidized multi-walled carbon nanotubes for the dispersive solid-phase extraction of quinolone antibiotics from water samples using capillary electrophoresis and large volume sample stacking with polarity switching. *J Chromatogr A* **2011,** *1218* (31), 5352-5361.

149.   Maijo, I.; Fontanals, N.; Borrull, F.; Neususs, C.; Calull, M.; Aguilar, C., Determination of UV filters in river water samples by in-line SPE-CE-MS. *Electrophoresis* **2013,** *34* (3), 374-382.

150.   Lombardo-Agui, M.; Gamiz-Gracia, L.; Garcia-Campana, A. M.; Cruces- Blanco, C., Sensitive determination of fluoroquinolone residues in waters by capillary electrophoresis with laser-induced fluorescence detection. *Anal Bioanal Chem* **2010,** *396* (4), 1551-1557.

151.   Rageh, A. H.; Klein, K.-F.; Pyell, U., Off-line and on-line enrichment of α-aminocephalosporins for their analysis in surface water samples using CZE coupled to LIF. *Chromatographia* **2016,** *79* (3-4), 225-241.

152.   Zhang, Z.; Zhang, D.; Zhang, X., Simultaneous determination of pharmaceutical and personal care products in wastewater by capillary electrophoresis with head-column field-amplified sample stacking. *Anal Methods* **2014,** *6* (19), 7978-7983.

153.   Ahrer, W.; Buchberger, W., Combination of aqueous and non-aqueous capillary electrophoresis with electrospray mass spectrometry for the determination of drug residues in water. *Monatsh Chem* **2001,** *132* (3), 329-337.

154.   Höcker, O.; Bader, T.; Schmidt, T. C.; Schulz, W.; Neusüss, C., Enrichment-free analysis of anionic micropollutants in the sub-ppb range in drinking water by capillary electrophoresis-high resolution mass spectrometry. *Anal Bioanal Chem* **2020**.

155.   Deng, B.; Xu, Q.; Lu, H.; Ye, L.; Wang, Y., Pharmacokinetics and residues of tetracycline in crucian carp muscle using capillary electrophoresis on-line coupled with electrochemiluminescence detection. *Food Chem* **2012,** *134* (4), 2350-2354.

156.   Sun, H.; Qi, H.; Li, H., Development of capillary electrophoretic method combined with accelerated solvent extraction for simultaneous determination of residual sulfonamides and their acetylated metabolites in aquatic products. *Food Anal Methods* **2012,** *6* (4), 1049-1055.

157.   Knoll, S.; Jacob, S.; Mieck, S.; Triebskorn, R.; Braunbeck, T.; Huhn, C., Relevance of charged micropollutants – Quantification of metformin and its transformation product guanylurea in biota by capillary electrophoresis-mass spectrometry. In *Anal Bioanal Chem*, 2020.

158.   Chapel, S.; Rouvière, F.; Heinisch, S., Pushing the limits of resolving power and analysis time in on-line comprehensive hydrophilic interaction x reversed phase liquid chromatography for the analysis of complex peptide samples. *J Chromatogr A* **2019**, 460753.

159.   Brudin, S. S.; Shellie, R. A.; Haddad, P. R.; Schoenmakers, P. J., Comprehensive two-dimensional liquid chromatography: ion chromatography x reversed-phase liquid chromatography for separation of low-molar-mass organic acids. *J Chromatogr A* **2010,** *1217* (43), 6742-6746.

160.   Beutner, A.; Kochmann, S.; Mark, J. J.; Matysik, F. M., Two-dimensional separation of ionic species by hyphenation of capillary ion chromatography x capillary electrophoresis-mass spectrometry. *Anal Chem* **2015,** *87* (6), 3134-3138.

161.   Ranjbar, L.; Foley, J. P.; Breadmore, M. C., Multidimensional liquid-phase separations combining both chromatography and electrophoresis - A review. *Anal Chim Acta* **2017,** *950*, 7-31.

162.   Stevenson, P. G.; Fairchild, J. N.; Guiochon, G., Retention mechanism divergence of a mixed mode stationary phase for high performance liquid chromatography. *J Chromatogr A* **2011,** *1218* (14), 1822-1827.

163.   Miller, L., Preparative enantioseparations using supercritical fluid chromatography. *J Chromatogr A* **2012,** *1250*, 250-255.

164.   Gomez Cortes, L., Marinov, D., Sanseverino, I., Navarro Cuenca, A., Niegowska, M., Porcel Rodriguez, E. and Lettieri, T. *Selection of substances for the 3rd Watch List under the Water Framework Directive*; 1018-5593; Luxembourg, 2020.

165.   Schymanski, E. L.; Singer, H. P.; Slobodnik, J.; Ipolyi, I. M.; Oswald, P.; Krauss, M.; Schulze, T.; Haglund, P.; Letzel, T.; Grosse, S.; Thomaidis, N. S.; Bletsou, A.; Zwiener, C.; Ibanez, M.; Portoles, T.; de Boer, R.; Reid, M. J.; Onghena, M.; Kunkel, U.; Schulz, W.; Guillon, A.; Noyon, N.; Leroy, G.; Bados, P.; Bogialli, S.; Stipanicev, D.; Rostkowski, P.; Hollender, J., Non-target screening with high-resolution mass spectrometry: critical review using a collaborative trial on water analysis. *Anal Bioanal Chem* **2015,** *407* (21), 6237-6255.

166.   Zhang, X.-H.; Deng, Y.; Zhao, M.-Z.; Zhou, Y.-L.; Zhang, X.-X., Highly-sensitive detection of eight typical fluoroquinolone antibiotics by capillary

electrophoresis-mass spectroscopy coupled with immunoaffinity extraction. *RSC Advances* **2018,** *8* (8), 4063-4071.

167.   Wuethrich, A.; Haddad, P. R.; Quirino, J. P., Field-enhanced sample injection micelle-to-solvent stacking capillary zone electrophoresis-electrospray ionization mass spectrometry of antibiotics in seawater after solid-phase extraction. *Electrophoresis* **2016,** *37* (9), 1139-1142.

168.   Höcker, O.; Bader, T.; Schmidt, T. C.; Schulz, W.; Neusüß, C., Enrichment-free analysis of anionic micropollutants in the sub-ppb range in drinking water by capillary electrophoresis-high resolution mass spectrometry. *Anal Bioanal Chem* **2020,** (412), 4857-4865.

169.   An, D.; Chen, Z.; Zheng, J.; Chen, S.; Wang, L.; Huang, Z.; Weng, L., Determination of biogenic amines in oysters by capillary electrophoresis coupled with electrochemiluminescence. *Food Chem* **2015,** *168*, 1-6.

170.   Jacob, S.; Knoll, S.; Huhn, C.; Kohler, H. R.; Tisler, S.; Zwiener, C.; Triebskorn, R., Effects of guanylurea, the transformation product of the antidiabetic drug metformin, on the health of brown trout (Salmo trutta f. fario). *PeerJ* **2019,** *7*, e7289.

171.   Jacob, S.; Köhler, H.-R.; Tisler, S.; Zwiener, C.; Triebskorn, R., Impact of the antidiabetic drug metformin and Its transformation product guanylurea on the health of the big ramshorn snail (Planorbarius corneus). *Front Environ Sci* **2019,** *7*.

172.   Knoll, S.; Jacob, S.; Mieck, S.; Triebskorn, R.; Braunbeck, T.; Huhn, C., Development of a capillary electrophoresis-mass spectrometry method for the analysis of metformin and its transformation product guanylurea in biota. *Anal Bioanal Chem* **2020,** *412* (20), 4985-4996.

173.   Wang, Y.-W.; He, S.-J.; Feng, X.; Cheng, J.; Luo, Y.-T.; Tian, L.; Huang, Q., Metformin: a review of its potential indications. *Drug Des Dev Ther* **2017,** *11*, 2421.

174.   Messerli, F. H.; Bangalore, S., Half a century of hydrochlorothiazide: facts, fads, fiction, and follies. *Am J Med* **2011,** *124* (10), 896-899.

175.   Schmitt-Kopplin, P., *Capillary electrophoresis: Methods and protocols*. Springer Science+Business Media: New York, 2008.

176.   Pantuckova, P.; Gebauer, P.; Bocek, P.; Krivankova, L., Electrolyte systems for on-line CE-MS: detection requirements and separation possibilities. *Electrophoresis* **2009,** *30* (1), 203-214.

177.   Stolz, A.; Jooss, K.; Höcker, O.; Romer, J.; Schlecht, J.; Neusüss, C., Recent advances in capillary electrophoresis-mass spectrometry: Instrumentation, methodology and applications. *Electrophoresis* **2019,** *40* (1), 79-112.

178.   Posch, T. Implementation of capillary electromigrativeseparation techniques coupled to massspectrometry in forensic and biological science. PhD thesis, Forschungszentrum Jülich, 2014.

179.   Kenndler, E., A critical overview of non-aqueous capillary electrophoresis. Part I: mobility and separation selectivity. *J Chromatogr A* **2014,** *1335*, 16-30.

180.   Barthel, J.; Gores, H.-J.; Schmeer, G.; Wachter, R., Non-aqueous electrolyte solutions in chemistry and modern technology. In *Physical and Inorganic Chemistry*, Springer-Verlag Berlin Heidelberg: 1983; pp 33-144.

181.   Sarmini, K.; Kenndler, E., Ionization constants of weak acids and bases in organic solvents. *J Biochem Biophys Methods* **1999,** *38* (2), 123-137.

182.   Bellini, M. S.; Deyl, Z.; Mikšík, I., Nonaqueous capillary electrophoresis. Application to the separation of complex mixtures of organic acids by ion-pairing mechanism. *Forensic Sci Int* **1998,** *92* (2-3), 185-199.

183.   Kenndler, E., A critical overview of non-aqueous capillary electrophoresis. Part II: separation efficiency and analysis time. *J Chromatogr A* **2014,** *1335*, 31-41.

184.   Miguel, E. L.; Silva, P. L.; Pliego, J. R., Theoretical prediction of pKa in methanol: testing SM8 and SMD models for carboxylic acids, phenols, and amines. *J Phys Chem B* **2014,** *118* (21), 5730-5739.

185.   Himmelsbach, M.; Buchberger, W.; Reingruber, E., Determination of polymer additives by liquid chromatography coupled with mass spectrometry. A comparison of atmospheric pressure photoionization (APPI), atmospheric pressure chemical ionization (APCI), and electrospray ionization (ESI). *Polym Degrad Stab* **2009,** *94* (8), 1213-1219.

186.   Robles-Molina, J.; Lara-Ortega, F. J.; Gilbert-Lopez, B.; Garcia-Reyes, J. F.; Molina-Diaz, A., Multi-residue method for the determination of over 400 priority and emerging pollutants in water and wastewater by solid-phase extraction and liquid chromatography-time-of-flight mass spectrometry. *J Chromatogr A* **2014,** *1350*, 30-43.

187.   Schifano, F., Misuse and abuse of pregabalin and gabapentin: cause for concern? *CNS drugs* **2014,** *28* (6), 491-496.

188.   Weiss, S.; Reemtsma, T., Determination of benzotriazole corrosion inhibitors from aqueous environmental samples by liquid chromatography-electrospray ionization-tandem mass spectrometry. *Anal Chem* **2005,** *77* (22), 7415-20.

189.   Freeling, F.; Scheurer, M.; Sandholzer, A.; Armbruster, D.; Nodler, K.; Schulz, M.; Ternes, T. A.; Wick, A., Under the radar - Exceptionally high environmental concentrations of the high production volume chemical sulfamic acid in the urban water cycle. *Water Res* **2020,** *175*, 115706.

190.   Sun, H.; Zuo, Y.; Qi, H.; Lv, Y., Accelerated solvent extraction combined with capillary electrophoresis as an improved methodology for simultaneous determination of residual fluoroquinolones and sulfonamides in aquatic products. *Anal Methods* **2012,** *4* (3), 670-675.

191.   Liu, L.; Chen, J.; He, X.; Hao, S.; Lian, Z.; Wang, B., First determination of extracellular paralytic shellfish poisoning toxins in the culture medium of toxigenic dinoflagellates by HILIC-HRMS. *Ecotoxicol Environ Saf* **2020,** *204*, 111042.

192.   Berry, D.; Millington, C., Analysis of pregabalin at therapeutic concentrations in human plasma/serum by reversed-phase HPLC. *Ther Drug Monit* **2005,** *27* (4), 451-456.

193.   Weber, W. H.; Müller, A.; Weiss, S.; Seitz, W.; Schulz, W., 1H-benzotriazole and tolyltriazoles in the aquatic environment. Occurrence in ground, surface and wastewater. *Vom Wasser* **2009,** *107*, 16-24.

194.   Seitz, W.; Schulz, W.; Winzenbacher, R., Advantage of liquid chromatography with high-resolution mass spectrometry for the detection of the small and polar molecules trifluoroacetic acid and sulfamic acid. *J Sep Sci* **2018,** *41* (24), 4437-4448.

195.   Dejaegher, B.; Vander Heyden, Y., HILIC methods in pharmaceutical analysis. *J Sep Sci* **2010,** *33* (6-7), 698-715.

196.   Ikegami, T.; Tomomatsu, K.; Takubo, H.; Horie, K.; Tanaka, N., Separation efficiencies in hydrophilic interaction chromatography. *J Chromatogr A* **2008,** *1184* (1-2), 474-503.

197.   Erkmen, C.; Gebrehiwot, W. H.; Uslu, B., Hydrophilic interaction liquid chromatography (HILIC): latest applications in the pharmaceutical researches. *Curr Pharm Anal* **2021,** *17* (3), 316-345.

198.   Dejaegher, B.; Mangelings, D.; Vander Heyden, Y., Method development for HILIC assays. *J Sep Sci* **2008,** *31* (9), 1438-1448.

199.   Nguyen, H. P.; Schug, K. A., The advantages of ESI-MS detection in conjunction with HILIC mode separations: Fundamentals and applications. *J Sep Sci* **2008,** *31* (9), 1465-1480.

200.   Lauber, M.; Mccall, S.; Alden, B.; Iraneta, P.; Koza, S., Developing High Resolution HILIC Separations of Intact Glycosylated Proteins Using a Wide-Pore Amide-Bonded Stationary Phase. *Waters application note 720005380EN* **2015**.

201.   Appelblad, P.; Jonsson, T.; Pontén, E.; Jiang, W., *A practical guide to HILIC including ZIC-HILIC applications*. MerckSeQuant AB: Darmstadt, Germany, 2009.

202.   Muller, K.; Zahn, D.; Fromel, T.; Knepper, T. P., Matrix effects in the analysis of polar organic water contaminants with HILIC-ESI-MS. *Anal Bioanal Chem* **2020,** *412* (20), 4867-4879.

203.   Fountain, K. J.; Xu, J.; Diehl, D. M.; Morrison, D., Influence of stationary phase chemistry and mobile-phase composition on retention, selectivity, and MS response in hydrophilic interaction chromatography. *J Sep Sci* **2010,** *33* (6-7), 740-751.

204.   Isokawa, M.; Funatsu, T.; Tsunoda, M., Evaluation of the effects of sample dilution and volume in hydrophilic interaction liquid chromatography. *Chromatographia* **2014,** *77* (21-22), 1553-1556.

205.   Zbornikova, E.; Knejzlik, Z.; Hauryliuk, V.; Krasny, L.; Rejman, D., Analysis of nucleotide pools in bacteria using HPLC-MS in HILIC mode. *Talanta* **2019,** *205*, 120161.

206.   Nurenberg, G.; Schulz, M.; Kunkel, U.; Ternes, T. A., Development and validation of a generic nontarget method based on liquid chromatography - high resolution mass spectrometry analysis for the evaluation of different wastewater treatment options. *J Chromatogr A* **2015,** *1426*, 77-90.

207.   Salas, D.; Borrull, F.; Fontanals, N.; Marce, R. M., Hydrophilic interaction liquid chromatography coupled to high-resolution mass spectrometry to determine artificial sweeteners in environmental waters. *Anal Bioanal Chem* **2015,** *407* (15), 4277-4285.

208.   Liang, S.-H., *A Novel Approach for Ultrashort-Chain PFAS Analysis in Water Samples*. Restek: Centre County, PA, USA, 2021.

209.   Wuethrich, A.; Haddad, P. R.; Quirino, J. P., The electric field – An emerging driver in sample preparation. *TrAC Trends Anal Chem* **2016,** *80*, 604-611.

210.   Stichlmair, J.; Schmidt, J.; Proplesch, R., Electroextraction: A novel separation technique. *Chem Eng Sci* **1992,** *47* (12), 3015-3022.

211.   Yamini, Y.; Seidi, S.; Rezazadeh, M., Electrical field-induced extraction and separation techniques: promising trends in analytical chemistry-a review. *Anal Chim Acta* **2014,** *814*, 1-22.

212.   Huang, C.; Chen, Z.; Gjelstad, A.; Pedersen-Bjergaard, S.; Shen, X., Electromembrane extraction. *TrAC Trends Anal Chem* **2017,** *95*, 47-56.

213.   Pedersen-Bjergaard, S.; Huang, C.; Gjelstad, A., Electromembrane extraction-recent trends and where to go. *J Pharm Anal* **2017,** *7* (3), 141-147.

214.   Pedersen-Bjergaard, S., Electromembrane extraction-looking into the future. *Anal Bioanal Chem* **2019,** *411* (9), 1687-1693.

215.   Eie, L. V.; Rye, T. K.; Hansen, F.; Halvorsen, T. G.; Pedersen-Bjergaard, S., Electromembrane extraction of peptides and amino acids - status and perspectives. *Bioanalysis* **2021,** *13* (4), 277-289.

216.   Huang, C.; Gjelstad, A.; Pedersen-Bjergaard, S., Electromembrane extraction with alkylated phosphites and phosphates as supported liquid membranes. *J Membr Sci* **2017,** *526*, 18-24.

217.   Hansen, F. A.; Kuban, P.; Oiestad, E. L.; Pedersen-Bjergaard, S., Electromembrane extraction of highly polar bases from biological samples - deeper insight into bis(2-ethylhexyl) phosphate as ionic carrier. *Anal Chim Acta* **2020,** *1115*, 23-32.

218.   Drouin, N.; Kloots, T.; Schappler, J.; Rudaz, S.; Kohler, I.; Harms, A.; Lindenburg, P. W.; Hankemeier, T., Electromembrane extraction of highly polar compounds: analysis of cardiovascular biomarkers in plasma. *Metabolites* **2019,** *10* (1).

219. See, H. H.; Hauser, P. C., Automated electric-field-driven membrane extraction system coupled to liquid chromatography-mass spectrometry. *Anal Chem* **2014,** *86* (17), 8665-8670.

220. Mamat, N. A.; See, H. H., Development and evaluation of electromembrane extraction across a hollow polymer inclusion membrane. *J Chromatogr A* **2015,** *1406*, 34-39.

221. See, H. H.; Hauser, P. C., Electric field-driven extraction of lipophilic anions across a carrier-mediated polymer inclusion membrane. *Anal Chem* **2011,** *83* (19), 7507-7513.

222. Nojavan, S.; Sirani, M.; Asadi, S., Investigation of the continuous flow of the sample solution on the performance of electromembrane extraction: Comparison with conventional procedure. *J Sep Sci* **2017,** *40* (19), 3889-3897.

223. Atarodi, A.; Chamsaz, M.; Moghaddam, A. Z.; Tabani, H., Introduction of fullerene as a new carrier in electromembrane extraction for the determination of ibuprofen and sodium diclofenac as model acidic drugs in real urine samples. *Chromatographia* **2017,** *80* (6), 881-890.

224. Nojavan, S.; Asadi, S., Electromembrane extraction using two separate cells: A new design for simultaneous extraction of acidic and basic compounds. *Electrophoresis* **2016,** *37* (4), 587-594.

225. Asl, Y. A.; Yamini, Y.; Rezazadeh, M.; Seidi, S., Electromembrane extraction using a cylindrical electrode: a new view for the augmentation of extraction efficiency. *Anal Methods* **2015,** *7* (1), 197-204.

226. Tabani, H.; Fakhari, A. R.; Shahsavani, A., Simultaneous determination of acidic and basic drugs using dual hollow fibre electromembrane extraction combined with CE. *Electrophoresis* **2013,** *34* (2), 269-276.

227. Seidi, S.; Yamini, Y.; Rezazadeh, M.; Esrafili, A., Low-voltage electrically-enhanced microextraction as a novel technique for simultaneous extraction of acidic and basic drugs from biological fluids. *J Chromatogr A* **2012,** *1243*, 6-13.

228. Mamat, N. A.; See, H. H., Simultaneous electromembrane extraction of cationic and anionic herbicides across hollow polymer inclusion membranes with a bubbleless electrode. *J Chromatogr A* **2017,** *1504*, 9-16.

229. See, H. H.; Stratz, S.; Hauser, P. C., Electro-driven extraction across a polymer inclusion membrane in a flow-through cell. *J Chromatogr A* **2013,** *1300*, 79-84.

230. Schmidt-Marzinkowski, J.; See, H. H.; Hauser, P. C., Electric field driven extraction of inorganic anions across a polymer inclusion membrane. *Electroanal* **2013,** *25* (8), 1879-1886.

231. See, H. H.; Hauser, P. C., Electro-driven extraction of low levels of lipophilic organic anions and cations across plasticized cellulose triacetate membranes: Effect of the membrane composition. *J Membr Sci* **2014,** *450*, 147-152.

232. Zarghampour, F.; Yamini, Y.; Baharfar, M.; Faraji, M., Simultaneous extraction of acidic and basic drugs via on-chip electromembrane extraction using a single-compartment microfluidic device. *Analyst* **2018,** *144* (4), 1159-1166.

233. See, H. H.; Mamat, N. A.; Hauser, P. C., Flow injection analysis with direct UV detection following electric field driven membrane extraction. *Molecules* **2018,** *23* (5).

234. Asl, Y. A.; Yamini, Y.; Seidi, S.; Rezazadeh, M., Simultaneous extraction of acidic and basic drugs via on-chip electromembrane extraction. *Anal Chim Acta* **2016,** *937*, 61-68.

235. Petersen, N. J.; Jensen, H.; Hansen, S. H.; Foss, S. T.; Snakenborg, D.; Pedersen-Bjergaard, S., On-chip electro membrane extraction. *Microfluid Nanofluid* **2010,** *9* (4), 881-888.

236. Drouin, N.; Rudaz, S.; Schappler, J., New supported liquid membrane for electromembrane extraction of polar basic endogenous metabolites. *J Pharm Biomed Anal* **2018,** *159*, 53-59.

237. Roman-Hidalgo, C.; Martin-Valero, M. J.; Fernandez-Torres, R.; Callejon-Mochon, M.; Bello-Lopez, M. A., New nanostructured support for carrier-mediated electromembrane extraction of high polar compounds. *Talanta* **2017,** *162*, 32-37.

238. Cristina, R. H.; Maria Jesus, M. V.; Rut, F. T.; Miguel Angel, B. L., Use of polymer inclusion membranes (PIMs) as support for electromembrane extraction ofnon-steroidal anti-inflammatory drugs and highly polar acidic drugs. *Talanta* **2018,** *179*, 601-607.

239. Han, C.; Sun, J.; Liu, J.; Cheng, H.; Wang, Y., A pressure-driven capillary electrophoretic system with injection valve sampling. *Analyst* **2015,** *140* (1), 162-173.

240. Almeida, M.; Cattrall, R. W.; Kolev, S. D., Polymer inclusion membranes (PIMs) in chemical analysis - A review. *Anal Chim Acta* **2017,** *987*, 1-14.

241. Breitenstein, C. *Untersuchungen von Polymerinclusionmembranen hinsichtlich ihrer Ionen-Durchlässigkeit mithilfe von Elektromembran-Extraktion*; Mastermodul Analytische Chemie, Eberhard Karls Universität Tübingen: 2020.

242. Pereira, N.; St John, A.; Cattrall, R. W.; Perera, J. M.; Kolev, S. D., Influence of the composition of polymer inclusion membranes on their homogeneity and flexibility. *Desalination* **2009,** *236* (1-3), 327-333.

243. Juriatti, E. *Optimierung der Elektromembran-Extraktion anionischer Analyten*; Mastermodul Analytische Chemie, Eberhard Karls Universität Tübingen: 2021.

244. Bock, S. *Optimierung des Elektromembranextraktionssystems*; Mastermodul Analytische Chemie, Eberhard Karls Universität Tübingen: 2020.

245. Onac, C.; Kaya, A.; Sener, I.; Alpoguz, H. K., An electromembrane extraction with polymeric membrane under constant current for the recovery of Cr(VI) from industrial water. *J Electrochem Soc* **2018,** *165* (2), E76-E80.

246. Slampova, A.; Kuban, P.; Bocek, P., Electromembrane extraction using stabilized constant d.c. electric current--a simple tool for improvement of extraction performance. *J Chromatogr A* **2012,** *1234*, 32-37.

247. Rahmani, T.; Rahimi, A.; Nojavan, S., Study on electrical current variations in electromembrane extraction process: Relation between extraction recovery and magnitude of electrical current. *Anal Chim Acta* **2016,** *903*, 81-90.

248. Hosseiny Davarani, S. S.; Pourahadi, A.; Ghasemzadeh, P., Quantification of controlled release leuprolide and triptorelin in rabbit plasma using electromembrane extraction coupled with HPLC-UV. *Electrophoresis* **2019,** *40* (7), 1074-1081.

249. Ferreira, S. L.; Bruns, R. E.; Ferreira, H. S.; Matos, G. D.; David, J. M.; Brandao, G. C.; da Silva, E. G.; Portugal, L. A.; dos Reis, P. S.; Souza, A. S.; dos Santos, W. N., Box-Behnken design: an alternative for the optimization of analytical methods. *Anal Chim Acta* **2007,** *597* (2), 179-186.

250. Aranda-Merino, N.; Ramos-Payan, M.; Callejon-Mochon, M.; Villar-Navarro, M.; Fernandez-Torres, R., Comparison of three electromembrane-based extraction systems for NSAIDs analysis in human urine samples. *Anal Bioanal Chem* **2020,** *412* (25), 6811-6822.

251. Chien, R. L.; Burgi, D. S., On-column sample concentration using field amplification in CZE. *Anal Chem* **1992,** *64* (8), 489A-496A.

252. Seip, K. F.; Jensen, H.; Kieu, T. E.; Gjelstad, A.; Pedersen-Bjergaard, S., Salt effects in electromembrane extraction. *J Chromatogr A* **2014,** *1347*, 1-7.

253. Hansen, F.; Jaghl, F.; Leere Oiestad, E.; Jensen, H.; Pedersen-Bjergaard, S.; Huang, C., Impact of ion balance in electromembrane extraction. *Anal Chim Acta* **2020,** *1124*, 129-136.

254. Middelthon-Bruer, T. M.; Gjelstad, A.; Rasmussen, K. E.; Pedersen-Bjergaard, S., Parameters affecting electro membrane extraction of basic drugs. *J Sep Sci* **2008,** *31* (4), 753-759.

255. Nasrollahi, S. S.; Davarani, S. S. H.; Moazami, H. R., Impedometric investigation of salt effects on electromembrane extraction: Practical hints for pH adjustment. *Electrochim Acta* **2019,** *296*, 355-363.

256. Bader, T.; Schulz, W.; Kummerer, K.; Winzenbacher, R., LC-HRMS Data Processing Strategy for Reliable Sample Comparison Exemplified by the Assessment of Water Treatment Processes. *Anal Chem* **2017,** *89* (24), 13219-13226.

List of scientific contributions

Publications

S. Knoll, <u>T. Rösch</u>, C. Huhn, "Trends in sample preparation and separation methods for the analysis of very polar and ionic compounds in environmental water and biota samples", *Anal. Bioanal. Chem.* 2020, *412*, 6149–6165.

T. <u>Rösch</u>, J. Troffer, C. Huhn, "Indirect CE-UV detection for the characterization of organic and inorganic ions of a broad mobility and pK_a range in engine coolants", *Electrophoresis* 2019, *40*, 2806-2809.

Oral presentations

<u>T. Rösch</u>, S. Bock, C. Breitenstein, N. Kalinke, B. Rudisch, C. Huhn, "Development of an electro-membrane extraction setup combined with CE-MS for the analysis of ionic micropollutants in surface waters"
Online CE- und FFE-Forum 2020

<u>T. Rösch</u>, J. Troffer, C. Huhn, "Fast and comprehensive analysis of inorganic and organic anions in car engine coolants by CE-UV"
CE- und FFE-Forum 2018, Fraunhofer Institute for Chemical Technology, Karlsruhe

Poster presentations

<u>T. Rösch</u>, S. Bock, C. Breitenstein, N. Kalinke, B. Rudisch, C. Huhn, "Development of an electro-membrane extraction setup combined with CE-MS for the analysis of ionic micropollutants in surface waters"
36th International Symposium on Microscale Separations and Bioanalysis 2020 (online)

<u>T. Rösch</u>, G. Weber, C. Huhn, "Analysis of ionic micropollutants using capillary electrophoresis-mass spectrometry and prefractionation with free flow electrophoresis"
CE- und FFE-Forum 2019, Agilent Technologies, Waldbronn

<u>T. Rösch</u>, C. Huhn, "Development of a non-target screening using CE-MS for the analysis of ionic micropollutants in surface waters"
26th International Symposium on Electro- and Liquid Phase- Separation Techniques 2019, University of Toulouse, Paul Sabatier and *ANAKON 2019, Westfälische Wilhelms-Universität Münster*

S. Knoll, <u>T. Rösch</u>, C. Knappe, C. Huhn, "Evaluation of different QuEChERS procedures for the extraction of selected environmental contaminants from fish tissue using LC- and CE-MS"
ANAKON 2019, Westfälische Wilhelms-Universität Münster

T. <u>Rösch</u>, J. Troffer, C. Huhn, "Fast and comprehensive analysis of inorganic and organic anions in car engine coolants by CE-UV"
1. International Conference on Ion Analysis 2018, Technische Universität Berlin